POLYTECHNIQUE MONTRÉAL

affiliée à l'Université de Montréal

et

l'Université du Québec en Abitibi-Témiscamingue

Caractérisation et traitement des contaminants émergents dans les effluents miniers

SÉBASTIEN RYSKIE

Département des génies civil, géologique et des mines

Thèse présentée en vue de l'obtention du diplôme de *Philosophiae Doctor*

Génie minéral

Février 2023

POLYTECHNIQUE MONTRÉAL

affiliée à l'Université de Montréal

et

l'Université du Québec en Abitibi-Témiscamingue

Cette thèse intitulée :

Caractérisation et traitement des contaminants émergents dans les effluents miniers

présentée par **Sébastien RYSKIE**

en vue de l'obtention du diplôme de *Philosophiæ Doctor*

a été dûment acceptée par le jury d'examen constitué de :

Isabelle DEMERS, présidente

Carmen M. NECULITA, membre et directrice

Eric ROSA, membre et codirecteur

Patrice COUTURE, membre et codirecteur

Vincent CLOUTIER, membre

Elliott SKIERSZKAN, membre externe

DÉDICACE

À ma famille

REMERCIEMENTS

Je remercie d'abord ma directrice de thèse Carmen Mihaela Neculita, professeure à l'Université du Québec en Abitibi-Témiscamingue (UQAT), qui m'a prodigué de précieux conseils tout au long de mon parcours aux études supérieures. Dès notre première rencontre, il y a plusieurs années, à la suite de mes études au baccalauréat, j'ai senti la gentillesse et la sagesse qui l'accompagnait. Elle a cru en moi dès le début et m'a toujours encouragé à continuer et à persévérer même dans les moments les plus difficiles. Je peux affirmer que sans elle, je n'aurais probablement pas été en mesure de terminer cette thèse.

Je remercie également mon co-directeur Éric Rosa, professeur à l'UQAT, qui m'a appuyé durant mon parcours au doctorat. Il m'a toujours donné d'excellents conseils et m'a appuyé dans les différentes étapes de cette réussite. J'apprécie énormément le temps qu'il m'a donné afin que je puisse terminer le projet et la rédaction de la thèse.

Je remercie aussi mon co-directeur Patrice Couture, professeur à l'Institut national de la recherche scientifique (INRS), qui a été une personne importante dans la réussite mes études. Bien qu'il y eût une bonne distance qui nous séparait, nous avons quand même réussi à demeurer en contact. Ses conseils judicieux ont été bénéfiques durant les différentes étapes de ce grand projet.

De plus, je remercie Étienne Bélanger, chimiste à l'UQAT, pour son support et son aide dans la réalisation des essais de laboratoire et la rédaction du 3e article. Nous avons eu d'excellentes discussions et nous avons délivré un excellent travail grâce à son aide.

Je remercie aussi Florence Laflamme qui a aussi participé étroitement aux différentes campagnes d'échantillonnage sur le terrain et à la réalisation des essais de laboratoire en tant que stagiaire. Elle a été une personne très importante dans la réussite de ce projet.

Je remercie également Lucie Coudert, professeure à l'UQAT, pour sa collaboration dans la rédaction du premier article. Cela a toujours été un bonheur de discuter avec elle. Un énorme merci à Bryce LeBourre qui a aidé à assembler et à démarrer le pilote d'ozonation ainsi que d'avoir rédigé et partagé le protocole d'opération. Merci à Marc Paquin qui a activement aidé aux différentes étapes du projet. Un remerciement spécial à l'équipe de l'URSTM dont Mélinda Gervais et Elvin Basto pour leur aide dans la réalisation des analyses et la préparation des essais. Je remercie aussi Magalie Roy pour son aide dans la préparation des fichiers pour la gestion des données

d'échantillonnage et des cartes de géolocalisation ainsi que Daniel Blanchette pour son aide durant les premières campagnes d'échantillonnage.

J'aimerais également remercier Gaëlle Triffault-Bouchet et Éloïse Veilleux du Centre d'Expertise en Analyse Environnementale du Québec (CEAEQ) pour leur aide dans la réalisation des essais de toxicité nécessaires à la rédaction du 3e article.

Je tiens sincèrement à remercier les membres du jury qui ont accepté d'évaluer ce travail de recherche ainsi que tous les professeurs de l'Institut de Recherche en Mines et Environnement (IRME) qui m'ont prodigué une formation de qualité exceptionnelle et indispensable mais aussi pour les liens créés.

Je remercie aussi Sylvain Lortie qui m'a permis de débuter ce projet de doctorat et de m'avoir donné l'opportunité de travailler avec une équipe exceptionnelle. Une merci également à Sylvain Rancourt qui a aidé activement aux différentes étapes d'échantillonnage sur le terrain, un collègue que j'ai vraiment apprécié. Je tiens aussi à remercier Martin Demontigny qui va demeurer gravé dans ma mémoire, c'était une personne extraordinaire qui est partie trop tôt.

Je remercie Stephane Brienne pour m'avoir donné la chance d'appliquer mes connaissances acquises durant ce projet et d'évoluer au sein d'une compagnie qui rejoint mes valeurs. Grâce à lui, j'ai un emploi de rêve dans l'un des plus beaux endroits au Canada.

Enfin, je remercie mes parents, beaux-parents, mes frères et ma sœur pour leurs encouragements tout au long de ce parcours. Un merci spécial à ma femme qui a été présente durant tout ce temps et qui m'a supporté malgré les embuches et les nombreux sacrifices de temps donnés à ce grand projet. Merci aussi à la vie (et à ma femme!) de m'avoir donné le plus beau cadeau du monde, une merveilleuse petite fille! Je termine ce doctorat juste à temps pour pouvoir lui donner tout mon temps et mon amour.

Merci à tous!

N.B. Merci aussi à ceux que j'ai oublié ainsi qu'à toi qui prend le temps de lire mon travail.

AVANT-PROPOS

Durant la réalisation de ce projet de doctorat, plusieurs publications ont été produites, soit trois articles soumis dans des revues scientifiques avec comité de lecture ainsi qu'une présentation et une affiche dans une conférence internationale et un symposium local. La liste des travaux est présentée dans cette section.

Revues avec comité de lecture

Ryskie, S., Neculita, C. M., Rosa, E., Coudert, L., Couture, P. (2021) Active treatment of contaminants of emerging concern in cold mine water using advanced oxidation and membrane-related processes: a review. *Minerals*, 11(3), 259.

Note : Cet article a été promu Feature Paper et Editor's Choice par les éditeurs de la revue.

Ryskie, S., Bélanger, E., Neculita, C. M., Couture, P., Rosa, E. (2023) Influence of ozone microbubble enhanced oxidation on mine effluent mixes and *Daphnia magna* toxicity. *Chemosphere*, 329: 138559.

Ryskie, S., Rosa, E., Neculita, C. M., Couture, P. (2023) Modeling the geochemical evolution of mine waters during mixing. *Applied Geochemistry* (en évaluation).

Conférence

Ryskie, S., Rosa, E., Neculita, C. M., Couture, P. (2021) A predictive geochemical modeling framework for improving mine water management. *Water Congress (9th International Congress on Water Management in Mining and Industrial Processes)*, Santiago, Chile, 7-9 juillet 2021.

Affiche

Ryskie, S., Rosa, E., Neculita, C. M., Couture, P. (2021) Un cadre de modélisation géochimique prédictive pour améliorer la gestion des eaux minières. *Symposium virtuel sur l'Environnement et les Mines*, Rouyn-Noranda, Québec, 14-16 juin 2021.

RÉSUMÉ

Les compagnies minières doivent mettre en priorité la vision du développement durable afin de diminuer leur emprunte environnementale tout en optimisant leurs opérations. Une saine gestion de l'eau est primordiale afin de respecter les normes environnementales telles la Directive 019 au Québec et le Règlement sur les effluents de mines de métaux et diamant au Canada ainsi que pour maintenir leur image face aux investisseurs et communautés environnantes. La présence de contaminants d'intérêt émergeant (CEC) pose son lot de défi quant à la caractérisation et au traitement des différents effluents seuls et en mélanges sur les sites miniers, dépendamment de la méthode de gestion de l'eau. Les CEC dans les effluents miniers, lesquelles ont vu leur intérêt augmenter suite au resserrement de la règlementation dans l'industrie minière, peuvent être classifiés dans les quatre groupes suivants : 1) les nouveaux contaminants d'intérêt (Mn, Se, xanthates, éléments de terres rares); 2) les contaminants communs ayant des concentrations cibles de traitement faibles en environnement sensible (As, Cu, Zn); 3) les contaminants difficiles à traiter (thiosels, salinité) et 4) les composés azotés ($N\text{-}NH_3$, NO_2^-, NO_3^-, CNO^-, SCN^-). Des méthodes de traitements conventionnelles augmentant la salinité résiduelle comportent des limites au niveau de l'efficacité de traitement. Ces dernières sont aussi souvent affectées par la température de l'eau pouvant être limitées en climat froid. Cette problématique peut être adressée par l'utilisation de méthodes de traitement par oxydation avancée ou de filtration membranaire. La prédiction de la qualité de l'eau à l'aide de la modélisation numérique est aussi très importante afin d'aider les opérateurs miniers à minimiser les risques environnementaux.

L'objectif principal de cette étude était de prédire la spéciation des CEC à l'aide du modèle PHREEQC ainsi que d'évaluer l'effet sur la toxicité aquatique sur le crustacé *Daphnia magna* avant et après traitement d'effluents seuls et en mélanges au moyen de l'ozonation en microbulles. Les objectifs spécifiques étaient de : 1) Réaliser une revue de littérature sur les CEC en milieu minier afin d'identifier ceux d'intérêt pour cette étude; 2) Prédire, par modélisation géochimique à l'aide du modèle PHREEQC, la concentration et la spéciation des CEC ciblés dans les mélanges d'effluents miniers avec un facteur de confiance de plus de 80%; 3) Augmenter l'efficacité de traitement des CEC ciblés par rapport aux méthodes conventionnelles par l'utilisation d'un procédé d'ozonation par microbulles.

La première partie de ce projet consistait à réaliser une revue de littérature sur les CEC en parallèle des campagnes d'échantillonnage et de la compilation des données historiques du site minier à l'étude. Les différents CEC du site ont été identifiés afin de choisir la méthode de traitement adaptée mais aussi de bien choisir la base de données thermodynamique en vue de la modélisation numérique des mélanges à l'aide de PHREEQC. La revue a aussi permis d'identifier les défis et opportunités en lien avec les CEC dans les eaux minières en concentrant sur les procédés d'oxydation avancée et de filtration membranaire.

La deuxième partie du projet s'est concentrée sur la modélisation numérique des différents mélanges d'effluents à l'aide de PHREEQC afin d'identifier les mécanismes de mobilisation des différents CEC. Pour ce faire, des échantillons de terrain ont été prélevés pour caractériser les effluents en amont et en aval des différents points de mélange. Des essais contrôlés de mélange en laboratoire ont ensuite été réalisés avec des effluents réels. Les paramètres physico-chimiques *in situ*, les concentrations des ions majeurs et éléments mineurs dissous et des isotopes stables de la molécule d'eau ont été analysés. Des analyses minéralogiques ont également été effectuées sur les précipités des mélanges de laboratoire. Les données ont été utilisées pour effectuer des analyses statistiques et pour modéliser l'évolution géochimique des effluents à l'aide du modèle PHREEQC avec la base de données wateq4f.dat. Les résultats suggèrent que la formation de minéraux secondaires tels que la schwertmannite, la goethite et la jarosite a un impact significatif sur l'évolution géochimique des effluents. La précipitation des minéraux secondaires a été identifiée comme un processus d'immobilisation des éléments traces par des processus de coprécipitation et de sorption. Les principales limites identifiées concernant l'utilisation de PHREEQC pour la modélisation des mélanges d'effluents miniers concernent l'évaluation du bilan ionique pour les échantillons à faible pH avec des concentrations élevées en Fe et Al et l'omission des processus biologiques. Néanmoins, l'approche de caractérisation et de modélisation développée ici fournit des informations utiles sur l'évolution géochimique des effluents miniers et pourrait être adaptée à plusieurs sites miniers.

La troisième étape du projet a évalué l'efficacité de l'oxydation avancée à l'aide d'ozone en microbulles combinées à la précipitation chimique des métaux utilisant de la chaux sur l'élimination des contaminants et son impact sur la toxicité pour *D. magna* avec cinq mélanges d'effluents miniers différents provenant du site à l'étude. Pour les mélanges non acides, deux scénarios ont été testés : premièrement, un prétraitement des métaux par précipitation à la chaux et ajout d'un

floculant a été effectué avant l'ozonation; et deuxièmement, l'ozonation a été effectuée avant le post-traitement des métaux en utilisant la même technique de précipitation et de floculation. Les résultats ont montré que l'efficacité d'élimination de $N\text{-}NH_3$ variait de 90% pour les concentrations faibles (1,1 mg/L) à plus de 99% pour les concentrations plus élevées (58,4 mg/L). De plus, l'ozonation sans prétraitement des métaux a amélioré l'efficacité du traitement $N\text{-}NH_3$ en termes de cinétique mais a entraîné des problèmes de toxicité anormale. Les résultats des bioessais effectués sur l'eau avec prétraitement des métaux n'ont montré aucun événement de toxicité, mais ont montré des schémas de toxicité anormaux sur les mélanges traités sans prétraitement des métaux (les effluents dilués étaient toxiques, tandis que ceux non dilués ne l'étaient pas). À 50% de dilution, l'eau était toxique, probablement en raison de la présence potentielle de nanoparticules d'oxydes métalliques.

Cette étude a permis d'approfondir les connaissances au niveau de l'évolution géochimique des CEC en contexte minier à l'aide d'outil de modélisation tout en validant avec des échantillons réels. Les limites de l'applicabilité de cette méthode ont aussi été identifiées tout en proposant des pistes de solution afin d'améliorer la précision de la prédiction de la qualité de l'eau et de l'effet sur la toxicité aquatique. Enfin, les connaissances acquises durant ce projet pourront potentiellement être utilisées par l'opérateur du site à l'étude mais aussi par les autres compagnies minières afin d'améliorer leur gestion de l'eau.

ABSTRACT

Mining companies must prioritize the vision of sustainable development to reduce their environmental footprint while optimizing their operations. An optimal water management is essential to comply with environmental standards such as Directive 019 in Quebec and the Metal and Diamond Mining Effluent Regulations in Canada, as well as to maintain their image with investors and surrounding communities. The presence of contaminants of emerging concern (CEC) poses its challenges for the characterization and treatment of the various effluents alone and in mixtures on mining sites, depending on the water management method. CECs in mining effluents, which have seen their interest increase following the tightening of regulations in the mining industry, can be classified into the following four groups: 1) new contaminants of interest (Mn, Se, xanthates, elements rare earth); 2) common contaminants with low treatment target concentrations in sensitive environments (As, Cu, Zn); 3) hard-to-treat contaminants (thiosalts, salinity) and 4) nitrogen compounds (NH_3-N, NO_2^-, NO_3^-, CNO^-, SCN^-). Conventional treatment methods that increase residual salinity have limitations in terms of treatment efficiency. These are also often affected by the temperature of the water which can be limited in cold climates. This problem can be overcome by using advanced oxidation or membrane filtration treatment methods. Predicting water quality using numerical modeling is also very important to help mine operators minimize environmental risks.

The main objective of this study was to predict the speciation of CECs using PHREEQC as well as to assess the effect on aquatic toxicity on the crustacean *Daphnia magna* before and after treatment of effluents alone and in mixtures using ozone microbubble. The secondary objectives were to: 1) conduct a literature review on CECs in the mining environment to identify those of interest for this study; 2) Predict, by geochemical modeling using the PHREEQC model, the concentration and speciation of targeted CECs in mining effluent mixtures with a confidence factor of more than 80%; 3) Increase the treatment efficiency of targeted CECs compared to conventional methods using an ozone microbubble process.

The first part of the project consisted in carrying out a literature review on CECs in parallel with the sampling campaigns and the compilation of historical data for the mine site under study. The different CECs of the site have been identified to select the appropriate treatment method but also to choose the right thermodynamic database for the numerical modeling of the mixtures using

PHREEQC. The review also identified the challenges and opportunities related to CECs in mining waters by focusing on advanced oxidation processes and membrane filtration.

The second part of the project focused on the numerical modeling of the different effluent mixtures using PHREEQC to identify the mobilization mechanisms of the different CECs. To do this, field samples were taken to characterize the effluents upstream and downstream of the various mixing points. Controlled laboratory mixing experiments were then carried out with real effluents. The in-situ physico-chemical parameters, the concentrations of dissolved major ions and minor elements and stable isotopes of the water molecule were analyzed. Mineralogical analyzes were also carried out on the precipitates of the laboratory mixtures. The data was used to perform statistical analyzes and to model the geochemical evolution of the effluents using the PHREEQC model with the wateq4f.dat database. The results suggest that the formation of secondary minerals such as schwertmannite, goethite and jarosite has a significant impact on the geochemical evolution of the effluents. The precipitation of secondary minerals has been identified as a process of immobilization of trace elements by co-precipitation and sorption processes. The main limitations identified regarding the use of PHREEQC for modeling mining effluent mixtures relate to the assessment of the ion balance for low pH samples with high Fe and Al concentrations and the omission of biological processes. Nevertheless, the characterization and modeling approach developed here provides useful information on the geochemical evolution of mining effluents and could be adapted to several mining sites.

The third stage of the project assessed the effectiveness of advanced oxidation using ozone microbubble combined with chemical precipitation using lime on contaminant removal and its impact on toxicity to *D. magna* with five different mine effluent mixtures from the study site. For the non-acid mixtures, two scenarios were tested: first, a pre-treatment of the metals by precipitation with lime and a flocculant was carried out before the ozonation; and second, ozonation was performed before metal post-treatment using the same precipitation and flocculation technique. The results showed that the NH_3-N removal efficiency ranged from 90% for low concentrations (1.1 mg/L) to over 99% for higher concentrations (58.4 mg/L). In addition, ozonation without metal pre-treatment improved the efficiency of NH_3-N treatment in terms of kinetics but resulted in abnormal toxicity issues. Results of bioassays performed on water with metal pre-treatment showed no toxicity events but anomalous toxicity patterns on treated mixtures

without metal pre-treatment (diluted effluents were toxic, while undiluted ones were not). At 50% dilution, the water was toxic, likely due to the potential presence of metal oxide nanoparticles.

This study allowed to advance the knowledge on the geochemical evolution of CECs in a mining context using a modeling tool while validating with real samples. The limits of the applicability of this method have also been identified while proposing solutions to improve the accuracy of the prediction of water quality and the effect on aquatic toxicity. Finally, the knowledge acquired during this project could potentially be used by the operator of the site under study but also by other mining companies to improve their water management.

TABLE DES MATIÈRES

LISTE DES TABLEAUX

LISTE DES FIGURES

LISTE DES SIGLES ET ABRÉVIATIONS

AMD	Acid Mine Drainage
ANFO	Ammonium Nitrate Fuel Oil
AOP	Advanced Oxidation Processes
BATEA	Best Available Technology Economically Achievable
Bio-EF	Bio-Electro-Fenton
BLM	Biotic Ligand Model
CCME	Canadian Council of Ministers of the Environment
CEAEQ	Centre d'Expertise en Analyse Environnementale du Québec
CEC	Contaminant of Emerging Concern
CI	Chromatographie Ionique
CN^-	Cyanide
CNO^-	Cyanates
DL	Detection Limit
DMA	Drainage Minier Acide
DNA	Deoxyribonucleic Acid
DO	Dissolved Oxygen
DOC	Dissolved Organic Carbon
DS	Draw Solution
EC	Electrical Conductivity
EC50	Effective Concentration for 50% of the organisms
EDS	Energy Dispersive Spectroscopy
EF	Electro-Fenton
E/I	Evaporation over Inflow

EPI	Équipement de Protection Individuelle
FO	Forward Osmosis
GRES	Groupe de Recherche sur l'Eau Souterraine
HDS	High Density Sludge
HFF	Hollow Fine Fiber
HMI	Human Machine Interface
HRT	Hydraulic Retention Time
IC25	Inhibition Concentration causing 25% reduction in growth or reproduction of the organisms
ICMC	International Cyanide Management Code
ICP-AES	Inductively Coupled Plasma Atomic Emission Spectroscopy
ICP-MS	Inductively Coupled Plasma Mass Spectrometry
INRS	Institut National de la Recherche Scientifique
IRME	Institut de Recherche en Mines et Environnement
LC50	Lethal Concentration for 50% of the organisms
LEL	Local Evaporation Line
LMWL	Local Meteoric Water Line
MBBR	Moving Bed Bioreactor
MDMER	Metal and Diamond Mining Effluent Regulations
MEB	Microscope Électronique à Balayage
MELCC	Ministère de l'Environnement et de la Lutte contre les changements climatiques
MEND	Mine Environment Neutral Drainage
MF	Microfiltration
MLA	Mineral Liberation Analyzer
MMER	Metal Mining Effluent Regulations

NF	Nanofiltration
$N\text{-}NH_3$	Azote ammoniacal
NSERC	Natural Sciences and Engineering Research Council of Canada
O_3	Ozone
OHR	Original Hydrodynamic Reaction technology
ORP	Oxidation-Reduction Potential
PAN	Polyacrylonitrile
PHREEQC	pH-Redox-Equilibrium programmé en C++
POR	Potentiel d'oxydo-réduction
PRO	Pressure-Retarded Osmosis
PVC	Polyvinyl Chloride
PVDF	Polyvinylidenediflouride
REE	Rare earth elements
REMMD	Règlement sur les Effluents de Mines de Métaux et Diamant
RIME	Research Institute in Mines and Environment
RO	Reverse Osmosis
ROS	Reactive Oxygen Species
SCN^-	Thyocyanates
SEM	Scanning Electron Microscopy
SI	Source Identification / Saturation Indice
SP	Setpoint
SRF	Saturated Rock Fill
SW	Spiral Wound
TDS	Total Dissolved Solids

TIE	Toxicity Identification Evaluation
TIMA	Tescan Integrated Mineral Analyser
TMP	Transmembrane Pressure
TRE	Toxicity Reduction Evaluation
TS	Total Solids
TSS	Total Suspended Solids
TTE	Toxicity Treatability Evaluation
TU	Toxic Units
UF	Ultrafiltration
UQAT	Université du Québec en Abitibi-Témiscamingue
USGS	U.S. Geological Survey
VMD	Vacuum Membrane Distillation
VSMOW	Vienna Standard Mean Ocean Water
ZLD	Zero Liquid Discharge
ZLW	Zero Liquid Waste

LISTE DES ANNEXES

CHAPITRE 1 INTRODUCTION

1.1 Mise en contexte et problématique

Afin de demeurer compétitives et rentables tout en ayant une vision de développement durable, les compagnies minières doivent trouver des moyens d'optimiser leurs activités opérationnelles et environnementales. Une grande importance doit être accordée à la gestion de l'eau car de graves problèmes peuvent en résulter. En effet, une gestion inadéquate de l'eau peut engendrer des effets néfastes sur les écosystèmes, freiner l'approbation d'un projet et l'acceptabilité sociale, bloquer les activités déjà existantes, augmenter les coûts de production et avoir un impact négatif sur la réputation de la compagnie. Par conséquent, avec la réglementation qui tend à devenir de plus en plus restrictive, dont la Directive 019 (MELCC, 2012) et le Règlement sur les effluents de mines de métaux et de diamant (REMMD) (Gouvernement du Canada, 2018), les procédés de traitement d'eau se doivent d'être efficaces, robustes et économiquement viables (MEND, 2014). Dans le contexte canadien, les compagnies doivent composer avec plusieurs défis associés aux eaux minières, soit des débits et niveaux de contamination élevés, parfois situées dans des endroits éloignés caractérisées par un climat froid et souvent une caractérisation incomplète. Depuis quelques années, il y a des préoccupations grandissantes reliées à la contamination des eaux par des contaminants d'intérêt émergent. Dans les eaux municipales et industrielles, ces contaminants sont de sources naturelles ou anthropiques, persistants et potentiellement toxiques, bien que les connaissances concernant leurs effets soient parfois très limitées (Sauvé et Desrosiers, 2014). Dans le secteur minier, tout au long de l'histoire, les contaminants nouveaux ou émergents ont évolué avec les défis de la métallurgie, les connaissances scientifiques et dérivés des réglementations (Neculita et al., 2020). Les contaminants d'intérêt émergent (ou CEC en anglais, pour Contaminant of Emerging Concern) dans les effluents miniers, lesquelles ont vu leur intérêt augmenter suite au resserrement de la règlementation dans l'industrie minière, peuvent être classifiés dans les quatre groupes suivants : 1) les nouveaux contaminants d'intérêt (Mn, Se, xanthates, éléments de terres rares); 2) les contaminants communs ayant des concentrations cibles de traitement faibles en environnement sensible (As, Cu, Zn); 3) les contaminants difficiles à traiter (thiosels, salinité) et 4) les composés azotés (N-NH_3, NO_2^-, NO_3^-, CNO^-, SCN^-) (Neculita et al., 2018, 2019, 2020). Il est question d'environnement sensible dans le milieu minier lorsque que la concentration des

paramètres présents naturellement est très faible et que les espèces aquatiques présentes sont sensibles aux variations.

Le traitement des CEC dans les effluents miniers représente un défi important pour les compagnies minières. En effet, cela peut s'expliquer par leur chimie complexe et leur persistance, le manque de connaissances sur leur comportement lors du mélange d'effluents ayant des concentrations et caractéristiques physicochimiques variables ainsi que les technologies de traitement économiquement viables qui ne sont pas applicables dans tous les cas. Pour pallier cette problématique, de nouvelles études doivent porter sur les méthodes de gestion et de traitement de ces contaminants que ce soit en lien avec la prédiction de la spéciation des CEC suivant le mélange d'effluents ou au sujet des différentes technologies potentiellement applicables tels les procédés de traitement physicochimique, notamment ceux limitant la production de salinité résiduelle dans l'eau traitée (p. ex. membranes, évaporation, procédés d'oxydation avancées utilisant de l'ozone et des ferrates) (Gonzalez-Merchan et al., 2016, 2018; Ryskie et al., 2020). Par exemple, dans cette étude, des essais de traitabilité ont été réalisés sur des mélanges d'effluents provenant de la mine Westwood en Abitibi-Témiscamingue, QC, Canada. Une usine de traitement à boue haute densité est présente pour le traitement des eaux acides mais ses capacités sont limitées quant au traitement de contaminants sensibles aux conditions redox (p.ex. : les composés azotés) pouvant être traités plus efficacement par des procédés d'oxydation avancée. Cette étude permettra, entre autres, de déterminer si une étape de traitement par oxydation avancée pourrait être plus efficace si elle est réalisée avant ou après l'étape de précipitation des métaux dans l'usine de boue haute densité. L'impact sur la toxicité aquatique est aussi un enjeu considérable vu son importance pour la protection des écosystèmes et le respect des normes prescrites par la réglementation. De plus, certains processus de traitement (ex. électrocoagulation) peuvent réduire la charge en contaminants, comme la salinité sulfatée, mais augmenter la toxicité aquatique (Foudhaili et al., 2020). Il s'agit d'une problématique majeure pour plusieurs minières car les sources de toxicité peuvent être, dans certains cas, très difficiles à cibler en raison de la grande complexité de la chimie de ces eaux, même si des méthodes d'identification bien établies existent.

1.2 Hypothèses

Une caractérisation détaillée des différents effluents du site, en amont et en aval des points de mélanges, ainsi que des essais de traitabilité permettront de déterminer un mode gestion de l'eau approprié.

- Une revue de littérature couplée à l'examen des analyses chimiques des effluents ciblés permettra d'identifier les CEC d'intérêt pour cette étude.
- L'utilisation du logiciel PHREEQC permettra de prédire la spéciation et les indices de saturation des phases présentes dans les mélanges.
- La cinétique des réactions modélisées permettra de prédire les concentrations à l'équilibre des éléments dissous.
- Le traitement des effluents miniers par oxydation avancée permettra d'obtenir des concentrations en CEC plus faibles que celles obtenues par des approches conventionnelles.

1.3 Objectifs

1.3.1 Objectif général

L'objectif général de cette thèse est d'utiliser des outils de modélisation pour prédire la spéciation des CEC et ses effets sur la toxicité pour des effluents traités par des procédés de nouvelle génération.

1.3.2 Objectifs spécifiques

- Réaliser une revue de littérature sur les CEC en milieu minier afin d'identifier ceux d'intérêt pour cette étude;
- Prédire, par modélisation géochimique à l'aide du modèle PHREEQC, la concentration et la spéciation des CEC ciblés dans les mélanges d'effluents miniers avec un facteur de confiance de plus de 80%;
- Augmenter l'efficacité de traitement des CEC ciblés par rapport aux méthodes conventionnelles par l'utilisation d'un procédé d'ozonation par microbulles.

1.4 Originalité

Les éléments d'originalité sont les suivants :

- Les mélanges contrôlés permettant d'anticiper les réactions géochimiques et de les identifier au moyen de la modélisation numérique permettront de prédire la qualité de l'eau et d'optimiser la gestion des effluents sur un site minier.

- L'utilisation d'une technologie émergente, soit l'ozone en microbulles, pour le traitement des mélanges d'eaux minières ainsi que l'effet sur la toxicité aquatique sur *D. magna* avant et après traitement ainsi qu'avec ou sans prétraitement des métaux est un autre élément d'originalité.

À terme, les résultats seront directement utilisés pour une meilleure gestion des eaux et pour l'identification d'une technologie de traitement optimale. Ces résultats pourront également être adaptés à d'autres sites miniers, selon la méthodologie employée.

1.5 Contenu de la thèse

Cette thèse est composée de 8 chapitres et chacun d'eux est présenté dans cette section. Le chapitre 1 est l'introduction de ce travail, débutant par une mise en contexte ainsi qu'en décrivant la problématique sur les CEC en milieu minier ainsi que les limites des méthodes de traitement. L'originalité est aussi décrite suivi par les hypothèses de recherche ainsi que les objectifs généraux et spécifiques.

Le chapitre 2 présente une revue de littérature sur les CEC en milieu minier. Ce dernier est divisé en deux parties. La première partie présente de façon détaillée les différents CEC, en évaluant l'évolution des connaissances au niveau des effets sur la toxicité aquatique. La seconde partie décrit les méthodes de traitement pouvant être adaptées à ces différents contaminants, soit les procédés d'oxydation avancée en général, l'ozonation par microbulles ainsi que la filtration membranaire. Ce chapitre est présenté sous la forme d'un article qui a été publié dans la revue *Minerals* (2021).

Le chapitre 3 contient une revue de littérature complémentaire en deux sections, une sur la modélisation numérique pour la prédiction de la qualité de l'eau ainsi qu'une sur l'utilisation des

traceurs isotopiques en milieu minier. Les travaux présentés dans l'article 2 sont basés sur ces deux volets, ils devaient donc être ajoutés en tant que revue de littérature complémentaire.

Le chapitre 4 présente la démarche méthodologique utilisée dans les travaux de recherche afin de répondre aux différents objectifs.

Le chapitre 5 présente les travaux de modélisation réalisés avec PHREEQC avec les échantillons prélevés sur le site durant les différentes campagnes d'échantillonnage. Ces travaux traite du deuxième objectif afin de démontrer la faisabilité de prédire la qualité de l'eau avec cette méthode. Ce chapitre est présenté sous la forme d'un article, en évaluation, pour publication potentielle dans la revue *Applied Geochemistry* (2023).

Le chapitre 6 traite du second et du troisième objectif présentant les travaux réalisés avec le pilote d'ozonation par microbulles des mélanges d'effluents du site à l'étude ainsi que de l'effet sur la toxicité aquatique sur *Daphnia magna.* Ce chapitre est présenté sous la forme d'un article publié dans la revue *Chemosphere* (2023).

Le chapitre 7, présenté sous la forme d'une discussion générale, fait état des résultats obtenus durant les travaux réalisés afin de répondre aux différents objectifs.

Le chapitre 8 termine cette thèse avec les conclusions des différents travaux ainsi que les recommandations pour de futurs travaux de recherche.

Finalement, le matériel supplémentaire est présenté dans les annexes.

CHAPITRE 2 ARTICLE 1 : ACTIVE TREATMENT OF CONTAMINANTS OF EMERGING CONCERN IN COLD MINE WATER USING ADVANCED OXIDATION AND MEMBRANE-RELATED PROCESSES: A REVIEW[1]

Cet article a été publié dans la revue *Minerals* le 2 mars 2021

2.1 Abstract

Responsible use and effective treatment of mine water are prerequisites of sustainable mining. The behavior of contaminants in mine water evolves in relation to the metastable characteristics of some species, changes related to the mine life cycle, and mixing processes at various scales. In cold climates, water treatment requires adaptation to site-specific conditions, including high flow rates, salinity, low temperatures, remoteness, and sensitivity of receiving waterbodies. Contaminants of emerging concern (CECs) represent a newer issue in mine water treatment. This paper reviews recent research on the challenges and opportunities related to CECs in mine water treatment, with a focus on advanced oxidation and membrane-based processes on mine sites operating in cold climates. Finally, the paper identifies research needs in mine water treatment.

Keywords: mine water treatment; contaminants of emerging concern (CECs); cold climates; advanced oxidation processes (AOPs), membranes

---

[1] Ryskie, S., Neculita, C.M., Rosa, E., Coudert, L., Couture, P., 2021. Active Treatment of Contaminants of Emerging Concern in Cold Mine Water Using Advanced Oxidation and Membrane-Related Processes: A Review. Minerals, vol. 11, n° 3. p. 259. DOI: 10.3390/min11030259.

Graphical abstract

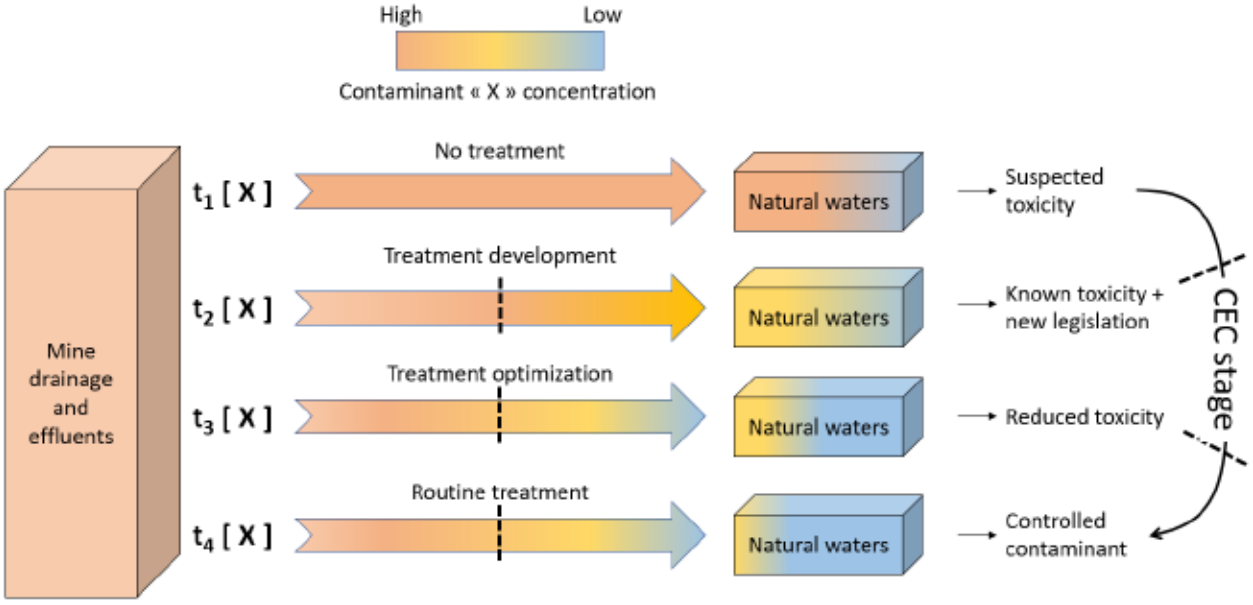

2.2 Introduction: Contaminants of Emerging Concern (CECs) in Mine Water

Sustainable mining implies a balance between economic profitability, safety, social acceptability, and environmental protection [1]. Given these factors, issues related to the mitigation of mining impacts on water resources inevitably arise. Optimizing low-cost water treatment approaches is critical to ensuring sustainable mining. This goal represents a major challenge as the global demand for mineral resources intensifies and diversifies [2], while the legislation regulating mining activities constantly evolves [3]. An integrated use of hydrological, geochemical, and isotopic tools in mining operations is also evolving [4]. Contaminants of emerging concern (CECs) are a central issue in this contemporary mining context.

In municipal and industrial wastewater, CECs include a wide range of highly soluble, persistent, and potentially toxic substances. Generally, there is limited knowledge about their concentrations (mostly because of poor knowledge on their quantification methods) and detrimental impacts [5]. These contaminants originate from natural or anthropic sources. Improved knowledge on the sources, transport, and spatiotemporal variability of CECs is an ongoing research need, especially for mixed-use watersheds, for better understanding of associated risks, and developing monitoring and mitigation strategies [6].

In mining, throughout history, new or emerging contaminants evolved with metallurgy challenges, scientific knowledge, and regulations [7,8]. As a result, new or CECs in mine water have specific features. They are not necessarily new chemicals and may have been present for a long time, but their presence or significance are only now being recognized, often because of increasing exploitation of low-grade ores, such as As from refractory gold mining [9]. The data about their characterization and toxicity are often scarce, the methods of detection are nonexistent or at an early stage, and there is no international definition of a new or emerging contaminant [10]. The CECs in mine water could even be contaminants that have already been treated but suddenly need to be mitigated to a new order of magnitude (especially in sensitive environments, such as cold climate (e.g. geographical isolation, extreme cold, strong winds, and erosion, salinity from de-icing agents or other, freeze-thaw cycles)). The definition of a CEC could also change geographically or for a different activity sector.

A review of Canadian legislation related to new contaminants or CECs in mine water and the development of treatment processes in the 1980s, 1990s, 2000s, and 2010s identified the following defining characteristics in each decade: (1) Before the 1980s, base metal mines were required to control metal concentrations in their effluents, but gold mines were not regulated [11]. Field-testing of cyanide destruction systems was reported (INCO or SO_2/air process discovery), followed by the testing, patenting, and implementing of all kinds of hydrogen peroxide-based processes. By the end of the 1980s, various types of water treatment systems were constructed and operated to control pH and treat dissolved metals, cyanides (and derivatives), total suspended solids, and so on. (2) In the 1990s, SO_2/air process was deployed at large scale. Acute aquatic toxicity was reportable but not regulated. There was a lot of research to lower copper and ammonia concentrations, but not much implementation of the findings. The 1990s also saw the first attempts to use metal precipitants. (3) In the 2000s, the International Cyanide Management Code (ICMC) and similar regulations meant that cyanide destruction now targeted the mill tailing pipe, not only final discharge, and the Metal Mining Effluent Regulations (MMER) meant that discharge water must not be acutely toxic. The decade also witnessed improved ammonia treatment as well as increased thiocyanates (SCN^-) biochemical treatment, and growing research on toxicity sources. (4) In the 2010s, the review of MMER saw the discussion and addition of new water targets, i.e., Metal and Diamond Mining Effluent Regulations (MDMER). Although Se was not mentioned, other parameters were tightened or introduced under MMER. Some mines in northern regions started to

work on desalination projects and were required to meet the Canadian Council of Ministers of the Environment (CCME) criteria at mine site closure. In some countries, mining permits involved respecting sulfate parameters; and zero liquid discharge (ZLD) and zero liquid waste (ZLW) were introduced. The evolution of regulations in Canada's (MMER) and Quebec's (Directive 019) mining industry is presented in Figure 2.1.

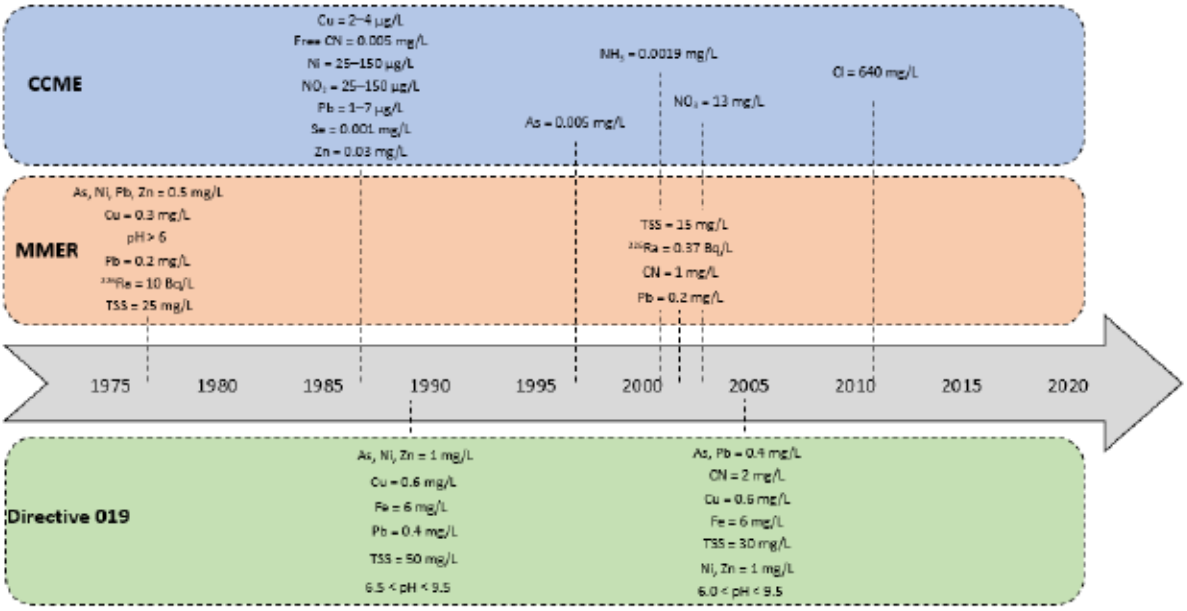

Figure 2.1 Regulation evolution for the mining industry in Canada [11–14]. CCME: Canadian Council of Ministers of the Environment; Metal Mining Effluent Regulations: MMER; TSS: Total Suspended Solids

Therefore, the current basic classification of CECs in mine water includes new contaminants (e.g. rare earth elements (REE), radioactive elements, Se, Mn); contaminants of emerging interest (e.g. salinity, sulfate), for which environmental contamination issues were not fully comprehended earlier; and "well-documented" contaminants (e.g. As, thiosalts, N-based compounds, xanthates, SCN^-), for which new issues (e.g. persistent aquatic toxicity) recently emerged, particularly in cold climates (at low temperature and high salinity) [7,8,15]. By their very nature, CECs are of growing concern for the mining industry. The definitions of some CECs based on scientific knowledge of different substances in mine water are presented in Figure 2.2.

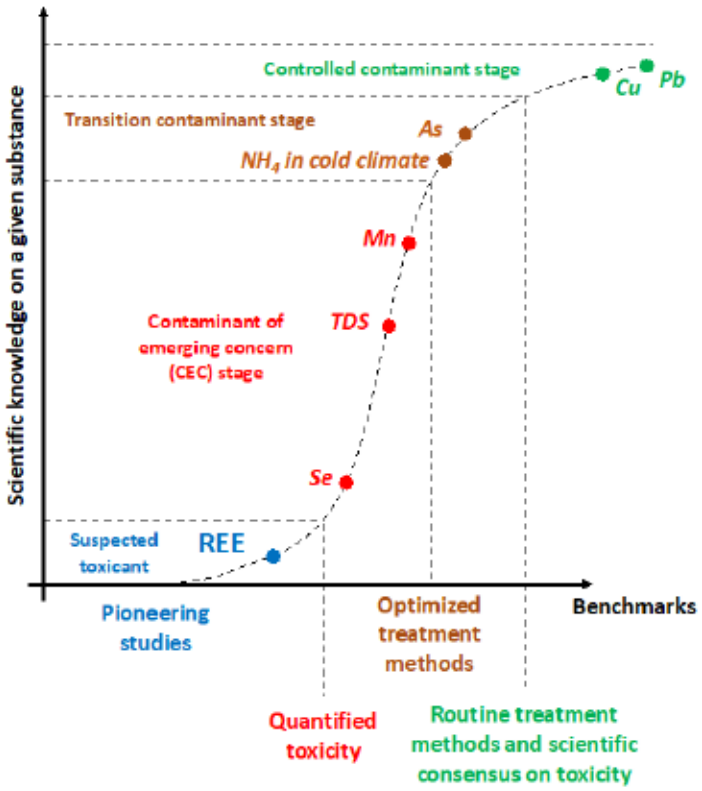

Figure 2.2 Contaminants of emerging concern (CECs) definitions based on scientific knowledge of different substances in mine water. REE: Rare Earth Elements; TDS: Total Dissolved Solids.

Based on the context outlined above, this paper provides an overview of the efficiency of selected processes and materials for the treatment of CECs from mine water. Background concentrations of selected CECs (As, Se, Mn, salinity, thiosalts, NH_3-N, and REE) in natural water are proposed as a basis for comparison with mine water. The treatment processes focus on As and Se, thiosalts, xanthates, N-based compounds (cyanides, NH_3-N, and SCN^-), and salinity. Regarding REE treatment, several comprehensive reviews are available, including two recent articles on the challenges and opportunities of their treatment and potential recovery from mine water [16–18]; thus, these elements will be not discussed in this review, even though they are of emerging concern. This review focuses on mine sites in cold climates to identify some priority issues related to the treatment of CECs. Questions relating to the treatment of CECs are of particular interest because of (1) the potential toxicity of these substances and (2) the gaps in the scientific knowledge required to define criteria for the discharge of mine water into the environment. The present study aims to contribute to the scientific efforts required to overcome this problem.

2.3 Characteristics of CECs

2.3.1 Background Concentrations of CECs

In this paper, As, Se, and Mn are considered as leading inorganic elements, given their importance as mine-related CECs and their known impacts on human health and the environment. In addition, xanthates, salinity, thiosalts, and nitrogen compounds were selected mainly because their ecotoxicological and cumulative effects remain uncertain even at low concentrations, especially with mixed contamination [7-9].

The geogenic sources of As include several minerals (e.g. arsenides, sulfides, oxides, arsenates, arsenites) that can be concentrated in mineralized areas [19]. In rocks, As typically ranges between 0.5 and 2.5 mg/kg [20], for an average crustal abundance of 1.5 mg/kg [21]. Common sources of As are As-bearing sulfides, which are often abundant in areas exploited for base metals, silver, and gold. In natural water, As mainly occurs as oxyanions of arsenite (As(III)) or arsenate (As(V)), while As-bearing organic species are generally less abundant [19]. In a review of worldwide data from large rivers, dissolved As concentrations of 0.11 to 2.71 µg/L, for a world average of 0.62 µg/L, were reported [22]. In groundwater, As concentrations can vary widely, with reported concentrations from < 0.05 µg/L to 79.0 µg/L, based on 813 samples from European aquifers [23]. In acid mine drainage, As concentrations up to 12 g/L (pH < 1.8) and Fe up to 20 g/L, in Carnoulès abandoned mine site, France [24], or droplets of liquid on the arsenolite (As_2O_3) crust with extreme high As concentrations (80–130 g/L, pH close to 0), have been reported [25].

Se concentrations in rocks are generally low, and the average crustal abundance is 0.05 mg/kg [21]. Se can be enriched in phosphate rocks (up to 300 mg/kg), coal (1–20 mg/kg), and black shales (up to 600 mg/kg) [21,26]. In natural water, Se mainly occurs as selenite (Se(IV)) and selenate (Se(VI)) [21]. In European surface water, reported Se concentrations range from <0.01 µg/L to 15.0 µg/L, for a median value of 0.340 µg/L [27], while, in European groundwater, Se ranges from < 0.015 to 247 µg/L, for a median value of 0.50 µg/L [23]. Se concentrations of 1.5 to 33 mg/L were reported in mine water [28].

Mn is the third most abundant transition metal on earth. The average concentrations found in natural water are 0.004 to 2 µg/L [7]. Mn is found in seven oxidation states in nature (0, 2+, 3+, 4+, 5+, 6+, and 7+), but the most common forms in water are Mn^{2+}, Mn^{3+}, and Mn^{4+}. Mine drainage, whether acidic or neutral, often contains a high concentration of Mn, which can have an

undesirable impact on ecosystems. In mine water, Mn concentrations range from 0.02 to 352 mg/L, depending on the location and type of mineralogy [7]. Studies demonstrate that Mn can have effects on aquatic organisms, but they are little known, and the impact of Mn on aquatic toxicity remains to be clarified to better guide the selection of treatment methods [7].

Xanthates are the most used collectors in the flotation of sulfurous minerals, and they can be found in mine tailings in concentrations sufficient to have a toxic effect on aquatic fauna [29]. More than 11,000 metric tons of xanthates are consumed annually worldwide in the form of sodium isopropylxanthate (40%), sodium ethylxanthate (30%), sodium isobutylxanthate (15%), and potassium isopentylxanthate (10%) [30]. These molecules act as collectors by rendering the surfaces of the mineral particles hydrophobic and, thus, help them to cling to air bubbles during the flotation process [31]. Xanthates can be toxic to aquatic organisms such as *Daphnia magna* at concentrations of 0.1 to 1 mg/L [31,32]. The concentrations in mine water can vary depending on the type of ore processed. In general, 300 to 500 g of xanthates per tonne of ore is required to obtain satisfactory separation [33]. Residual concentrations ranging from 0.2 to 9 mg/L have been reported in process water [34]. Xanthates can also increase the bioaccumulation of metals by forming hydrophobic complexes with metals such as Zn, Cd, Pb, and Cu. These complexes facilitate the assimilation of metals by organisms through cell membranes [33]. The toxicity of xanthates is mainly linked to their degradation path, which causes the formation of carbon disulfide, which is volatile and slightly soluble in water. The xanthates have a half-life varying between 2 and 8 days, depending on the length of the alkyl chain, for a temperature of 15 °C. However, degradation in cold climates has not yet been studied [33].

Mine water salinity is an integrative parameter, which is characterized by the cumulative concentration of the most common ions (Na^+, K^+, Ca^{2+}, Mg^{2+}, Cl^-, HCO_3^-, CO_3^{2-}, and SO_4^{2-}) [35]. Salinity, electrical conductivity (EC), and total dissolved solids (TDS) are correlated. TDS may include an inorganic fraction (Na^+, K^+, Ca^{2+}, Mg^{2+}, Cl^-, HCO_3^-, CO_3^{2-}, and SO_4^{2-}) and an organic fraction (dissolved organic carbon—DOC) [36]. In mine water, TDS and salinity consist mainly of inorganic ions. The EC, which is defined by water's ability to allow the transport of electric charge, is an indication of the degree of water mineralization, providing information on dissolved elements (in ionic form) [37]. The high concentration of TDS results in an increase in the salinity of mine water. Salinity persists after the treatment of the mine water, which often even increases it. Moreover, salinity can have a detrimental impact on the aquatic toxicity depending on the species

present in water and their concentrations. For example, the concentration of Ca^{2+} or water hardness can reduce the toxicity of Cl^- and SO_4^{2-} [38]. Once dissolved solids that form salinity are transported into the environment, they are likely to cause toxicity [39].

Thiosalts are metastable sulfur oxyanions, naturally present in concentrations ranging from very low to a few hundred mg/L, such as in highly acidic crater-lake water [40]. Thiosalts are the common intermediate species of sulfur oxidation in metal sulfides (e.g. pyrite, pyrrhotite), in the presence of sulfur-oxidizing bacteria [41,42]. The main thiosalts species are thiosulfate ($S_2O_3^{2-}$), trithionate ($S_3O_6^{2-}$), and tetrathionate ($S_4O_6^{2-}$), with $S_2O_3^{2-}$ being the dominant thiosalt species [43,44]. In mine water, thiosalts are mainly generated (up to 60%) during the milling and flotation of sulfide ores, and at high pH (9.4–10.7) and alkalinity [45]. Other factors that contribute to the acceleration of thiosalt formation include the following: sulfides content of ores (5 times more thiosalts generated in ores with 80 to 90% sulfides vs. 25 to 30% sulfides); residence time during flotation (proportional); temperature (double amount at 40 °C vs. 25 °C); agitation rate in flotation (accelerated oxidation kinetics); and grinding operation (significant reduction of thiosalts generation (86%) during grinding at pH 10.7 in a solution deaerated with nitrogen gas) [46]. A recent study evaluated the effect of freeze/thaw cycles on thiosalts concentrations using column tests with tailings mainly dominated by pyrrhotite and serpentine [47]. Results showed that $S_2O_3^{2-}$ could top up to 10 g/L for columns subjected to freeze/thaw cycles relative to 7.2 g/L for those at an ambient temperature. Additionally, $S_4O_6^{2-}$ reached concentrations of 2.6 g/L in freeze/thaw columns and 2.2 g/L in the ambient columns. Another study showed the increased reactivity of minerals during freeze/thaw cycles [48], thus, supporting previous observations [47].

Nitrogen compounds, including NH_3-N, NO_2^-, and NO_3^-, are naturally present in the environment, usually at low concentrations. Human activity tends to add more nitrogen compounds in natural streams. In the presence of phosphorus, the eutrophication of stagnant or low-flow water sources can often occur, even in cold climates [49]. In the mining industry, the two major sources of nitrogen compounds are explosives and cyanides. Nitrogen-based blasting agents (e.g. ANFO—ammonium nitrate fuel oil) are used in mining to extract the commodities from their ore bodies. The explosives that are not completely degraded in the explosion can be dissolved in the water and then pumped at the surface during the dewatering process [50]. In addition to explosives, which are common to all types of mines, in the gold and silver extraction process, cyanides are also needed for their efficient recovery (> 90%, at 71 mg Au/t) [51].

Cyanidation, which was deemed a major advance at the end of the 19th century, remains the most efficient and least expensive separation process for gold and silver extraction, even though cyanides are toxic and nonselective, and generate effluents that are highly complex to treat [52,53]. The main issue related to these effluents is their mixed contamination with several groups of undesirable substances (e.g. cyanides and their derivatives, such as NH_3-N and SCN^-, metals), which requires multiple treatment steps for the final effluents to respect the physicochemical and toxicity discharge criteria. Two contaminants closely related to aquatic toxicity, even though not regulated by the Canadian law, are NH_3-N and SCN^- [52]. While the major source of NH_3-N (i.e. cyanides) is specific to gold mining, a nitrogen source associated with explosives (ANFO) is common to all mine effluents. The efficient treatment of NH_3-N and SCN^- requires their oxidation to bicarbonate and nitrate, in addition to sulfate (for SCN^-). The high flow rates of mine effluents, together with the very slow kinetics of NH_3-N oxidation, especially at low temperatures, supports the need for new, robust, adapted, and low-cost processes with low or no temperature and pH dependence [50], in addition to limited residual salinity creation.

Cyanides require treatment before wastewater is discharged into natural streams and can lead to the formation of NH_3-N [52]. If sulfur is present in the processed ores (as sulfide minerals and partially oxidized sulfur intermediates), toxic derivatives (SCN^-) can also be formed at high pH and alkalinity [51]. Even though SCN^- is less toxic than CN^-, its higher stability makes it more complex and difficult to treat [52].

The compilation of different contaminants, including their typical concentration in natural and mining environments, sources, and treatment methods is presented in Table 2.1. The schematic representation of the CECs evolution in the mining environment is presented in Figure 2.3.

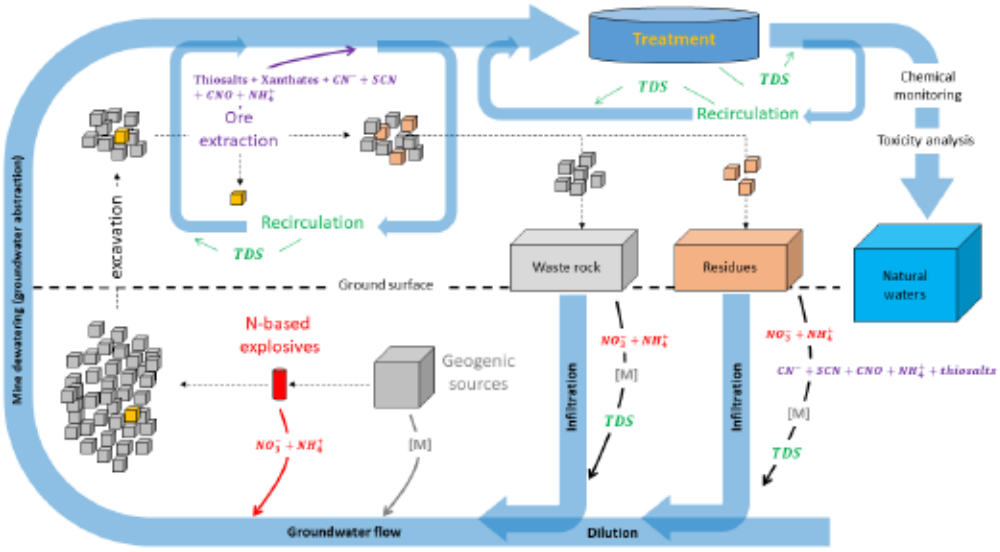

Figure 2.3 Schematic representation of the CECs evolution in the mining environment. [M]: metal or metalloid; TDS: Total Dissolved Solids.

Table 2.1 Compilation of different contaminants, including their typical concentration, source, and treatment methods.

Contaminant	Natural Environment Concentration (µg/L)	Mining Environment Concentration (mg/L)	Possible Source of Contamination	Applicable Processing Methods	References
Mn	0.004–2	0.02–352	Acid and neutral mine drainage	Co-precipitation Sorption Ion exchange Membrane filtration Oxidation and precipitation Biological	[7,54]
Se	< 0.01–15	1.5–33	Mine drainage	Membrane filtration Ion exchange Evaporation Co-precipitation Electrocoagulation Photoreduction Adsorption Biological	[27,28,55,56]
Xanthates	N/A	0.2–9	Flotation process	Advanced oxidation processes Natural degradation	[34,57]
Thiosalts	N/A	< 700	Acid mine drainage and mineral processing	Advanced oxidation processes Lime neutralization Biological Natural degradation Electrochemical oxidation Membrane filtration	[43,45,58]
Salinity (TDS)	< 1000	< 16,000	Mine drainage	Thermal processes Coagulation-flocculation Membrane filtration Aerobic treatment	[15,59,60]
SO_4^{2-}	3000–30,000	100–5000	Mine drainage	High density sludge treatment ChemSulphide process Biopaq – Bioteq Sulfatogenic bioreactor Passive treatment Sorption Dispersed alkaline substrates Membrane filtration	[15,61]
As	0.11–2.71	< 130,000	Mine drainage and hydrometallurgical processes	Co-precipitation Membrane filtration	[9,25]

Contaminant	Natural Environment Concentration (µg/L)	Mining Environment Concentration (mg/L)	Possible Source of Contamination	Applicable Processing Methods	References
NH_3-N	< 1000	46	Explosives and cyanide treatment	High pH stripping Membrane filtration Nitrification-denitrification Natural degradation Anammox Electro-oxidation Electrocoagulation Adsorption Advanced oxidation processes	[50,62–64]
NO_2^-	< 1600	4.4	Explosives Biological treatment	Denitrification Membrane filtration Advanced oxidation processes	[50,64,65]
NO_3^-	< 10,000	25–100	Explosives Cyanide treatment Biological treatment	Denitrification Membrane filtration	[50,65,66]
CNO^-	N/A	28	Cyanide treatment	Natural degradation Ozone Biological	[64,67]
SCN^-	N/A	168–680	Cyanide treatment	Ozone Electrochemical oxidation Biological treatment Ferrates Advanced oxidation processes	[52,64]

N/A: Not Applicable; TDS: Total Dissolved Solids.

2.3.2 Persistent Aquatic Toxicity

The aquatic toxicity of mine water is an important parameter to consider during mining operations. As an example of cold climate, the Canadian context is discussed. At the provincial level in Quebec, operating mining companies must comply with the guidelines set out in Directive 019 [68]. In Canada, at the federal level, they must comply with the Metal and Diamond Mining Effluent Regulations (MDMER) [14]. In addition to maximum authorized concentrations of several contaminants in mine water, the MDMER stipulates that the acute toxicity testing on rainbow trout (*Oncorhynchus mykiss*) and water fleas (*Daphnia magna*) must be performed once a month. Because *D. magna* is generally more sensitive to acutely lethal environments than rainbow trout, research often relies on *D. magna* as a representative indicator for acute toxicity. Even though *D.*

magna is used widely in regulatory assessment, *D. pulex* is commonly found in Canadian lakes, streams, and rivers—that is, in almost all eutrophic and permanent watercourses [69]. Comparative evaluation of the acute toxicity for *D. magna* and *D. pulex* of sulfate-rich neutral mine water from active gold mines showed a greater sensitivity of *D. pulex* compared to *D. magna*, before and after the treatment by electrocoagulation, in toxicity tests using standard reconstituted hard or natural dilution water [70].

Water from mining activities tends to be highly charged with contaminants such as metal(loid)s, salinity, nitrogen compounds, and, in some cases, xanthates. Aquatic toxicity of some CECs (e.g. xanthates, thiosalts) in mine water is incompletely assessed and under-documented, as opposed to others (e.g. As, Se) for which the literature is abundant. A compilation of lethal (LC50) and effective (EC50) concentrations of the different contaminants for *D. magna* is presented in Table 2.2.

Several studies have demonstrated the impact of these various contaminants on aquatic fauna. Although mining companies are governed by standards for aquatic toxicity, even when the acute toxicity criteria for regulated species (*D. magna* and rainbow trout) are met, the entire wildlife food chain can be affected by chronic effects [71,72]. Depending on the contaminant speciation and water mixes, bioavailability and synergistic or competitive effects in their fixation on binding sites on a biotic ligand might occur [71].

Table 2.2 Lethal (LC50) and effective (EC50) concentrations of CECs reported for *Daphnia magna*.

Contaminant	LC50 (mg/L)	EC50 (mg/L)	Test duration (h)	Hardness (mg $CaCO_3$/L)	Temperature (°C)	pH	References
Mn	N/A	9.3 10.27	48	45 240	21	6.5–8.5	[73]
Se	N/A	0.71	48	72	21	6.5–8.5	[73]
Na-ethyl xanthate Na-isopropyl xanthate Na-isobutyl xanthate K-amyl xanthate K-pentyl xanthate	N/A	0.35 3.7 3.6 3.67 3.0	N/A	N/A	15	N/A	[33]
$S_2O_3^{2-}$ $S_4O_6^{2-}$	N/A	300 750	N/A	N/A	N/A	N/A	[45]

Ca^{2+}	N/A	52 560	48	45 240	21	6.5–8.5	[73]
Cl^-	2600	N/A	24	N/A	N/A	N/A	[74]
Na^+	N/A	1640 423.13	48	45 240	21	6.5–8.5	[73]
K^+	N/A	93 160.45	48	45 240	21	6.5–8.5	[73]
SO_4^{2-}	7000	N/A	48	N/A	N/A	N/A	[74]
As	N/A	2.4 7.4 74	48	72 45 240	21	6.5–8.5	[73]
Cu	0.004 0.012	N/A N/A	48 48	44 ± 4 150 ± 10	N/A N/A	N/A	[75]
Zn	0.82 0.1 0.655 0.3 1.29	N/A N/A N/A N/A N/A	48 24 24 48 48	N/A 45 196 44 ± 4 150 ± 10	N/A N/A N/A N/A N/A	N/A	[69] [76] [76] [75] [75]
NH_3-N	1.980	N/A	24	N/A	20	7	[77]
NO_3^-	2047	N/A	48	156–172	N/A	N/A	[78]
N-NO_2^-	N/A	23	48	N/A	20	N/A	[79]
CNO^-	18	N/A	48	N/A	N/A	N/A	[80]
SCN^-	57.4 0.63–32	11.3 N/A	48 96	N/A 75	N/A 8–16	N/A	[52]

N/A: Not Applicable.

To reduce the dispersion of contaminants in the environment and prevent the deterioration of aquatic fauna, the federal government has introduced regulations. The MDMER requires that all metal mines produce an effluent that is nontoxic for rainbow trout and *D. magna*, in accordance with Environment and Climate Change Canada's methods of analysis. If there is mortality for more than 50% of the organisms in 100% of the whole effluent concentration during a period of 48 h for *D. magna* or 96 h for rainbow trout, the sample is considered as having failed the toxicity test [14]. If the lethality test is failed, the mining company must investigate the causes of toxicity.

The most common approach to determining the causes of toxicity is the Toxicity Reduction Evaluation (TRE) method. A step-by-step protocol was developed to help identify and confirm the causes and sources of toxicity and to eliminate them [58]. The first step of this protocol, known as Toxicity Identification Evaluation (TIE), is to identify the contaminant(s) responsible for the toxicity. Once the identification has been carried out, the next step is Source Identification (SI). The final step, Toxicity Treatability Evaluation (TTE), is to evaluate possible treatments or modify water management approaches to eliminate toxicity. During this process, it is important to have optimal communication and coordination between the various stakeholders, such as operators, toxicologists, chemists, and the engineering team, so that the TRE is a success [58].

Studies on the direct and indirect toxicity of thiosalts do not show a correlation between concentration and mortality of the species regulated by provincial and federal laws for acute and sublethal toxicity tests. In general, it is agreed that thiosalts are not directly acutely toxic at concentrations commonly found in mining effluents but rather indirectly due to the generation of latent acidity, which causes a decrease in pH [43]. Concentrations up to 4.1 g/L of $S_2O_3^{2-}$ did not entail acute toxicity to rainbow trout [45]. However, toxicity occurred when the pH of the water dropped to below 5. Direct toxicity test results consistently showed that sublethal toxicity, sublethal toxicity to *C. dubia* was high but total thiosalts concentrations were low, and vice versa [45]. The same report found that $S_2O_3^{2-}$ is more toxic to all organisms (96 h LC50 for *C. dubia* = 59 mg/L; 96 h LC50 for *L. minor* = 498 mg/L; 96 h LC50 for *P. promelas* = 665 mg/L) than $S_4O_6^{2-}$ (96 h LC50 for *C. dubia* = 562 mg/L; 96 h LC50 for *L. minor* > 901 mg/L; 96 h LC50 for *P. promelas* > 891 mg/L), which results in a non-additive toxicity of the polythionates, thus, explaining the absence of correlation between total thiosalts and toxicity [45]. The IC25 values for indirect toxicity are low (high toxicity) for all organisms when the pH drops below 5, except for *L. minor* (IC25 > 100% at pH 3.1; no toxicity) [45]. Confirmed toxicity at circumneutral pH indicates that other contaminants such as Cu and Se may add to thiosalts toxicity [45]. Further research on thiosalts toxicity is required considering the extreme concentrations recently reported [47] and the increased reactivity of minerals (and, therefore, leaching of other contaminants) during freeze/thaw cycles [48], especially for mines operating in cold climates. These studies should focus on the cooperative toxic effect with other metals and non-additive toxicity of polythionates.

Mixed contamination of mining effluents can entail complexities because of the interactions between the contaminants. The thermodynamic equilibrium between the mineral and chemical phases determines the speciation of the contaminants. These reactions are dependent on the temperature and the balance of the mineral, gas, and aqueous phases. Bacterial activities can also have a role as a biocatalyst for the various reactions that occur [81].

Several models of aquatic toxicity prediction that consider the mixture of different contaminants as well as the physiology of biota already exist. These models determine the speciation of inorganic elements according to the physicochemical parameters of water and then determine the LC50 values. For example, the Biotic Ligand Model (BLM) can be used for this type of prediction [82–84]. Mixed contamination can significantly contribute to aquatic toxicity. One of the most widely used bioassays in the world for acute aquatic toxicity is that of *D. magna*, one of the most sensitive

crustaceans [85]. Examples of *D. magna* toxicity in the mining industry are presented in Table 2.3. Mixed contamination can sometimes have pronounced effects on *D. magna*. The combination of various contaminants according to different physicochemical properties modifies speciation, bioavailability, and equilibrium concentrations in the final effluent. For example, the hardness of water, a parameter that has a significant effect on the toxicity of metals, reduces the bioavailability of these metals and, therefore, increases the toxic concentration [83]. At high concentrations, the hardness can have an opposite effect by increasing osmotic stress in biota [86]. Calcium can also have a protective effect on *D. magna* by reducing the absorption of metals such as Ni, Zn, Se, and Cd [83,86].

Another study has shown that water with very high hardness and alkalinity and containing high concentrations of Ca^{2+}, Mg^{2+}, CO_3^{2-}, and HCO_3^- can have a toxic effect on *D. magna*. A calcite shell ($CaCO_3$) forms over its entire surface and causes its disintegration following its death (LC50, 72 h). In this case, the head disintegrated first [87].

Table 2.3 Examples of D. magna toxicity in mine water.

Location	Exploitation Type	Parameters	*D. magna* Toxicity (Toxic units - TU)	References
South Korea	Metal plating plant final effluent	pH = 7.58 DOC = 131.1 mg/L Hardness = 46 mg $CaCO_3$/L Cu dissolved = 0.36 mg/L Cl^- = 12,841 mg/L Br^- = 2307 mg/L	6.5	[88]
	After treatment by ion exchange	Cl^- = 2840 mg/L	< 1	
South Korea	Final effluent of acid rock drainage treatment plant before pH correction	pH = 4.51 DO = 4.11 mg/L DOC = 3.87 mg/L Hardness = 2408 mg $CaCO_3$/L Al dissolved = 31.87 mg/L Cu dissolved = < DL Fe dissolved = 13.92 mg/L Zn dissolved = 1.39 mg/L	5.66	[88]
	After pH correction	pH = 7.0 Al dissolved = 0.093 mg/L Cu dissolved = 0.001 Fe dissolved = 0.011 mg/L Zn dissolved = 0.05 mg/L	< 1	
South Korea	Mixed effluents of electronics plant	pH = 8.55 DOC = 139.5 mg/L Hardness = 178.8 mg $CaCO_3$/L Cu total = 1.5624 mg/L Cu dissolved = 0.4793 mg/L	35.46	[88]

Location	Exploitation Type	Parameters	*D. magna* Toxicity (Toxic units - TU)	References
Canada (QC)	Final effluent, LaRonde mine, Agnico Eagle (04-03-1999 to 20-02-2001)	pH = 7.8–9.2 CN total = 0.005–0.36 mg/L CNO^- = 3.9–231 mg/L SCN^- = 73–293 mg/L NH_3-N = 20–88 mg/L SO_4^{2-} = 1350–2370 mg/L DOC = 35–93.6 mg/L Ca = 470–670 mg/L Cu = 0.02–0.14 mg/L Zn = < 0.01–0.26 mg/L	1–50.5	[89]
Canada (QC)	Final effluent, LaRonde mine, as reported by SGS Lakefield (06-05-2001)	pH = 8.05 TDS = 3320 mg/L CN total = 0.05 mg/L CNO^- = 21 mg/L SCN^- = 57 mg/L NH_3-N = 32.6 mg/L NO_2-N = 2.78 mg/L NO_3-N = 22 mg/L SO_4^{2-} = 2200 mg/L DOC = 12.4 mg/L Ca = 713 mg/L Cu = 0.016 mg/L Cu dissolved = 0.011 mg/L Na = 177 mg/L Zn = 0.02 mg/L Zn dissolved = < 0.01 mg/L Conductivity = 2710 µmhos/cm Hardness = 1820 mg $CaCO_3$/L DO = 9.4 mg/L	1.68	[89]
South Korea (Daeduck, Damyang county)	Mine drainage	pH = 6.1 Hardness = 16 mg $CaCO_3$/L Zn = 0.156 mg/L Pb = 0.0402 mg/L Cu = < DL Cd = 0.0013 mg/L	1.6	[75]
South Korea (Myungbong, Boseong county)	Mine drainage	pH = 7.8 Hardness = 50 mg $CaCO_3$/L Zn = 4.797 mg/L Pb = 0.0015 mg/L Cu = 0.0296 mg/L Cd = 0.0176 mg/L	22.9	[75]

DL: Detection Limit; DOC: Dissolved Organic Carbon; DO: Dissolved Oxygen; TDS: Total Dissolved Solids; TU: Toxicity units

One way to predict the aquatic toxicity of mixed contamination is to sum the toxic units (TU). The TU is equal to the concentration of a contaminant in the water divided by the LC50. If the sum of the TUs of all the contaminants in the mixture is greater than 1, the water is considered toxic to the organism in reference. The validity of this principle was confirmed with real effluents, but the LC50 were corrected in relation to water hardness [75]. Considering the reduction in toxicity in response to an increase in hardness, formulas can be used to correct the LC50. Although this method predicts aquatic toxicity with a confidence rate of up to 89% in some cases, a high iron

concentration can be an inhibiting factor in the estimation of toxicity because of amorphous iron precipitates [90]. A high DOC concentration can also have an important role in the complexation of metals and decreases the confidence rate of the prediction of aquatic toxicity by this method [88].

2.4 Treatment of CECs in Mine Water

Treatment strategies usually begin by identifying the problem, followed by setting objectives, and considering potential solutions based on constraints related to Best Available Technology Economically Achievable (BATEA), specific regulatory criteria, environmental impacts (residual contamination and aquatic toxicity), social acceptability, and license to operate [91,92]. The review of available literature showed that at least three main priorities can be identified in responsible management of mine water in cold climates: (1) development of sustainable treatment processes with limited energy consumption; (2) control of the residual salinity, after treatment; and (3) safe handling of produced sludge, after the recovery of potential economical elements or the immobilization of undesired ones. Contrary to temperate climates, the characteristics of cold climates contribute to additional challenges and opportunities in mine water treatment. The technologies presented in this paper can be used in cold climates with good treatment performance as the cold temperature has less impact on their treatability mechanisms compared to conventional treatments.

2.4.1 Advanced Oxidation Processes (AOPs)

Some AOPs fit into these requirements as they are efficient at low temperatures and allow for the complete oxidation of several contaminants in water using environmentally friendly oxidants, based on the hydroxyl radical, such as peroxone (H_2O_2+O_3) [93], Fenton-like (H_2O_2 and Fe^{3+} catalyst) [94,95], ferrates (Fe(VI)) [96], and O_3 microbubbles [63,64,97] or persulfate-based AOPs [98]. The peroxone was found more effective in the degradation of naphthenic acids and toxicity reduction than ozonation (at high doses), a costly treatment for oil sands process-affected water [99]. However, peroxone proved inefficient or inhibitory for NH_3-N treatment in a synthetic effluent [64].

In a recent study, the use of H_2O_2 to remove thiosalts from a synthetic and real mine effluent at 8 °C and 22 °C showed that a long reaction time was required for optimal efficiency [100]. The

important role of temperature on the removal of thiosalts was confirmed. In fact, results showed that low temperatures enhance the stability of polythionates, but also seem to partially oxidize $S_2O_3^{2-}$ in the presence of H_2O_2 as oxidizing agent. At higher temperatures, 96% thiosalts removal from a real effluent was reached, but the oxidation of intermediate S species was incomplete and reaction time was 7 days.

The Fenton process consists of H_2O_2 activation with basically an iron catalyst to generate a hydroxyl radical, a powerful and nonselective, environmentally friendly oxidant. The Fenton-like process was found highly efficient (> 99% of 1 g/L SCN^-) and a potential economical option for SCN^- partial oxidation (at pH 2.5–3) into cyanides to be returned to the leaching of gold and silver from their ores [94]. Consistently, at 21 °C, Fenton-like gave 84% and 22% of SCN^- and NH_3-N removal (at initial concentrations of 1 g/L and 40 mg/L, respectively), whereas at 4 °C the efficiency of SCN^- degradation decreased to 73% [95]. This AOP has major advantages, as the iron catalyst is easily available; the process is environmentally friendly and entails low residual toxicity and operating costs [101].

Electrochemical AOPs have been gaining popularity for limiting As toxicity, through oxidation of As(III) to As(V), and its subsequent removal. Electrochemical treatment methods have the advantage of using electrons as a reagent, thus, reducing the amount of added chemicals and residual salinity [102]. Bio-electrochemical AOPs have also received growing interest for organic CECs treatment in municipal wastewater because of the reduced cost of electricity. In fact, electro-Fenton (EF) and bio-electro-Fenton (bio-EF) are the eco-friendliest and most cost-efficient processes for the treatment of recalcitrant contaminants compared to other electrochemical methods [102,103]. In bio-EF, electrons are generated through microbial activity at the anode, and H_2O_2 is *in situ* generated at the cathode. H_2O_2 is then available to react with an iron catalyst to form hydroxyl radicals, as in the conventional Fenton process. In a study on EF in a dual chamber microbial fuel cell, results showed that As(III) removal efficiency was of 94% at optimal oxidation current efficiency. However, the removal process was incomplete for As(V) [103], and the final concentration did not meet the criteria specified by federal law [14].

Most publications focus on EF/bio-EF efficiency for the degradation of organic contaminants. Very little information is available on their performance for oxidation and removal of micropollutants, despite a promising application to the mining industry. Therefore, forthcoming research should

focus on assessing EF and bio-EF performance on removal of oxidizable CECs in synthetic and especially real mine water, including As, NH_3-N, and thiosalts [104].

New research reported the satisfactory efficiency of ferrates for NH_3-N and SCN^- removal from highly contaminated mine effluents, but not simultaneously [105]. The wet Fe(VI) efficiency was evaluated on three synthetic and two real gold mine effluents contaminated by SCN^- and/or NH_3-N. Results showed that Fe(VI) oxidized more than 97% of SCN^-, while the NH_3-N increased up to 50%, after SCN^- oxidation in the presence of NH_3-N, within 1 h. A second step of NH_3-N treatment would, thus, be warranted. The main concerns, especially with wet Fe(VI) use, are the high pH and dissolved solids content of treated water (when high doses are required), that can adversely affect water quality downstream of discharge and its toxicity [96,106]. However, as the Fe(III) salt source for wet Fe(VI) production could be nitrates, chlorides, or sulfates, the residual contamination could vary: (1) from a four-time increase of residual nitrates with $Fe(NO_3)_3$, to (2) high residual chlorides with $FeCl_3$ and the oxidant used in the Fe(III) to Fe(VI) oxidation (sodium hypochlorite, NaClO), and (3) to no increase of residual sulfates with $Fe_2(SO_4)_3$ [106].

2.4.2 Ozone Microbubbles

The efficiency of several AOPs (O_3 microbubbles, UV, and H_2O_2) was also tested for NH_3-N removal from several synthetic (70 mg/L NH_3-N) and five actual mine effluents [64]. The tests started in batch mode, for optimizing the performance, followed by in continuous flow with one real effluent. Results showed that O_3 microbubbles gave the best efficiency. Indeed, more than 92.6% of the initial NH_3-N was treated, at pH 9, within 90 min. The use of Br^- as a catalyst increased treatment efficiency, whereas the combination of UV with O_3 was less efficient than O_3 alone under the conditions tested. Moreover, the presence of cyanides, cyanate, SCN^-, and metals adversely influenced NH_3-N removal efficiency, which ranged from 27.8 to 99.3%. Polishing final steps were required for the removal of the coloration that developed in some treated mine effluents. These results were consistent with previous findings on O_3 microbubbles that showed NH_3-N complete removal in a synthetic effluent (100 mg/L), at pH 9, in about 7.2 ks, whereas at pH 6 only 20 mg/L of NH_3-N were removed [63]. Moreover, they are consistent with reported findings on the oxidation of As(III) (50–200 µg/L) to As(V), at pH 7, within less than 25 min in a synthetic effluent [107]. The O_3 microbubbles process showed also satisfactory efficiency in thiosalts removal (99%) from a synthetic effluent [100]. The use of O_3 microbubbles for NH_3-N treatment in mine water has

distinctive advantages, including the fast kinetics of the process, complete oxidation of several contaminants in mixing effluents, and no residual salinity creation in the treated water. Recently, the ultrasounds combined with ozonation and $SrO\text{-}Al_2O_3$ as a catalyst showed to be promising for NH_3-N treatment [108]. With a combination of ultrasounds at a frequency of 25 kHz vs. 270 W ultrasonic power and ozone, the NH_3-N conversion and N_2 gas yield were 83.2% and 51.8%, respectively.

The mode of diffusion of O_3 in water is an important process, allowing mass transfer to the gas-liquid interface. Indeed, due to the low solubility of O_3 in water, the injection method can increase the process efficiency, for example, by using microbubbles [109]. The microbubbles have a diameter of 10 to 50 µm, and a very high gas-liquid interfacial contact surface, then a very low ascent rate. The phenomenon that makes the use of microbubbles attractive for water treatment is the reduction in their size until their implosion in the liquid phase, unlike the coarse bubbles that always rise to the surface [109]. Two major advantages characterize microbubbles. First, there is higher ozone solubilization with higher internal pressure, forcing greater mass exchange at the gas-liquid interface. Ozone then forms hydroxyl radicals depending on the physicochemical properties of water. Second, microbubbles implosion phenomenon also generates hydroxyl radicals [109].

The use of AOPs such as ozone, microbubbles, and sonochemical cavitation in the mining sector is very rare. In recent years, these processes were also adapted for use with mine effluents, with satisfactory results. Comparative performance of ozone, microbubbles, peroxone (mixture of ozone and hydrogen peroxide), and sonochemical cavitation for mine water at different scales are presented in Table 2.4.

Table 2.4 Treatment performance of ozone, microbubbles, and ultrasound on mine water or compounds used in flotation processes.

Treatment type	Industry	Influent	Effluent	Scale	References
Ozone microbubbles followed by coagulation-flocculation	Gold mine underground water	pH = 6.7 Eh = 445 mV T = 22°C NH_3-N = 22 mg/L NO_2^- = 5.5 mg/L NO_3^- = 185 mg/L Cu = 0.154 mg/L Fe = 1.06 mg/L Mn = 3.41 mg/L Zn = 9.6 mg/L	pH = 8.7 Eh = 410 mV T = 22°C NH_3-N = 0.78 mg/L NO_2^- = < DL NO_3^- = 180 mg/L Cu = 0.01 mg/L Fe = 0.16 mg/L Mn = 0.58 mg/L Zn = 0.2 mg/L	Pilot in continuous flow	[64]
Ozone microbubbles	Gold mine process water after cyanide destruction	pH = 9 Eh = 295 mV T = 22°C NH_3-N = 34.6 mg/L	pH = 9.3 Eh = 382 mV T = 36°C NH_3-N = 5.4 mg/L	Pilot in batch mode	[64]

		NO_2^- = 6 mg/L NO_3^- = 48 mg/L CNO^- = 15.8 mg/L SCN^- = 135 mg/L Total CN = 0.04 mg/L Cu = 1.52 mg/L Fe = 0.5 mg/L Mn = 0.3 mg/L Zn = 0.29 mg/L	NO_2^- = < DL NO_3^- = 151 mg/L CNO^- = 12.5 mg/L SCN^- = < DL Total CN = 0.05 mg/L Cu = < DL Fe = < DL Mn = 0.06 mg/L Zn = < DL		
$O_3 + H_2O_2$	Gold mine process water	CN = 172.5 mg/L pH = 11 Turbidity = 56 NTU TOC = 137.8 mg/L DOC = 496 mg/L	CN = 0.08 mg/L pH = 7 Turbidity = 68 NTU TOC = 24.5 mg/L DOC = 118.5 mg/L	Laboratory	[110]
Air micro-nanobubbles	Mine effluent	T = 21°C pH = 11.99 Turbidity = 170 NTU Conductivity = 4.06 mS/cm DO = < 0.1 mg/L TS = 4740 mg/L TSS = 251 mg/L Pb = 51.3 mg/L Zn = 17.601 mg/L	T = 22°C pH = 11.72 Turbidity = 15.93 NTU Conductivity = 2.39 mS/cm DO = 8.53 mg/L TS = 4120 mg/L TSS = 31 mg/L Pb = 0.98 mg/L Zn = 0.128 mg/L	Laboratory	[111]
O_3 + ultrasound	Synthetic water with surfactant	pH = 8.3 Sodium lauryl sulfate = 100 mg/L	pH = 8.3 Sodium lauryl sulfate = 16.7 mg/L	Laboratory	[112]
Ozone microbubbles	Synthetic water with As(III)	pH = 7 As(III) = 200 µg/L As(V) = < DL	pH = 7 As(III) = < DL As(V) = 200 µg/L	Laboratory	[107]

DL: Detection Limit; TOC: Total Organic Carbon; DOC: Dissolved Organic Carbon; DO: Dissolved Oxygen; TS: Total Solids; TSS: Total Suspended Solids

More research is required to systematically evaluate the performance of O_3 microbubbles process with mine effluents at low temperatures and scaling-up conditions. Further techno-economic studies are also necessary prior to full-scale mine site applications.

2.4.3 Membrane Filtration

Membrane-based processes include microfiltration (MF), ultrafiltration (UF), nanofiltration (NF), reverse osmosis (RO), vacuum membrane distillation (VMD), and forward osmosis (FO). A combination of these filtration techniques is often required to ensure good performance and minimize clogging membranes. Membrane filtration processes treat a variety of contaminants, from suspended solids and colloidal material to more persistent and soluble ones as salinity [59,113].

The nature of contamination determines the type of membrane to be used for effective treatment. Direct membrane filtration, or FO, achieves good contaminant removal rates by reducing release

rates and treatment costs [114]. In addition, VMD increases the recovery rate of permeate when used alone or in combination with conventional filtration types [115–117].

The operating principle of all these processes lies in the pressure gradient exerted on the membranes, commonly called transmembrane pressure (TMP) [113,118]. The feed can pass directly through the membrane but is usually recirculated at high speed on the face of the membrane (crossflow configuration) [118]. This type of operation is recommended because the turbulence generated causes erosion and makes it possible to reduce the accumulation of solids on the membrane [118]. Membrane processes, their separation mechanisms, the materials used to manufacture the membranes, and their typical treatment objectives are presented in Table 2.5.

Table 2.5 Technical characteristics of the different types of membrane process [113,118,119].

Process	Separation Mechanism	Material / Type	Typical Transmembrane Pressure (kPa)	Recuperation (%)	Typical Objective	Regime
Microfiltration (MF)	Separation by sieving through macropores (> 50 nm)	Polymer and inorganic / Porous	10–100	90–99+	Removal of suspended matter and coarse colloidal particles including microorganisms	Pore size Exclusion at the membrane interface
Ultrafiltration (UF)	Separation by sieving through mesopores (2–50 nm)	Polymer and inorganic / Porous	50–300	85–95+	Removal of coarse molecules in solution and colloidal particles in suspension including bacteria and macromolecules such as proteins	
Nanofiltration (NF)	Separation by a combination of charge rejection, diffusion of solubility, and sieving through micropores (< 2 nm)	Polymer and inorganic / Dense	200–1500	75–90+	Removal of multivalent ions and specific charged or polar molecules	Solution Diffusion through the membrane
Reverse osmosis (RO)	Separation based on the difference in solubility and diffusion rate of water and solutes	Polymer / Dense	500–8000	60–90	Removal of low molecular weight compounds such as inorganic ions	

The membranes can be made of polymers based on materials such as polyacrylonitrile (PAN) and polyvinylidene difluoride (PVDF). The cost of these membranes is relatively low, and their life cycle is around seven years [113]. Inorganic membranes are more resistant to chemical and thermal stress than polymer-based membranes. They are divided into four categories according to their

constituents: ceramic membranes, glass membranes, metal membranes, and zeolite membranes. These are mainly used for MF and UF [113].

Two types of membrane configuration dominate the saline water treatment market with NF and RO: spiral wound and fine hollow fiber commonly known as spiral wound (SW) and hollow fine fiber (HFF). SW elements are constructed with flat membrane sheets and materials that provide mechanical strength. The materials of these membranes can be cellulosic or non-cellulosic. Cellulose acetate membranes are composed of two layers of different shapes of the same polymer; they are called asymmetric [120]. Composite membranes are two layers of different polymers separated from a porous substrate, which is often polysulphone [120]. The materials used in the manufacture of HFF can be polyaramide or a mixture of cellulose acetate. The membranes usually have an external diameter between 100 and 300 µm and an internal diameter between 50 and 150 µm. Saline water is inserted into the media from the outside of the HFF; by applying pressure, the permeate passes through and is then collected [120].

Clogging of membranes is the main problem related to their use. Indeed, the presence of elements that clog the pores of the membranes reduces their effectiveness and even their lifespan. For example, the presence of organic species and suspended matter can have a high clogging effect [121]. Calcium sulphate and calcium carbonate can also clog the membranes [122]. In the treatment of mine water, the main clogging elements were identified as Sb, Al, Si, and Na [119]. Pretreatment steps can help overcome this problem [119]. Higher water temperatures can reduce the clogging effect as the membrane pores expand. By expanding, contaminants can more easily pass through the membrane and, thus, reduce the quality of the permeate [123].

The membrane cleaning methods depend on whether the clogging is reversible or not. If the clogging is reversible, the use of physical methods such as a pulsed reverse flow with purge, vibrations with ultrasound, air, or CO_2 jets, or reverse permeation at regular intervals can clear the pores. This type of cleaning tends to have less impact on the degradation of the membranes and their lifespan than a chemical cleaning [118,122]. Chemical cleaning uses a chemical to react with the sealing layer to facilitate physical cleaning. The most used membrane cleaners are alkaline or acidic cleaners, surfactants, and saline solutions; their choice is related to the type of sealant [122]. The use of ozone also reduces clogging by organic matter [121,124]. The parameters to consider during chemical cleaning are product concentration, pH, temperature, pressure, flow rate, and cleaning time [122].

Reported efficiency of membranes for mine water at different scales is presented in Table 2.6. For example, the MF and UF can be used to remove total suspended solids (TSS) and colloidal chemical oxygen demand as pretreatment prior to RO, which can remove salinity [59]. The management of RO reject is an important consideration because of its high TDS concentrations. A treatment of this brine can reduce the reject and can be used as byproduct with resale value [125]. The VMD technology that uses hydrophobic membrane and heat can be a good way to concentrate the RO brine and recover metals. The removal of 99.9% of TDS with VMD technology was reported. The mine water tested contained 2332 mg/L of TDS, 14.4 mg/L of Ca, 2.72 mg/L of Mg, 1.92 mg/L of Fe, and 3.38 mg/L of Al. Removal efficiency was higher than 95% for all these elements after 90 min [126]. The EC of the treated water could be lower than 50 µS/cm [116]. The VMD can be used as a treatment for low concentration of heavy metals and to achieve better performance than conventional treatment [127].

As newer technology, FO has promising potential for the desalination of high salinity mine water streams (60–240 g/L TDS). FO utilizes a thin film composite membrane and draws solutions to recover the metals. The principle of FO is based on the osmotic difference between a dilute feed solution (FS, i.e., contaminated water to be treated) and a more concentrated draw solution (DS, with higher osmotic potential than FS), which is diluted during the salinity treatment. The next step of the process—the separation of clean water from the diluted draw solution—is energy consuming and, as a result, the limiting and decisive step in FO overall feasibility. A crystallization process can then be used to recover the metals and salts after the separation [128]. The major advantages of FO for water recovery are the non-selectivity (high rejection of a wide variety of contaminants), less fouling of membrane, the simpler osmotic cells, and the overall lower cost (no external hydraulic pressure is applied for the water to cross the membrane relative to pressure-driven processes such as in RO) [128]. FO was found efficient in metal removal from acid mine drainage close or over 98% using NaCl-DS [129]. However, with mine water, the reverse flux of ions from the DS into the FS, especially when they can react with feed solutes, could prove one of the major downsides of this process, in addition to the precipitation of some secondary minerals on the separating membrane when inorganic salts are used in DS (e.g. NH_4HCO_3) [129]. More recently, the FO membranes showed to be promising in power production by the pressure-retarded osmosis (PRO) process [130]. Notably, osmotic energy generation (using PRO) was proposed more than 70 years ago, but it was limited by the lack of effective membranes. As recently as 2009, a prototype

plant was constructed in Norway, but the project was terminated in 2014 due to technology immaturity [131].

Table 2.6 Treatment efficiency using membrane filtration with mine water at different scales.

Treatment	Industry	Influent	Effluent (permeate)	Scale	References
MF + NF + RO	Gold mine pressure oxidation process water effluent	pH = 1.46 EC = 28.07 mS/cm TSS = 571 mg/L TDS = 23 973 mg/L Cu = 156.8 mg/L Co = 40.01 mg/L Ni = 256.8 mg/L Ca = 487.6 mg/L Mg = 2561 mg/L Fe = 436.5 mg/L Mn = 105.5 mg/L Al = 348 mg/L As = 34.6 mg/L Total Acidity = 10.28 g $CaCO_3$/L Free Acidity = 6.89 g $CaCO_3$/L SO_4^{2-} = 21 480 mg/L	pH = 2.56 EC = 0.79 mS/cm TSS = 0 mg/L TDS = 192 mg/L Cu = 0.22 mg/L Co = 0.09 mg/L Ni = 1.24 mg/L Ca = 1.61 mg/L Mg = 11.96 mg/L Fe = 0.56 mg/L Mn = 0.13 mg/L Al = 0.63 mg/L As = 2 mg/L - - SO_4^{2-} = 270 mg/L	Pilot	[132]
NF	Acid mine drainage from abandoned mercury mine	Fe = 515 mg/L Al = 23 mg/L As = 6 mg/L Hg = 2.3 µg/L SO_4^{2-} = 2300 mg/L pH = 2.47 ORP = 592 mV DO = 3.3 mg/L	Fe = 7.5 mg/L Al = 1.7 mg/L As = 0.08 mg/L - SO_4^{2-} = 245 mg/L - - -	Pilot	[133]
MF + NF	Acidic bioleaching mining waste process	Co = 4.04 mg/L Ge = 1.33 mg/L Mo = 14.30 mg/L Re = 3.26 mg/L Cu = 54 mg/L Fe = 1980 mg/L Zn = 720 mg/L	Co = 0.04 mg/L Ge = 1.18 mg/L Mo = 0.39 mg/L Re = 2.96 mg/L Cu = 0.74 mg/L Fe = 15 mg/L Zn = 7.8 mg/L	Laboratory	[134]
RO	Final effluent of antimony mine in operation	Turbidity = 39.4 NTU TDS = 7910 mg/L Sb = 49.8 mg/L As = 0.038 mg/L Ni = 0.052 mg/L Zn = 0.052 mg/L Fe = 0.05 mg/L Cd = 0.0001 mg/L Cr = 0.001 mg/L Cu = 0.002 mg/L Pb = 0.001 mg/L	Turbidity = 1 NTU TDS = 218 mg/L Sb = 0.1 mg/L As = 0.001 mg/L Ni = 0.001 mg/L Zn = 0.001 mg/L Fe = 0.05 mg/L Cd = 0.0001 mg/L Cr = 0.001 mg/L Cu = 0.001 mg/L Pb = 0.001 mg/L	Industrial	[119]

ORP: Oxidation-reduction potential

The use of membrane filtration processes is common in the field of desalination for drinking water but less in the mining field. In recent years, research has made it possible to apply this technology to mine water and obtain satisfactory results [135].

2.5 Challenges and Opportunities in Mine Water Treatment in Cold Climates

Additional challenges in cold climates mean that system designs for effective performance of mine water treatment must also properly integrate specific characteristics, including the following: (1) high sensitivity and limited resilience of ecosystems, (2) unusual faster dissolution of carbonates at low temperatures, (3) the increased salinity in response to the very narrow window of water flow (2–3 months/year), (4) high costs of freshwater, (5) enhanced detrimental impacts of salinity on treatment efficiency and solubility of minerals from the gangue, (6) accelerated clogging of membranes, (7) limited knowledge about the suitable management of residual materials in a continuously evolving context (e.g. the increasing thickness of the active layer of permafrost), and (8) slower kinetics of most of the chemical processes. The impact from the mixing of different effluents on aquatic toxicity is also a big challenge. All these challenges must be targeted for future research to ensure sustainable mining in the North.

Nevertheless, few opportunities are arising in relation to mine water treatment in cold climates. Energy production from salinity, such as osmotic power generation by PRO using seawater brine as the DS and wastewater retentate as the feed, showed potential as a renewable energy source [130,136]. The use of promising membrane filtration technologies can help to recover the metals and reduce the salinity. The membrane fouling with high calcium and sulfate concentrations (i.e., gypsum scaling) is still an issue with some membrane materials. Further studies are necessary to solve these issues [137]. Finally, some AOPs could limit the creation of residual salinity and allow the simultaneous treatment of mixed contaminants.

2.6 Conclusion

This paper provided an overview of the issues related to the removal of CECs from mine water, with focus on As, Mn, Se, salinity, thiosalts, xanthates, and N-based compounds (cyanides, NH_3-N, and SCN^-) in cold climates. The background concentrations of As, Mn, Se, salinity, thiosalts, xanthates, and N-based compounds in natural water were first discussed. The performance of AOPs

and membrane filtration processes in CECs treatment in mine water were then emphasized. Further studies are required for optimal treatment performance under cold climate conditions and high flow rates, including field-scale tests. In the contemporary context, the mining industry's ability to strengthen its capacity to adapt to increasingly stringent criteria related to CECs is central to sustainable development. Such adaptation will necessarily depend on close collaboration between mining operators and scientists conducting applied research, and the challenges will most likely increase in complexity in the very near future, which highlights the critical need for intensifying research on the treatment of CECs.

Author Contributions: Conceptualization, Original Draft Preparation, Writing – Review and Editing, S.R., C.M.N., E.R., L.C., and P.C.; Supervision, C.M.N., E.R., and P.C. All authors have read and agreed to the published version of the manuscript.

Acknowledgments: This research was supported by the Natural Sciences and Engineering Research Council of Canada (NSERC), Canada Research Chairs Program, and RIME UQAT-Polytechnique industrial partners, including Agnico Eagle, Canadian Malartic Mine, Iamgold, Raglan Mine–Glencore, Newmont, and Rio Tinto. The authors would like thank Mario Drapeau, senior metallurgist at Agnico Eagle Mines Ltd., for his valuable contribution on the review of historical and new CECs in mine water. The authors also wish to thank Alexandre Royer-Lavallée and Jennifer Dubuc for their contributions during the preparation of the manuscript.

Conflicts of Interest: The authors declare no conflict of interest. The funders had no role in the design of the study; in the collection, analyses, or interpretation of data; in the writing of the manuscript, or in the decision to publish the results.

2.7 References

1. Laurence, D. Establishing a sustainable mining operation: An overview. *J. Clean. Prod.* **2011**, *19*, 278–284.
2. Krausmann, F.; Gingrich, S.; Eisenmenger, N.; Erb, K.H.; Haberl, H.; Fischer-Kowalski, M. Growth in global materials use, GDP and population during the 20th century. *Ecol. Econ.* **2009**, *68*, 2696–2705.

3. Roach, B.; Walker, T.N. Aquatic monitoring programs conducted during environmental impact assessments in Canada: Preliminary assessment before and after weakened environmental regulation. *Environ. Monit. Assess.* **2017**, *189*, 109.
4. Wolkersdorfer, C.; Nordstrom, D.K.; Beckie, R.D.; Cicerone, D.S.; Elliot, T.; Edraki, M.; Valente, T.; Alves França, S.C.; Kumar, P.; Oyarzún Lucero, R.A.; Gil, A.L. Guidance for the integrated use of hydrological, geochemical, and isotopic tools in mining operations. *Mine Water Environ.* **2020**, *39*, 204–228.
5. Sauvé, S.; Desrosiers, M. A review of what is an emerging contaminant. *Chem. Cent. J.* **2014**, *8*, 15.
6. Fairbairn, D.J.; Arnold, W.A.; Barber, B.L.; Kaufenberg, E.F.; Koskinen, W.C.; Novak, P.J.; Rice, P.J.; Swackhamer, D.L. Contaminants of emerging concern: Mass balance and comparison of wastewater effluent and upstream sources in a mixed-use watershed. *Environ. Sci. Technol.* **2016**, *50*, 36–45.
7. Neculita, C.M.; Rosa, E. A review of the implications and challenges of manganese removal from mine drainage. *Chemosphere* **2019**, *214*, 491–510.
8. Neculita, C.M.; Coudert, L.; Rosa, E.; Mulligan, C. Future prospects for treating contaminants of emerging concern in water and soils/sediments. In *Advanced Nano-Bio Technologies for Water and Soil Treatment*; Filip, J., Cajthaml, T., Najmanová, P., Černík, M., Zbořil, R., Eds.; Springer International Publishing: Berlin/Heidelberg, Germany, 2020; pp. 589–605.
9. Coudert, L.; Bondu, R.; Rakotonimaro, T.V.; Rosa, E.; Guittonny, M.; Neculita, C.M. Treatment of As-rich mine effluents and produced residues stability: Current knowledge and research priorities for gold mining. *J. Hazard. Mater.* **2020**, *386*, 121920.
10. OECD. *New and Emerging Water Pollutants arising from Agriculture*; OECD: Paris, France, 2012; 49.
11. Fisheries and Environment Canada. *Metal Mining Liquid Effluent Regulations and Guidelines*; Report EPS 1-WP-77-1; Fisheries and Environment Canada: Ottawa, ON, Canada, 1977.
12. D019. *Directive 019 Sur l'Industrie Minière*; Government of Quebec: Quebec, QU, Canada, 2005.
13. CCME Summary Table. Available online: http://st-ts.ccme.ca/en/index.html (accessed on 18 October 2020).

14. Minister of Justice. *MMER (Metal and Diamond Mining Effluent Regulations);* SOR/2002–222; Government of Canada: Ottawa, ON, Canada, 2019.
15. Ben Ali, H.E.; Neculita, C.M.; Molson, J.W.; Maqsoud, A.; Zagury, G.J. Performance of passive systems for mine drainage treatment at low temperature and high salinity: A review. *Miner. Eng.* **2019**, *134*, 325–344.
16. Royer-Lavallée, A.; Neculita, C.M.; Coudert, L. Removal and potential recovery of rare earth elements from mine water. *J. Ind. Eng. Chem.* **2020**, *89*, 47–57.
17. Costis, S.; Mueller, K.; Coudert, L.; Neculita, C.M.; Reynier, N.; Blais, J.F. Recovery potential of rare earth elements from mining and industrial residues: A review and case studies. *J. Geochem. Explor.* **2021**, *221*, 106699.
18. Olías, M.; Cánovas, C.; Basallote, M.D.; Lozano, A. Geochemical behaviour of rare earth elements (REE) along a river reach receiving inputs of acid mine drainage. *Chem. Geol.* **2018**, *493*, 468–477.
19. Smedley, P.L.; Kinniburgh, D.G. A review of the source, behaviour and distribution of arsenic in natural waters. *Appl. Geochem.* **2002**, *17*, 517–568.
20. Mandal, B.K.; Suzuki, T. Arsenic round the world: A review. *Talanta* **2002**, *58*, 201–235.
21. Plant, J.A.; Kinniburgh, D.G.; Smedley, P.L.; Fordyce, F.M.; Klinck, B.A. Arsenic and selenium. In: *Treatise on Geochemistry*; Holland, H.D., Turekian, K.K., Eds.; Pergamon: Oxford, UK, 2003, pp. 17–66.
22. Gaillardet, J.; Viers, J.; Duprée, B. Trace elements in river waters. In: *Treatise on Geochemistry*; Drever, J.I., Ed.; Pergamon: Oxford, UK, 2003, pp. 225–272.
23. Shand, P.; Edmunds, W.M. The baseline inorganic chemistry of European groundwaters. In: *Natural Groundwater Quality*; Edmunds, M.W., Shand, P., Eds.; Blackwell Publishing: Hoboken, NJ, USA, 2008, pp. 22–58.
24. Giloteaux, L.; Duran, R.; Casiot, C.; Bruneel, O.; Elbaz-Poulichet, F.; Goni-Urriza, M. Three-year survey of sulfate-reducing bacteria community structure in Carnoulès acid mine drainage (France), highly contaminated by arsenic. *FEMS Microbiol. Ecol.* **2013**, *83*, 724–737.
25. Majzlan, J.; Plášil, J.; Škoda, R.; Gescher, J.; Kögler, F.; Rusznyak, A.; Küsel, K.; Neu, T.R.; Mangold, S.; Rothe, J. Arsenic-rich acid mine water with extreme arsenic concentration: Mineralogy, geochemistry, microbiology and environmental implications. *Environ. Sci. Technol.* **2014**, *48*, 13685–13693.

26. Fordyce, F. Selenium geochemistry and health. *Ambio* **2007**, *36*, 94–97.
27. Flem, B.; Reimann, C.; Fabian, K.; Birke, M.; Filzmoser, P.; Banks, D. Graphical statistics to explore the natural and anthropogenic processes influencing the inorganic quality of drinking water, ground water and surface water. *Appl. Geochem.* **2018**, *88*, 133–148.
28. Ji, Y.; Li, L.; Wang, Y. Selenium removal by activated alumina in batch and continuous-flow reactors. *Water Environ. Res.* **2020**, *92*, 51–59.
29. Sun, Z.; Forsling, W. The degradation kinetics of ethyl-xanthate as a function of pH in aqueous solution. *Miner. Eng.* **1997**, *10*, 389–400.
30. Xu, Y.; Lay, J.; Korte, F. Fate and effects of xanthates in laboratory freshwater systems. *Bull. Environ. Contam. Toxicol.* **1988**, *41*, 683–689.
31. Alto, K.; Broderius, S.; Smith, L. *Toxicity of Xanthates to Freshwater Fish and Invertebrates*; Minnesota Environmental Quality Council: Minneapolis, MN, USA, 1978.
32. Rostad, C.E.; Schmitt, C.J.; Schumacher, J.G.; Leiker, T.J. An exploratory investigation of polar organic compounds in waters from a lead–zinc mine and mill complex. *Water Air Soil Pollut.* **2011**, *217*, 431–443.
33. Bach, L.; Nørregaard, R.D.; Hansen, V.; Gustavson, K. *Review on Environmental Risk Assessment of Mining Chemicals Used for Mineral*; Scientific Report; DCE–Danish Centre for Environment and Energy: Roskilde, Denmark, 2016.
34. Muzinda, I.; Schreithofer, N. Water quality effects on flotation: Impacts and control of residual xanthates. *Miner. Eng.* **2018**, *125*, 34–41.
35. Van Dam, R.A.; Harford, A.J.; Lunn, S.A.; Gagnon, M.M. Identifying the cause of toxicity of a saline mine water. *PLoS ONE* **2014**, *9*, e106857.
36. Pinto, P.X.; Al-Abed, S.R.; Balz, D.A.; Butler, B.A.; Landy, R.B.; Smith, S.J. Bench-scale and pilot-scale treatment technologies for the removal of total dissolved solids from coal mine water: A review. *Mine Water Environ.* **2016**, *35*, 94–112.
37. Cohen, B.; Lazarovitch, N.; Gilron, J. Upgrading groundwater for irrigation using monovalent selective electrodialysis. *Desalination* **2018**, *431*, 126–139.
38. Simmons, J.A. Toxicity of major cations and anions (Na^+, K^+, Ca^{2+}, Cl^-, and SO_4^{2-}) to a macrophyte and an alga. *Environ. Toxicol. Chem.* **2012**, *31*, 1370–1374.
39. Bowell, R.J. A review of sulfate removal options for mine waters. SRK Consulting, Cardiff, Wales, United Kingdom, **2004**; 24 p.

40. Takano, B.; Ohsawa, S.; Glover, R.B. Surveillance of Ruapehu Crater Lake, New Zealand by aqueous polythionates. *J. Volcanol. Geoth. Res.* **1994**, *60*, 29–57.
41. Johnson, D.B. Chemical and microbiological characteristics of mineral spoils and drainage waters at abandoned coal and metal mines. *Water Air Soil Pollut.* **2003**, *3*, 47–66.
42. Range, B.M.K.; Hawboldt, K.A. Adsorption of thiosulphate, trithionate, tetrathionate using biomass ash/char. *J. Environ. Chem. Eng.* **2018**, *6*, 5401–5408.
43. Miranda-Trevino, J.C.; Pappoe, M.; Hawboldt, K.; Bottaro, C. The importance of thiosalts speciation: Review of analytical methods, kinetics, and treatment. *Crit. Rev. Environ. Sci. Technol.* **2013**, *43*, 2013–2070.
44. Range, B.M.K.; Hawboldt, K.A. Removal of thiosalt/sulfate from mining effluents by adsorption and ion exchange. *Min. Proc. Ext. Met. Rev.* **2019**, *40*, 79–86.
45. Schwartz, M.; Vigneault, B.; McGeer, J. *Evaluating the Potential for Thiosalts to Contribute to Toxicity in Mine Effluents*; ; Report presented for Thiosalts Consortium, Project: 602591, Report CANMET-MMSL 06-053 (CR); CANMET Mining and Mineral Sciences Laboratories (CANMET-MMSL): Ottawa, ON, Canada, 2006; 101.
46. Wasserlauf, M.; Dutrizac, J.E. *The Chemistry, Generation and Treatment of Thiosalts in Milling Effluents: A Non-Critical Summary of CANMET Investigations 1976–1982*; Report: 82-4E; CANMET: Ottawa, ON, Canada, 1982; 104.
47. Schudel, G.; Plante, B.; Bussière, B.; McBeth, J.; Dufour, G. The effect of arctic conditions on the geochemical behaviour of sulphidic tailings. In: Proceedings of the Tailings and Mine Waste, Vancouver, BC, Canada, 17–20 November 2019.
48. Jouini, M.; Neculita, C.M.; Genty, T.; Benzaazoua, M. Freezing/thawing effects on geochemical behaviour of residues from acid mine drainage passive treatment systems. *J. Water Process. Eng.* **2020**, *33*, 101807.
49. Chlot, S. Nitrogen and Phosphorus Interactions and Transformations in Cold-Climate Mine Water Recipients. Ph.D. Thesis, Lulea University of Technology, Lulea, Sweden, 2013.
50. Jermakka, J.; Wendling, L.; Sohlberg, E.; Heinonen, H.; Vikman, M. Potential technologies for the removal and recovery of nitrogen compounds from mine and quarry waters in subarctic conditions. *Crit. Rev. Environ. Sci. Technol.* **2015**, *45*, 703–748.
51. Mudder, T.I.; Botz, M.M.; Smith, A. *Chemistry and Treatment of Cyanidation Wastes*, 2nd ed.; Mining Journal Books Limited: London, UK, 2001.

52. Gould, D.W.; King, M.; Mohapatra, B.R.; Cameron, R.A.; Kapoor, A.; Koren, D.W. A critical review on destruction of thiocyanate in mining effluents. *Miner. Eng.* **2012**, *34*, 38–47.
53. Johnson, C.A. The fate of cyanide in leach wastes at gold mines: An environmental perspective. *Appl. Geochem.* **2015**, *57*, 194–205.
54. Marsidi, N.; Hasan, H.A.; Abdullah, S.R.S. A review of biological aerated filters for iron and manganese ions removal in water treatment. *J. Water Process. Eng.* **2018**, *23*, 1–12.
55. Staicu, L.C.; Morin-Crini, N.; Crini, G. Desulfurization: Critical step towards enhanced selenium removal from industrial effluents. *Chemosphere* **2017**, *172*, 111–119.
56. Golder Associates Inc. *Literature Review of Treatment Technologies to Remove Selenium from Mining Influenced Water*; Teck Coal Limited: Calgary, AB, Canada, 2009.
57. Molina, G.C.; Cayo, C.H.; Rodrigues, M.A.S.; Bernardes, A.M. Sodium isopropyl xanthate degradation by advanced oxidation processes. *Miner. Eng.* **2013**, *45*, 88–93.
58. Novak, L.; Holtze, K.; Wagner, R.; Feasby, G.; Liu, L. *Guidance Document for Conducting Toxicity Reduction Evaluation (TRE) Investigations of Canadian Metal Mining Effluents*; Prepared ESG International Inc. and SGC Lakefield for TIME Network; ON, Canada, 2002, 85.
59. Lefebvre, O.; Moletta, R. Treatment of organic pollution in industrial saline wastewater: A literature review. *Water Res.* **2006**, *40*, 3671–3682.
60. Nordstrom, D.K.; Blowes, D.W.; Ptacek, C.J. Hydrogeochemistry and microbiology of mine drainage: An update. *Appl. Geochem.* **2015**, *57*, 3–16.
61. Katz, M. The Canadian sulphur problem. *Sulphur and Its Inorganic Derivatives in the Canadian Environment*; National Research Council of Canada, NRC Associate Committee on Scientific Criteria for Environmental Quality: Ottawa, ON, Canada, 1977; pp. 21–67.
62. CCME (Canadian Water Quality Guidelines for the Protection of Aquatic Life). *Ammonia*; Canadian Council of Ministers of the Environment: Winnipeg, MB, Canada, 2010; pp. 1–8.
63. Khuntia, S.; Majumder, S.K.; Ghosh, P. Removal of ammonia from water by ozone microbubbles. *Ind. Eng. Chem. Res.* **2013**, *52*, 318–326.
64. Ryskie, S.; Gonzalez-Merchan, C.; Genty, T.; Neculita, C.M. Efficiency of ozone microbubbles for ammonia removal from mine effluents. *Miner. Eng.* **2019**, *145*, 106071.
65. Health Canada. Guidelines for Canadian drinking water quality: Guideline technical document-Nitrate and nitrite. In *Water and Air Quality Bureau*; Healthy Environments and Consumer Safety: Ottawa, ON, Canada, 2013; 128.

66. Baker, J.A.; Gilron, G.; Chalmers, B.A.; Elphick, J.R. Evaluation of the effect of water type on the toxicity of nitrate to aquatic organisms. *Chemosphere* **2017**, *168*, 435–440.
67. di Biase, A.; Wei, V.; Kowalski, M.S.; Bratty, M.; Hildebrand, M.; Jabari, P.; Oleszkiewicz, J.A. Ammonia, thiocyanate, and cyanate removal in an aerobic up-flow submerged attached growth reactor treating gold mine wastewater. *Chemosphere* **2020**, *243*, 125395.
68. D019. *Directive 019 Sur l'Industrie Minière*; Government of Quebec: Quebec, QC, Canada; 2012.
69. Shaw, J.R.; Dempsey, T.D.; Chen, C.Y.; Hamilton, J.W.; Folt, C.L. Comparative toxicity of cadmium, zinc, and mixtures of cadmium and zinc to daphnids. *Environ. Toxicol. Chem.* **2006**, *25*, 182–189.
70. Foudhaili, T.; Jaidi, R.; Neculita, C.M.; Rosa, E.; Triffault-Bouchet, G.; Veilleux, E.; Coudert, L.; Lefebvre, O. Effect of the electrocoagulation process on the toxicity of gold mine effluents: A comparative assessment of *Daphnia magna* and *Daphnia pulex*. *Sci. Total Environ.* **2020**, *708*, 134739.
71. Couture, P.; Pyle, G. Field studies on metal accumulation and effects in fish. In *Homeostasis and Toxicology of Essential Metals*; Wood, C.M., Farrell, A.P., Brauner, C.J., Eds.; Fish Physiology, Vol. 31, Part 1. Academic Press: Cambridge, MA, USA, 2012; pp. 417–473.
72. Simate, G.S.; Ndlovu, S. Acid mine drainage: Challenges and opportunities. *J. Environ. Chem. Eng.* **2014**, *2*, 1785–1803.
73. Okamoto, A.; Yamamuro, M.; Tatarazako, N. Acute toxicity of 50 metals to *Daphnia magna*. *J. Appl. Toxicol.* **2015**, *35*, 824–830.
74. Vinot, H.; Larpent, J. Water pollution by uranium ore treatment works. *Hydrobiologia* **1984**, *112*, 125–129.
75. Yim, J.H.; Kim, K.W.; Kim, S.D. Effect of hardness on acute toxicity of metal mixtures using *Daphnia magna*: Prediction of acid mine drainage toxicity. *J. Hazard. Mater.* **2006**, *138*, 16–21.
76. USEPA (US Environmental Protection Agency). *Ambient Water Quality Criteria for Zinc;* Office of Research and Development: Washington, DC, USA, 1980.
77. USEPA. *Aquatic Life Ambient Water Quality Criteria for Ammonia–Freshwater*; Office of Water: Washington, DC, USA, 2013.

78. CCME. *Nitrate Ion*; Canadian Council of Ministers of the Environment: Winnipeg, MB, Canada, 2012; pp. 1–17.
79. Eytcheson, S.A.; LeBlanc, G.A. Hemoglobin levels modulate nitrite toxicity to *Daphnia magna*. *Sci. Rep.* **2018**, *8*, 1–8.
80. Dauchy, J.W.; Waller, T.W.; Piwoni, M.D. Acute toxicity of cyanate to *Daphnia magna*. *Bull. Environ. Contam. Toxicol.* **1980**, *25*, 194–196.
81. Banks, D.; Younger, P.L.; Arnesen, R.T.; Iversen, E.R.; Banks, S.B. Mine-water chemistry: The good, the bad and the ugly. *Environ. Geol.* **1997**, *32*, 157–174.
82. Paquin, P.R.; Gorsuch, J.W.; Apte, S.; Batley, G.E.; Bowles, K.C.; Campbell, P.G.; Galvez, F. The biotic ligand model: A historical overview. *Comp. Biochem. Phys. C.* **2002**, *133*, 3–35.
83. Deleebeeck, N.M.; De Schamphelaere, K.A.; Heijerick, D.G.; Bossuyt, B.T.; Janssen, C.R. The acute toxicity of nickel to *Daphnia magna*: Predictive capacity of bioavailability models in artificial and natural waters. *Ecotoxicol. Environ. Safe.* **2008**, *70*, 67–78.
84. Kozlova, T.; Wood, C.M.; McGeer, J.C. The effect of water chemistry on the acute toxicity of nickel to the cladoceran *Daphnia pulex* and the development of a biotic ligand model. *Aquat. Toxicol.* **2009**, *91*, 221–228.
85. Persoone, G.; Baudo, R.; Cotman, M.; Blaise, C.; Thompson, K.C.; Moreira-Santos, M.; Han, T. Review on the acute *Daphnia magna* toxicity test—Evaluation of the sensitivity and the precision of assays performed with organisms from laboratory cultures or hatched from dormant eggs. *Knowl. Manag. Aquat. Ec.* **2009**, *393*, 1–29.
86. Sivula, L.; Vehniainen, E.R.; Karjalainen, A.K.; Kukkonen, J.V.K. Toxicity of biomining effluents to *Daphnia magna*: Acute toxicity and transcriptomic biomarkers. *Chemosphere* **2018**, *210*, 304–311.
87. Bogart, S.J.; Woodman, S.; Steinkey, D.; Meays, C.; Pyle, G.G. Rapid changes in water hardness and alkalinity: Calcite formation is lethal to *Daphnia magna*. *Sci. Total Environ.* **2016**, *559*, 182–191.
88. Kang, S.W.; Seo, J.; Han, J.; Lee, J.S.; Jung, J. A comparative study of toxicity identification using *Daphnia magna* and *Tigriopus japonicus*: Implications of establishing effluent discharge limits in Korea. *Mar. Pollut. Bull.* **2011**, *63*, 370-375.

89. Wagner, R.; Liu, L.; Grondin, L. *Toxicity Treatment Evaluation of Mine Final Effluent—Using Chemical and Physical Treatment Methods*; Technical paper; SGS Minerals Services: Canada, 2002.
90. Lee, S.H.; Kim, I.; Kim, K.W.; Lee, B.T. Ecological assessment of coal mine and metal mine drainage in South Korea using *Daphnia magna* bioassay. *Springer Plus* **2015**, *4*, 518.
91. Kratochvil, D. Sustainable water treatment technologies for the treatment of acid mine drainage. In Proceedings of the International Conference on Acid Rock Drainage (ICARD), Ottawa, ON, Canada, 20–26 May 2012.
92. MEND (Mine Environment Neutral Drainage). *Study to Identify BATEA for the Management and Control of Effluent Quality from Mines*; MEND Report 3.50.1 prepared by HATCH for MEND Program; MEND: Canada, 2014; 614.
93. Miklos, D.B.; Remy, C.; Jekel, M.; Linden, K.G.; Drewes, J.E.; Hubner, U. Evaluation of advanced oxidation processes for water and wastewater treatment: A critical review. *Water Res.* **2018**, *139*, 118–131.
94. Budaev, S.L.; Batoeva, A.A.; Tsybikova, B.A. Effect of Fenton-like reactions on the degradation of thiocyanate in water treatment. *J. Environ. Chem. Eng.* **2014**, *2*, 1907–1911.
95. Gonzalez-Merchan, C.; Genty, T.; Bussière, B.; Potvin, R.; Paquin, M.; Benhammadi, M.; Neculita, C.M. Influence of contaminant to hydrogen peroxide to catalyzer molar ratio in the advanced oxidation of thiocyanates and ammonia using Fenton-based processes. *J. Environ. Chem. Eng.* **2016**, *4*, 4129–4136.
96. Yates, B.J.; Zboril, R.; Sharma, V.K. Engineering aspects of ferrate in water and wastewater treatment: A review. *J. Environ. Sci. Heal.* **2014**, *49*, 1603–1614.
97. Khuntia, S.; Majumder, S.M.; Ghosh, P. Microbubbles-aided water and wastewater purification: A review. *Rev. Chem. Eng.* **2012**, *28*, 191–221.
98. Lee, J.; von Gunten, U.; Kim, J.H. Persulfate-based advanced oxidation: Critical assessment of opportunities and roadblocks. *Environ. Sci. Technol.* **2020**, *54*, 3064–3081.
99. Meshref, M.N.A.; Klamerth, N.; Islam, M.S.; McPhedran, K.N.; Gamal El-Din, M. Understanding the similarities and differences between ozone and peroxone in the degradation of naftenic acids: Comparative performance for potential treatment. *Chemosphere* **2017**, *180*, 149–159.

100. Gervais, M.; Dubuc, J.; Paquin, M.; Gonzalez-Merchan, C.; Genty, T.; Neculita, C.M. Comparative efficiency of three advanced oxidation processes for thiosalts treatment in mine impacted water. *Miner. Eng.* **2020**, *152*, 106349.

101. Bokare, A.D.; Choi, W. Review of iron-free Fenton-like systems for activating H2O2 in advanced oxidation processes. *J. Hazard. Mater.* **2014**, *275*, 121–135.

102. Babu, D.S.; Nidheesh, P.V. A review on electrochemical treatment of arsenic from aqueous medium. *Chem. Eng. Commun.* **2021**, *208*, 389–410.

103. Wang, X.Q.; Liu, C.P.; Yuan, Y.; Li, F.B. Arsenite oxidation and removal driven by a bio-electro-Fenton process under neutral pH conditions. *J. Hazard. Mater.* **2014**, *275*, 200–209.

104. Olvera-Vargas, H.; Dubuc, J.; Wang, Z.; Coudert, L.; Neculita, C.M.; Lefebvre, O. Electro-Fenton beyond the degradation of organics: Treatment of thiosalts in contaminated mine water. *Environ. Sci. Technol.* **2021**, *55*, 2564–2574.

105. Gonzalez-Merchan, C.; Genty, T.; Bussière, B.; Potvin, R.; Paquin, M.; Benhammadi, M.; Neculita, C.M. Ferrates performance in thiocyanates and ammonia degradation in gold mine effluents. *Miner. Eng.* **2016**, *95*, 124–130.

106. Gonzalez-Merchan, C.; Genty, T.; Paquin, M.; Gervais, M.; Bussière, B.; Potvin, R.; Neculita, C.M. Influence of ferric iron source on ferrate's performance and residual contamination during the treatment of gold mine effluents. *Miner. Eng.* **2018**, *127*, 61–66.

107. Khuntia, S.; Majumder, S.K.; Ghosh, P. Oxidation of As(III) to As(V) using ozone microbubbles. *Chemosphere* **2014**, *97*, 120–124.

108. Liu, C.; Chen, Y.; He, C.; Yin, R.; Liu, J.; Qiu, T. Ultrasound-enhanced catalytic ozonation oxidation of ammonia in aqueous solution. *Int. J. Env. Res. Public Health* **2019**, *16*, 2139.

109. Xiong, X.; Wang, B.; Zhu, W.; Tian, K.; Zhang, H. A review on ultrasonic catalytic microbubbles ozonation processes: Properties, hydroxyl radicals generation pathway and potential in application. *Catalysts* **2019**, *9*, 10.

110. Esparza, J.M.; Cueva, N.C.; Pauker, C.S.; Jentzsch, P.V.; Bisesti, F.M. Combined treatment using ozone for cyanide removal from wastewater: A comparison. *Revista Internacional de Contaminacion Ambiental* **2019**, *35*, 459–467.

111. Vicente C.; Valverde Flores J. Removal of lead and zinc from mining effluents by applying air micro-nanobubbles. *J. Nanotechnol.* **2017**, *1*, 73–78.

112. Ghanem, H.; Kravchenko, V.; Makedon, V.; Shulha, O.; Oleksandr, S. Preliminary water purification from surfactants and organic compounds through ozone oxidation, intensified by electrical impulses. In Proceedings of the 2019 IEEE 6th International Conference on Energy Smart Systems (ESS), Kyiv, Ukraine, 17–19 April 2019.
113. Elshorbagy, W.; Chowdhury, R. *Water Treatment*; InTech: London, UK, 2013; 392.
114. Hube, S.; Eskafi, M.; Hrafnkelsdóttir, K.F.; Bjarnadóttir, B.; Bjarnadóttir, M.Á.; Axelsdóttir, S.; Wu, B. Direct membrane filtration for wastewater treatment and resource recovery: A review. *Sci. Total Environ.* **2020**, *710*, 136375.
115. Drioli, E.; Ali, A.; Macedonio, F. Membrane distillation: Recent developments and perspectives. *Desalination* **2015**, *356*, 56–84.
116. Andrés-Mañas, J.A.; Ruiz-Aguirre, A.; Acién, F.G.; Zaragoza, G. Assessment of a pilot system for seawater desalination based on vacuum multi-effect membrane distillation with enhanced heat recovery. *Desalination* **2018**, *443*, 110–121.
117. Karanasiou, A.; Kostoglou, M.; Karabelas, A. An experimental and theoretical study on separations by vacuum membrane distillation employing hollow-fiber modules. *Water* **2018**, *10*, 947.
118. Speed, D. Environmental aspects of planarization processes. In *Advances in Chemical Mechanical Planarization (CMP)*; Elsevier: Amsterdam, The Netherlands, 2016; pp. 229–269.
119. Samaei, S.M.; Gato-Trinidad, S.; Altaee, A. Performance evaluation of reverse osmosis process in the post-treatment of mining wastewaters: Case study of Costerfield mining operations, Victoria, Australia. *J. Water Process. Eng.* **2020**, *34*, 101116.
120. Watson, I.C.; Morin, O.; Henthorne, L. *Desalting Handbook for Planners*; Desalination Research and Development Program Report; Bureau of Reclamation: Washington, DC, USA, 2003; 72.
121. Van Geluwe, S.; Braeken, L.; Van der Bruggen, B. Ozone oxidation for the alleviation of membrane fouling by natural organic matter: A review. *Water Res.* **2011**, *45*, 3551–3570.
122. Aguiar, A.; Andrade, L.; Grossi, L.; Pires, W.; Amaral, M. Acid mine drainage treatment by nanofiltration: A study of membrane fouling, chemical cleaning, and membrane ageing. *Sep. Purif. Technol.* **2018**, *192*, 185–195.

123. Andrade, L.; Aguiar, A.; Pires, W.; Miranda, G.; Amaral, M. Integrated ultrafiltration-nanofiltration membrane processes applied to the treatment of gold mining effluent: Influence of feed pH and temperature. *Sep. Sci. Technol.* **2017**, *52*, 756–766.

124. Fujioka, T.; Hoang, A.T.; Okuda, T.; Takeuchi, H.; Tanaka, H.; Nghiem, L.D. Water reclamation using a ceramic nanofiltration membrane and surface flushing with ozonated water. *Int. J. Env. Res. Public Health* **2018**, *15*, 799.

125. Loganathan, K.; Chelme-Ayala, P.; Gamal El-Din, M. Pilot-scale study on the treatment of basal aquifer water using ultrafiltration, reverse osmosis and evaporation/crystallization to achieve zero-liquid discharge. *J. Environ. Manage.* **2016**, *165*, 213–223.

126. Sivakumar, M.; Ramezanianpour, M.; O'Halloran, G. Mine water treatment using a vacuum membrane distillation system. *APCBEE Proc*. **2013**, *5*, 157–162.

127. Ji, Z. Treatment of heavy-metal wastewater by vacuum membrane distillation: Effect of wastewater properties. *IOP Conf. Ser.: Earth Environ. Sci.* **2018**, *108*, 042019.

128. Kolliopoulos, G.; Shum, E.; Papangelakis, V.G. Forward osmosis and freeze crystallization as low energy water recovery processes for a water-sustainable industry. *Environ. Process.* **2018**, *5*, 59–75.

129. Vital, B.; Bartacek, J.; Ortega-Bravo, J.; Jeison, D. Treatment of acid mine drainage by forward osmosis: Heavy metal rejection and reverse flux of draw solution constituents. *Chem. Eng. J.* **2018**, *332*, 85–91.

130. Altaee, A.; AlZainati, N. Novel thermal desalination brine reject-sewage effluent salinity gradient for power generation and dilution of brine reject. *Energies* **2020**, *13*, 1756.

131. Chung, T.S.; Luo, L.; Wan, C.F.; Cui, Y.; Amy, G. What is next for forward osmosis (FO) and pressure retarded osmosis (PRO)? *Sep. Purif. Technol.* **2015**, *156*, 856–860.

132. Ricci, B.C.; Ferreira, C.D.; Aguiar, A.O.; Amaral, M.C. Integration of nanofiltration and reverse osmosis for metal separation and sulfuric acid recovery from gold mining effluent. *Sep. Purif. Technol.* **2015**, *154*, 11–21.

133. Sierra, C.; Saiz, J.R.Á.; Gallego, J.L.R. Nanofiltration of acid mine drainage in an abandoned mercury mining area. *Water Air Soil Pollut.* **2013**, *224*, 1734.

134. Meschke, K.; Hofmann, R.; Haseneder, R.; Repke, J.-U. Membrane treatment of leached mining waste–A potential process chain for the separation of the strategic elements germanium and rhenium. *Chem. Eng. J.* **2020**, *380*, 122476.

135. Naidu, G.; Ryu, S.; Thiruvenkatachari, R.; Choi, Y.; Jeong, S.; Vigneswaran, S. A critical review on remediation, reuse, and resource recovery from acid mine drainage. *Environ. Pollut.* **2019**, 247, 1110–1124.

136. Skilhagen, S.E.; Dugstad, J.E.; Aaberg, R.J. Osmotic power—Power production based on the osmotic pressure difference between waters with varying salt gradients. *Desalination* **2008**, *220*, 476–482.

137. Shaffer, D.L.; Werber, J.R.; Jaramillo, H.; Lin, S.; Elimelech, M. Forward osmosis: Where are we now? *Desalination* **2015**, *356*, 271–284.

CHAPITRE 3 REVUE DE LITTÉRATURE COMPLÉMENTAIRE

La revue de littérature complémentaire couvre des notions qui n'ont pas été couvertes dans la revue de littérature publiée dans l'article présenté au chapitre 2 et qui sont utilisés dans les travaux réalisés durant le projet. Afin d'avoir une vue d'ensemble sur les thématiques de la modélisation numérique pour la prédiction de la qualité des eaux ainsi que sur le traçage isotopique, ces informations seront brièvement présentées dans cette section. La section sur la modélisation numérique portera majoritairement sur l'utilisation de PHREEQC sur les mélanges d'eaux minières et celle sur le traçage isotopique portera principalement sur l'utilisation des isotopes de la molécule d'eau en domaine minier.

3.1 Modélisation numérique pour la prédiction de la qualité des eaux

La modélisation numérique est un excellent outil pouvant aider à résoudre des problèmes complexes, prédire la qualité des eaux, designer et optimiser les procédés permettant ainsi de prendre des décisions mieux éclairées pour les opérations (Wolkersdorfer et al., 2020). Avec les années, ces outils se sont développés et affinés afin de les rendre plus pratique et précis. Leur utilisation est devenue un incontournable pour l'industrie et la recherche. Cependant, selon l'outil de modélisation choisi, qui dépend de l'application visée, certaines limites y sont associées. L'utilisateur doit bien connaître ces limites afin d'obtenir des résultats qui se rapprochent de la réalité. Certains outils laissent plus de liberté que d'autres quant au choix des paramètres de base, ce qui complique parfois les interprétations. Par exemple, le choix de la base de données thermodynamique est un des paramètres ayant le plus d'impact sur les résultats obtenus (Lu et al., 2022). Une bonne connaissance de la minéralogie est aussi importante car les outils, bien qu'ils puissent être précis, ne peuvent pas déterminer avec exactitude la présence d'une espèce minérale en particulier.

3.1.1 Différents outils de modélisation

Plusieurs outils de modélisation sont disponibles et selon les besoins ou l'application, certains peuvent être plus adaptés que d'autres. Le tableau 3.1 compile les différents outils de modélisation, incluant leurs utilités, leurs limites et des exemples d'applications.

Tableau 3.1 Compilation des différents outils de modélisation

Outil	Utilités	Avantages	Limites	Références
PHREEQC	Calcul de la spéciation et des indices de saturation Calcul des réactions batch et transport en une dimension Modélisation inverse	Programme open source gratuit facilement accessible Utilisation simple	Besoin de bien connaître les fonctions afin d'obtenir des résultats cohérents	Parkhurst & Appelo, 2013
OLI	Prédiction de la concentration électrolytique de mélanges Simulation de procédés multiphasiques permettant de hautes températures et pressions Calcul des indices de saturation et corrosion	Calcul et ajustement automatique des paramètres afin de réduire les erreurs Choix automatique de la base de données thermodynamique en fonction des paramètres d'entrée Support technique facile d'accès	Coût élevé de la licence	OLI Systems, 2021
Geochemist Workbench	Production de diagramme de phases Calcul des réactions de transport en une et deux dimensions Calcul des équilibres et cinétiques de réaction avec prise en compte de la catalyse microbienne ainsi que des colloïdes	Calcul et ajustement automatique des paramètres afin de réduire les erreurs Plusieurs types de licences disponibles selon les besoins Support technique facile d'accès	Coût élevé de la licence	Bethke et al., 2022

Outil	Utilités	Avantages	Limites	Références
FactSage	Calcul thermodynamique afin de produire des diagrammes de phases Calcul des équilibres de mélange Calcul des réactions permettant de modéliser les procédés	Précision des calculs dans des systèmes multiphasiques à haute température et pression Modules disponibles pour multiple applications	Coût élevé de la licence Surtout utilisé en métallurgie	Bale et al., 2002
Mine3P	Calcul des réactions de transport en une, deux et trois dimensions Surtout utilisé pour modéliser les réactions dans les stériles et résidus miniers Calcul de transport en milieu poreux saturés et non saturés dans des systèmes à l'équilibre partiel	Interface visuelle et interactive Programme très flexible Prise en compte des processus biogéochimiques et de sorption	Moins adapté pour modéliser les mélanges d'effluents	Yi et al., 2021
Hytec	Calcul des réactions de transport en milieu poreux Calcul de la spéciation des espèces minérales et de leur concentration Calcul des équilibres thermodynamiques	Prise en compte des phénomènes de sorption Prise en compte des colloïdes organiques et inorganiques Faible coût	Réactions biogéochimiques demandant une grande ressource en processeur	Van Der Lee et al., 2003
GoldSim	Calcul des bilans hydriques et processus géochimiques	Programme très flexible	Coût élevé de la licence	GoldSim Technology Group, 2021

Outil	Utilités	Avantages	Limites	Références
	Utilisé dans le domaine minier pour aider à gérer l'eau et le dépôt des résidus minier Calcul statistique et prédictif	Interface visuelle facile d'utilisation Intégration de PHREEQC pour aider aux calculs géochimiques Ouvert à d'autres utilisations que la gestion des eaux		
NETPATH	Calcul des réactions géochimiques et bilan de masse Calcul de la spéciation des espèces minérales et de leur concentration	Permet de modéliser des mélanges Prise en compte des compositions isotopiques	Langage de programmation Fortran peu utilisé aujourd'hui Nombre limite d'effluents pouvant être mélangés Base de données thermodynamique limitée	Plummer et al., 1994

3.1.2 Description de PHREEQC

PHREEQC est un programme distribué par United States Geological Survey (USGS) gratuitement pouvant simuler des réactions chimiques et processus de transport pour des eaux naturelles ou contaminées, en se basant sur les équilibres de réaction multiphasique solide-liquide-gaz (Parkhurst et Appelo, 2013). Maintenant rendu à la version 3, PHREEQC a évolué depuis les années, initialement programmé en Fortran dans la version PHREEQE, il est maintenant programmé en C++, un langage de programmation plus utilisé aujourd'hui. Son nom vient de l'acronyme pH-Redox-EQuilibrium car ses fonctions primaires étaient basées sur les équilibres des réactions d'oxydo-réduction (Parkhurst et Appelo, 2013). Plusieurs fonctions sont disponibles dans la dernière version du programme, en passant par le mélange d'eaux, la dissolution et précipitation de phases afin d'atteindre l'équilibre, l'effet de changement de température, l'échange ionique, la complexation de surface, le transport advectif, la modélisation inverse, les réactions cinétiques contrôlées, les équilibres de solution solide, la diffusion et dispersion de transport en une dimension la modélisation inverse pour les bilans isotopiques (Parkhurst et Appelo, 2013).

Le programme est utilisé dans plusieurs domaines, que ce soit pour les eaux souterraines, naturelles de surface ou même pour les eaux usées (Eary et al., 2003; Frau et Ardau, 2003; Balistrieri et al., 2007). Les fonctions de mélanges peuvent être, par exemple, utilisées en domaine minier afin de prédire la qualité des eaux pour différents scénarios de mélanges mais aussi pour évaluer la qualité sur plusieurs années (AECOM, 2019; Maest et al., 2020). Les fonctions de mélanges peuvent être aussi combinées à la fonction d'équilibre lorsque la minéralogie est connue et ainsi prédire la quantité de solide qui précipite ou se dissout (AECOM, 2019). La fonction de modélisation inverse est aussi pratique afin de déterminer les phases minérales ayant précipité ou dissout et ainsi réconcilier les paramètres d'un chemin d'écoulement, tout en prenant en considération le transfert et les interactions de la phase gazeuse (Lecompte et al., 2005; Sharif et al., 2008).

3.1.3 Importance de la minéralogie

Il est d'un grand intérêt de connaître la minéralogie présente dans les échantillons analysés lors de travaux de modélisation. Cela apporte une confidence supplémentaire lors de la validation des résultats. En effet, PHREEQC ne permet pas de prédire les phases minérales présentes avec précision, mais il permet de déterminer quelles sont les phases potentiellement présentes. La

combinaison des analyses minéralogiques ainsi que des connaissances de base selon les paramètres physico-chimiques de l'eau tel le pH, aide à la précision des modèles (Nordstrom, 2020). Par exemple, les phases minérales identifiées peuvent être mise dans le modèle avec la fonction « equilibrium ». La connaissance de l'évolution des phases présentes selon le pH permet aussi de déterminer les constantes d'équilibre K_s dans la base de données thermodynamique (Nordstrom, 2020).

3.1.4 Choix de la base de données thermodynamique

Le choix de la base de données thermodynamique est très important afin de bien représenter les conditions de la modélisation. Des résultats différents peuvent être obtenus selon la base de données, il est donc nécessaire d'identifier celle sélectionnée. D'abord, il doit y avoir de la constance dans la base de données thermodynamique choisie, c'est-à-dire, les fonctions thermodynamiques doivent être compatibles pour toutes les substances du modèle (Lu et al., 2022). Un mélange de données thermodynamiques d'une base à une autre qui ne sont pas compatibles peut amener des problèmes de convergence vers la bonne solution. Selon le problème étudié, il est important de considérer la plage de température et pression représentée par la base de données thermodynamique, elles peuvent varier substantiellement. Les valeurs log K_s doivent être adéquates pour les températures et pressions données. La plupart utilisent un log K_s à 25°C et 1 bar mais d'autres, utilisées surtout pour les hautes pressions et températures, utilisent des facteurs de corrections (Lu et al., 2022). La force ionique et les coefficients d'activité sont aussi des facteurs importants. Pour des solutions salines, il est pertinent de sélectionner la base de données qui comportent les coefficients d'activité pertinents (Lu et al., 2022). En présence de drainage minier acide contenant des concentrations élevées en Fe, la base de données thermodynamique wateq4f.dat est celle qui est communément utilisée car elle prend en considération les particules colloïdales, diminuant ainsi l'erreur associée aux concentrations ioniques versus solides (Nordstrom, 2020).

3.1.5 Études de cas

L'utilisation de PHREEQC est très répandue dans le domaine minier et peut être employé dans plusieurs applications. Le tableau 3.2 compile différentes études de cas dans le domaine minier.

Tableau 3.2 Études de cas avec l'utilisation de PHREEQC en domaine minier

Endroit à l'étude	Objectifs	Conclusions	Références
Mine Leviathan en Californie et fosse Berkeley au Montana, États-Unis	Déterminer la quantité de chaux et de caustique nécessaire pour neutraliser un effluent provenant de DMA à l'aide de PHREEQC Modéliser des mélanges de DMA avec des eaux neutres afin d'évaluer les paramètres à l'équilibre	Démonstration que PHREEQC peut calculer la quantité de neutralisant à ajouter pour augmenter le pH et que celle-ci varie selon l'acidité et les concentrations de Fe et Al. La comparaison des données mesurées et modélisées a permis de déterminer les meilleurs paramètres à considérer pour la modélisation afin de diminuer l'erreur des modèles.	Nordstrom, 2020
Projet minier Pebble en Alaska, États-Unis	Prédire la qualité de l'eau et l'effet de mélange avec le milieu récepteur 105 ans après la fermeture en utilisant PHREEQC et MIKE SHE afin d'analyser les impacts potentiels d'un bris du système de traitement perpétuel prévu après l'arrêt des opérations	Prédiction que la qualité de l'eau affecterait les populations de saumon dans le ruisseau South Fork Koktuli à plus de 35 km advenant un bris du système de traitement d'eau durant 20 ans. Démonstration de l'importance d'évaluer plusieurs scénarios utilisant les outils de modélisation disponibles afin d'évaluer correctement les risques environnementaux de projets miniers en vue du design et des demandes de permis.	Maest et al., 2020

Endroit à l'étude	Objectifs	Conclusions	Références
Mine de cuivre abandonnée Elizabeth au Vermont, États-Unis	Déterminer les processus de dissolution de métaux à l'aide de PHREEQC, évaluer la spéciation des éléments dissouts à l'aide de BLM et lier l'information géochimique des éléments dissouts et leur spéciation à la toxicité associée	Identification des processus de dissolution et précipitations des métaux, surtout liés à la co-précipitation avec les précipités de Fe, soit schwertmannite et ferrihydrite, nouvellement formés mais aussi du pH. Identification des endroits où les concentrations de métaux dissous et labiles, surtout Cd, Cu and Zn, dépassent la CL50 pour la tête de boule et la daphnie.	Balistrieri et al., 2007
Mine abandonnée Montevecchio à Sardaigne, Italie	Évaluer la variation des contaminants depuis la fermeture de la mine Évaluer la dégradation naturelle des contaminants et les processus associés à l'aide de PHREEQC	Identification de l'ampleur de la contamination ainsi que des endroits impactés, mais aussi de l'évolution des concentrations à la baisse avec les années. Les processus d'atténuation sont reliés à la précipitation du Fe ainsi que de la co-précipitation et adsorption des autres métaux/metalloïdes comme As, Zn, Cd, Mn, Ni et REE sur les particules de Fe formées mais aussi dû à la dilution avec des ruisseaux non contaminés.	Cidu et al., 2011

3.2 Traçage isotopique en milieu minier

Le traçage isotopique est un outil pratique permettant d'identifier la provenance et le chemin des contaminants, l'évolution biogéochimique de contaminants dans le processus de mobilisation, l'origine de l'eau et son âge, les bilans de mélanges à différents points sur un site autant pour les eaux de surface que souterraines (Spangenberg et al., 2007). En contexte minier, la combinaison du traçage isotopique et des différents outils disponibles tels que les analyses géochimiques, physico-chimiques, bilans hydriques, permettent de mieux connaître les différents processus, tant pour les eaux que pour les contaminants, sur un site afin d'en améliorer la gestion et diminuer l'impact environnemental en contrôlant la problématique à la source (Wolkersdorfer et al., 2020; Kurukulasuriya et al., 2022). Bien que le traçage isotopique commence à être utilisé de façon plus fréquente depuis quelques années dans le domaine de l'hydrologie en général, peu d'études utilisent cet outil en contexte minier (Yu et al., 2021). Cette partie décrira principalement l'utilisation des isotopes de la molécule d'eau puis survolera les autres différentes applications utilisant d'autres isotopes.

3.2.1 Différents isotopes utilisés pour le traçage

3.2.1.1 Eau

Plusieurs isotopes sont utilisés en milieu minier dépendamment de l'objectif. Les isotopes stables de la molécule d'eau (δ^2H et $\delta^{18}O$) permettent de déterminer l'évolution hydrologique et sont utilisés dans différentes études à travers le monde afin d'expliquer les processus affectant les eaux de surface et souterraines (Spangenberg et al., 2007; Rey et al., 2018). La façon d'utiliser la signature de ces isotopes d'eau afin de produire un hydrographe de séparation est d'utiliser l'approche bilan de masse (Klaus et McDonnell, 2013) :

$$Q_t = Q_p + Q_e$$

$$C_t Q_t = C_p Q_p + C_e Q_e$$

$$F_p = \frac{C_t - C_e}{C_p - C_e}$$

Où Q_t est le débit d'eau, Q_p est la contribution de l'eau pré-événement, Q_e est la contribution de l'eau de l'événement, C_t, C_p, C_e sont les valeurs δ du débit d'eau, l'eau pré-événement et l'eau de

l'événement et F_p est la fraction pré-événement dans le cours d'eau. L'abondance des isotopes stable de l'eau, noté δ et exprimé en parties par millier (‰), est basé sur les ratios isotopique de la fraction lourde sur la fraction légère soit $^{18}O/^{16}O$ et $^{2}H/^{1}H$ (Klaus et McDonnell, 2013).

$$\delta^2 H \text{ ou } \delta^{18} O = \left(\frac{R_{échantillon}}{R_{standard}} - 1\right) \times 1000$$

où $R_{échantillon}$ est le ratio $^{2}H/^{1}H$ ou $^{18}O/^{16}O$ et $R_{standard}$ est la valeur Vienna Standard Mean Ocean Water (VSMOW).

Les valeurs standard VSMOW respectives des ratios sont $155,76 \pm 0,05 \times 10^{-6}$ pour $^{2}H/^{1}H$ et $2005,2 \pm 0,45 \times 10^{-6}$ pour $^{18}O/^{16}O$ (Klaus et McDonnell, 2013). Les données sont souvent représentées dans un graphique qui inclut la droite « local meteoric water line » (LMWL) qui est représentatif de l'endroit à l'étude (Rey et al., 2018). Les analyses des échantillons du site définissent une droite « local evaporation line » (LEL) qui est aussi incluse dans le même graphique. Avec l'application *Hydrocalculator* il est possible de calculer les ratios évaporation sur intrant (E/I) (Skrzypek et al., 2015). Les isotopes de la molécule d'eau peuvent être utilisés pour identifier les variations saisonnières, les bilans de masse des différentes provenances de l'eau, le taux d'évaporation (Lewicka-Szczebak et Jedrysek, 2013; Singh et al., 2018). Ils sont même utiles pour quantifier l'apport d'eau plus âgée versus nouvelle, par exemple, en calculant les ratios d'eau de l'ère glaciale, d'eau météorique et d'eau de saumure dans une mine souterraine à différentes profondeurs (Douglas et al., 2000; Hamed et al., 2014). L'identification des processus hydrologiques dans les systèmes affectés par le DMA est aussi une des applications qui permet d'améliorer la gestion des résidus miniers (Spangenberg et al., 2007). L'élévation de la recharge de l'eau souterraine peut aussi être calculé à l'aide de cet outil (Huang et Wang, 2017).

3.2.1.2 Azote

L'isotope d'azote est utilisé pour identifier les différents processus de transformation de NO_3 et NH_4^+ dans les eaux minières (Hu et al., 2021). En combinaison avec l'isotope d'oxygène, il permet de quantifier les réactions de nitrification, volatilisation ainsi qu'adsorption (Nilsson et Widerlund, 2017; Jung et al., 2020). Des études ont démontré leur utilité dans le domaine minier afin d'identifier les mécanismes de transport et de réaction dans les différentes infrastructures des sites (Hendry et al., 2018; Marcotte et al., 2022; Hendry et al., 2023).

3.2.1.3 Soufre

L'isotope de S est utilisé comme traceur dans le domaine minier surtout afin de déterminer l'évolution des concentrations de SO_4. La combinaison de $\delta^{18}O$ et $\delta^{34}S$ permettent de mesurer l'apport de SO_4 provenant de l'oxydation des minéraux sulfurés (Elliot et Younger, 2007; Migaszewski et al., 2018). La réduction bactérienne peut aussi être identifiée par le traçage isotopique de ^{34}S (Edraki et al., 2005; Wen et al., 2016).

3.2.1.4 Strontium

L'isotope de strontium est aussi un traceur utilisé dans le domaine minier afin de déterminer la provenance de la contamination. Il est présent dans plusieurs types de minéralogies et très soluble dans l'eau. Il n'est pas affecté par les phénomènes de sorptions, contrairement à la plupart des métaux présents dans les eaux usées, ce qui fait que le ratio original de l'isotope de Sr est maintenu permettant ainsi une meilleure identification de la source de contamination (Vengosh et al., 2022). Il est par exemple utilisé comme traceur dans les mines de phosphate (Vengosh et al., 2022). Le ratio d'isotope est $^{87}Sr/^{86}Sr$ et est utilisé par exemple pour déterminer les processus géochimiques et la mobilisation de différents contaminants dans les eaux minières (Négrel et al., 2007; Hamel et al., 2010; Wen et al., 2018).

3.2.1.5 Carbone

L'isotope ^{13}C est utilisé dans le domaine minier afin d'identifier les sources de carbone inorganique dissous. La dissolution de la calcite permettant de tamponner le pH dans les eaux minières est un facteur important et la quantification de cette réaction peut être réalisée à l'aide de $\delta^{13}C$ (Salifu et al., 2020). En plus de déterminer l'apport des carbonates, il est aussi utilisé pour le carbone organique et les processus biogéochimiques (Elliot et Younger, 2007; Salifu et al., 2020; Yi et al., 2021; Cesar et al., 2021).

3.2.1.6 Autres

D'autres isotopes sont utilisés dans le domaine minier afin de tracer l'évolution des contaminants dans les eaux. Les isotopes de métaux peuvent être utiles dans certains cas où une contamination spécifique doit être identifier. Par exemple, des combinaisons de ^{204}Pb, ^{206}Pb, ^{207}Pb et ^{208}Pb ont été utilisés afin d'identifier et quantifier les sources ainsi que l'étendue de contamination de la mine

(Miller et al., 2007; Mendova et al., 2016). D'autre part, les isotopes $\delta^{66}Zn$ et $\delta^{65}Cu$ sont utilisés pour identifier les processus biogéochimiques dans les effluents miniers (Borrok et al., 2008; Kimball et al., 2009).

3.2.2 Méthodes d'analyse des isotopes

La méthode d'analyse des isotopes de l'eau ^{18}O et ^{2}H la plus utilisée est celle réalisé à l'aide d'un spectromètre de masse gazeux où l'échantillon est comparé avec la référence. La référence est préparée en laboratoire à partir d'un volume reçu représentant la VSMOW (Clark et Fritz, 1997). Afin de mesurer ^{18}O dans l'eau, l'échantillon est équilibré avec du CO_2 et le pH de ce dernier est ajusté d'abord à une valeur inférieure à 4,5 afin d'accélérer l'échange de l'oxygène entre l'eau et le CO_2, selon la réaction suivante :

$$CO_2 + H_2O \leftrightarrow H_2CO_3$$

La valeur de $\delta^{18}O$ est ensuite calculée à l'aide d'un facteur de fractionnement α, ayant une valeur de 1,0412 pour le CO_2 et H_2O (Clark et Fritz, 1997). Pour l'analyse de ^{2}H, toute l'eau est réduite afin de la convertir en H_2 gazeux. Pour cette analyse, il n'est pas nécessaire d'utiliser un facteur de correction.

3.2.3 Études de cas

L'utilité des isotopes est variée dans le domaine minier tel que présenté dans les sections précédentes. Le tableau 3.3 compile plusieurs études de cas utilisant différents isotopes pour de multiples applications.

Tableau 3.3 Compilation des études de cas

Isotopes utilisés	Endroit à l'étude	Objectifs	Conclusions	Référence
$\delta^{15}N$ et $\delta^{18}O_{NO_3^-}$	Mines de charbon dans la Elk Valley, Colombie-Britannique, Canada	Déterminer les mécanismes de transformation de l'azote et la provenance dans les haldes à stériles	Nitrates issus principalement des explosifs non détonnés. Identification de zone anoxiques et sub-oxiques permettant la dénitrification.	Hendry et al., 2018
$^{87}Sr/^{86}Sr$	Mine de phosphate en Israël	Déterminer les sources de contamination de l'eau souterraine	La mer morte a été identifiée comme étant la source de la salinité de l'eau souterraine et non pas les eaux usées de la mine.	Vengosh et al., 2022
$\delta^{2}H_{H_2O}$, $\delta^{18}O_{H_2O}$, $\delta^{15}N_{NO_3^-}$, $\delta^{18}O_{NO_3^-}$ $\delta^{15}N_{NH_4^+}$	Mine d'or au Québec, Canada	Déterminer les bilans de masse sur le site avec les isotopes de la molécule d'eau Déterminer la provenance et les mécanismes de transformation des composé azotés	Le taux d'évaporation sur les intrants (E/I) se situe entre 0 et 34%. La combinaison du traceur Cl^- avec les isotopes de la molécule d'eau ont permis de déterminer les pourcentages des différents composés azotés provenant de l'eau de dénoyage. Les isotopes de l'azote ont permis d'identifier la nitrification et la dénitrification comme les principaux mécanismes de transformation dans les parcs à résidus.	Marcotte et al., 2022

Isotopes utilisés	Endroit à l'étude	Objectifs	Conclusions	Référence
$\delta^{2}H$ et $\delta^{18}O$	Mine de sables bitumineux en Alberta, Canada	Déterminer les bilans de hydriques du site en identifiant les intrants provenant des précipitations, les pertes par évaporation et les infiltrations potentielles	Modèle conceptuel a été produit mettant en lumière les rôles du mélange, la purge de la tour de refroidissement et la demande en eau sur la signature isotopique de l'eau de procédé. L'étude a permis de déterminé le bilan de masse et l'effet saisonnier sur l'apport en eau sur le site et les effets sur l'eau de procédé.	Chad et al., 2022
$\delta^{13}C$	Rivière Wujiang dans la province de Guizhou en Chine	Caractériser les changements dans les sources et composition de carbone organique, quantifier comment le réservoir transporte et transforme le carbone organique et proposer un modèle conceptuel sur l'effet du réservoir sur le cycle du carbone	Les particules de carbone organique terrestre sont remplacées par du carbone organique dérivé de phytoplancton, pendant qu'il y a un enlèvement graduel de particules de carbone organique colorées et une addition de carbone organique dérivé de phytoplancton au carbone dissous organique pendant l'écoulement vers le réservoir. Dans le réservoir, la production a surpassé la dégradation dans les premiers 5 m pour ensuite diminuer, la dégradation microbienne était plus importante en profondeur. Le carbone inorganique dissous (10-21%) a été intégré au carbone organique par le processus de pompe carbone biologique.	Yi et al., 2021

Isotopes utilisés	Endroit à l'étude	Objectifs	Conclusions	Référence
$\delta^{15}N$ et $\delta^{18}O$	Mine Kiruna en Suède	Identifier les sources et les processus de transformation de l'azote dans les eaux du site minier	Identification des sources de NO_3^- et $N\text{-}NH_3$ dans les eaux du site. Les NO_3^- proviennent surtout du drainage des haldes à stériles. Des concentrations naturelles de NO_3^- sont aussi présentent. Une quantité substantielle de N provient des explosifs soit entre 28 et 39% de la concentration mesurée au réservoir.	Nilsson & Widerlund, 2017
$\delta^{18}O$, $\delta^{2}H$, $\delta^{34}S$, ^{3}H, ^{13}C et ^{14}C	Puits de mine abandonné à Frances Colliery en Écosse	Identifier l'évolution à long terme et les possibles sources de contamination durant le pompage du puits à l'aide des différents traceurs isotopiques	Identification d'une source de salinité provenant de la mer et d'une autre provenant du sel de déglaçage utilisé à la surface. Une fuite provenant des bassins à la surface a été identifiée. Identification de la source de SO_4 provenant de l'oxydation des sulfures. La présence de carbonates et de mélantérite explique la présence de signature isotopique de C et S. L'eau des anciennes galeries de moins bonne qualité pourrait remplacer l'eau de recharge de meilleure qualité si elle est toute pompée.	Elliot & Younger, 2007
$\delta^{34}S$	Mine Mount Morgan en Australie	Utiliser l'hydrogéochimie, les isotopes stables ainsi que la minéralogie pour investiguer l'évolution du DMA ainsi que le	Les résultats ont montré que la réduction de SO_4 dans un environnement saturé réducteur et la formation de minéraux évaporitiques jouent un rôle important dans le contrôle des	Edraki et al., 2005

Isotopes utilisés	Endroit à l'étude	Objectifs	Conclusions	Référence
		rôle des précipités et différencier les sources naturelles et minières de SO_4	concentrations de SO_4. Des sources naturelles et anthropogéniques ont aussi été identifiées. Le traçage isotopique de SO_4 permet d'identifier les processus biogéochimiques et peut aider à estimer le taux de réduction de la concentration.	
$\delta^{15}N$ et $\delta^{18}O$	Elkview Operations dans la Elk Valley en Colombie-Britannique, Canada	Déterminer et quantifier la réaction de dénitrification pour l'enlèvement de NO_3^- dans le Saturated Rock Fill (SRF)	L'étude a montré qu'il est possible d'identifier les réactions de dénitrification dans le système de traitement SRF mais la quantification doit être prise avec précaution et doit être supportée par d'autres données. Le bio traitement par SRF a été un succès et est maintenant considéré pour être utilisé à plus grande échelle et déployé sur les autres sites miniers.	Hendry et al., 2023
$\delta^{66}Zn$ et $\delta^{65}Cu$	Six sites miniers historiques aux États-Unis et en Europe	Déterminer si la signature isotopique est unique selon l'installation géologique et si elle change selon la concentration en métaux dissous dépendamment des cycles quotidiens	La signature isotopique de Zn et Cu est hétérogène et ne reflète pas une moyenne dans un endroit donnée. Le Zn et Cu sont transférés de la phase dissoute à la phase solide en réponse aux processus de contrôle par photo cycle et est possiblement attribuée à l'absorption métabolique des micro-organismes.	Borrok et al., 2008

CHAPITRE 4 DÉMARCHE MÉTHODOLOGIQUE

Le projet s'est déroulé en plusieurs étapes soit la caractérisation, le traitement ainsi que la prédiction de la qualité physico-chimique des mélanges d'effluents. La première étape consistait à la compilation des données historiques suivi d'un échantillonnage des différents effluents sur une période de 3 ans afin d'avoir les différentes qualités physico-chimiques durant toutes les saisons actives. Les données historiques ainsi que les nouvelles données récoltées lors des différentes campagnes d'échantillonnage ont été compilées dans une géodatabase à l'aide du logiciel ArcGIS. Les données ont aussi été analysées de façon statistique avec le logiciel RStudio permettant de produire des graphiques.

L'étape suivante était la prédiction des propriétés physico-chimiques des mélanges d'effluents. La modélisation de ces propriétés a été réalisée à l'aide des données de caractérisation ainsi que du programme PHREEQC. En parallèle, des mélanges avec des effluents réels ont été produits afin d'en analyser les paramètres physico-chimiques réels à l'équilibre. À l'aide des résultats obtenus, une prédiction de la qualité des différents effluents selon les saisons pourrait être réalisée pour le site à l'étude, selon les bilans de pompage actuel, et ainsi permettre une méthode de gestion de l'eau optimale tout en validant si un traitement est nécessaire afin de respecter les critères de toxicité aquatiques à l'effluent final.

L'étape de traitement a été réalisée sur des effluents réels provenant de différents endroits sur le site à l'étude. Les effluents ont été testés en mélanges afin de voir l'impact sur les performances de traitement. La méthode de traitement utilisée a été l'oxydation avancée avec l'ozone sous forme de microbulles. L'ajustement des paramètres d'opération afin d'obtenir une efficacité de traitement optimale a été fait durant les essais puis analysé. Avant et après les essais, des tests écotoxicologiques sur les effluents traités ont été réalisés avec la *D. magna* afin de vérifier les performances des méthodes de traitement sur la toxicité aquatique. La figure 4.1 montre le schéma des différentes étapes du projet.

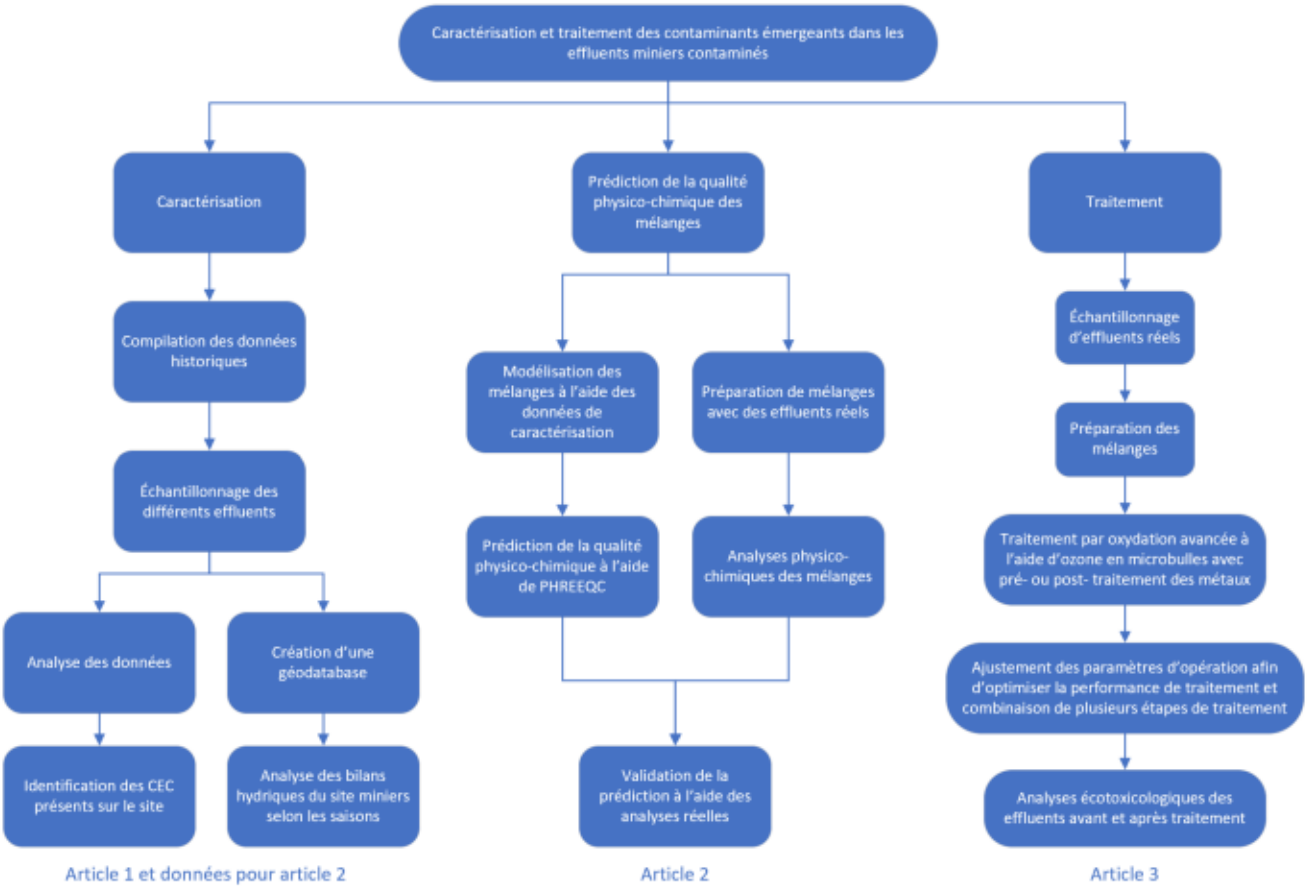

Figure 4.1 Schéma du déroulement du projet

4.1 Site à l'étude

Le projet s'est déroulé sur le site de la mine Westwood appartenant à la compagnie Iamgold. Ce site regroupe les installations de la mine Doyon, lesquelles incluent, sur une superficie d'environ 28 km^2, les parcs à résidus (parc 1, parc 2, parc 3 est et parc 3 ouest), les haldes à stériles (halde sud et halde nord), les bâtiments administratifs, l'usine de traitement de minerai, l'usine de traitement d'eau acide, la fosse Doyon qui sert comme parc à résidus pour les opérations en cours, les bassins collecteurs (bassin sud, réservoir ouest et bassin B), le bassin de polissage (bassin A) et l'effluent final. La mine Westwood se sert donc d'une partie de ces installations pour le déroulement de ses opérations. Les installations exclusives à la mine Westwood, ayant une superficie de près de 2 km^2, incluent le chevalement Westwood, la rampe d'accès, la ventilation, le bassin collecteur d'eau d'exhaure (bassin Westwood), l'usine de remblais en pâte et la station d'eau potable. Le projet s'est intéressé à la qualité et la gestion des eaux sur le site en prenant en

considération les impacts des mélanges sur la qualité physico-chimique de l'eau ainsi que l'effet sur la toxicité aquatique. La figure 4.2 illustre le site de la mine Westwood et les différents points d'échantillonnage qui sont intégrés dans la géodatabase.

Figure 4.2 Site de la mine Westwood d'Iamgold (tiré de ArcGIS)

4.2 Compilation et analyse des données historiques

La compilation des données historiques du site a été réalisée à l'aide de tous les fichiers Excel qui étaient disponibles sur le réseau informatique de la compagnie. Les données étaient compilées dans différents fichiers Excel d'année en année et pour différents points d'échantillonnage. Un seul fichier a été créé rassemblant ainsi tous les points d'échantillonnage pour toutes les années, remontant jusqu'en 2002, en uniformisant les tableaux. Ceci permet de faciliter la création de la géodatabase dans ArcGIS mais aussi de pouvoir analyser les données à l'aide du logiciel RStudio. Pour la création de la géodatabase avec ArcGIS, l'arpentage de tous les points d'échantillonnage a

été réalisé à l'aide d'un système d'acquisition de données GPS afin de localiser tous les points sur la carte.

4.3 Essais de traitabilité avec ozonation par microbulles

Le système d'ozonation par microbulles a été dimensionné sur mesure avec des équipements qui ont été sélectionnés pour être compatibles les uns avec les autres. Le modèle du générateur d'ozone est le GM1 fabriqué par la compagnie Primozone. Il peut produire 35 g O_3/h à une concentration de 20% mais peut aussi produire jusqu'à 60 g O_3/h à une concentration de 10%. Le générateur est refroidi au liquide à l'aide d'une unité de refroidissement Lauda UC2. Le générateur est alimenté par de l'oxygène de qualité médicale en bonbonne. Afin de protéger le générateur d'un retour de liquide dans la ligne d'injection d'ozone, un système anti-retour est installé sur la ligne d'injection. Pour une question de santé-sécurité reliée à la manipulation d'ozone, un détecteur d'ozone dans l'air ambiant est installé sur l'équipement et provoque l'arrêt du générateur si la concentration dépasse la limite sécuritaire. Le système d'injection d'ozone est composé d'une pompe à microbulle KTM20N de la compagnie Nikuni ainsi qu'un mélangeur statique MX-E10 de la compagnie OHR (Original Hydrodynamic Reaction Technology). Afin d'améliorer la qualité des microbulles à l'intérieur du réacteur d'ozonation, un séparateur de gaz éliminant les bulles grossières est installé à la suite du mélangeur statique, celui-ci peut être court-circuité au besoin. Le modèle du séparateur est le DS-150-P de la compagnie Mazzei. Le réacteur d'ozonation est en polycarbonate, un matériau transparent compatible avec l'ozone. Il a été fabriqué sur mesure pour le système de traitement. Les équipements principaux utilisés pour le système d'ozonation sont illustrés dans le tableau 4.1.

Tableau 4.1 Principaux équipements utilisés pour l'ozonation en microbulles (images tirées des sites web des fournisseurs)

	
Générateur d'ozone GM1 de Primozone	Unité de refroidissement UC2 de Lauda
	
Pompe à microbulles KTM20N de Nikuni	Mélangeur statique MX-E10 de OHR
	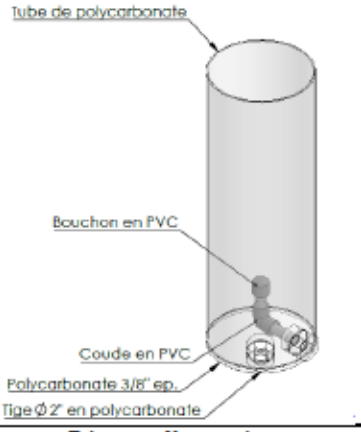
Séparateur de gaz en excès DS-150-P de Mazzei	Réacteur d'ozonation

Le choix de combiner la pompe à microbulles avec le mélangeur statique est pour augmenter la qualité des microbulles générées. En effet, à l'aide de l'action du mélangeur statique, pratiquement toutes les bulles grossières sortant de la pompe sont transformées en microbulles dans le mélangeur statique. Le principe de fonctionnement du mélangeur statique est présenté à la figure 4.3.

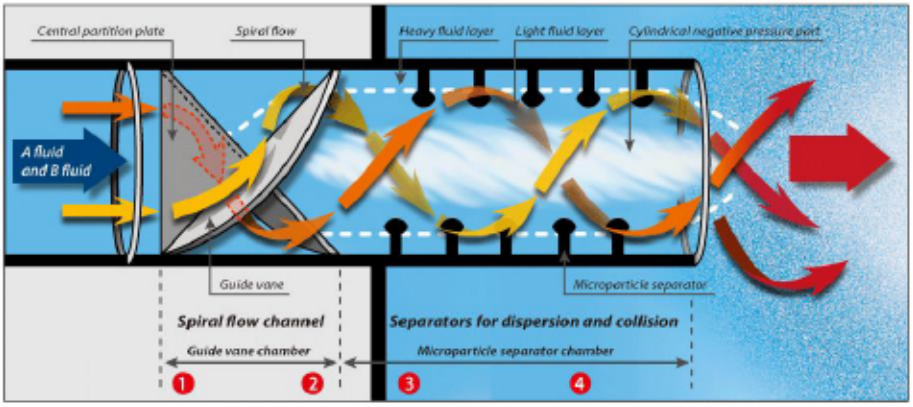

Figure 4.3 Principe de fonctionnement du mélangeur statique OHR (tiré de ohr-labo.com)

Le système d'ozonation permet de traiter un volume de 20 L d'eau en mode batch. Afin de maintenir le pH dans le réacteur d'ozonation durant le traitement, un système d'injection de NaOH automatique avec une sonde de pH est branché sur le réacteur. Plusieurs essais ont été réalisés durant la maîtrise (Ryskie, 2017) et les recommandations ont été prises en compte dans le montage et les paramètres d'opération.

4.4 Modélisation de la spéciation des mélanges d'effluents

La modélisation des différents mélanges d'effluents a été réalisée à l'aide du modèle PHREEQC version 3. PHREEQC est un modèle géochimique sous forme de code permettant d'identifier et de quantifier les réactions chimiques ainsi que de simuler des procédés de transport en une dimension impliquant les phases minérales solides, aqueuses et gazeuses (Parkhurst et Appelo, 2013). D'autres chercheurs ont utilisé ce modèle afin de prédire la qualité géochimique de l'eau dans le temps selon les mélanges déterminés par les bilans hydriques d'un site minier (Lewis-Russ et al., 2019). Le choix de ce modèle vis-à-vis d'autres est que celui-ci est robuste, éprouvé, gratuit, code libre accès et simple d'utilisation.

Des données physico-chimiques historiques ainsi que les données issues des différentes campagnes d'échantillonnage ont permis de calibrer le modèle des différents points de mélange. Le bilan hydrique du site à l'étude a permis de déterminer les ratios de mélange aux différentes périodes de l'année. Un modèle conceptuel du site a été réalisé, sous forme de diagramme, afin de faciliter l'entrée de données dans le modèle PHREEQC et ainsi augmenter le niveau de confiance des prédictions. Les données issues du bilan hydrique du site à l'étude ont été compilées afin de réaliser

des statistiques. Le modèle peut ainsi suivre les variations temporelles selon la période de l'année et les précipitations historiques. Le choix des bases de données thermodynamiques pour le modèle a aussi été un enjeu en ce qui a trait à la fiabilité de la prédiction. Ces bases de données peuvent être ajustées afin de fiabiliser l'utilisation du modèle prédictif.

La modélisation des mélanges a ensuite été validée en analysant les propriétés physico-chimiques des mélanges d'effluents réels. Des quantités d'eau prélevées lors des différentes campagnes d'échantillonnage ont été congelées afin de les préserver. Des mélanges ont été réalisés avec les échantillons préservé selon les même ratios précédemment calculés et utilisés pour la modélisation numérique avec PHREEQC. Les résultats obtenus avec les mélanges d'effluents réels peuvent ensuite déterminer le niveau de confiance des différentes modélisations.

CHAPITRE 5 ARTICLE 2 : MODELING THE GEOCHEMICAL EVOLUTION OF MINE WATERS DURING MIXING[2]

Cet article a été soumis le 30 mai 2023, présentement en évaluation pour considération dans la revue *Applied Geochemistry*.

5.1 Abstract

Mine water management often involves the mixing of effluents with contrasting chemical compositions. However, the impacts of mixing processes on the geochemical evolution of effluents are poorly understood, which complicates the prediction of the quality of the water to be treated before discharge to the environment. This article specifically targets this problem and is based on data collected from an active mine site located in Québec, Canada. Field samples were collected to characterize effluents upstream and downstream of various mixing points. Controlled laboratory mixing experiments were performed with real effluents. In situ physicochemical parameters, concentrations of dissolved major ions and trace elements, and stable isotopes of the water molecule were analyzed. Mineralogical analyses were also performed on precipitates from the laboratory mixtures. The data were used for statistical analyses and for modeling the geochemical evolution of the effluents using the PHREEQC model with the *wateq4f.dat* database. The results suggest that the formation of secondary minerals such as schwertmannite, $Fe(OH)_3$, and jarosite significantly impact the geochemical evolution of effluents. The precipitation of secondary minerals was identified as an immobilization process for trace elements through coprecipitation and sorption processes. The main limitations of modeling mine effluent mixtures with PHREEQC include the evaluation of the ion balance for low pH samples with high Fe and Al concentrations and the omission of biological processes. Nevertheless, the characterization and modeling approach developed here provides useful insights into the geochemical evolution of mine effluents and could be adapted to several mining sites.

Keywords: PHREEQC; Mine water modeling; Water mixtures; Iron precipitation; Sorption; Mineralogical analyses

---

[2] Ryskie, S., Rosa, E., Neculita, C.M., Couture, P., 2023. Modeling the geochemical evolution of mine waters during mixing. *Applied Geochemistry*. En évaluation for consideration dans une perspective de publication.

5.2 Introduction

The management of mine water often involves (1) the temporary storage of waters from various sources in basins and ponds (dewatering, process waters, runoff), (2) the mixing of waters from these sources as a function of water management needs, (3) the treatment of the mixed waters, and (4) the release of treated and, sometimes, untreated effluents to the environment (Wolkersdorfer et al., 2020; Spellman et al., 2022). Mine operators must manage water to minimize environmental and operational risks by considering water levels in ponds and basins, discharge rates, forecasted precipitations, and onsite water usage. Mine operators must further ensure that enough water remains available for treatment needs during the winter season to maintain water treatment plant operations.

The effluent mixing processes required for water management approaches can result in changes in the activity, speciation, toxicity, and mobility of contaminants. Contaminants such as Fe, Al, As, Cu, Mn, Se, and Zn can be immobilized through precipitation, coprecipitation, and sorption processes involving oxyhydroxides (Hem, 1985; Bigham & Nordstrom, 2000). During mixing processes involving mine effluents, the formation of Fe and Al oxides, oxyhydroxides, and hydroxysulfates can also be pH-dependent (Bigam & Nordstrom, 2000; Barge et al., 2016; Nordstrom, 2020). For example, at pH < 2, jarosite can precipitate (Nordstrom, 2020), whereas schwertmannite can precipitate at pH 2–4 (Nordstrom, 2020; Schoepfer et al., 2021) and ferrihydrite is more likely to precipitate at higher pH (Nordstrom, 2020). These mineral phases are likely to initially form amorphous precipitates during mixing processes and can convert to crystalline phases with time. For example, poorly-crystalline schwertmannite and basaluminite can convert to microcrystalline goethite/jarosite and alunite, respectively (Nordstrom, 2020). Changes in the speciation and mobility of contaminants such as As and Se can also influence the toxicity of effluents (Ryskie et al., 2021; Lemly, 2002). Furthermore, seasonal changes in precipitation, ice and snow accumulation and melting, and evaporation can strongly influence the chemical composition of mine effluents through dilution and concentration mechanisms.

Considering the multitude of processes dictating the geochemical evolution of mine effluents, integrative approaches including hydrological balances and geochemical and isotopic analyses must be preconized for their characterization (Hendry et al., 2018; Papp et al., 2020; Marcotte et

al., 2022; Wolkersdorfer et al., 2020). Geochemical modeling tools such as PHREEQC can further highlight key mechanisms controlling the geochemical evolution of waters (Parkhurst & Appelo, 1999; Lecomte et al., 2005). The application of numerical modeling for evaluating the geochemical evolution of mine effluents during mixing processes and water treatment is widely used by the scientific community (Cravotta et al., 2014; Burrows et al., 2017; Cravotta, 2021; Spellman et al., 2022). Despite the many scientific advances in geochemical modeling in a mining context, challenges remain in the use of modeling to support mine water management (Cravotta, 2021). On the one hand, the use of oxidoreduction potential (ORP) and pH values from *in situ* field measurements as inputs for calculating the speciation of dissolved substances in geochemical models can lead to important biases. For example, it is known that in situ ORP measurements made with field probes are often inconsistent with other indicators (e.g., redox couples) for estimating the redox potential of a solution (Appelo and Postma, 2005). In addition, *in situ* pH measurements can be affected by undesirable effects such as the suspension effect, leading to biased values. Furthermore, field procedures often involve the filtration of samples with 0.45 or 0.22 µm membranes, and results from chemical analyses conducted on filtered samples are often assumed to represent «dissolved» concentrations, even though colloids can pass the filtration membranes (Nordstrom, 2020). As a result, the inputs (Eh-pH and «dissolved» concentrations) used for geochemical modeling can be imprecise. On the other hand, the understanding of the precipitation processes of Fe, Mn and Al oxides and co-precipitation and sorption of trace metals remains imperfect. The comparison of field measurements at different mixing points in different seasons and laboratory tests under controlled conditions with calculations based on geochemical modeling represents a relevant approach to address these issues.

Fitting in the preestablished context, the general objective of this study is to assess the advantages and limitations of geochemical modeling for quantifying the impacts of mixing processes on the geochemical evolution of mine waters under field and laboratory conditions. The specific objectives are (1) to document the changes in the concentrations, activities, speciation, and saturation indices of contaminants in response to mixing through a comparison of measurements (field and laboratory data) and simulations and (2) to decipher the potential immobilization/mobilization processes controlling the activities of contaminants in mixed waters.

5.3 Study mine site

The study site was a gold mine located near the Cadillac-Larder Lake fault, within the Abitibi greenstone belt (Abitibi-Témiscamingue, Québec, Canada), one of the largest mining regions in the world (Figure 5.1).

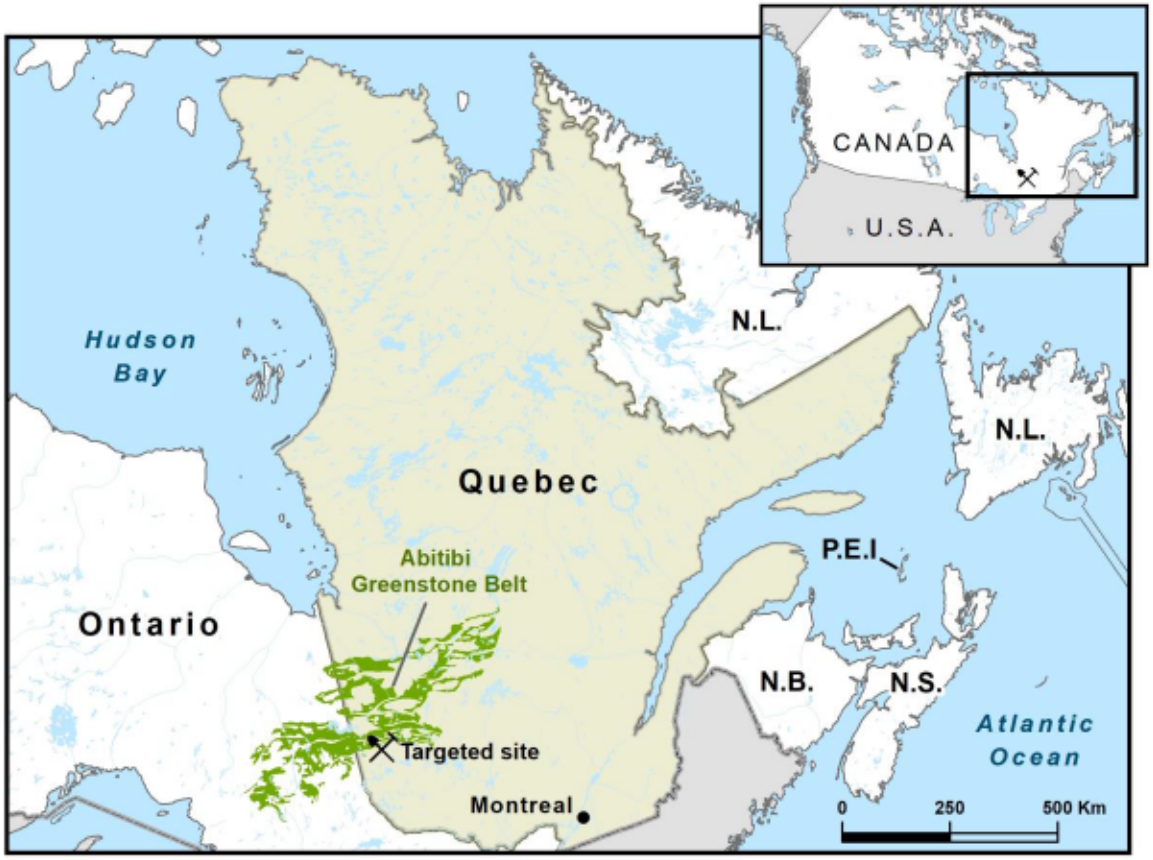

Figure 5.1 Study mine site location.

The gold extraction process at the mine site uses cyanidation with a carbon in pulp approach, at a maximum rate of 850,000 tonnes of ore per year. The residual cyanide is treated with the INCO (SO_2-air) process (Botz et al., 2005) before discharge in the tailings pond, which corresponds to an open pit.

The local climate is characterized by strong seasonality with cold, sub-zero temperatures in winter (mean air temperature of approximately –15°C in January) and warm temperatures in the summer (mean air temperature of approximately 18°C in July). The mean annual precipitation is approximately 948 mm (climate-data.org, 2022).

Sulfur-rich acid-generating rocks occur locally, and large volumes of acidic waters are generated. The mine is located on a legacy site and utilizes the old infrastructure in place; water management involves several ponds, reservoirs, and basins. The mine operation also involves dewatering from underground infrastructure. The actual depth of the mine is approximately 2 km, and multiple underground pumping stations are used to route the dewatering effluent towards a surface settling pond. The mining site flow diagram is shown in Figure 5.2 and the different sampling sites are identified in Table 5.1. As illustrated in Figure 5.2, the onsite managed waters are mixed before reaching a high-density sludge (HDS) treatment plant (Coulton et al., 2003).

Table 5.1 Description of water locations on the mine site used in this study (acronyms used for site privacy).

Effluent	Water type and mix
DP	Active tailings pond collecting process water after destruction of cyanides by the SO_2-air process as well as acid mine drainage.
TSF1	Inactive tailings storage facility containing acid mine drainage.
TSF2	Inactive tailing storage facility containing acid mine drainage and pumping water from TSF1 at certain times of the year.
TSF3W	Tailings storage facility used for the recirculation of process water from ore treatment before cyanidation.
TSF3E	Inactive tailings storage facility containing acid mine drainage and the overflow of TSF3W at certain times of the year.
SB	Pond containing acid mine drainage from the south waste rock pile and surrounding roads.
NP	Waste rock pile located in the northern part of the site. The pile generates acid drainage, which is collected by a creek flowing through BB.
WWB	Pond containing dewatering effluents pumped from the underground mining infrastructure.
WR	Pond containing acid mine drainage from the south waste rock pile, water from SB, and water from the WWR.
BB	Pond containing acid mine drainage from NP, waters from all TSFs, depending on the time of year, and water from the WR. This pond also serves as a buffer tank for the high-density sludge water treatment plant.

HDS	High-density sludge water treatment plant.
PP	Polishing pond containing treated water from the HDS treatment plant.
EFF	Final effluent at the outflow of the polishing pond.
River	Naturally flowing river receiving the effluent. In this study, the river was sampled upstream of the effluent release point to estimate a baseline composition for surface waters.

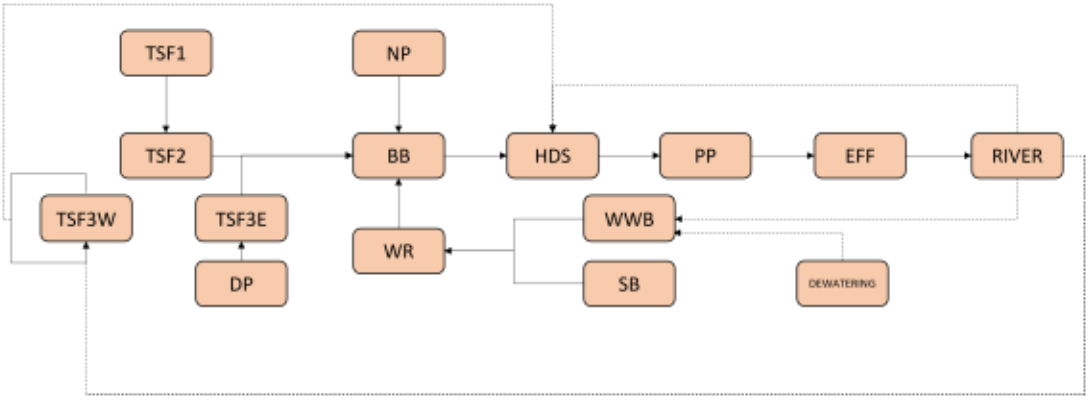

Figure 5.2 Schematic flow diagram of the different water infrastructures on the mine site.

5.4 Methods and data sources

5.4.1 Onsite geochemical monitoring

The compilation of historical site data was carried out using the data made available by the mine operator. A comprehensive database was created with all available data between 2002 and 2018. Sampling campaigns were further conducted in November 2018, August 2019, October 2019, May 2020, and June 2021. A total of 47 effluent samples were collected during these campaigns. In the field, the in situ physicochemical parameters (pH, ORP, temperature, electrical conductivity (adjusted for temperature), and dissolved oxygen) were measured using a *YSI ProPlus* multiparameter probe. Samples were collected using a *Nasco Swing Sampler* pole equipped with a dedicated sampling bottle. The sampling bottles were rinsed three times with the effluents before sampling. Samples were filtered onsite using syringes equipped with 0.45 µm membranes; some samples were acidified to pH 2 with HNO_3 for metal analysis, while others remained unacidified for anion analysis. Unfiltered samples collected for ammonia nitrogen analysis were acidified to pH 2 using H_2SO_4 and stored in 125 mL high density polyethylene (HDPE) bottles. Unfiltered

samples collected for alkalinity measurements were stored in 1 L HDPE bottles. All samples were preserved at 4°C before analysis.

5.4.2 Laboratory mixing experiments

Mixtures were produced from different effluents sampled in June 2021. In the field, a submersible pump was used to fill 20 L plastic buckets with the selected effluents. The submersible pump was rinsed onsite before collecting samples by pumping water at a high discharge rate during several minutes before sample collection. In situ physicochemical parameters (pH, ORP, temperature, electrical conductivity (adjusted for temperature), and dissolved oxygen) were measured using a *YSI ProPlus* multiparameter probe. The plastic buckets were quickly transported to the laboratory, agitated, and then mixed to the desired proportions using a graduated cylinder (Table 5.2). The mixing ratios used for mixtures were calculated from the site hydrological balance, based on discharge rates evaluated for the active season (from May to December). The resulting mixtures were sampled following the procedures described in section 3.4. The mixtures were then stored and resampled after 18 days, following the same procedures. In situ physicochemical parameters were measured every day to see if the values stabilized before stopping the experiment. Sample collection was completed with a syringe to minimize water movement in the bucket. Once water samples were collected, the water remaining in the bucket was filtered to recover the precipitated solids; these solids were analyzed by scanning electron microscopy (SEM).

Table 5.2 Volumes (in L) used for the preparation of mixtures in the laboratory.

Sampling point	Mix 1 (L)	Mix 2 (L)	Mix 3 (L)	Mix 4 (L)
TSF1				0.13
TSF2		1.31		0.60
TSF3E		0.42		0.31
TSF3W			1.73	
WWB	2.07			
SB	3.52			
NP		2.47		0.81
WR		1.20		1.16
DP			3.45	
DP+TSF3W				2.78

5.4.3 Isotopic analyses

The isotopic analyses (δ^2H–$\delta^{18}O$ of the water molecule) were conducted at the Geotop laboratory (Montreal, Canada) and the methodological procedures described below are from the Geotop analyses report. Exactly 200 ml of sample water was pipetted in a 3 ml vial, closed with a septum cap and transferred to a 40°C heated rack. For δ^2H analyses, a hydrophobic platinum catalyst (Hokko beads) was added. After 1 hour, air in the vials was replaced with CO_2 (for $\delta^{18}O$) or H_2 (for δ^2H) using the AquaPrep. Samples were left to equilibrate for 7 hours for $\delta^{18}O$ or 4 hours for δ^2H. The equilibrated samples were analyzed with a Micromass model Isoprime isotope ratio mass spectrometer coupled to an AquaPrep system in dual inlet mode. 3 internal reference waters ($\delta^{18}O$=0,23±0.06‰, -13,74±0.07‰ & -20,35±0.10‰; δ^2H=1,28±0.27‰, -98,89±1,12‰ & -155,66±0.69‰) were used to normalize the results on the VSMOW-SLAP scale. A 4th reference water ($\delta^{18}O$=-4,31±0.08‰; δ^2H=-25,19±0.83‰) was analyzed as an unknown to assess the exactness of the normalization. Results are given in delta units (δ) in ‰ vs VSMOW. The overall analytical uncertainty (1σ) is better than ±0.1‰ for $\delta^{18}O$ and ±2.0 ‰ for δ^2H. These uncertainties are based on the propagation of uncertainties of the normalization of the internal reference materials and the samples but does not include the homogeneity nor the representativity of the sample.

5.4.4 Chemical analyses

The chemical analyses were performed in an external laboratory that is accredited by the *Centre D'expertise en Analyses Environnementales du Québec* (H2Lab, Rouyn-Noranda, QC, Canada). Metals were analyzed by inductively coupled plasma mass spectrometry (ICP-MS) after sample filtration using 0.45 µm membranes (CEAEQ, 2020; MA. 200 – Mét. 1.2). Anions (NO_2^-, NO_3^-, SO_4^{2-}, PO_4^{3-}, Cl^-, Br^-, and OCN^-) were analyzed by ion chromatography (IC 945 Professional Detector Vario Metrohm) (CEAEQ, 2020; MA. 300 – Ions 1.3). The NH_3-N concentrations were analyzed using a selective electrode (Orion ThermoFisher Scientific Orion for Ammonia) according to the standard method (APHA, 2017; Method 4500-NH_3 D). Total CN^- was measured using the automated colorimetric method with isonicotinic acid and barbituric acid (CEAEQ, 2016; MA. 300 – CN 1.2).

5.4.5 Mineralogical analyses

The remaining water from the five laboratory mixtures was filtered at 0.45 µm after the experiments. The cakes were then dried in an oven (Shel Lab) at 60 °C. An aliquot of each dry powder sample was stub-mounted using double-sided carbon tape. The stub mount was carbon coated before it was loaded into the SEM for inspection. The SEM used for this study was a mineral liberation analyzer (MLA; FEI Mark II) on a Quanta platform. Spot chemical analyses and elemental mapping were performed using energy dispersive spectroscopy (EDS). Bruker X-ray detectors and the Bruker Esprit™ software were employed for the EDS analyses, with the aim to identify the main phases present in each sample. The elemental composition (in %) provided by the software at each spot analyzed was compared to web mineralogical databases to tentatively identify the mineral phases.

Additional mineralogical analyses were performed on three samples (mixtures 2-3-4) using a TESCAN TIMA G4 Field Emission Gun SEM to obtain an improved resolution. Because of the quantity of solids available, only these three mixtures were processed for these additional analyses. The TIMA system was equipped with four Element Peltier-cooled solid state EDS detectors, which were calibrated using a manganese standard. The accelerating voltage was 25 kV and the probe current was in the range of ~6 nA. Spot chemical analyses and elemental mapping (Essence™ EDS software) were performed using EDS, with the aim to identify the main phases present in each sample.

5.4.6 Statistical approaches

Correlations between measured chemical species were evaluated by creating heatmaps following the procedure described by Bondu et al. (2020). The heatmap consists of a graphical representation of the correlation coefficients between the variables, where a dendrogram from a hierarchical cluster analysis (HCA) is used to identify possible groups of parameters with similarities. The data were processed using the *CorCoDa* function from the *robCompositions* package and heatmaps were produced using the *heatmap.2* function from the *gplots* package in R (Warnes et al., 2016). This approach is increasingly used in geochemistry to detect similarities and differences among groups of chemical parameters (Kynclova et al., 2017; Bondu et al., 2020).

5.4.7 Geochemical modeling

Geochemical modeling was performed with PHREEQC (Parkhurst & Appelo, 2013) using the *wateq4f.dat* database (Ball & Nordstrom, 1991), which accounts for colloidal phases likely to precipitate in acid mine effluents (Nordstrom, 2020). Forward modeling was first performed to verify the electroneutrality of samples and calculate saturation indices (SI). Mineral phases with SI close to 0 and likely to be in contact with the monitored effluents were selected and inverse models were produced to estimate the sources and sinks of chemical elements during effluent mixing processes. The gas phases used in the models were oxygen and carbon dioxide. The phases selected for the EQUILIBRIUM_PHASES function were derived from the literature and the mineralogical observations. The addition of thermodynamic data for mineral species such as schwertmannite to the *wateq4f.dat* database was from Nordstrom (2020) using a log k value of 18.5. The choice of redox was based on calculated pe with Eh.

5.5 Results and discussion

5.5.1 Laboratory mixing experiments

5.5.1.1 Laboratory observations

The dissolved concentrations obtained for the laboratory mixtures on the day of mixing and after 18 days are presented in Table 5.3. The aqueous chemical analyses revealed marked changes in dissolved solids concentrations over the duration of the experiment. For a more convenient representation of the data, the absolute and relative changes in concentrations observed for dissolved species are presented in Figure 5.3. The calculated changes in concentrations show that Ca, Fe, Mg, Si, and Na were the dissolved phases that exhibited the greatest absolute decreases in concentration. The calculated relative changes in concentrations further indicate that most of the analyzed parameters showed decreasing concentrations over the duration of the experiment. It is postulated here that the largest absolute decreases in dissolved concentrations of the major phases are related to precipitation phenomena, while the relative decreases in concentrations of the minor and trace phases are mainly related to coprecipitation and sorption phenomena.

Table 5.3 Measured concentrations (mg/L) of dissolved elements in laboratory mixtures (LM) on day 1 (D1) and day 18 (D18) and relative changes in concentrations ($\Delta\% = \frac{([day\ 18] - [day\ 1])}{[day\ 1]}$).

	LM1 D1 (mg/L)	LM1 D18 (mg/L)	Δ%	LM2 D1 (mg/L)	LM2 D18 (mg/L)	Δ%	LM3 D1 (mg/L)	LM3 D18 (mg/L)	Δ%	LM4 D1 (mg/L)	LM4 D18 (mg/L)	Δ%
Al	2.28E-02	1.38E-02	-40	6.01E-03	5.20E-03	-13	2.38E-06	3.98E-06	67	1.99E-03	9.60E-04	-52
As	2.32E-06	1.36E-06	-41	5.66E-07	5.41E-07	-5	2.14E-08	2.14E-08	0	1.06E-07	9.50E-08	-10
Ba	3.92E-07	2.78E-07	-29	3.15E-08	4.39E-08	39	8.51E-07	6.87E-07	-19	2.61E-07	2.73E-07	5
Cd	2.27E-07	1.34E-07	-41	9.03E-08	4.55E-08	-50	1.96E-09	1.79E-10	-91	1.79E-10	1.55E-08	8593
Ca	2.97E-02	1.74E-02	-41	1.28E-02	1.09E-02	-14	1.54E-02	1.24E-02	-20	1.17E-02	8.12E-03	-31
Cl	2.03E-02	2.06E-02	1	4.65E-03	4.39E-03	-6	1.90E-03	1.71E-03	-10	4.35E-03	4.21E-03	-3
Cu	9.65E-05	5.65E-05	-41	4.51E-05	3.84E-05	-15	1.44E-06	5.04E-07	-65	1.54E-05	7.16E-06	-54
Fe	3.15E-02	1.68E-02	-47	1.67E-02	1.37E-02	-18	1.80E-07	2.70E-06	1400	4.91E-03	1.35E-03	-73
Li	7.16E-05	4.85E-05	-32	2.22E-05	2.13E-05	-4	3.91E-06	2.89E-06	-26	7.23E-06	5.20E-06	-28
Mg	2.64E-02	1.60E-02	-39	8.91E-03	7.83E-03	-12	7.15E-03	5.33E-03	-26	5.38E-03	2.74E-03	-49
Mn	7.69E-04	4.39E-04	-43	3.13E-04	2.72E-04	-13	1.79E-04	1.06E-04	-41	1.69E-04	8.13E-05	-52
Ni	2.58E-05	1.48E-05	-43	1.16E-05	9.96E-06	-14	1.62E-06	1.21E-06	-25	3.49E-06	1.85E-06	-47
Pb	8.30E-10	8.29E-10	0	8.25E-10	8.25E-10	0	8.24E-10	8.23E-10	0	8.23E-10	3.68E-09	347
K	4.91E-05	3.33E-05	-32	1.90E-05	2.65E-05	39	2.49E-03	1.82E-03	-27	8.94E-04	4.59E-04	-49
Se	6.13E-06	3.73E-06	-39	2.07E-06	2.37E-06	15	2.42E-08	7.63E-09	-68	4.97E-07	4.67E-07	-6
Si	2.90E-03	7.02E-04	-76	1.67E-03	6.57E-04	-61	3.57E-04	2.37E-04	-34	1.92E-04	3.01E-04	57
Na	2.70E-03	1.63E-03	-40	1.16E-03	1.07E-03	-8	1.55E-02	1.15E-02	-26	5.84E-03	3.17E-03	-46
Sr	1.25E-04	7.31E-05	-42	2.26E-05	1.98E-05	-12	1.92E-05	1.91E-05	0	1.88E-05	1.73E-05	-8
SO_4	6.16E-02	7.08E-02	15	3.67E-02	3.59E-02	-2	2.30E-02	2.57E-02	12	2.42E-02	2.09E-02	-14
U	1.66E-07	1.10E-07	-33	6.76E-08	6.76E-08	0	2.11E-08	2.11E-08	0	2.95E-08	2.11E-08	-29
Zn	1.37E-04	7.65E-05	-44	3.69E-05	3.16E-05	-14	1.26E-06	1.54E-07	-88	1.76E-05	8.65E-06	-51

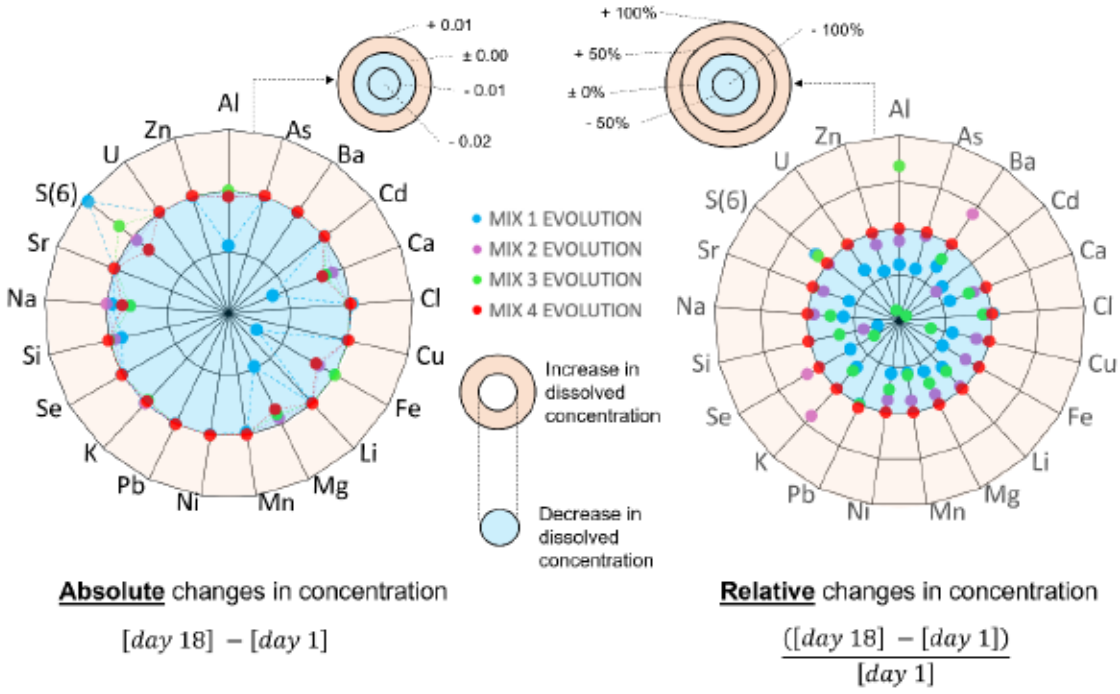

Figure 5.3 Absolute (concentration difference) and relative (% difference) changes in dissolved solids concentrations in laboratory mixtures over an 18-day period.

The solid samples retrieved from the Fe-rich acidic mixtures (mixtures 1–2–4) after day 18 of the experiment contained jarosite and Fe–SO_4–P–Si-rich particles that were deemed to be schwertmannite (Figure 5.4). The SI calculated using PHREEQC for these three mixtures also suggested supersaturation with respect to schwertmannite and jarosite. It was thus deduced that jarosite and schwertmannite were newly-formed precipitates rather than particles that were originally present on the day of mixing that settled (Kim & Kim, 2021; Schoepfer & Burton, 2021). In addition, SI calculations revealed supersaturation with respect to $Fe(OH)_3$ in the three Fe-rich acidic mixtures, suggesting that this Fe-oxyhydroxide could also influence liquid–solid equilibriums. Given their stoichiometry, the precipitation of jarosite-K ($KFe_3(SO_4)_2(OH)_6$), jarosite-Na ($NaFe_3(SO_4)_2(OH)_6$), $Fe(OH)_3$, and schwertmannite ($Fe_8O_8(SO_4)_{1.26}(OH)_{5.48}$) could explain the removal of Fe, SO_4^{2-}, K, and Na from solution through direct incorporation into mineral structures. Oxyanions of As, Cr, Se, Mo, Sb can further be immobilized by schwertmannite through sorption and coprecipitation (Schoepfer & Burton, 2021), whereas Al can be incorporated into the structure of schwertmannite (Carrero et al., 2022). It is thus likely that schwertmannite and jarosite

precipitation were the key mechanisms dictating the chemical evolution of the Fe-rich acidic mixtures. It is noteworthy that Pb can be released from schwertmannite during its transformation to goethite, whereas Cd and Co can be released into the water with slight changes in pH, Eh, and temperature (Kim & Kim, 2021). Such processes could explain the increase in Cd and Pb observed in mixture 4 after 17 days (Table 5.3). The observed decreases in Ca and Mg can be explained by the precipitation of gypsum. The presence of small amounts of gypsum in the solids retrieved from the mixtures could account for the decrease in Ca and SO_4^{2-} in the dissolved phase. It is also possible that Mg was included in gypsum as an impurity (Choi et al., 2019). Mixture 3 ($pH \geq 7.7$) showed low dissolved Fe concentrations in comparison to the Fe-rich acidic mixtures (mixtures 1–2–4) discussed above. Mixture 3 exhibited a translucent appearance throughout the entire duration of the experiment and some dark deposits were observed at the bottom of the mixing bucket on day 18 (Figure 5.4). The SEM images obtained for solids from this mixture show well-defined gypsum crystals forming a cluster, which is most likely the result of precipitation following the preparation of the mixture. The SI calculated for gypsum in mixture 3 further revealed supersaturation on the day of mixing and near-equilibrium conditions on day 18, supporting the hypothesis that gypsum precipitation occurred. An increase in NH_3-N was also observed for mixture 3 (see supplementary electronic material, SEM1); this could be explained by the presence of cyanide compounds such as OCN^- that transformed to NH_3-N by hydrolysis over time (di Biase et al., 2020).

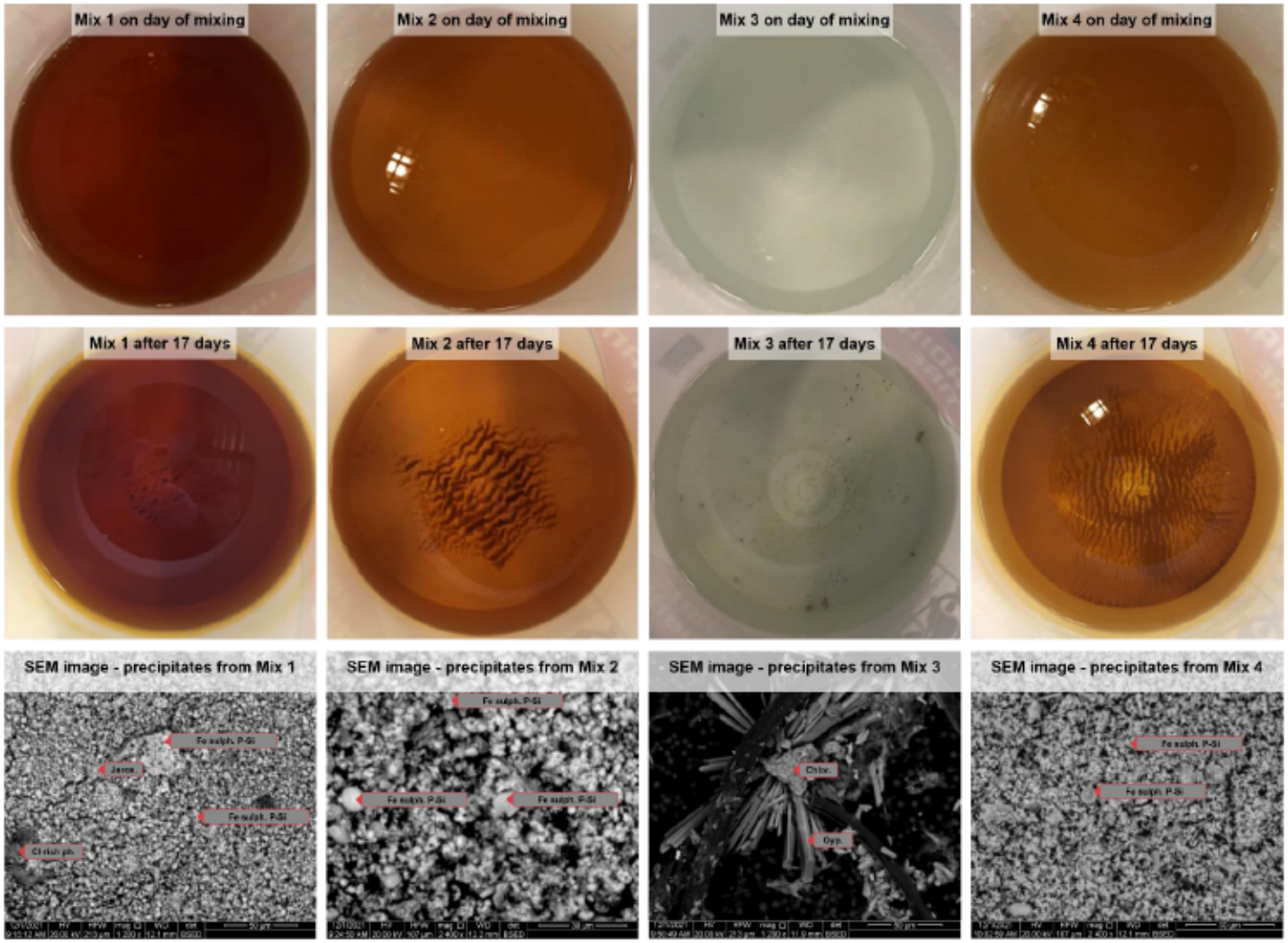

Figure 5.4 Visual observations and mineralogical analyses conducted on the solids from effluent mixtures prepared in the laboratory and allowed to react for 17 days.

Further to the mineralogical analyses discussed above, it is noteworthy that microbiological activity could have significantly influenced the formation of solids during the mixing experiments. As an example, Figure 5.5 shows SEM images at 5 and 10 µm (collected with the TIMA) of precipitates from mixture 4. The circular shape of the Fe–S–O-rich solids suggests that they could have been formed through a bacterial reaction. The fibrous outer sphere and sheaths visible in the images is characteristic of this type of reaction (Konhauser, 1997). Thus, further modeling efforts focusing on the evaluation of bacterially-mediated processes will be needed to improve models based on inorganic geochemistry.

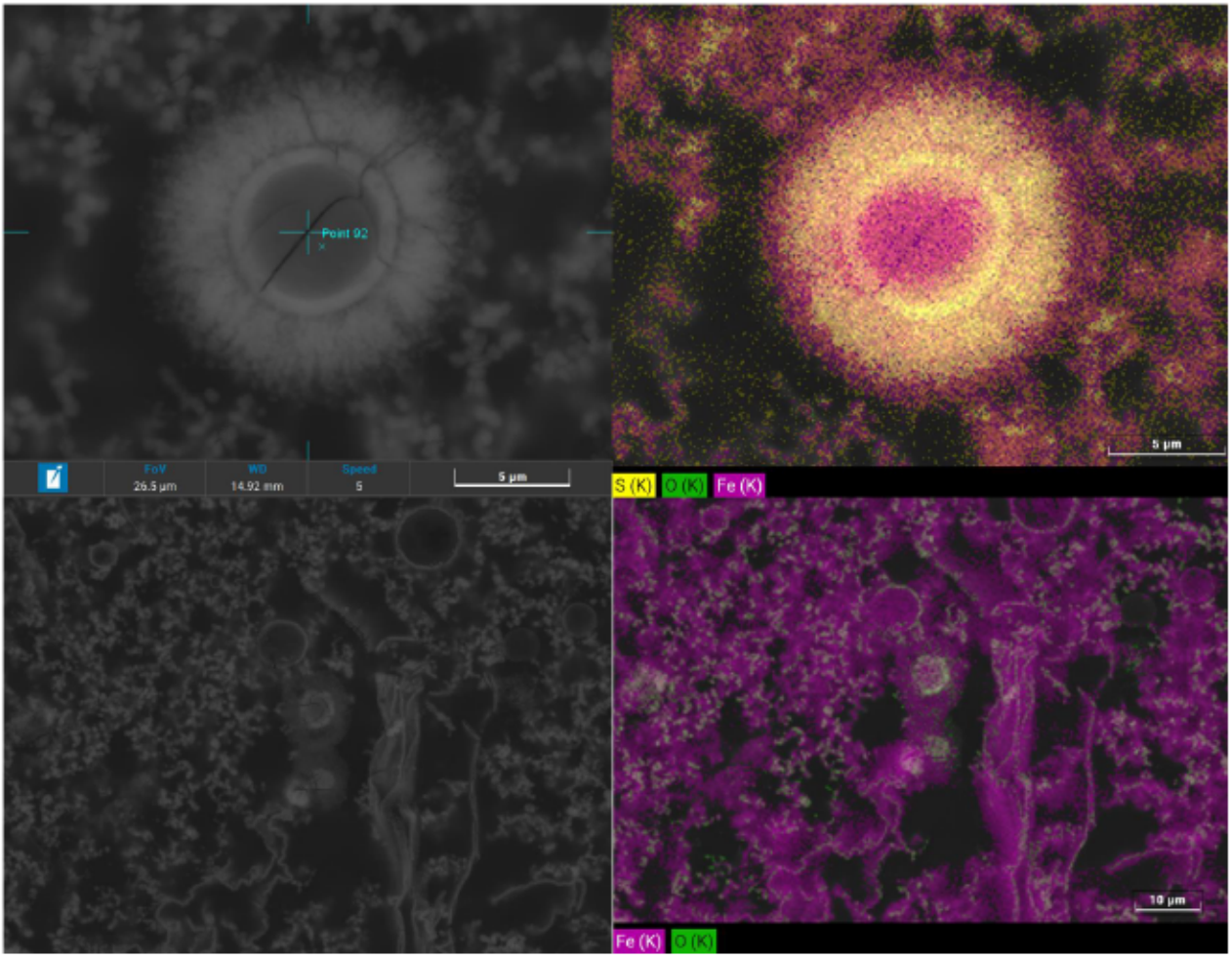

Figure 5.5 Scanning electron microscopy (SEM) images of Fe–S–O precipitates in mixture 4 showing typical characteristics of a solid formed through a bacterial reaction.

5.5.1.2 Geochemical modeling of laboratory experiments

The first step related to the modeling of laboratory mixing experiments consisted of comparing the predicted mixture compositions using the MIX keyword in PHREEQC (y-axis) with the actual dissolved solids concentrations measured on days 1 and 18 (x-axis) (Figure 5.6 A-B). With this approach, the modeled concentrations simply represent the amount-weighted average composition of the mixture. The points plotted above the 1:1 line (predicted concentration > observed concentration) were deemed to be associated with phases undergoing immobilization processes (precipitation, sorption), whereas the points plotted below the 1:1 line (predicted concentration < observed concentration) were deemed to be associated with phases undergoing mobilization processes (dissolution, desorption). The second modeling step consisted of comparing the predicted mixture compositions using the MIX and EQUILIBRIUM PHASES keywords in PHREEQC (y-axis) with the actual dissolved solids concentrations measured on days 1 and 18 (x-axis) (Figure 5.6 C-D). The equilibrium calculations were forced to allow only mineral precipitation (no dissolution). With this approach, the modeled dissolved solids concentrations represent the composition of the mixtures after equilibrium was reached for the selected mineral phases, following precipitation processes. The mineral phases included for the equilibration of the mixtures in PHREEQC were $Fe(OH)_3$, gypsum, jarosite-K, jarosite-Na, and schwertmannite, which was consistent with the laboratory observations (section 4.1.1). The gas phases included for the calculations were O_2 and CO_2, using their respective partial pressures in the atmosphere (Nordstrom, 2020). The points plotted above the 1:1 line (predicted concentration > observed concentration) were deemed to be associated with phases undergoing immobilization processes (precipitation, sorption) through a mechanism not accounted for by the model, whereas the points plotted below the 1:1 line (predicted concentration < observed concentration) were deemed to be associated with phases undergoing precipitation with slow kinetics (equilibrium not reached). Considering the mineral phases retained for the models, a focus was placed on the elements included in the stoichiometry of the minerals, namely Fe, S (SO_4^{2-}), K, and Na.

The results suggest that a simple mixing calculation using the MIX keyword in PHREEQC allowed for a realistic estimate of the dissolved solids concentrations in the mixtures day 1. This is seen in Figure 5.7 A, where most points fall close to the 1:1 line. However, the data showed more variability when modeled concentrations obtained with the MIX keyword were compared with measured concentrations on day 18, with most of the modeled concentrations falling above the 1:1

line (Figure 5.7 B). This is consistent with the effect of precipitation processes leading to a decrease in dissolved solids concentrations, a process not accounted for when solely using the MIX keyword. When using the MIX and EQUILIBRIUM PHASES keywords, most of the modeled concentrations for day 18 fall closer to the 1:1 line in comparison to the modeled concentrations obtained using solely the MIX keyword (mixtures 1–2–4) (Figure 5.7 B-D). The general observation from these results is that both straightforward mixing calculations and mixing calculations combined with equilibrium calculations can be used to realistically estimate the dissolved solids concentrations in the mixtures on day 18 of the experiment. Inverse models were also tested using the INVERSE MODELING keyword in PHREEQC to model the phase mole transfers of the selected mineral phases in the laboratory mixtures between day 1 and day 18 (see SEM1 for PHREEQC script). As for the EQUILIBRIUM PHASES calculations, the mineral phases included for the inverse models in PHREEQC were $Fe(OH)_3$, gypsum, jarosite-K, jarosite-Na, and schwertmannite, along with O_2 and CO_2, using their respective partial pressures in the atmosphere. The uncertainty in the model input was iteratively adjusted to limit the number of possible solutions while ensuring that at least one solution could converge. The obtained inverse model solutions are presented in Figure 5.8. The results suggest jarosite precipitation for all Fe-rich acid mixtures (mixtures 1–2–4). The inverse models suggest that schwertmannite precipitation was less prevalent than jarosite precipitation; this is potentially explained by the difference in the stochiometric formula of the two species, with 8 Fe atoms and 3 Fe atoms, respectively. Gypsum precipitation was also modeled for mixture 3, which was consistent with the mineralogical observations for this mixture (Figure 5.4). Overall, the inverse models only represent first-order estimates of the phase mole transfers in the modeled systems due to the limited number of phases included in the calculations and the multiple possible solutions.

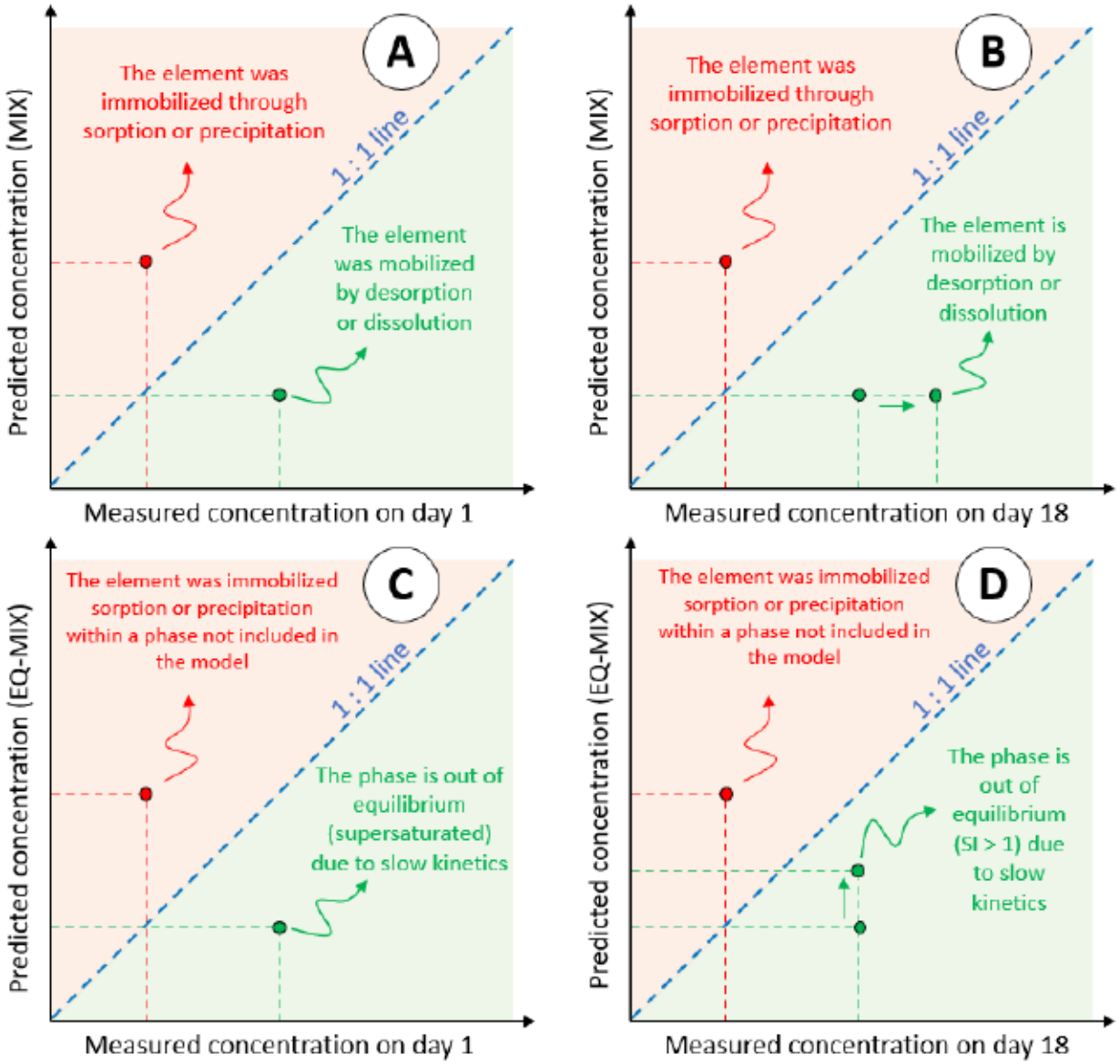

Figure 5.6 Interpretation key for comparisons between modeled and observed dissolved solids concentrations.

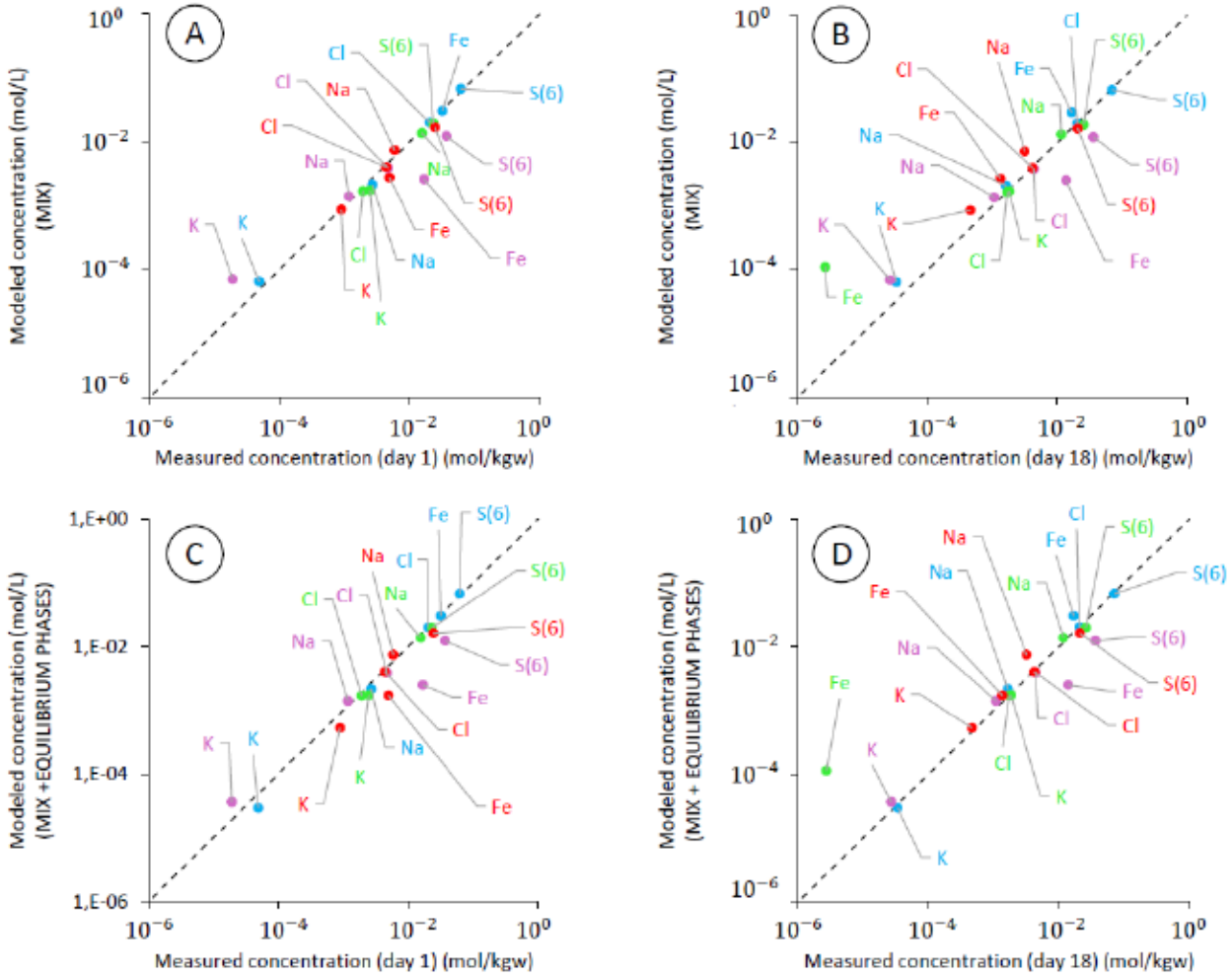

Figure 5.7 Comparisons between modeled and observed dissolved solids concentrations (the color code for data is the same as in Figure 5.3).

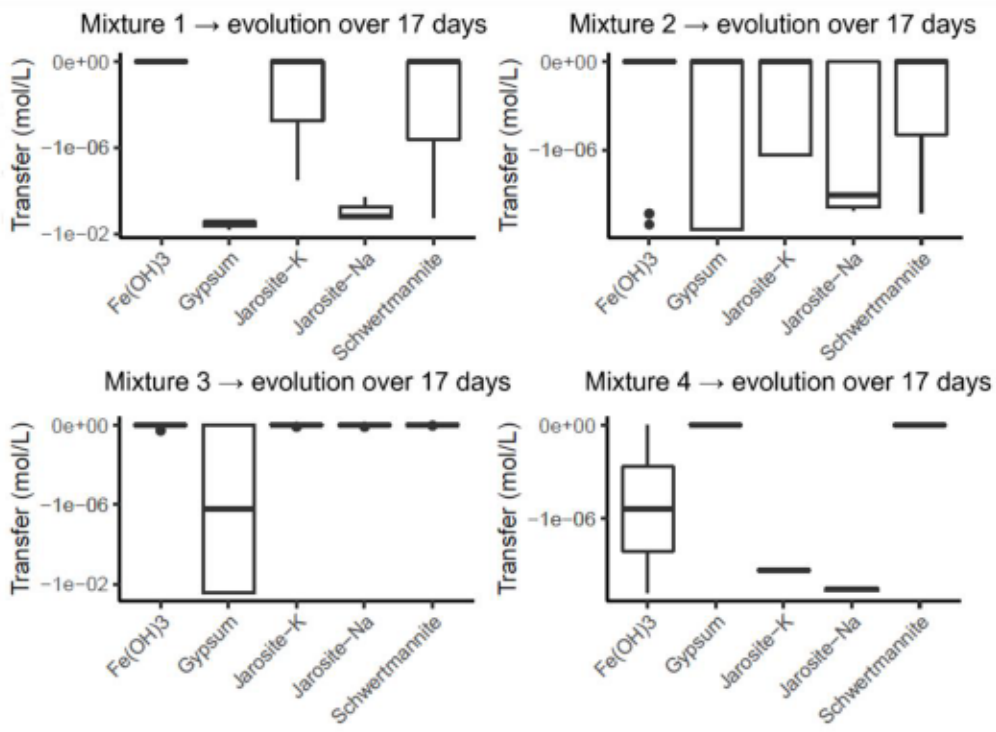

Figure 5.8 Phase mole transfer calculated from the inverse models for the laboratory experiments.

5.5.2 On site geochemical monitoring

5.5.2.1 Observations pertaining to the hydrological processes occurring onsite

The isotopic data associated with the June 2021 sampling campaign were selected to assess the hydrological processes occurring at the site, with a focus on mixing and evaporation processes. The measured $\delta^{18}O$ and $\delta^{2}H$ values ranged from –12.88‰ to –7.22‰ and from –95.9‰ to –67.7, respectively. All data plotted below the local meteoric water line (LMWL, as defined by Rey et al. (2018)) and defined a local evaporation line (LEL) line with $\delta^{2}H = 5.05 \times \delta^{18}O - 29.51‰$ (R^2 = 0.95) (Figure 5.9). The intercept between the LEL and MWL yielded $\delta^{18}O$ and $\delta^{2}H$ values of –13.87‰ and –99.58‰, respectively. These values are very close to the amount-weighted mean annual isotopic composition of precipitation in the study region as calculated by Rey et al. (2018), suggesting that the waters at the site were uniformly recharged by precipitation throughout the seasons. The data suggest that evaporation over inflow (E/I) ratios were greatest at the NP, TSF1, and TSF3W sites and lowest in the nearby river. Such observations are consistent with the conceptual flowchart of the site, as the NP and TSF1 sites correspond to inactive basins where shallow waters can evaporate while TSF3W is a basin where water is recirculated, allowing for

increased evaporation with time. The E/I ratios were estimated using the *Hydrocalculator (v. 1.03)* application, which is based on the revised Craig & Gordon (1965) model (Skrzypek et al., 2015). The calculations were performed assuming steady state conditions, a known LEL, a relative humidity of 70%, an average temperature of 15°C, and precipitation presenting an isotopic composition equal to that of the mean annual precipitation. The estimates suggested E/I ratios ranging between 3% in the nearby natural river and 39% at the site NP. These data reveal that evaporation is likely to impart a significant influence on the site hydrological and chemical balances, as dissolved solids concentrations increased with increasing E/I. The significant evaporation rates revealed by the isotopic data suggest that they should not be used for the calculation of mixing ratios. In a system without evaporation, the isotopic composition of water from a mixture (δ_{MIX}) of n components should represent the amount (Q_i) -weighted average of the different mixture components (δ_i):

$$\delta_{MIX} = \sum_{i=1}^{n} \delta_i Q_i \qquad \text{Equation 1}$$

$$\sum_{i=1}^{n} Q_i = 1 \qquad \text{Equation 2}$$

In such a context, isotopic data (δ_{MIX}; δ_i) can be used to calculate the contributions of various sources to a mixture (Q_i) when $n = 2$. However, for a system where water from a mixture is affected by evaporation, the amount-weighted average approach (Eq. 1–2) to calculating mixing ratios is no longer valid. Therefore, pumping data estimated by the site operator was selected rather than isotopic data for the calculation of the mixing ratios, and the calculated E/I ratios were used to evaluate the potential influence of evaporation on the dissolved solids concentrations.

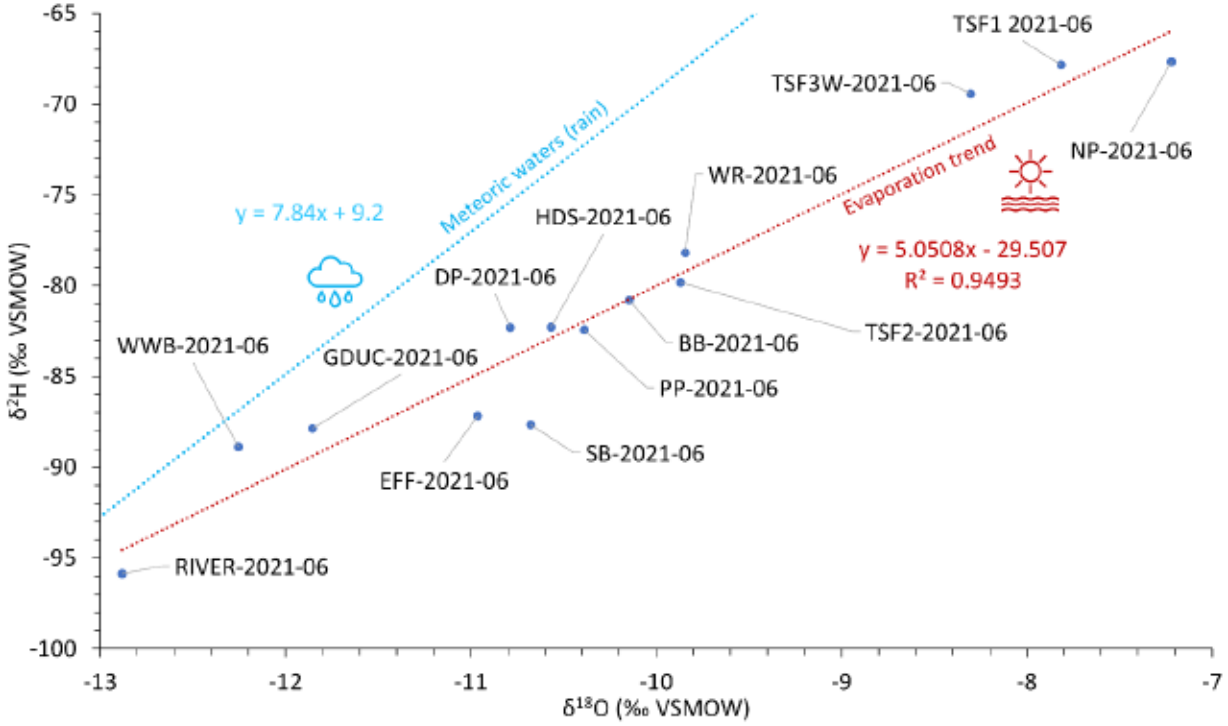

Figure 5.9 Isotopic composition of the samples collected in June 2021 and calculated LEL (LMWL from Rey et al. (2018)). GDUC represents a sampling point in a new open pit on the mine site.

5.5.2.2 Observations pertaining to the spatiotemporal variability of onsite water quality

The statistical summary of geochemical data for the five sampling campaigns is presented in Table 5.4 (see SEM1 for complete dataset). The data show that the dominant major cations were Ca > Na > K. One noticeable feature is that Fe and Al concentrations were high in most of the samples, thus significantly contributing to positive charges in solution. The dominant anions were SO_4^{2-} > Cl^- > NO_3^-, whereas alkalinity was low, except for sites TSF3W, TSF3E, WWB, and DP. The simulations conducted using PHREEQC revealed that several samples showed positive charge balance errors, especially when the pH was less than 3 (Figure 5.10). Four main hypotheses could explain this observation. First, this could be due to sample preservation techniques. Samples for cation analyses were kept at pH < 2, whereas samples for anion analyses were not subjected to pH adjustment. Under such conditions, it is possible that precipitation occurred in some samples aimed at anion analyses or that the dissolution of suspended sediments occurred in samples used for cation analyses. The second hypothesis is that the speciation calculations performed here failed to

adequately represent positively charged dissolved species. This could be due to the speciation calculations associated with Al and Fe, as these two elements were abundant in low-pH samples and can form dissolved species with different charges. Thus, errors in speciation calculations for Al and Fe species could lead to charge balance errors. The third hypothesis is that colloidal particles of Al and Fe were present; these particles can pass through the 0.45 µm filter during the sampling process, resulting in an overestimation of the real dissolved concentrations (Nordstrom, 2020). The presence of Al and Fe colloidal particles can then decrease the concentration of trace elements such as As, Cd, Cu, Mn, Ni, and Zn by coprecipitation and adsorption (Hem, 1985; Balistrieri et al., 2007). The fourth hypothesis is that the pH measurements were affected by the suspension effect or that clogging of the porous frit of the pH electrode occurred, leading to erroneous pH values.

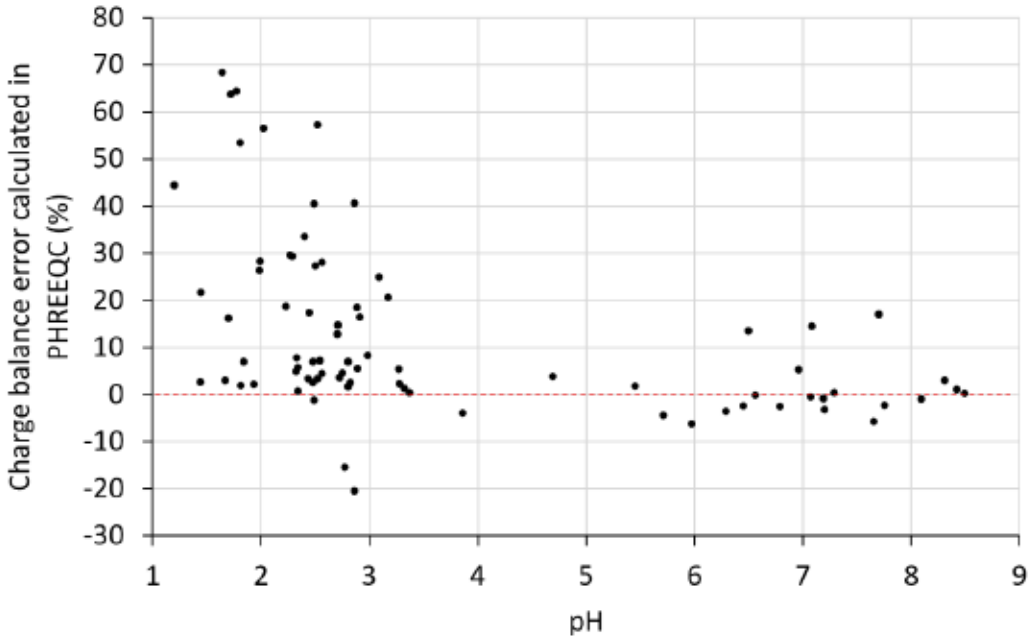

Figure 5.10 Calculated charge balance errors as a function of pH

The electrical conductivity of the water (corrected to 25°C) can further be compared to the ionic strength of the water calculated in PHREEQC to check the quality of the results. In Figure 5.11, all samples with charge balance errors < 10% (shown in green) were used to evaluate the regression line between conductivity and ionic strength. The points plotted far above the regression line most likely correspond to samples in which the dissolution of colloids has occurred (see hypothesis 3

above). Under such circumstances, it seems realistic to propose that the ionic strength calculated from the analytical results was overestimated as compared to the in situ water conductivity measurement. The points plotted close to the regression line that present large charge balance errors could be associated with hypotheses 2 and 4 above. Overall, when interpreting results, it should be recognized that some samples show a non-negligible excess of dissolved cations.

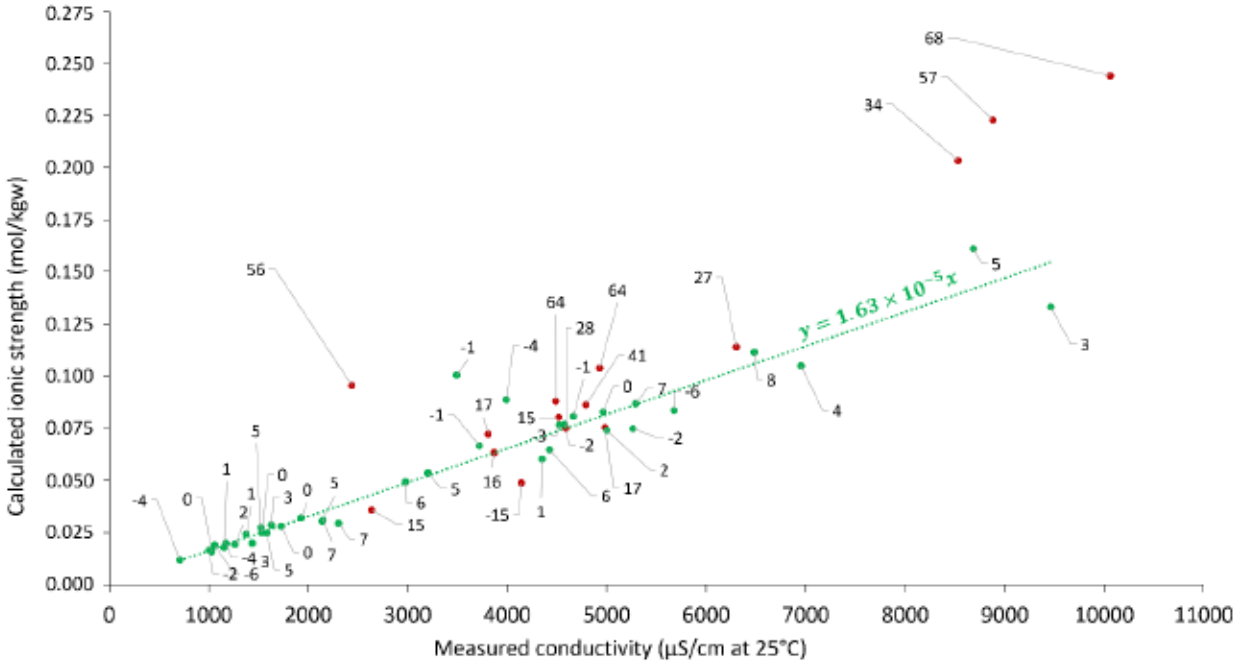

Figure 5.11 Calculated ionic strength plotted against in situ water conductivity. The green dots correspond to samples with charge balance errors < 10%; these were used to calculate the illustrated correlation line. The red dots correspond to samples with charge balance errors > 10%. Labels correspond to the charge balance errors (%) calculated in PHREEQC.

Table 5.4 Data from the five campaigns used for the models. Presented as min-max (average)

	TSF1	TSF2	TSF3W	TSF3E	BB	WWB	SB	WR	DP	NP
Temp.	6.9–19.7 (13.52)	6.4–20.4 (13.54)	6.5–20.2 (13.44)	6.4–20.5 (13.66)	7.1–20.8 (14.3)	10–22.4 (16.94)	7.5–21.1 (15.06)	7.3–22.2 (14.3)	6.9–18.7 (11.4)	10–16 (13)
pH	2.02–2.82 (2.59)	2.8–3.86 (3.32)	6.56–8.49 (7.73)	6.29–8.31 (7.39)	1.77–2.89 (2.45)	4.69–6.45 (5.65)	1.64–2.5 (2.24)	1.72–2.49 (2.29)	6.79–7.2 (7.07)	2.86
O_2	4.77–11.55 (7.53)	4.87–12.16 (8.86)	6.4–10.14 (8.91)	7.72–11.03 (9.72)	6.68–12.38 (9.4)	6.32–9.32 (7.70)	0.17–9.29 (5.14)	0.22–11.18 (7.44)	1.01–7.12 (4.86)	10.5
pe	11.25–18.17 (13.25)	10.27–15.18 (11.93)	6.72–14.04 (9.22)	6.99–13.84 (9.04)	11.59–18.82 (13.51)	7.16–14.25 (8.95)	11.94–15.08 (12.80)	7.96–19.28 (12.88)	2.40–13.65 (7.41)	11.81
Alk.			25–51 (36.6)	18–28 (23.75)		4–12 (8)			124–177 (161.8)	
Al	12.6–184.16 (51.65)	6.53–11.3 (8.73)	0.069–0.42 (0.18)	0.079–0.32 (0.18)	42.1–137.10 (80.74)	0.051–0.88 (0.39)	381–788.05 (565.61)	111–162 (124.33)	0.0025–0.075 (0.043)	13.20–25.78 (19.49)
As	0.0004–0.18 (0.051)	0.0004–0.125 (0.032)	0.0002–0.087 (0.022)	0.0002–0.069 (0.020)	0.0036–0.072 (0.027)	0.0011–0.068 (0.021)	0.03–0.2572 (0.084)	0.0068–0.06 (0.029)	0.00025–0.068 (0.020)	0.0041–0.0049 (0.0045)
NH_3-N	0.08–3.8 (2.23)	1.2–3.44 (2.62)	0.09–17 (7.80)	0.01–0.2 (0.088)	0.34–2.6 (1.69)	0.48–12.9 (9.02)	0.05–0.38 (0.16)	0.28–5.1 (2.67)	54.5–60.02 (56.64)	0.79–3.19 (1.99)
Ba	0.0003–0.03 (0.012)	0.0083–0.022 (0.016)	0.012–0.018 (0.014)	0.004–0.012 (0.0087)	0.0006–0.023 (0.016)	0.086–0.14 (0.11)	0.0003–0.035 (0.020)	0.0064–0.036 (0.025)	0.056–0.12 (0.08)	0.006–0.022 (0.014)
Br	0.0059–0.7 (0.36)	0.0006–0.7 (0.35)	0.00025–0.7 (0.44)	0.00025–0.7 (0.36)	0.002–8.6 (4.46)	0.00025–25 (18.28)	0.028–1.13 (0.58)	0.0018–13 (7.54)	0.00025–7.5 (3.54)	0.0007–0.03 (0.015)
Cd	0.0015–0.007 (0.0044)	0.0015–0.007 (0.0044)	0.00001–0.006 (0.0038)	0.00001–0.005 (0.0029)	0.0015–0.009 (0.0057)	0.0015–0.042 (0.022)	0.00001–0.003 (0.0021)	0.0015–0.012 (0.0064)	0.00008–0.015 (0.0055)	0.00056–0.00077 (0.00067)
Ca	140–520 (274.4)	123–279.4 (10)	246–318 (274.5)	110–319 (210)	239–517 (335.6)	898–1,380 (1,060)	180–785 (354)	304–667 (467.6)	556–615 (587.4)	102–256 (179)
Cl	16–32.7 (24.4)	11.7–24.2 (17)	17–26.3 (22.3)	4.6–31.2 (11.36)	125–376.3 (215.7)	1,052–1,912 (1,469)	2.9–5.3 (4.26)	328–562 (477)	78–106 (87)	2.8–39.8 (21.3)
Cu	0.61–1.56 (0.91)	0.724–1.67 (1.33)	0.035–0.12 (0.064)	0.0015–0.010 (0.0058)	1.04–1.65 (1.37)	0.12–0.54 (0.26)	3.42–9.07 (5.45)	1.3–2.10 (1.76)	0.038–0.36 (0.18)	0.49–0.53 (0.51)
Fe	15–66.5 (35.8)	0.598–15.9 (3.45)	0.024–19.51 (4.90)	0.005–0.032 (0.020)	162–481.34 (337.87)	0.044–4.21 (1.61)	1,060–2,667 (1,850)	380–817 (575.30)	0.005–8.66 (1.78)	17.63–160 (88.8)
F	0.1–0.97 (0.37)	0.1–1.21 (0.33)	0.2–1.15 (0.52)	0.1–1.03 (0.38)	0.1–1.44 (0.49)	0.1–0.6 (0.28)	0.1–3.72 (1.06)	0.1–0.2 (0.16)	0.1–0.8 (0.33)	0.91
Li	0.01–0.021 (0.017)	0.005–0.013 (0.0092)	0.009–0.013 (0.01)	0.004–0.012 (0.009)	0.045–0.10 (0.072)	0.039–0.05 (0.043)	0.28–0.47 (0.39)	0.093–0.14 (0.11)	0.028–0.051 (0.042)	0.013–0.025 (0.019)
Mg	24.1–248.27 (82.21)	17.3–82.33 (35.8)	10.8–13.6 (12.3)	12.8–32.1 (22.16)	53.4–162.91 (102.62)	27.6–46.1 (37.20)	380–852 (606.75)	113–172 (148.6)	156–221 (178.3)	30–35.7 (32.9)
Mn	2.02–19.50 (6.46)	2.58–6.46 (4.04)	0.002–0.28 (0.12)	0.005–0.036 (0.020)	4.28–10.94 (6.55)	3.38–5.34 (4.65)	21.5–58.34 (33.01)	6.17–12.43 (8.68)	10.2–13.6 (11.49)	2.51–3.00 (2.75)
Ni	0.043–0.79 (0.22)	0.033–0.06 (0.21)	0.0071–0.021 (0.014)	0.0022–0.009 (0.0056)	0.13–0.33 (0.21)	0.028–0.064 (0.041)	0.70–2.14 (1.17)	0.23–0.38 (0.29)	0.10–0.15 (0.12)	0.060–0.096 (0.078)

	TSF1	TSF2	TSF3W	TSF3E	BB	WWB	SB	WR	DP	NP
NO_3^-	0.03–8.3 (3.22)	0.1–11 (3.96)	0.84–11 (5.81)	0.01–8.7 (3.63)	0.37–15 (7.6)	1.42–81 (46.44)	0.14–6.8 (2.01)	0.29–34 (14.64)	0.01–28 (11.41)	0.05–0.2 (0.13)
NO_2^-	0.01–0.7 (0.36)	0.005–0.7 (0.35)	0.07–1.07 (0.64)	0.01–0.7 (0.37)	0.005–0.7 (0.35)	0.02–0.7 (0.49)	0.01–0.7 (0.36)	0.005–0.7 (0.36)	0.02–2.7 (0.85)	0.005–0.06 (0.033)
P	0.45–0.9 (0.75)	0.45–0.9 (0.75)	0.9–0.9 (0.9)	0.45–0.9 (0.75)	5.5–24 (13.8)	0.45–0.9 (0.75)	0.45–0.9 (0.75)	6–24 (14.67)	0.45–0.9 (0.75)	0.14
Pb	0.00009–0.01 (0.0035)	0.0046–0.012 (0.0037)	0.0001–0.0017 (0.0008)	0.0001–0.01 (0.0023)	0.0001–0.025 (0.0079)	0.00009–0.01 (0.0026)	0.00009–0.056 (0.027)	0.0001–0.036 (0.018)	0.00009–0.01 (0.0030)	0.00008–0.00009 (0.000085)
K	0.025–5.4 (2.81)	3.36–6.24 (2.55)	10.7–23.8 (19)	4.76–12 (9.15)	1.55–7.46 (4.10)	6.82–13.1 (10.75)	0.025–0.32 (0.16)	0.99–4.05 (2.94)	55–95.27 (65.49)	1.24–1.73 (1.49)
Se	0.001–0.15 (0.033)	0.0004–0.038 (0.021)	0.0004–0.0005 (0.00043)	0.0003–0.0059 (0.0015)	0.012–0.10 (0.042)	0.0004–0.063 (0.015)	0.039–0.20 (0.12)	0.012–0.103 (0.046)	0.00025–0.0096 (0.0053)	0.018–0.022 (0.020)
Si	6.66–122.85 (36.16)	3.96–36.53 (11.83)	0.38–0.61 (0.49)	0.064–0.95 (0.29)	12.1–75.86 (27.47)	4.82–21.07 (9.28)	0.005–57.9 (37.18)	17.4–37.96 (23.69)	4.41–22.31 (9.29)	17.3–51.9 (34.6)
Na	10.57–34.2 (23.35)	25.3–40.4 (30)	45.67–101 (80.37)	15.6–48.7 (33.89)	27.5–49.53 (37.65)	96.3–128.91 (107.30)	1.93–5.45 (3.56)	27–47.6 (40.54)	265–445.88 (308.18)	6.06–26.5 (16.28)
Sr	0.029–0.26 (0.19)	0.14–0.86 (0.26)	0.46–0.69 (0.57)	0.15–0.52 (0.32)	0.30–2.49 (1.42)	11.2–18.23 (13.89)	0.12–0.21 (0.16)	2.83–5.14 (4.36)	1.77–2.36 (1.99)	0.1–0.25 (0.18)
SO_4^{2-}	630–3,880 (1,516)	470–1,513 (744)	753–1,001 (840)	312–879 (621)	1,130–2,887 (1,803)	749–1,057 (893)	5,290–11,371 (8,563)	1,540–3,861 (2,606)	2,460–2,774 (2,664)	492–1350 (921)
U	0.0008–0.018 (0.0047)	0.0007–0.002 (0.001)	0.0005–0.0007 (0.00065)	0.0005–0.0007 (0.00062)	0.003–0.009 (0.006)	0.0007–0.009 (0.0025)	0.018–0.082 (0.035)	0.007–0.013 (0.0094)	0.001–0.005 (0.0023)	0.001–0.002 (0.0015)
Zn	0.13–1.08 (0.39)	0.38–0.65 (0.53)	0.007–0.09 (0.045)	0.005–0.13 (0.032)	0.99–3.63 (1.81)	5.14–9.97 (7.45)	1.46–4.38 (2.36)	2.26–5.47 (3.36)	0.069–1.43 (0.52)	0.13–0.16 (0.15)

All concentrations are in mg/L. Temperature is expressed in °C. Alkalinity is expressed as mg $CaCO_3$/L

The heatmap produced for the monitoring data suggests that four main groups of dissolved substances can be identified (Figure 5.12; Table 5.5). Groups 1A and 1B contain major alkali (Na, K) and alkaline earth elements (Ca, Sr) along with Cl^- and Br^-. The correlations in dissolved species concentrations observed for these groups of elements likely represent mobilization processes related to the dissolution of carbonates (potential source of Ca and Sr), silicates (potential source of Na and K), and Cl^- and Br^--bearing salts. Groups 2A and 2B contain dissolved SO_4^{2-} along with several transition metals and metalloids such as As, Fe, Mn, Cu, Zn, and Pb. The correlations in dissolved species concentrations observed for these groups of elements likely represent mobilization/immobilization processes related to the dissolution of sulfide minerals (potential source of SO_4^{2-}, metals, and metalloids) and secondary mineral precipitation, such as schwertmannite, $Fe(OH)_3$, and jarosite. These minerals were indeed identified as potential sinks of Fe, Na, K, and S through precipitation and potential sinks of metals and metalloids through coprecipitation and sorption (see section 4.1). The saturation indices (SI > 1) calculated using PHREEQC for these minerals are shown in Figure 5.13. The highest SI values were obtained for schwertmannite > $Fe(OH)_3$ > jarosite-ss, while jarosite-K and gypsum were generally characterized by SI $\approx$ 0 and jarosite-Na was generally undersaturated. These observations suggest that precipitation mechanisms occurring onsite did not reach equilibrium for schwertmannite and $Fe(OH)_3$, the two most important minerals found in the laboratory experiments, whereas gypsum and jarosite-K could have reached equilibrium for several samples. It thus seems likely that the covariation of the phases included in groups 2A and 2B of the heatmap was governed by the weathering of primary sulfides found in the host rocks followed by the precipitation of schwertmannite, $Fe(OH)_3$, gypsum, and jarosite. The geochemical behavior of the phases in groups 1A and 1B was decoupled from that of the groups 2A and 2B. This is likely because the primary minerals that were the sources of the dissolved solids differed (mainly silicates for group 1 and sulfides for group 2) and because the secondary phases that precipitated did not incorporate enough of the elements included in group 1 to drive correlations with elements from group 2. Based on the hypothesis that schwertmannite (and $Fe(OH)_3$) could impart a significant control on Fe, SO_4^{2-}, and trace metal and metalloid concentrations, as discussed in section 4.1, it appears that water management strategies aimed at increasing water residence times in ponds and basins could lead to decreases in dissolved solids concentrations in most of the waters onsite.

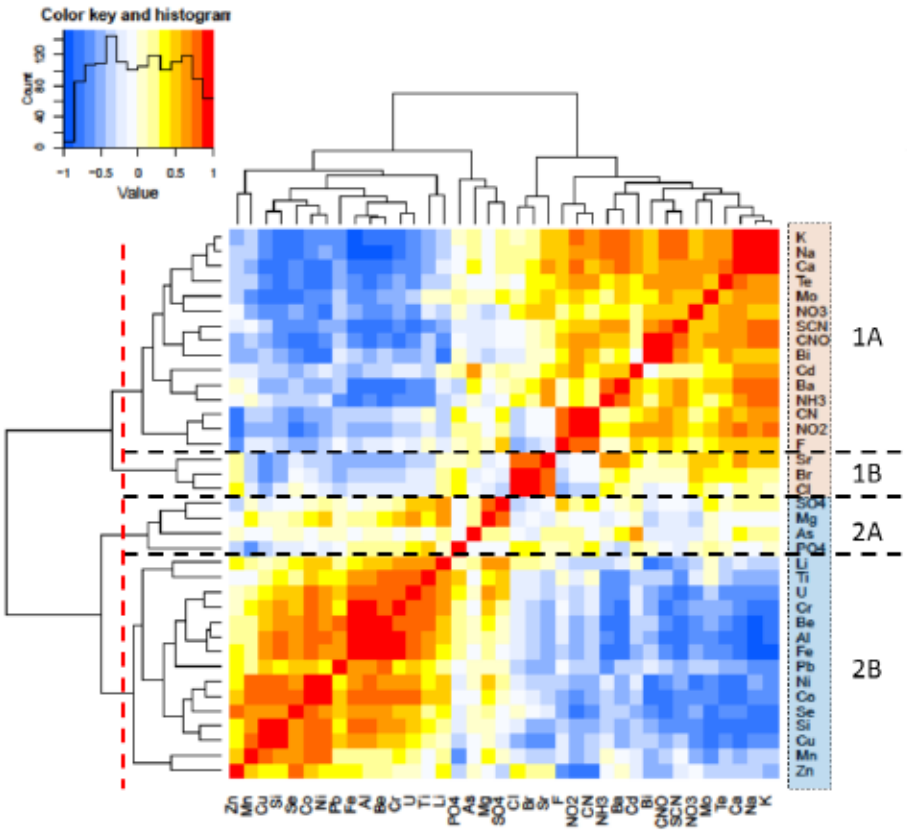

Figure 5.12 Heatmap generated from the data collected during the sampling campaigns.

Table 5.5 Classification of the different parameters based on the heatmap analysis.

Groups		Parameters	Potential mineral phases	Potential key reactions	Potential indicators
1	A	K, Na, Ca, NO_3^-, Cd, Ba, NH_3, NO_2^-, F	The presence of alkali and alkaline earth elements in this group suggests that silicates and carbonates could be involved.	Silicate hydrolysis and carbonate dissolution, controlled by pH.	Silicate hydrolysis and carbonate dissolution should entail an increase in pH.
	B	Sr, Br, Cl			
2	A	SO_4^{2-}, Mg, As, PO_4^{3-}	Sulfur and transition metals (+metalloids) are abundant; thus, oxides, hydroxides, and sulfides could be involved.	The stability of oxides and sulfides should strongly depend on Eh and pH.	Sulfide dissolution should entail an increase in SO_4^{2-} and a decrease in pH.
	B	Li, Ti, U, Cr, Be, Al, Fe, Pb, Ni, Co, Se, Si, Cu, Mn, Zn			

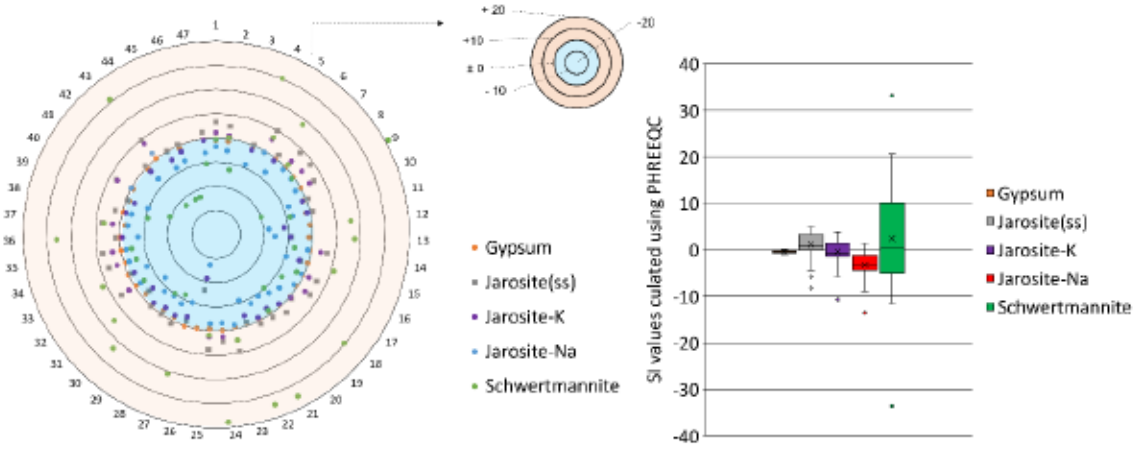

Solution numbers are shown on the left-hand diagram (refer to SEM1)

Figure 5.13 Saturation indices calculated using PHREEQC for the field samples

5.5.2.3 Geochemical modeling of onsite mixing processes

The three approaches used for modeling laboratory mixing experiments were also applied to evaluate onsite mixing processes. The interpretation key developed for interpreting model results for the laboratory experiments was used for the field observations. Figure 5.14 presents the comparisons between the calculated concentrations (MIX keyword and MIX + EQUILIBRIUM PHASES keywords) and the observed concentrations. The focus was set on field mix 1 (WWB + SB → WR) and field mix 2 (TSF2 + NP + TSF3E + WR → BB) (Table 5.2 indicates mixing ratios). The observations pertaining to field mixing processes are similar to those obtained for laboratory mixing experiments. Overall, simulation results obtained using only the MIX keyword generally exceeded field observations (i.e., the model overestimated dissolved solids concentrations) (Figure 5.14 A and C). This is most likely because precipitation processes occurred in WR following mixing of the influents. When using the MIX + EQUILIBRIUM PHASES keywords (Figure 5.14 B and D), the modeled K concentrations fell far below the 1:1 line, suggesting that schwertmannite and/or jarosite precipitation was relatively slow and that the system remained supersaturated with respect to these minerals. This is consistent with the SI indexes calculated onsite.

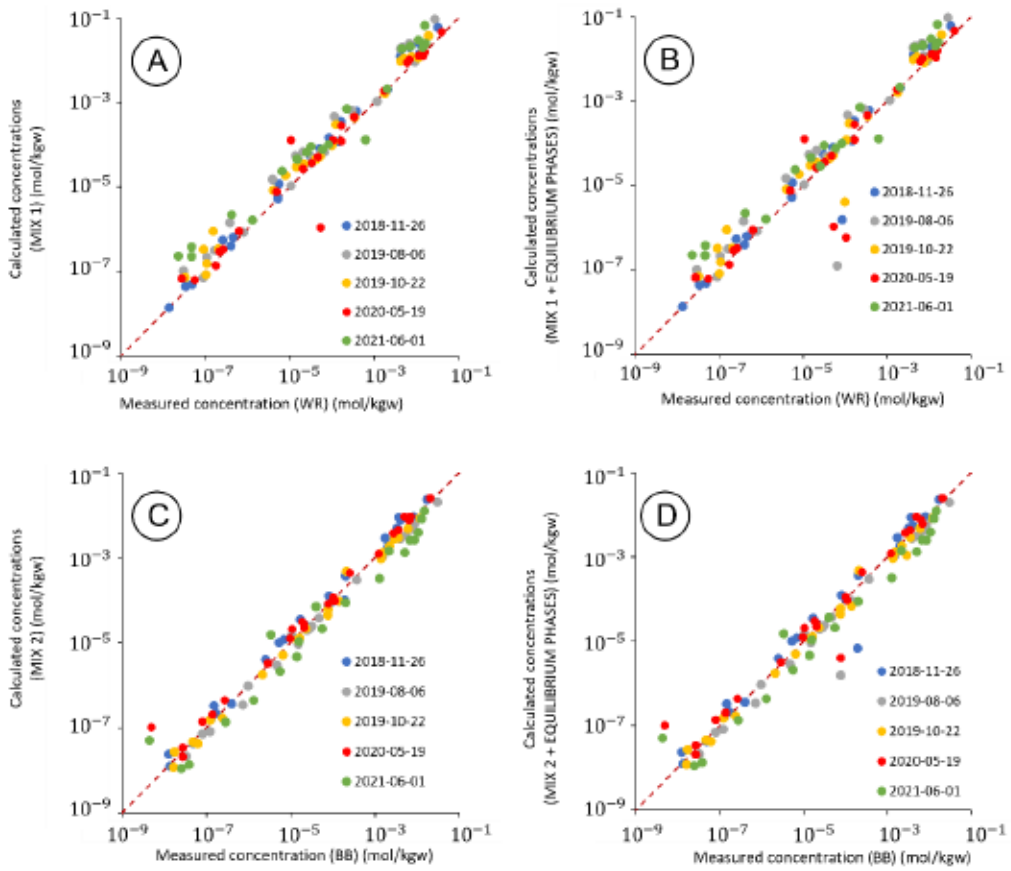

Figure 5.14 Modeled vs observed dissolved concentrations for the field mixtures.

The inverse models developed to represent mixtures 1 and 2 under field conditions consisted of using the INVERSE MODEL keyword to obtain (a) the WR composition from WWB and SB with the mineralogical phases identified in section 4.1 (WWB + SB → WR) and (b) the BB from TSF2, NP, TSF3E, and WR with the mineralogical phases identified in section 4.1 (TSF2 + NP + TSF3E + WR → BB). The inverse models only allowed for mineral precipitation (no dissolution). The results obtained for mixtures 1 and 2 under field conditions for different dates are presented in Figure 5.15. The results suggest that jarosite (and schwertmannite, to a lesser extent) precipitation was important in mixture 1. However, the results varied greatly with time, suggesting that mixing and precipitation processes onsite vary over time in a manner that cannot be predicted using the simple inverse model used here. A similar interpretation applies for mixture 2 (Figure 5.15), which showed considerable variability with time. The overall conclusion from the models discussed above is that the combined MIX and MIX + EQUILIBRIUM PHASES simulations allowed for the

most simple and realistic interpretation of the data when using the interpretation key presented in Figure 5.6.

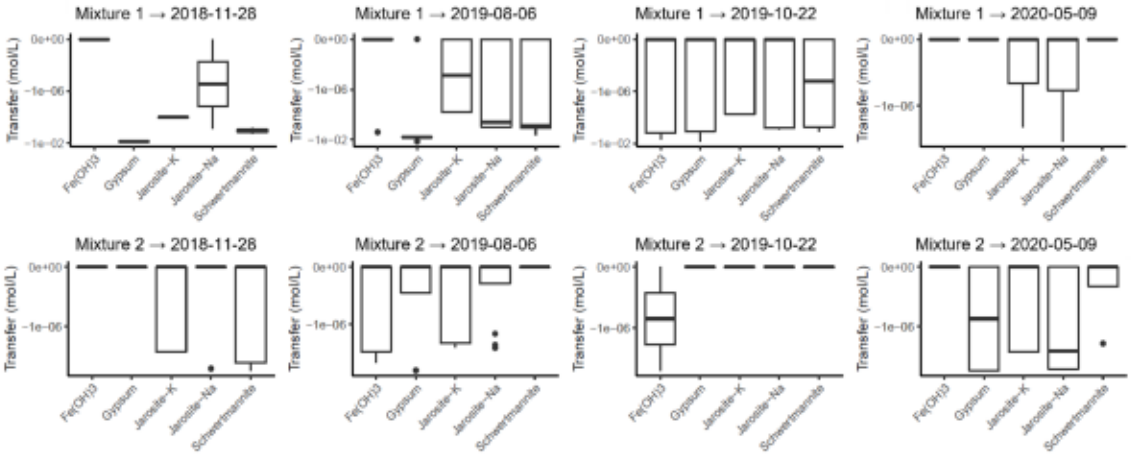

Figure 5.15 Phase mole transfer calculated from the inverse models for field observations.

5.5.3 Main limitations

The approach of modeling the geochemical evolution of effluents during mixing processes has a strong application potential for mining issues. On the one hand, the results obtained suggest that the saturation indices calculated in PHREEQC with the *wateq4f.dat* database for different mining effluents can predict the formation of key minerals in the geochemical evolution of mining waters. In particular, the forward model allowed the identification of the formation potential of jarosite, schwertmannite, $Fe(OH)_3$, and gypsum, four phases observed in the controlled laboratory experiments. On the other hand, the use of the keywords MIX and EQUILIBRIUM_PHASES allowed the approximate prediction of the concentrations of dissolved substances in mine effluent mixtures. Comparisons between predicted vs observed concentrations revealed that predicted concentrations were generally overestimated using the MIX keyword due to the precipitation of secondary phases. Predicted concentrations using the MIX and EQUILIBRIUM_PHASES keywords suggest that laboratory and field waters were out of equilibrium with respect to jarosite, schwertmannite, and $Fe(OH)_3$, with these phases often remaining supersaturated. However, the two approaches mentioned above allow an estimation of the maximum and minimum concentrations likely to be observed in the effluent mixtures. Therefore, modeling approaches using the

wateq4f.dat database in PHREEQC could represent a useful tool for predicting mine effluent compositions during mixing processes.

Despite the potential applications described below, some important limitations remain and represent research opportunities. The first critical limitation concerns the evaluation of the ion balance of acidic mine effluents (pH < 3) with high Fe and Al contents. Data from the present study suggest that ion balance errors are significant for these effluents. Potential causes include colloid dissolution in samples for metal analysis, uncertainties associated with calculating Fe and Al speciation for these solutions, and errors related to pH measurements. A second important limitation that should stimulate future research is the consideration of biological processes in the modeling of mixing processes. The observations made on the solids precipitated during the laboratory mixing experiments revealed the presence of Fe–Si-rich phases with morphologies characteristic of solids resulting from biological processes. However, biological processes were not considered in the models proposed here. In addition, considering the kinetics of schwertmannite, jarosite, $Fe(OH)_3$, and gypsum formation under field conditions and properly estimating the average residence time of waters in basins, ponds, and reservoirs is critical to evaluate the mass of solid phases likely to precipitate during mixing processes. Finally, studies focusing on the coprecipitation, sorption, and desorption of trace metals and metalloids with schwertmannite, jarosite, and $Fe(OH)_3$ are necessary. Indeed, the observations from this study reveal that most of the trace metals and metalloids tend to decrease in concentration with time following mixing processes. This supports the hypothesis that trace elements are immobilized by the precipitation of the main phases (schwertmannite, jarosite, $Fe(OH)_3$). However, it is still unclear how these elements are immobilized by the precipitated solids. The potential impact of remobilization processes (e.g., desorption) should also be addressed as the precipitated solids resulting from mixing processes could represent a significant pool of contaminants over the long term.

5.6 Conclusion

The combination of chemical, isotopic, and mineralogical analyses with statistical analyses and forward and inverse modeling approaches allowed the key processes controlling the geochemical evolution of mixed mine effluents to be deciphered. The formation of secondary minerals such as schwertmannite, jarosite, and $Fe(OH)_3$ was identified as a key process controlling the geochemistry

of the studied mine effluents. These phases can incorporate Fe, SO_4^{2-}, K, and Na from solution through direct incorporation into mineral structures; it is likely that other metals and metalloids (i.e., Li, Ti, U, Cr, Be, Al, Pb, Ni, Co, Se, Si, Cu, Mn, Zn) are also immobilized by schwertmannite, jarosite, and $Fe(OH)_3$ through sorption or coprecipitation processes. The kinetics of schwertmannite, jarosite, and $Fe(OH)_3$ formation appeared to play an important role in the geochemical evolution of mixed effluents, as the mixtures often remained out of equilibrium with respect to these phases. Biological activity can further influence the formation of secondary minerals. In the present study, inorganic processes were modeled using PHREEQC. However, observations made on the solids formed during laboratory experiments strongly suggest the occurrence of biologically mediated processes, which brings certain additional uncertainties to the models. The results presented here reveal that forward and inverse modeling approaches performed using PHREEQC (with the *wateq4f.dat* database) can provide valuable insights into the range of dissolved solids concentrations to be expected in mixed mine effluents and the key mineral phases likely to drive the geochemical evolution of mixtures. Other type of modeling tool like PHREEQ-N-AMDTreat could be used to validate the models. Such knowledge is critical to better manage mine effluents and predict the chemical composition of effluents reaching the mine water treatment plants in an effort to optimize treatment processes.

Credit authorship contribution statement

Sébastien Ryskie: Conceptualization, Methodology, Visualization, Formal analysis, Investigation, Writing - original draft. Eric Rosa: Conceptualization, Methodology, Formal analysis, Visualization, Supervision, Writing - review & editing. Carmen M. Neculita: Conceptualization, Methodology, Visualization, Formal analysis, Supervision, Writing - review & editing, Project administration, Funding acquisition. Patrice Couture: Conceptualization, Methodology, Formal analysis, Visualization, Supervision, Writing - review & editing.

Funding

This work was funded by the Natural Sciences and Engineering Research Council of Canada (NSERC), the Canada Research Chairs Program, and the industrial partners of the Research Institute on Mines and Environment (RIME) UQAT (University of Quebec in Abitibi-Temiscamingue)-Polytechnique Montreal, including Agnico Eagle, Canadian Malartic Mine, Iamgold Corporation, Newmont, Raglan Mine-Glencore, and Rio Tinto.

Declaration of Competing Interest

The authors declare that there is no conflict of interest.

Acknowledgements

The authors want to sincerely thank the collaboration of Louis Coetzee, Senior Process Mineralogist from Teck for the mineralogical analyses as well as the active help of Florence Laflamme during the lab trials and sampling.

5.7 References

AECOM (2019). New Britannia Mill Water Quality Assessment. Memo for Hudbay Minerals Inc., 49 p.

American Public Health Association (APHA), 2017. Standard Methods for the Examination of Water and Wastewater. Method 4500-NH_3 D. 23rd Ed. Washington, DC, USA.

Appelo, C.A.J., Postma, D., 2005. Geochemistry, Groundwater and Pollution (2nd). Balkema, Leiden, p. 678.

Balistrieri, L. S., Seal II, R. R., Piatak, N. M., & Paul, B. (2007). Assessing the concentration, speciation, and toxicity of dissolved metals during mixing of acid-mine drainage and ambient river water downstream of the Elizabeth Copper Mine, Vermont, USA. *Applied Geochemistry, 22*(5), 930-952.

Ball, J. W. & D. K. Nordstrom (1991). "User's manual for wateq4f, with revised thermodynamic data base and test cases for calculating speciation of major, trace, and redox elements in natural waters." US Geological Survey.

Barge, L. M., Cardoso, S. S., Cartwright, J. H., Doloboff, I. J., Flores, E., Macías-Sánchez, E., Sobrón, P. (2016). Self-assembling iron oxyhydroxide/oxide tubular structures: laboratory-grown and field examples from Rio Tinto. *Proceedings of the Royal Society A: Mathematical, Physical and Engineering Sciences, 472*(2195), 20160466.

Bigham, J., & Nordstrom, D. K. (2000). Iron and aluminum hydroxysulfates from acid sulfate waters. *Reviews in Mineralogy and Geochemistry, 40*(1), 351-403.

Bondu, R., Cloutier, V., Rosa, E., & Roy, M. (2020). An exploratory data analysis approach for assessing the sources and distribution of naturally occurring contaminants (F, Ba, Mn, As) in groundwater from southern Quebec (Canada). *Applied Geochemistry, 114*, 104500.

Botz, M. M. (2001). Overview of cyanide treatment methods. *Mining Environmental Management, Mining Journal Ltd., London, UK, 28*, 30.

Burrows, J.E., Cravotta, C.A. III, and Peters, S.C. (2017). Enhanced Al and Zn removal from coal-mine drainage during rapid oxidation and precipitation of Fe oxides at near-neutral pH. *Applied Geochemistry, 78*, 194-210.

Carrero, S., Fernandez-Martinez, A., Pérez-López, R., Cama, J., Dejoie, C., & Nieto, J. M. (2022). Effects of aluminum incorporation on the schwertmannite structure and surface properties. *Environmental Science: Processes & Impacts,* 24, 1383-1391.

CEAEQ, 2016. Détermination des cyanures: méthode colorimétrique automatisée avec l'acide isonicotinique et l'acide barbiturique – distillation manuelle. MA. 300 – CN 1.2, Rév. 4. Ministère du Développement durable, de l'Environnement et de la Lutte contre les changements climatiques du Québec, Qc, Canada, 26p.

CEAEQ, 2020. Détermination des anions: méthode par chromatographie ionique. MA. 300 – Ions 1.3, Rév. 6. Ministère de l'environnement et de la lutte contre les changements climatiques, Qc, Canda, 14p.

CEAEQ, 2020. Détermination des métaux: méthode par spectrométrie de masse à source ionisante au plasma d'argon. MA. 200 – Mét. 1.2, Rév. 7. Ministère de l'environnement et de la lutte contre les changements climatiques, Qc, Canada, 35p.

Choi, J. Y., Lee, T., Cheng, Y., & Cohen, Y. (2019). Observed crystallization induction time in seeded gypsum crystallization. *Industrial & Engineering Chemistry Research, 58*(51), 23359-23365.

climate-data.org (2022). Historic Weather for Rouyn-Noranda, Québec, Canada. https://fr.climate-data.org/amerique-du-nord/canada/quebec/rouyn-noranda-21931/#climate-table (last access: January 20, 2023).

Craig, H., & Gordon, L. I. (1965). Deuterium and oxygen 18 variations in the ocean and the marine atmosphere. Stable Isotopes in Oceanographic Studies and Paleotemperatures. Spoleto, July 26-30.

Cravotta, C. A. III (2021). "Interactive PHREEQ-N-AMDTreat water-quality modeling tools to evaluate performance and design of treatment systems for acid mine drainage." *Applied Geochemistry, 126*, 104845.

Cravotta, C.A. III, Goode, D.J., Bartles, M.D., Risser, D.W., Galeone, D.G. (2014). Surface-water and groundwater interactions in an extensively mined watershed, upper Schuylkill River, Pennsylvania, USA. *Hydrological Processes, 28*, 3574–3601.

Coulton, R., Bullen, C., & Hallett, C. (2003). The design and optimisation of active mine water treatment plants. *Land Contamination and Reclamation, 11*(2), 273-280.

di Biase, A., Wei, V., Kowalski, M. S., Bratty, M., Hildebrand, M., Jabari, P., & Oleszkiewicz, J. A. (2020). Ammonia, thiocyanate, and cyanate removal in an aerobic up-flow submerged attached growth reactor treating gold mine wastewater. *Chemosphere, 243*, 125395.

Hem, J. D. (1985). *Study and interpretation of the chemical characteristics of natural water* (Vol. 2254): Department of the Interior, US Geological Survey.

Hendry, M. J., Barbour, S. L., Schmeling, E. E., Wassenaar, L. L., Shaw, S., & Schabert, M. S. (2023). Quantifying denitrification in a field-scale bioremediation experiment. *Science of the Total Environment*, 854, 158762.

Hendry, M. J., Wassenaar, L. I., Barbour, S. L., Schabert, M. S., Birkham, T. K., Fedec, T., & Schmeling, E. E. (2018). Assessing the fate of explosives derived nitrate in mine waste rock dumps using the stable isotopes of oxygen and nitrogen. *Science of the Total Environment, 640*, 127-137.

Kim, H.-J., & Kim, Y. (2021). Schwertmannite transformation to goethite and the related mobility of trace metals in acid mine drainage. *Chemosphere, 269*, 128720.

Konhauser, K. O. (1997). Bacterial iron biomineralisation in nature. *FEMS Microbiology Reviews, 20*(3-4), 315-326.

Kynčlová, P., Hron, K., & Filzmoser, P. (2017). Correlation between compositional parts based on symmetric balances. *Mathematical Geosciences, 49*(6), 777-796.

Lecomte, K. L., Pasquini, A. I., & Depetris, P. J. (2005). Mineral weathering in a semiarid mountain river: its assessment through PHREEQC inverse modeling. *Aquatic Geochemistry, 11*(2), 173-194.

Lemly, A. D. (2002). Symptoms and implications of selenium toxicity in fish: the Belews Lake case example. *Aquatic Toxicology, 57*(1-2), 39-49.

Marcotte, P., Neculita, C. M., Cloutier, V., Bordeleau, G., & Rosa, E. (2022). Tracing the sources and fate of nitrogen at a Canadian underground gold mine. *Applied Geochemistry, 142*, 105238.

Mosley, L. M., Daly, R., Palmer, D., Yeates, P., Dallimore, C., Biswas, T., & Simpson, S. L. (2015). Predictive modelling of pH and dissolved metal concentrations and speciation following mixing of acid drainage with river water. *Applied Geochemistry, 59*, 1-10.

Nordstrom, D. K. (2020). Geochemical Modeling of Iron and Aluminum Precipitation during Mixing and Neutralization of Acid Mine Drainage. *Minerals, 10*(6), 547.

Papp, D. C., Baciu, C., Turunen, K., & Kittilä, A. (2020). Applicability of selected stable isotopes to study the hydrodynamics and contaminant transport within mining areas in Romania and Finland. *Geological Society, London, Special Publications, 507*(1), 169-192.

Parkhurst, D. L., & Appelo, C. (1999). User's guide to PHREEQC (Version 2): A computer program for speciation, batch-reaction, one-dimensional transport, and inverse geochemical calculations. *Water-resources investigations report, 99*(4259), 312.

Parkhurst, D. L. & C. Appelo (2013). Description of input and examples for PHREEQC version 3: a computer program for speciation, batch-reaction, one-dimensional transport, and inverse geochemical calculations, US Geological Survey.

Rey, N., Rosa, E., Cloutier, V., & Lefebvre, R. (2018). Using water stable isotopes for tracing surface and groundwater flow systems in the Barlow-Ojibway Clay Belt, Quebec, Canada. *Canadian Water Resources Journal/Revue Canadienne des Ressources Hydriques, 43*(2), 173-194.

Ryskie, S., Neculita, C. M., Rosa, E., Coudert, L., & Couture, P. (2021). Active treatment of contaminants of emerging concern in cold mine water using advanced oxidation and membrane-related processes: a review. *Minerals, 11*(3), 259.

Schoepfer, V. A., & Burton, E. D. (2021). Schwertmannite: A review of its occurrence, formation, structure, stability and interactions with oxyanions. *Earth-Science Reviews, 221*, 103811.

Skrzypek, G., Mydłowski, A., Dogramaci, S., Hedley, P., Gibson, J. J., & Grierson, P. F. (2015). Estimation of evaporative loss based on the stable isotope composition of water using Hydrocalculator. *Journal of Hydrology, 523*, 781-789.

Spellman, C.J. Jr., Smyntek, P.M., Cravotta, C.A. III, Tasker, T.L., & Strosnider, W.H.J. (2022). Pollutant co-attenuation via in-stream interactions between mine drainage and municipal wastewater. *Water Research, 214*, 118173.

Turunen, K., Räsänen, T., Hämäläinen, E., Hämäläinen, M., Pajula, P., Nieminen, S. P. (2020). Analysing contaminant mixing and dilution in river waters influenced by mine water discharges. *Water, Air, & Soil Pollution, 231*(6), 1-15.

Warnes, M. G. R., Bolker, B., Bonebakker, L., Gentleman, R., & Huber, W. (2016). Package 'gplots'. *Various R programming tools for plotting data*.

Wolkersdorfer, C., Nordstrom, D. K., Beckie, R. D., Cicerone, D. S., Elliot, T., Edraki, M., Lucero, R. A. O. (2020). Guidance for the integrated use of hydrological, geochemical, and isotopic tools in mining operations. *Mine Water and the Environment, 39*(2), 204-228.

CHAPITRE 6 ARTICLE 3 : INFLUENCE OF OZONE MICROBUBBLE ENHANCED OXIDATION ON MINE EFFLUENT MIXES AND DAPHNIA MAGNA TOXICITY[3]

Cet article a été publié dans la revue *Chemosphere* le 1er avril 2023.

6.1 Abstract

The mining industry often must mix different kinds of water on the mine site during pre-treatment or post-treatment before the final discharge of the treated water to the environment. Microbubble ozonation has proven to be efficient in the removal of contaminants of concern from mine water, such as metals, metalloids, and nitrogen compounds, which can persist in the environment and entail toxicity issues. This study evaluated the efficiency of ozone microbubbles combined with lime precipitation on contaminant removal and its impact on toxicity for Daphnia magna with five different mine effluent mixes from an active mine site located in Abitibi-Témiscamingue, Qc, Canada. For the non-acidic mixes, two scenarios were tested: first, pre-treatment of metals using lime precipitation and a flocculant was conducted prior to ozonation; and second, ozonation was conducted prior to metals post-treatment using the same precipitation and flocculation technique. Results showed that the NH_3-N removal efficiency ranged from 90% for the lower initial concentrations (1.1 mg/L) to more than 99% for the higher initial concentrations (58.4 mg/L). Moreover, ozonation without metals pre-treatment improved NH_3-N treatment efficiency in terms of kinetics but entailed abnormal toxicity issues. Results of bioassays conducted on water with metals pre-treatment did not show any toxicity events but showed abnormal toxicity patterns on the mixes treated without metals pre-treatment (diluted effluents were toxic, while undiluted were not). At 50% dilution, the water was toxic, probably due to the potential presence of metal oxide nanoparticles. The confirmation of the source of toxicity requires further investigation.

---

[3] Ryskie, S., Bélanger, E., Neculita, C.M., Couture, P., Rosa, E., 2023. Influence of ozone microbubbles enhanced oxidation on mine effluent mixtures and *Daphnia magna* toxicity. *Chemosphere*, 329: 138559, ISSN 0045-6535, https://doi.org/10.1016/j.chemosphere.2023.138559.

Keywords: Ozone microbubbles, AOP (advanced oxidation process), toxicity, *Daphnia magna*, metal oxide nanoparticles

Graphical abstract

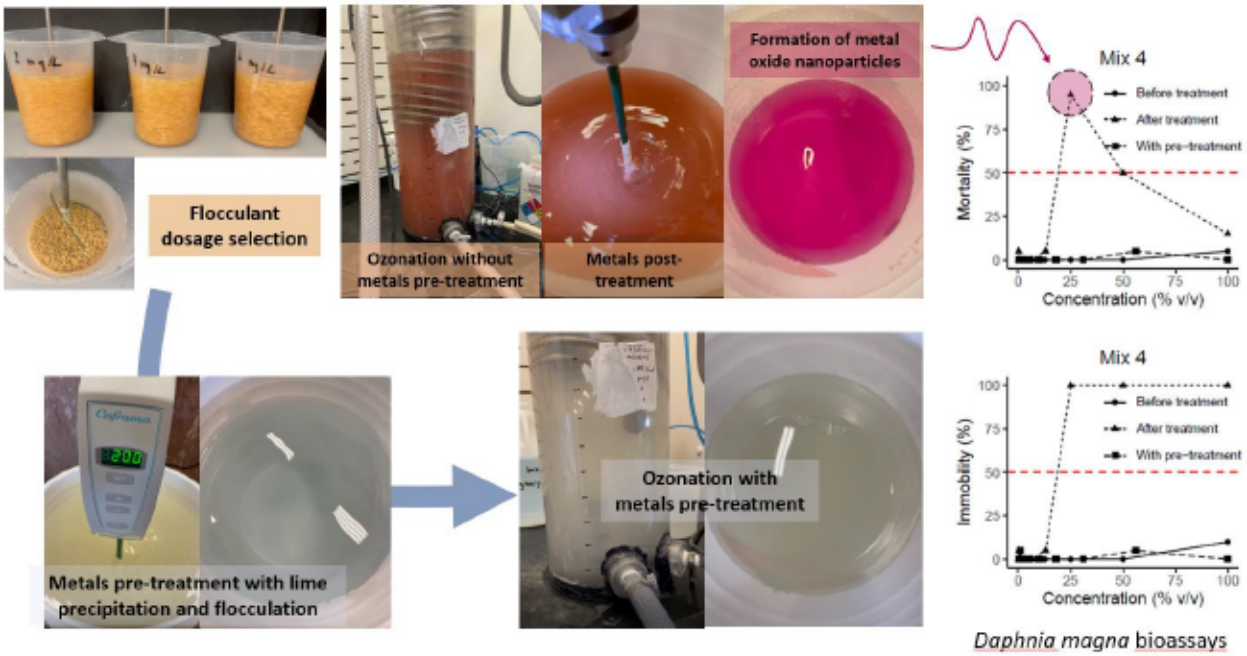

6.2 Introduction

Mining activities generate large volumes of contaminated waters that need to be treated before final discharge to the environment. Different types of waters are often mixed on mining sites to manage effluents (e.g.: acid rock drainage, process water, dewatering water, precipitation). These mixes include several contaminants (metals, metalloids, salinity, N-compounds), and the change in the physicochemical parameters occurring when different waters are mixed can change their geochemical speciation (Wolkersdorfer et al., 2020). This phenomenon can entail the mobilization or sequestration of some of the compounds in the water, which can also affect toxicity. For example, As and Se are sensitive to the redox potential and pH, and depending on their speciation, some forms can be more toxic (Hem, 1985; Coudert et al., 2020; Etteieb et al., 2020). The reduced form of As, arsenite, is known to be more toxic than the oxidized form, arsenate (Bondu et al., 2017). Similarly, Se in its oxidized form, selenate, is less bioavailable due to its higher mobility than the reduced form, selenite (Hamilton, 2004; Gonzalez et al., 2019). Therefore, the use of advanced oxidation processes (AOPs) to treat these contaminants can help to decrease their toxicity

for the receiving environment (Khuntia et al., 2014; Gonzalez et al., 2019). An increase in alkalinity and hardness can decrease the toxicity of the mix, which can be less impacted by metals (Yim et al., 2006); however, the opposite effect can also occur when the concentration is too high and entails undesired precipitation and osmotic stress on the body of aquatic organisms such as *Daphnia magna* (*D. magna*) (Bogart et al., 2016).

With regulations becoming more stringent over time, some of the contaminants that were not a concern in the past are now considered contaminants of emerging concern (CEC) (Neculita et al., 2020; Ryskie et al., 2021). The technologies available to treat the classical contaminants and CEC are numerous. Mines need the Best Available Technology Economically Achievable (BATEA), which must also be robust and efficient (MEND, 2014). In cold climates, BATEA is sometimes a more challenging solution to find, as in the case of nitrogen compounds that are more complex to treat using a biological process in cold waters (Jermakka et al., 2015; Ryskie et al., 2020).

The AOP is an emerging technology to treat contaminants in water (Mousset et al., 2021). Some recent studies reported the efficiency of AOP using ferrates (Gonzalez-Merchan et al., 2016; Gervais et al., 2020), electro-oxidation (Foudhaili et al., 2020; Olvera-Vargas et al., 2021; Dubuc et al., 2022), and ozone microbubbles (Kunthia et al., 2013, 2014; Ryskie et al., 2020, Marcotte et al., 2021). The efficiency of the treatment for different contaminants is water-chemistry related and depends on both the technology and the targeted contaminants. In some cases, the AOP impact on the aquatic toxicity of treated waters has also been assessed (Foudhaili et al., 2020; Marcotte et al., 2021). Ozone microbubbles showed removal of up to 97–99% for the N-compounds (SCN^-, CNWAD, $N\text{-}NH_3$, OCN^-), while the toxicity after treatment for *D. magna* had a toxic unit (TU) value of less than 1 (i.e.: not toxic)(Marcotte et al., 2021). In another study, some metals that are difficult to treat at low concentrations using conventional methods (e.g.: flocculation-based methods), like Mn and Zn, had a good removal efficiency with ozone microbubbles, up to 99% and 96%, respectively (Ryskie et al., 2020). A removal efficiency of more than 99% for N-compounds was also reported (Ryskie et al., 2020). The use of microbubbles instead of coarse bubbles is a promising way to use ozone as an efficient and viable treatment for the mining industry. Some studies have shown the improved efficiency of ozone mass transfer in water using microbubbles (Takahashi et al., 2007; Zheng et al., 2015; Xiong et al., 2019). However, the use of ozone can also lead to the generation of metal oxide nanoparticles, which are recognized to be highly toxic, even at low concentrations (Renzi & Blaskovic, 2019; Sengul & Asmatulu, 2020).

To the authors' best knowledge, no study has yet evaluated the efficiency of ozone microbubbles on water mixes from multiple locations of a mine site, for multiple contaminants classified as CEC, combined with toxicity analysis. Therefore, the main objective of this study was to evaluate the efficiency of ozone microbubbles on water mixes from an active gold mine located in Québec, Canada. The removal efficiency for different CEC, including some metals, metalloids, and N-compounds, in a cold climate was analyzed for multiple operation parameters with an ozonation pilot, and the toxicity of the waters on *D. magna* was assessed before and after treatment.

6.3 Materials and methods

The methodology used for the preparation of the mixes, the physicochemical analyses, the treatment tests, and the toxicity tests before and after treatment is represented in a schematic flow diagram in **Figure 6.1**. The details are provided in the next section.

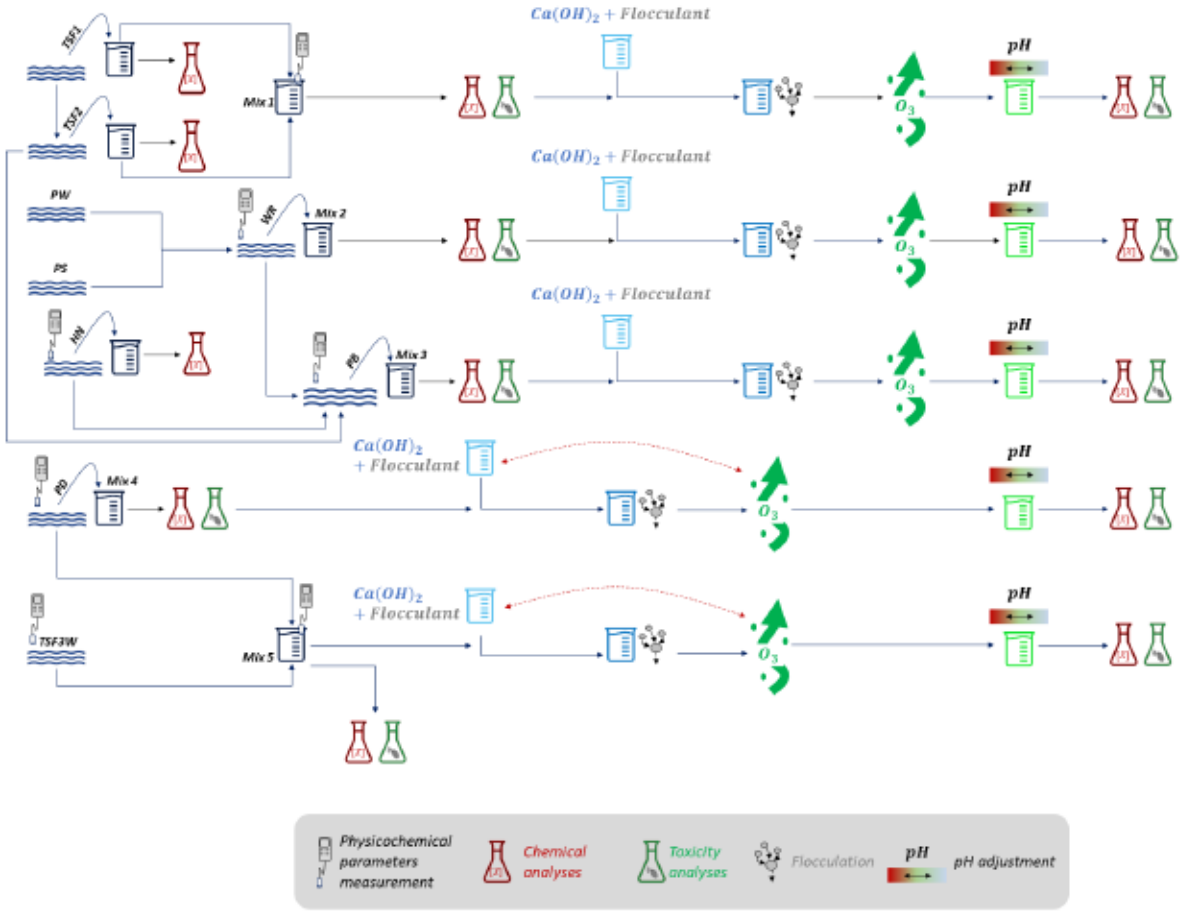

Figure 6.1 Schematic flow diagram of the methodology

6.3.1 Sampling, preparation, and characterization of effluent mixes before and after treatment

Real mine effluents from a gold mine located in Abitibi-Témiscamingue, Qc, Canada were sampled and mixed (**Table 6.1**). The effluents were sampled from six different points at the mine: 1) inactive tailings storage facility containing acid mine drainage (AMD) waters from precipitation (TSF1 and TSF2); 2) active tailings pond collecting process waters after destruction of cyanides by the SO_2-air process, as well as AMD waters from precipitation (DP); 3) pond containing AMD water from the north and south waste dumps (WR and SB); and 4) tailings storage facility used for the recirculation of process water from ore treatment before cyanidation (TSF3W). The flow diagram schematic of the mine site is shown in **Figure 6.2**, which also defines all the mix numbers. Samples were mixed in different proportions, in which pH varied from 2.60 to 8.39 (**Table 6.2**).

Table 6.1 Description of every water location on the studied mine site (map showed in **Figure 6.2** and effluent names are the abbreviation of the different sampling points)

Effluent	Water type and mix
DP	Active tailings pond collecting process water after destruction of cyanides by the SO_2-air process, as well as AMD water from precipitation
TSF1	Inactive tailings storage facility containing AMD water from precipitation
TSF2	Inactive tailings storage facility containing AMD water from precipitation and pumping water from TSF1 at certain times of the year
TSF3W	Tailings storage facility used for the recirculation of process water from ore treatment before cyanidation
TSF3E	Inactive tailings storage facility containing AMD water from precipitation and the overflow of TSF3W at certain times of the year

Effluent	Water type and mix
SB	Pond containing AMD water from the south waste dump and surrounding roads
NP	Waste rock dump located at the north, generating acid water that is collected by a creek flowing through BB
WWB	Pond containing dewatering pumped from underground to allow mine operations
WR	Pond containing AMD water from the south waste dump, water from SB, and water from the WWB
BB	Pond containing AMD water from the north waste dump, water from all TSFs depending on the time of year, and water from the WR. This pond also serves as a buffer tank for the high-density sludge water treatment plant
HDS	High-density sludge water treatment plant
PP	Polishing pond containing treated water from the HDS
EFF	Final effluent at the end of the polishing pond
River	Receiving medium for the final effluent. The sampling point is upstream

The physicochemical parameters of the effluents were analyzed before and after each treatment step, including pH, oxidation reduction potential (ORP), temperature, electrical conductivity (EC), alkalinity/acidity, ammonia nitrogen (NH_3-N), nitrites (NO_2^-), nitrates (NO_3^-), sulfates (SO_4^{2-}), phosphates (PO_4^{3-}), chlorine (Cl^-), bromide (Br^-), cyanates (OCN^-), thiocyanates (SCN^-), total cyanide (total CN^-), and dissolved and total metals. The pH, temperature, EC, and ORP were analyzed using a YSI ProDSS multiparameter meter. During the ozonation treatment step, the NH3-N concentrations were analyzed at room temperature with a selective electrode (Orion ThermoFisher Scientific Orion for Ammonia) according to the standard method (APHA, 2017; Method 4500-NH3 D). The anions analyses (NO_2^-, NO_3^-, Cl^-, Br^-, SO_4^{2-}, SCN^-, OCN^-, and PO_4^{3-}) were performed by ion chromatography (945 Professional Detector Vario Metrohm) with a UV/VIS detector (944 Professional UV/VIS detector Vario Metrohm) and an automatic sampler

(858 Professional Processor Metrohm) (CEAEQ, 2020a; MA. 300 – Ions 1.3). Alkalinity and acidity measurements were performed by automatic titration (855 Robotic Titrosampler) according to the standard method (CEAEQ, 2016a; MA. 315 – Alc-Aci 1.0). Metal analyses were performed by inductively coupled plasma mass spectrometry (ICP-MS) before and after sample filtration using 0.45 µm membranes (CEAEQ, 2020b; MA. 200 – Mét. 1.2). The total CN- concentrations were measured using an automated colorimetric method with isonicotinic acid and barbituric acid manual distillation (CEAEQ, 2016b; MA. 300 – CN 1.2); these analyses were carried out by an accredited external laboratory (H2Lab, Rouyn-Noranda, Qc, Canada).

Table 6.2 Description of the proportion and physicochemical characteristics of the effluent mixes

Mix	Proportion	pH	EC (µS/cm)	ORP (mV)
1	TSF1 (47.6%) + TSF2 (52.4%)	3.10	1,680	502.5
2	WR (100%)	2.60	4,571	549.7
3	BB (100%)	2.64	3,775	518.7
4	DP (100%)	7.59	3,700	233.1
5	DP (80.6%) + TSF3W (19.4%)	8.39	3,634	219.4

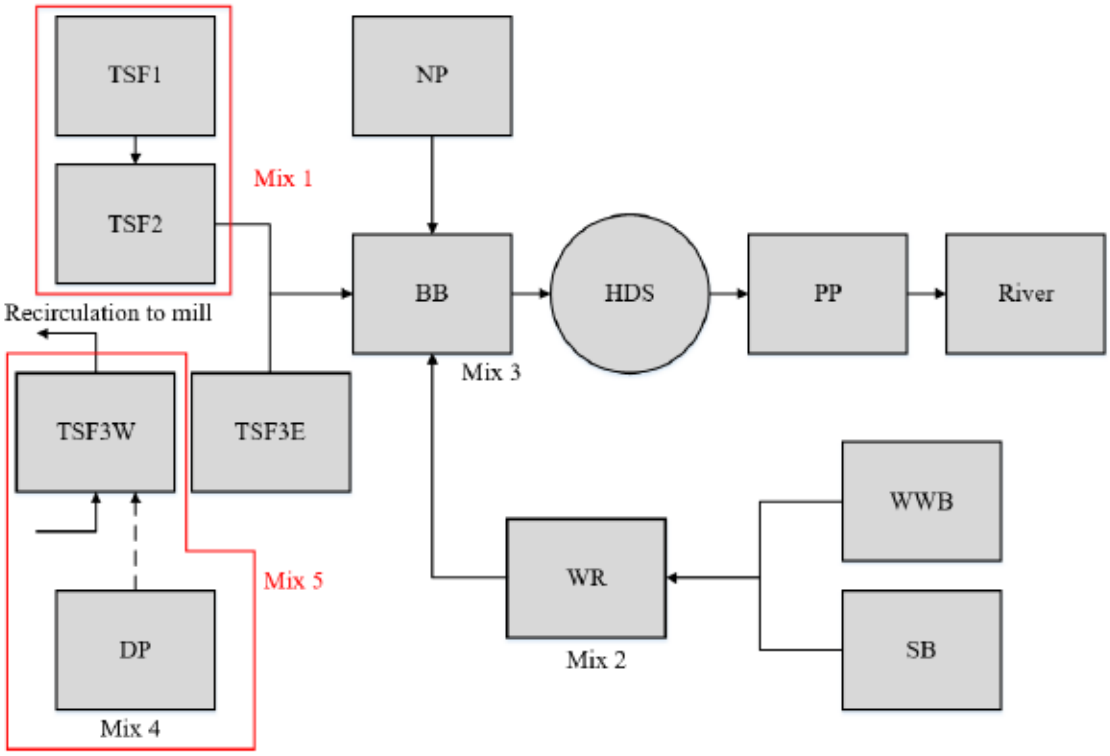

Figure 6.2 Schematic flow diagram of the mine site, including the mix numbers

6.3.2 Treatment using ozone microbubbles

A Primozone® GM1 ozone generator system equipped with a microbubble Nikuni KTM20N pump was used along with an OHR MX-F15 (Original Hydrodynamic Reaction Technology) static mixer. The ozone generator was equipped with a cooling water system to maintain the temperature ~10°C during the process, while a safety alarm device was installed to prevent O_3 leakage. The concentration capacity of O_3 was 20% and the pilot system provided a flow rate of 11 g O_3/h when operated at 30 psi with oxygen (O_2). An 18 L tank reactor was used, and the standard operating pressure of the microbubble pump was 36.3 psi at the outlet and -3.6 psi at the suction. Effluent mixes were treated under recirculated flow with the ozonation pilot-scale system (**Figure 6.3**). The method and system used are improved from a previous study (Ryskie et al., 2020). The bubble size was not measured during the study.

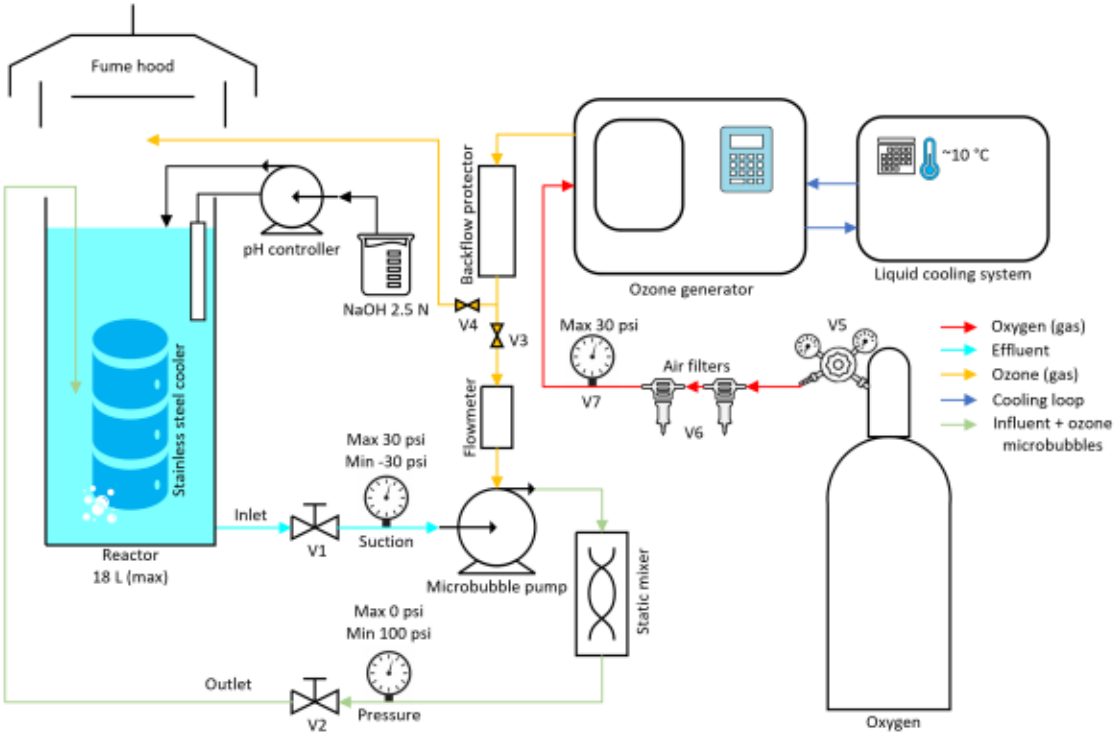

Figure 6.3 Schematic pilot-scale ozonation system under recirculated flow, V1 to V7 represent the valves (modified from ©Le Bourre, 2020)

The volume of water treated under recirculated flow was 15 L, at a flow rate of 1.3 L/min and with 1.5 to 2 h of hydraulic retention time (HRT) (until NH_3-N concentration was below 0.1 mg/L). The pH was adjusted to 9 before the start of the tests and maintained at 9 during the treatment using a pH controller with ACS grade NaOH (2.5 N). The physicochemical characteristics (pH, ORP, EC, and temperature) were monitored continuously during the process. Concentrations of NH_3-N, alkalinity, anions, and metals were measured on samples collected every 15 minutes to assess their evolution.

6.3.3 Pre- and post-treatment using lime and flocculant

Real mine effluents were pre- or post-treated using lime and a flocculant. A polyacrylamide base polymer (FLOPAM AN 905 VHM (MC)) was used for the flocculation. Laboratory jar tests were conducted to optimize flocculant concentration (2, 4, or 6 mg/L) before ozonation treatment. A freshly prepared aqueous lime solution (10% w/w) was slowly added using a pH controller until

the pH reached 10. Then, a freshly prepared flocculant solution (0.2% w/w) was directly added, and the mix was agitated at 50 rpm for 2 min. The flocs were allowed to settle for 30 min and the optimal flocculant concentration was determined based on the turbidity of the supernatant. Mixes 1 to 5 were pre-treated and mixes 4 and 5 were post-treated using this procedure. Liquid/solid separation was performed carefully by suction using a peristaltic pump.

6.3.4 Toxicity tests

Toxicity tests were performed to evaluate the influence of ozone microbubble oxidation on the toxicity of mine effluent mixes on *D. magna*. The choice of using *D. magna* for this study is justified as the most sensitive species of the two regulated species (*D. magna* and rainbow trout) in the mining industry in Québec, Canada (Minister of Justice, 2021; Ministère de l'environnement et de la lute contre les changements climatiques MELCC, 2012). Sample analyses were conducted according to the standard analysis method (MA. 500 – D. mag 1.1) of the Centre d'Expertise en Analyse Environnementale du Québec (CEAEQ, 2021). The pH of the samples, which was basic after treatment, was adjusted to ~7 using 0.1 N sulfuric acid (H_2SO_4) to respect the regulation (Minister of Justice, 2021; Ministère de l'environnement et de la lute contre les changements climatiques MELCC, 2012) and to eliminate pH as a possible cause of toxicity on *D. magna*. Treated and untreated samples were immediately refrigerated and kept at 4°C prior to testing. The samples were brought to room temperature and homogenized, and physicochemical parameters such as temperature, pH, dissolved oxygen (DO), EC, and hardness were measured just before starting the tests. The reconstituted hard water used to dilute the samples for the toxicity tests was characterized by a pH of 6.5–8.5 (recommended 7.0–8.0) and DO of 90–100% saturation, and the hardness was adjusted to 160–180 mg/L $CaCO_3$ with a concentrated solution of calcium chloride ($CaCl_2$; 187.1 g/L) and magnesium chloride ($MgCl_2$; 55.8 g/L). Neonates (< 24 h old) were used for the tests. The toxicity test consisted of mixing the effluents with dilution water in different proportions (0, 6.25, 12.5, 25, 50, 100% - v/v) for untreated samples. Eleven concentrations were tested for each treated sample, with a final volume of 150 mL per container: mixes 1 and 4 without pre-treatment (0, 0.2, 0.39, 0.78, 1.6, 3.1, 6.3, 13, 25, 50, 100% - v/v); mix 2 (0, 7.5, 10, 13, 18, 24, 32, 42, 56, 75, 100% - v/v); and mixes 3 and 4 with pre-treatment and 5 with and without pre-treatment (0, 0.54, 0.97, 1.73, 3.1, 5.5, 9.8, 18, 31, 56, 100% - v/v). A total of 20 neonates were used for each concentration: precisely, four tubes per concentration were filled with 10 mL of

sample and five neonates. The number of organisms per test was selected to not exceed a maximum load of living organisms of 0.65 g/L. The organisms were exposed to a photoperiod of 16 h under lighting intensity between 500 and 1,000 Lux and 8 h in darkness, for 48 h at 20 ± 2.0°C. The tests determined the lethal concentration 50% (LC_{50}) and the effective concentration 50% (EC_{50}), which provide an indication of mortality and immobility factors (CEAEQ, 2021). After a 48-h period of incubation, immobile and dead daphnia were counted (immobility is defined as inability to swim for 15 s after a slight agitation of the solution, whereas mortality is determined by the absence of movement of the appendages and antennas, and by the absence of heartbeats). A positive quality control was conducted with potassium dichromate ($K_2Cr_2O_7$) as the reference toxicant. Immediately after neonate counting, pH, temperature, EC, and DO concentrations were measured in all dilutions tested and in the quality control. According to the regulation (Minister of Justice, 2021; Ministère de l'environnement et de la lute contre les changements climatiques MELCC, 2012), effluent mixes causing the mortality of > 50% (LC_{50}) of the *D. magna* population after 48 h of exposure were considered acutely toxic, while effluent mixes causing the mortality of ≤ 50% of the population were considered non-acutely toxic.

6.3.5 Data processing

The NH_3-N treatment efficiency was calculated as shown in equation 1:

$$\text{Efficiency} = \frac{C_0 - C_1}{C_0} \times 100\% \quad (1)$$

where C_0 and C_1 are concentrations before and after treatment, respectively. The treated mass of NH_3-N (mg) was calculated as shown in equation 2:

$$\text{Treated mass of } NH_3\text{-N} = (C_0 - C_x) \times V \quad (2)$$

where C_0 is the concentration before treatment, C_x is the remaining concentration, and V is the treated volume. Ozone consumption (g/g NH_3-N) was calculated as shown in equation 3:

$$O_3 \text{ consumption} = \left(\frac{T_1}{60}\right) \times \left(F \times \left(\frac{\text{Treated mass of } NH_3\text{-N}}{1000}\right)\right) \quad (3)$$

where T_1 is the treatment time and F is the O_3 flow rate.

6.4 Results and discussion

6.4.1 Data before and after ozonation with pre- and post-treatment

The results obtained from five mixes of real mine effluents (mixes 1 to 5) using microbubble ozonation under continuous flow, at pH 9, combined with metals pre- or post-treatment, are presented in **Figure 6.4**; a summary of physicochemical characteristics is presented in **Table 6.3**. The NH_3-N concentrations in the effluent mixes varied from 1.1 to 58.5 mg/L, while the OCN^- was present only in mixes 4 and 5, with concentrations of 4.9 and 4.8 mg/L, respectively (**Table 6.3**). For all mixes, initial SCN^- concentrations were below the detection limit (< 0.05 mg/L). Moreover, the known catalytic influence of bromine on NH_3-N oxidation rate was limited because initial concentrations were also below detection limits (Zuttah, 1999). Mixes 1 to 3 had to be pre-treated before NH_3-N ozonation because they were acidic (pH 2.6 to 3.1) and contained metals, with high concentrations of Al (15.1–111.8 mg/L) and Fe (9.1–399.2 mg/L) (**Table 6.3**). After pre-treatment, results showed good efficiency for metal removal, with final concentrations below the Canadian regulation (MDMER, 2022). For example, in mixes 2 and 3, Al concentrations decreased from 114 mg/L and 82 mg/L, and Fe concentrations from 399 mg/L and 335 mg/L, respectively, to below the detection limits (**Table 6.3**). Better initial water qualities were observed for mixes 4 and 5, with low concentrations of metals and neutral pH, but higher NH_3-N concentrations of 58.5 and 53.6 mg/L, respectively. For mixes 4 and 5, metal treatment was performed before and after the ozonation process to compare the effect on toxicity.

For mixes 1 to 3, NH_3-N concentrations were relatively low (1.1 to 3.9 mg/L), and ozonation treatment was complete in 30 min. However, the O_3 consumption per g NH_3-N was higher for the treatment of low NH_3-N concentrations (**Figure 6.4 d**). In mix 3, the NH_3-N concentration decreased from 1.1 to 0.1 mg/L in 30 min and required 366.7 g O_3/g NH_3-N, compared to 11.4 g O_3/g NH_3-N for a decrease from 56.1 to 24.0 mg/L NH_3-N in mix 5.

For mixes 4 and 5, the presence of low concentrations of metals did not affect the ozonation efficiency (**Table 6.3**). Ozone microbubbles were also efficient to remove low concentrations of metals (**Table 6.3**), making this treatment complementary to a lime plant for mine contaminated water. The concentrations of Cu, Fe, Mn, Ni, and Zn decreased during the ozonation process without pre-treatment. For example, in mixes 4 and 5, the concentration of Mn decreased from 8.8

to 0.7 mg/L and from 6.8 to 0.7 mg/L with 91% and 89.3% removal efficiencies, respectively. In addition, in mixes 4 and 5, ozonation was more efficient for Cu and Co removal than metal pre-treatment, probably because it is more difficult to treat low concentrations through precipitation. For all mixes, the final NH_3-N concentrations were below 0.1 mg/L with removal efficiencies ranging from 90.9 to 99.7% (**Figure 6.4**). These results are consistent with the previous studies using ozone microbubbles, where a high efficiency of NH_3-N and metal removal was observed (Khuntia et al., 2013; Ryskie et al., 2020). The presence of metals in mixes 4 and 5 without pre-treatment showed a small difference in the kinetics of NH_3-N removal compared to those with pre-treatment: the slope in **Figure 6.4 a** was more pronounced in the presence of metals, but O_3 consumption (**Figure 6.4 d**) was also slightly lower without metal pre-treatment. The presence of dissolved metals (Fe^{2+}, Mn^{2+}, Co^{2+}, Cd^{2+}, Cu^{2+}, Ag^{2+}, Cr^{3+}, and Zn^{2+}) in low concentrations in mixes 4 and 5 may have had the effect of catalysts during the ozonation (Wang & Xu, 2012). The increase in microbubble formation in the presence of higher total dissolved solids (TDS) concentrations, increasing the gas-liquid transfer efficiency because of higher surface tension, could also explain differences in the kinetics (Zheng et al., 2015; Xiong et al., 2019). The increase in the number of smaller bubbles also resulted in better NH_3-N treatment efficiency than using coarse bubbles in a comparative study of nanobubbles vs coarse bubbles (Wu et al., 2022).

Table 6.3 Contaminant concentrations before and after treatment[1]

Sample name	Al	As	NH_3-N	Co	Cu	CNO^-	Fe	Mn	Ni	NO_3^-	Se	Zn
Detection Limit (DL)	**0.005**	**0.0005**	**0.01**	**0.0005**	**0.0005**	**0.01**	**0.01**	**0.0005**	**0.0005**	**0.01**	**0.0005**	**0.001**
Mix 1	15.1	0.003	3.9	0.1	1.0	< DL	9.1	4.2	0.07	0.5	0.03	0.3
Mix 1 after metal pre-treatment	1.1	0.003	3.8	0.006	0.005	< DL	< DL	0.06	0.001	0.04	< DL	0.001
Mix 1 after ozonation	0.01	< DL	0.02	0.001	< DL	< DL	< DL	0.001	< DL	4.4	< DL	0.001
Mix 2	113.8	0.02	1.3	0.4	1.4	< DL	399.2	8.9	0.3	0.8	0.1	4.2
Mix 2 after metal pre-treatment	< DL	0.005	1.4	0.0005	0.01	< DL	< DL	< DL	< DL	1.1	0.004	< DL
Mix 2 after ozonation	0.014	0.0006	< DL	< DL	0.001	N/A2	< DL	0.001	0.0006	2.7	0.003	0.005
Mix 3	82.0	0.007	1.1	0.3	1.1	< DL	335.3	7.1	0.2	0.5	0.09	2.2
Mix 3 after metal pre-treatment	< DL	0.004	0.9	0.001	0.007	< DL	0.02	0.001	< DL	0.4	0.007	< DL
Mix 3 after ozonation	< DL	< DL	0.05	< DL	0.0005	N/A	< DL	0.01	< DL	1.9	0.007	< DL
Mix 4	0.06	< DL	58.5	0.1	0.05	4.9	0.1	8.8	0.08	0.8	0.0009	0.04
Mix 4 without metal pre-treatment after ozonation	< DL	0.0005	0.04	0.003	< DL	0.7	< DL	0.9	< DL	52.5	0.002	< DL
Mix 4 after metal treatment after ozonation	< DL	0.01	0.04	0.003	< DL	0.7	0.01	0.7	< DL	49.9	< DL	< DL
Mix 4	0.06	< DL	58.5	0.1	0.05	4.9	0.1	8.8	0.08	0.8	0.0009	0.04
Mix 4 after metal pre-treatment	< DL	0.006	60.6	0.03	0.009	2.9	0.01	0.001	0.01	1.0	0.002	< DL
Mix 4 after ozonation	< DL	0.002	0.09	0.003	0.0006	0.7	< DL	0.01	< DL	60.3	0.004	0.001
Mix 5	0.07	< DL	53.6	0.08	0.05	4.8	0.2	6.9	0.06	1.1	0.001	0.02
Mix 5 without metal pre-treatment after ozonation	< DL	0.0005	0.09	0.003	< DL	0.8	0.01	0.7	0.002	62.1	< DL	< DL
Mix 5 after metal treatment after ozonation	< DL	0.003	0.07	0.002	< DL	N/A	< DL	0.07	< DL	60.3	0.0006	< DL
Mix 5	0.07	< DL	53.6	0.08	0.05	4.8	0.2	6.9	0.06	1.1	0.001	0.02
Mix 5 after metal pre-treatment	0.02	0.02	51.3	0.03	0.01	3.0	< DL	0.07	0.02	0.9	0.002	< DL
Mix 5 after ozonation	< DL	< DL	0.1	0.002	< DL	0.6	< DL	< DL	< DL	57.5	0.001	< DL

1. While all the parameters were analyzed, only the important ones that showed variation during the treatment steps are presented. Concentrations are presented as dissolved in mg/L and as mg N/L for NH_3-N and NO_3^-.
2. N/A: Not Available

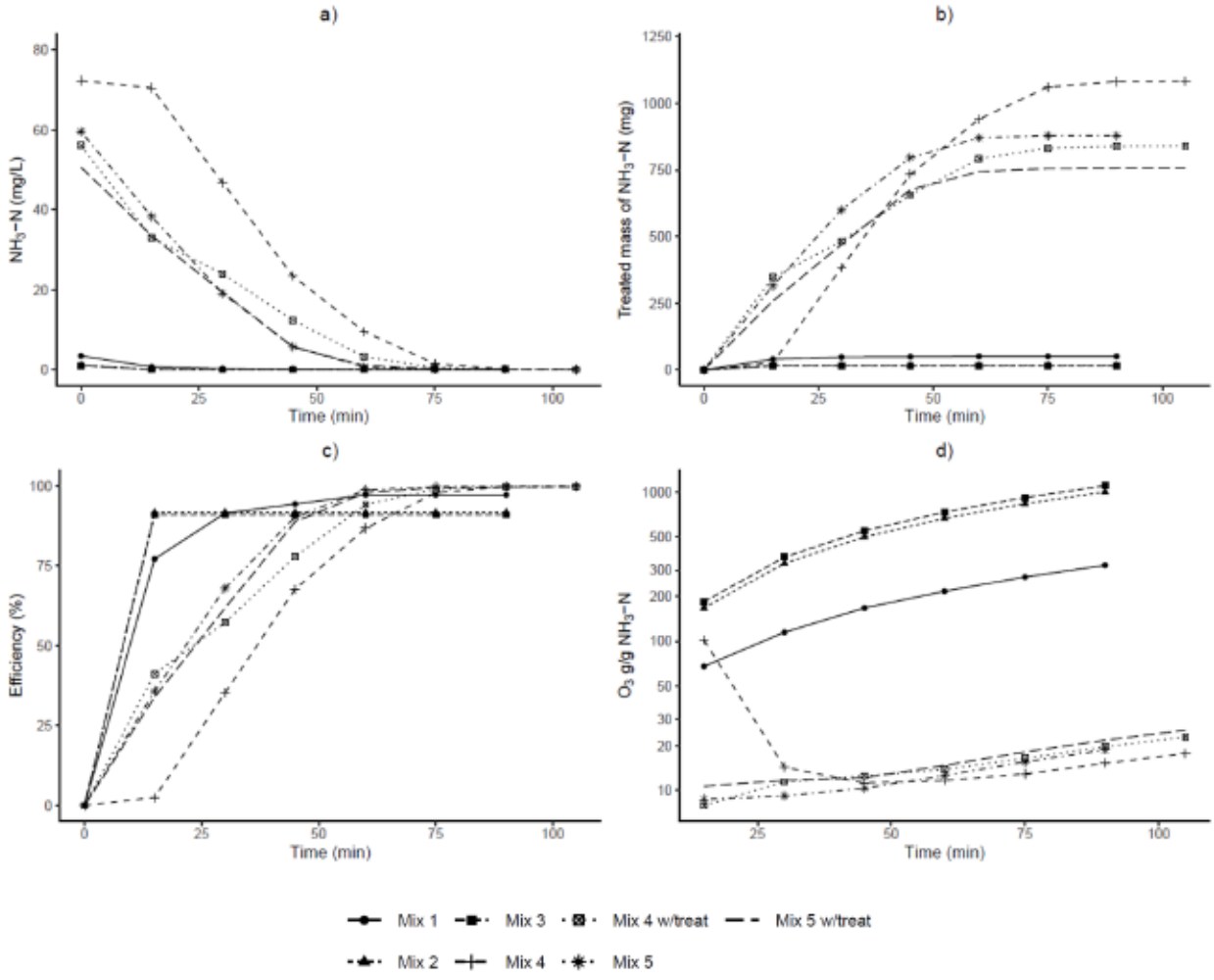

Figure 6.4 Evolution of concentration, treated mass of NH_3-N, removal efficiency, and O_3 consumption during the ozonation process

6.4.2 Treatment impact on *Daphnia magna* toxicity

The results from toxicity tests before and after treatment, including those pre-treated for metals prior to ozonation, are presented in **Figure 5**. For mixes 1 to 3, the samples were all acutely toxic to *D. magna* before treatment (100% mortality at a dilution of 6.25% v/v), while mixes 4 and 5 were not toxic (< 5% mortality). For mixes 1 to 3, the effect on *D. magna* immobility was present at the lowest dilution (6.25% v/v), where 100% of all the neonates were immobile. For mixes 4 and 5, the % of immobility was 10 and 0, respectively, without dilution. Toxicity results showed that none of the effluents were toxic once the ozonation treatment was complete when there was a pre-

treatment for metals removal and pH adjustment prior to collecting the sample. However, the tests with direct ozonation on mixes 4 and 5 prior to a treatment for metals showed inconsistent toxicity results, invalidating the analysis: the samples were not toxic at 100% v/v concentration, but they were toxic at 25% and 56% v/v dilution, respectively. Moreover, the immobility concentration for mixes 4 and 5 was 25% and 56%, respectively, and showed a common irregular pattern.

6.4.2.1 Effect of pre-treatment on toxicity

Pre-treatment of the metals before ozonation prevented toxicity events during the tests. The effect on the immobility was small with a pre-treatment of metals. However, both mixes 4 and 5 without pre-treatment were toxic, but not at 100% concentration (**Figure 5**). At a dilution of 25% and 56%, respectively, these samples were toxic. At these concentrations, the dead *D. magna* were swollen and had lost appendages. The unusual toxicity curves invalidated the test, as the undiluted samples were not toxic. The effect on the immobility was also elevated considering that these two mixes were not toxic before treatment and did not have effects on immobility. Without the pre-treatment of metals, a pink color developed after ozonation, probably explained by the presence of metal oxides in nanoparticle forms. Considering this effect on the toxicity, a pre-treatment of metals before ozonation is suggested to avoid toxicity events.

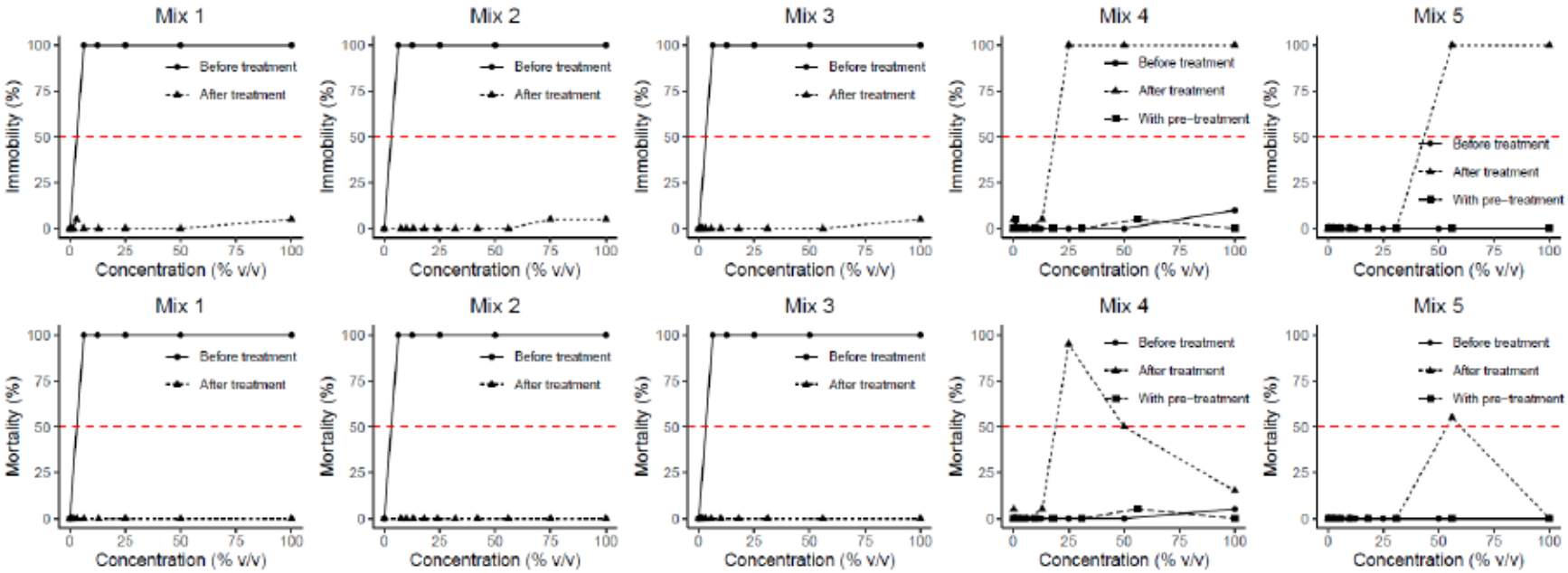

Figure 6.5 Bioassays results representing the % of immobility and mortality at different dilutions

6.4.3 Possible causes of toxicity

For mixes 1 to 3, the toxicity before treatment was probably mainly due to the pH of the samples. On the mine site, these three mixes contained AMD, which is highly toxic due to low pH and high metal concentrations. For mixes 4 and 5, the toxicity was possibly due to the presence of nanoparticles of metal oxides. The toxicity of nanoparticles on *D. magna*, which can induce many side effects (e.g., formation of gas bubble inside the body, body burial coating inducing immobilization, direct toxicity, avoidance behavior response, intestinal problems), depends on the concentration and particle size, while the side effects of the gas bubble disease could cause a swelling of the crustacean (Renzi & Blaskovic, 2019). The protective effect of Ca and Mg has also been documented, with higher concentrations limiting the toxicity of metals, including metal oxide nanoparticles (Tipping & Woof, 1992; Martin & Kempton, 2003; Ritter & Luckenbach, 2003; Dobbs & Stillman, 2006; Bogart et al., 2016; Renzi & Blaskovic, 2019; Foudhaili et al., 2020). The presence of metal oxide nanoparticles can induce the production of reactive oxygen species (ROS), which can cause oxidative stress, inflammation, and damage to cell membranes, proteins, and DNA (Sengul & Asmatulu, 2020). The remaining pink color in the treated water during the bioassays could be attributed to the presence of nanoparticles due to the oxidation of metals in the ozonation process. The water analyses showed that the dissolved metal concentrations decreased considerably, but a mix of all the trace metals in oxidized form could have the potential to increase the toxicity and induce the production of ROS, leading to toxicity (Renzi & Blaskovic, 2019; Sengul & Asmatulu, 2020). Since these metals were present in trace concentrations, the contribution of the protective effect of Ca and Mg at lower dilutions during the bioassays was probably enough to protect the daphnia. The dilution water used during the bioassays had a lower hardness (adjusted to 160–180 mg $CaCO_3$/L) than the treated water of mixes 4 and 5 at 100% concentration (2,008 and 1,927 mg $CaCO_3$/L, respectively). The non-linear relation between the hardness and the metal mix toxicity could be an indication that a higher hardness may have sufficed to provide protection prior to dilution during the bioassays (Yim et al., 2006).

6.5 Conclusion

This study evaluated the removal efficiency of NH_3-N and metals for real mine effluent mixes, as well as the effect on the *D. magna* toxicity. The treatability tests showed satisfactory treatment

results using ozone microbubbles and lime precipitation with a flocculant. On the tests completed with the five mixes, three (mixes 1 to 3) contained low NH_3-N concentrations (< 4 mg/L) and two (mixes 4 and 5) contained higher concentrations (58 and 54 mg/L, respectively). In all cases, the treatment efficiency of NH_3-N was > 90% for the lower concentrations and > 99% for the higher concentrations. While the treatment showed a slightly better performance using ozone without metals pre-treatment, the bioassays showed that the pre-treatment of metals was necessary to prevent toxicity issues due to the possible presence of metal oxide nanoparticles generated by the ozonation. A pink color was still present in the water of mixes 4 and 5 without metals pre-treatment during the bioassays, suggesting the possible presence of metal oxides. Toxicity was observed only at 50% dilution, but not undiluted, with the control water during the bioassay, only for mixes 4 and 5. The lower hardness of the control water could have played a role in the toxicity, decreasing the protective effect of Ca on metals toxicity during dilution. This study showed the importance of treating for metals before ozonation due to toxicity issues and water coloring. For further evaluation, a polishing step could be conducted to remove the color and assess if the toxicity issue is linked to the presence of metal oxide nanoparticles.

Acknowledgements

This work was funded by the Natural Sciences and Engineering Research Council of Canada (NSERC), the Canada Research Chairs Program, and the industrial partners of the Research Institute on Mines and Environment (RIME) - University of Québec in Abitibi-Témiscamingue (UQAT) - Polytechnique Montréal, including Agnico Eagle, Canadian Malartic Mine, Iamgold Corporation, Newmont, Raglan Mine-Glencore, and Rio Tinto. The authors want to sincerely thank the collaboration of Gaëlle Thiffault-Bouchet, Éloïse Veilleux and their team from CEAEQ for conducting the bioassays, as well as the active help of Florence Laflamme during the lab tests and sampling.

6.6 References

American Public Health Association (APHA), 2017. Standard Methods for the Examination of Water and Wastewater. Method 4500-NH_3 D. 23rd Ed. Washington, DC, USA.

Bogart, S. J., Woodman, S., Steinkey, D., Meays, C., Pyle, G. G., 2016. Rapid changes in water hardness and alkalinity: Calcite formation is lethal to *Daphnia magna*. *Science of the Total Environment, 559*, 182-191.

Bondu, R., Cloutier, V., Rosa, E., Benzaazoua, M., 2017. Mobility and speciation of geogenic arsenic in bedrock groundwater from the Canadian Shield in western Québec, Canada. *Science of the Total Environment, 574*, 509-519.

Centre d'Expertise en Analyse Environnementale du Québec (CEAEQ), 2021. Détermination de la toxicité: létalité (CL50 48h) chez la daphnie *Daphnia magna*. MA. 500 – D.mag. 1.1, Rév. 3. Ministère de l'environnement et de la lutte contre les changements climatiques du Québec, Qc, Canada, 18p.

CEAEQ, 2016. Détermination de l'alcalinité de de l'acidité: méthode titrimétrique automatisée. MA. 315 – Alc-Aci 1.0, Rév. 3. Ministère du Développement durable, de l'environnement et de la lutte contre les changements climatiques du Québec, Qc, Canada, 12p.

CEAEQ, 2016. Détermination des cyanures: méthode colorimétrique automatisée avec l'acide isonicotinique et l'acide barbiturique – distillation manuelle. MA. 300 – CN 1.2, Rév. 4. Ministère du Développement durable, de l'Environnement et de la Lutte contre les changements climatiques du Québec, Qc, Canada, 26p.

CEAEQ, 2020. Détermination des anions: méthode par chromatographie ionique. MA. 300 – Ions 1.3, Rév. 6. Ministère de l'environnement et de la lutte contre les changements climatiques, Qc, Canda, 14p.

CEAEQ, 2020. Détermination des métaux: méthode par spectrométrie de masse à source ionisante au plasma d'argon. MA. 200 – Mét. 1.2, Rév. 7. Ministère de l'environnement et de la lutte contre les changements climatiques, Qc, Canada, 35p.

Coudert, L., Bondu, R., Rakotonimaro, T. V., Rosa, E., Guittonny, M., Neculita, C. M., 2020. Treatment of As-rich mine effluents and produced residues stability: Current knowledge and research priorities for gold mining. *Journal of Hazardous Materials*, 121920.

Dobbs, M. G., Stillman, J. H., 2006. Influence of water hardness on the toxicity of zinc to Daphnia magna. *Environmental Toxicology and Chemistry: An International Journal, 25*(5), 1425-1429.

Dubuc, J., Coudert, L., Lefebvre, O., Neculita, C. M., 2022. Electro-Fenton treatment of contaminated mine water to decrease thiosalts toxicity to *Daphnia magna*. *Science of the Total Environment*, 835, 155323.

Etteieb, S., Magdouli, S., Zolfaghari, M., Brar, S., 2020. Monitoring and analysis of selenium as an emerging contaminant in mining industry: A critical review. *Science of the Total Environment*, 134339.

Foudhaili, T., Jaidi, R., Neculita, C. M., Rosa, E., Triffault-Bouchet, G., Veilleux, É., Lefebvre, O., 2020. Effect of the electrocoagulation process on the toxicity of gold mine effluents: A comparative assessment of *Daphnia magna* and *Daphnia pulex*. *Science of the Total Environment, 708*, 134739.

Gervais, M., Dubuc, J., Paquin, M., Gonzalez-Merchan, C., Genty, T., Neculita, C. M., 2020. Comparative efficiency of three advanced oxidation processes for thiosalts oxidation in mine-impacted water. *Minerals Engineering, 152*, 106349.

Gonzalez, J. A., Ghobaeiyeh, F. V., Mckay, D. J., 2019. Process for treatment of mine impacted water. In: Google Patents.

Gonzalez-Merchan, C., Genty, T., Bussière, B., Potvin, R., Paquin, M., Benhammadi, M., Neculita, C. M., 2016. Ferrates performance in thiocyanates and ammonia degradation in gold mine effluents. *Minerals Engineering, 95*, 124-130.

Hamilton, S. J., 2004. Review of selenium toxicity in the aquatic food chain. *Science of the Total Environment, 326*(1-3), 1-31.

Hem, J. D., 1985. *Study and interpretation of the chemical characteristics of natural water* (Vol. 2254): Department of the Interior, US Geological Survey.

Jermakka, J., Wendling, L., Sohlberg, E., Heinonen, H., Vikman, M., 2015. Potential technologies for the removal and recovery of nitrogen compounds from mine and quarry waters in subarctic conditions. *Critical Reviews in Environmental Science and Technology, 45*(7), 703-748.

Khuntia, S., Majumder, S. K., Ghosh, P., 2013. Removal of ammonia from water by ozone microbubbles. *Industrial & Engineering Chemistry Research, 52*(1), 318-326.

Khuntia, S., Majumder, S. K., Ghosh, P., 2014. Oxidation of As (III) to As (V) using ozone microbubbles. *Chemosphere, 97*, 120-124.

Le Bourre, B., 2020. Protocole d'essais de traitement de l'azote ammoniacal par ozonation. RIME (Research Institute on Mines and Environment), UQAT (Université du Québec en Abitibi-Témiscamingue), Rouyn-Noranda, Qc, Canada, 28 p.

Marcotte, P., Aubé, E., Dubé, C., Neculita, C.M., 2021. Performance of microbubbles ozonation for the removal of nitrogen-based contaminants in mine impacted water. Proceedings of the Symposium on Mines and the Environment, Rouyn-Noranda, Qc, Canada, June 14-16.

Martin, C. W., Kempton, J. H., 2003. Effects of water hardness on the toxicity of copper to *Daphnia magna*: implications for the biotic ligand model. *Environmental Toxicology and Chemistry: An International Journal, 22*(7), 1466-1472.

Ministère de l'environnement et de la lutte contre les changements climatiques (MELCC), 2012. Directive 019 sur l'industrie minière. Gouvernement du Québec, ISBN : 978-2-550-64507-8, 105p. http://www.mddefp. gouv.qc.ca/milieu_ind/directive019/directive019.pdf.

Minister of Justice, 2021. MDMER (Metal and Diamond Mining Effluent Regulations); SOR/ 2002–222. Government of Canada, Ottawa, ON, Canada. https://laws-lois.justice.gc.ca/ PDF/SOR-2002-222.pdf.

MEND (Mine Environment Neutral Drainage), 2014. Study to identify BATEA for the management and control of effluent quality from mines. MEND Report 3.50.1, Hatch, Canada, 527 p.

Mousset, E., Loh, W. H., Lim, W.S., Jarry, L., Wang, Z., Lefebvre, O., 2021. Cost comparison of advanced oxidation processes for wastewater treatment using accumulated oxygen-equivalent criteria. *Water Research*, 200, 117234.

Neculita, C. M., Coudert, L., Rosa, E., Mulligan, C. N., 2020. Future prospects for treating contaminants of emerging concern in water and soils/sediments. In *Advanced Nano-Bio Technologies for Water and Soil Treatment* (pp. 589-605): Springer.

Olvera-Vargas, H., Dubuc, J., Wang, Z., Coudert, L., Neculita, C. M., Lefebvre, O., 2021. Electro-Fenton beyond the degradation of organics: Treatment of thiosalts in contaminated mine water. *Environmental Science & Technology, 55*(4), 2564-2574.

Renzi, M., Blašković, A., 2019. Ecotoxicity of nano-metal oxides: A case study on *Daphnia magna*. *Ecotoxicology, 28*(8), 878-889.

Ritter, C., Luckenbach, T., 2003. Hardness-dependent toxicity of metals to *Daphnia magna*: a study using the biotic ligand model. *Aquatic toxicology, 65*(1), 29-44.

Ryskie, S., Gonzalez-Merchan, C., Neculita, C. M., Genty, T., 2020. Efficiency of ozone microbubbles for ammonia removal from mine effluents. *Minerals Engineering, 145*, 106071.

Ryskie, S., Neculita, C. M., Rosa, E., Coudert, L., Couture, P., 2021. Active treatment of contaminants of emerging concern in cold mine water using advanced oxidation and membrane-related processes: a review. *Minerals, 11*(3), 259.

Sengul, A. B., Asmatulu, E., 2020. Toxicity of metal and metal oxide nanoparticles: a review. *Environmental Chemistry Letters, 18*(5), 1659-1683.

Takahashi, M., Chiba, K., Li, P., 2007. Formation of hydroxyl radicals by collapsing ozone microbubbles under strongly acidic conditions. *The Journal of Physical Chemistry B, 111*(39), 11443-11446.

Tipping, E., Woof, C., 1992. The influence of pH and water hardness on the toxicity of aluminium to *Daphnia magna*. *Water research, 26*(4), 515-522.

Wang, J. L., Xu, L. J., 2012. Advanced oxidation processes for wastewater treatment: Formation of hydroxyl radical and application. *Critical Reviews in Environmental Science and Technology, 42*(3), 251-325.

Wolkersdorfer, C., Nordstrom, D. K., Beckie, R. D., Cicerone, D. S., Elliot, T., Edraki, M., Valente, T., Alves Franca, S. C., Kumar, P., Lucero, R. A. O., Soler i Gil, A., 2020. Guidance for

the integrated use of hydrological, geochemical, and isotopic tools in mining operations. *Mine Water and the Environment, 39*(2), 204-228.

Wu, Y., Tian, W., Zhang, Y., Fan, W., Liu, F., Zhao, J., Lyu, T., 2022. Nanobubble technology enhanced ozonation process for ammonia removal. *Water, 14*(12), 1865.

Xiong, X., Wang, B., Zhu, W., Tian, K., Zhang, H., 2019. A review on ultrasonic catalytic microbubbles ozonation processes: Properties, hydroxyl radicals generation pathway and potential in application. *Catalysts, 9*(1), 10.

Yim, J. H., Kim, K. W., Kim, S. D., 2006. Effect of hardness on acute toxicity of metal mixtures using *Daphnia magna*: Prediction of acid mine drainage toxicity. *Journal of Hazardous Materials, 138*(1), 16-21.

Zheng, T., Wang, Q., Zhang, T., Shi, Z., Tian, Y., Shi, S., Wang, J., 2015. Microbubble enhanced ozonation process for advanced treatment of wastewater produced in acrylic fiber manufacturing industry. *Journal of Hazardous Materials, 287*, 412-420.

Zuttah, Y., 1999. Destruction de l'ammoniac dans les effluents miniers. MSc thesis, Department of mines and metallurgy, Laval University, Qc, Canada, 107p.

CHAPITRE 7 DISCUSSION GÉNÉRALE

7.1 Retour sur les objectifs

Cette étude concernant les CEC en contexte minier avait pour objectifs de 1) réaliser une revue de littérature afin d'identifier les contaminants d'intérêt sur le site minier à l'étude; 2) de prédire, par modélisation numérique à l'aide du modèle PHREEQC, la concentration et la spéciation des CEC ciblés à l'équilibre dans les mélanges d'effluents miniers et ce, avec un facteur de confiance d'au moins 80%; 3) augmenter l'efficacité de traitement des CEC ciblé de plus de 50% par rapport aux méthodes conventionnelles par l'utilisation d'un procédé d'ozonation en microbulles. Chacun des trois objectifs a été présenté sous forme d'un article.

Concernant le premier objectif, la revue de littérature a en effet pu identifier les contaminants d'intérêt présents sur le site tout en identifiant d'autres contaminants pouvant se retrouver sur d'autres sites miniers. L'évolution d'un contaminant considéré émergent vers un état plus connu, c'est-à-dire, lorsque les effets sur l'environnement sont connus et que les méthodes de traitement adaptées sont développées, est présentée dans la revue de littérature. Une description détaillée de chaque contaminant, à savoir, la concentration naturellement présente, les concentrations typiques en milieu minier, leur effet sur la toxicité aquatique ainsi que des méthodes de traitement émergentes y sont inclus. Les méthodes de traitement par oxydation avancée utilisant l'ozone en microbulles ainsi que la filtration membranaire sont présentées en détails avec quelques exemples d'études de cas. Bref, les besoins en recherche y sont détaillés identifiant ainsi les défis en traitement des eaux minières en climat froid. Bref, les principaux résultats montraient que : 1) l'utilisation de l'ozone en microbulles permet de traiter efficacement l'azote ammoniacal et améliore le traitement de certains métaux 2) l'ozonation sans prétraitement des métaux peut changer la couleur des effluents traités. De plus, cette synthèse de la littérature récente et pertinente sur le sujet a permis d'identifier les besoins en recherche suivants : les procédés d'oxydation avancée peuvent limiter la création de salinité résiduelle ainsi que permettre de traiter simultanément les mélanges d'effluents.

Les résultats reliés au second objectif ont démontré les limites du modèle PHREEQC avec les mélanges d'eaux minières acides et fortement contaminées en Fe. En effet, les prédictions pour la majorité des contaminants étaient pratiquement toutes dans l'intervalle de confiance visé de 80%

sauf pour les mélanges où il y avait une concentration élevée en Fe. Les mécanismes de sorption, coprécipitation ainsi que la précipitation due à l'activité microbiologique ont été identifiés à l'aide des différents modèles effectués durant l'étude tout en validant à l'aide des analyses physico-chimiques et minéralogiques.

Les essais réalisés afin de répondre au troisième objectif ont pu démontrer que l'utilisation de l'ozone en microbulles augmente l'efficacité de traitement pour $N\text{-}NH_3$, NO_2^-, et certains métaux comparativement aux méthodes conventionnelles. En effet, la cinétique de réaction pour l'oxydation de $N\text{-}NH_3$ et NO_2^- en NO_3^- est plus rapide qu'un procédé biologique conventionnel de type MBBR et est moins affecté par la température (Young et al., 2017). Le traitement de certains métaux est aussi amélioré comme il est possible de voir dans l'étude. Il est important de mentionner qu'il est impératif de traiter les métaux avant l'oxydation avec ozone car il peut y avoir formation de nanoparticules d'oxydes métalliques ayant un effet toxique pour les espèces aquatiques.

7.2 Validation des hypothèses

Les hypothèses de recherche ont été validées en partie durant cette étude. La première hypothèse consistait à l'identification des CEC d'intérêt à l'aide d'une revue de littérature, ce qui a été validé. En effet, les différents contaminants identifiés sur le site ont aussi été présentés dans la revue de littérature. Pour la deuxième hypothèse, l'utilisation de PHREEQC a permis de prédire la spéciation et les indices de saturation des différentes phases présentes dans les mélanges. Cependant, la modélisation des cinétiques de réaction à l'aide de PHREEQC est assez limitée et il est difficile de prédire des concentrations lorsque l'état d'équilibre n'est pas atteint. Tel que mentionné précédemment, la troisième hypothèse a été validée en démontrant qu'il est possible de réduire les concentrations à l'aide de l'ozonation en microbulles à une valeur plus faible que par l'utilisation d'une méthode conventionnelle utilisant la précipitation à l'aide de chaux et de floculant.

7.3 Présence des CEC sur le site à l'étude

Durant l'étude, plusieurs campagnes d'échantillonnage ont eu lieu afin d'avoir des données étalées sur différentes saisons actives. L'analyse de ces données conjointement réalisée à l'aide de la revue de littérature a permis d'identifier les CEC présents sur le site à l'étude et ce, pour les travaux de modélisation ainsi que les essais de traitabilité. Le choix des paramètres reliés à la modélisation et

les essais de traitement ont été choisis grâce à la connaissance des différents contaminants présents. L'analyse de ces différents contaminants a aussi été réalisée en compilant les données historiques du site à l'aide de la géodatabase ainsi que le programme R. Les graphiques des différents points d'échantillonnage sont présentés à l'annexe D.

Une analyse sous forme graphique de l'évolution de la température et des précipitations selon la période de l'année est présentée à la figure 7.1. La période active, durant laquelle l'eau n'est pas gelée, est généralement d'avril à novembre soit printemps, été et automne.

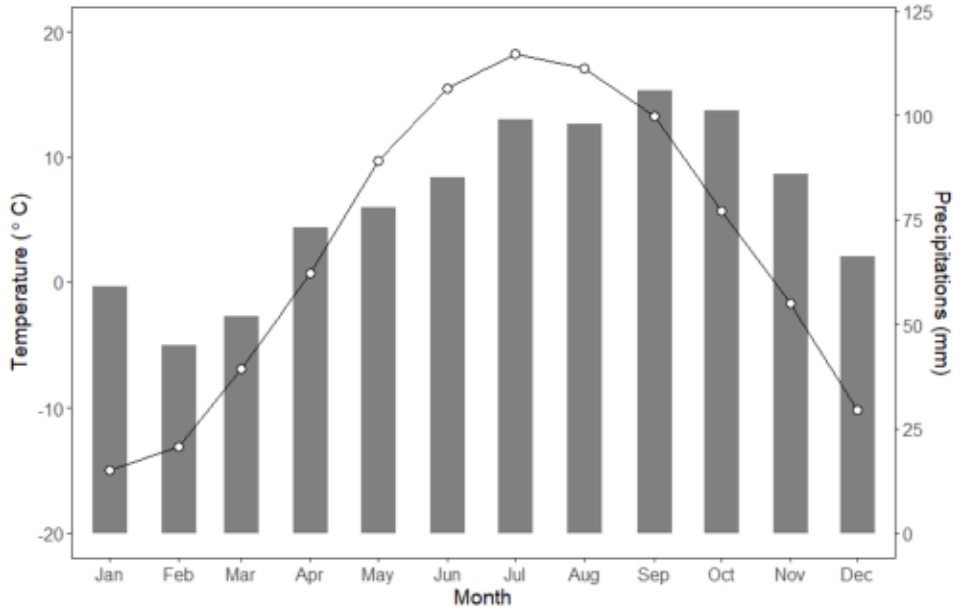

Figure 7.1 Évolution de la température et des précipitations en fonction de la période de l'année (climate-data.org, 2022)

7.4 Choix de la base de données thermodynamique pour PHREEQC

Le choix de la base de données thermodynamique lors des modélisations des différents mélanges a été un facteur important à considérer. En effet, plusieurs bases de données sont disponibles dans PHREEQC et chacune d'elles diffère l'une de l'autre, parfois légèrement, parfois énormément et sont utilisées dépendamment de la qualité de l'eau étudiée (Lu et al., 2022). Dans cette étude, la base de données thermodynamique wateq4f.dat a été utilisée car c'est la seule disponible actuellement pouvant modéliser avec plus de précision les eaux minières acides comportant des métaux, tels le Fe et Al, sous forme colloïdale (Nordstrom, 2020). Il est cependant plus difficile de modéliser les composés azotés avec cette dernière. La base de données thermodynamique

minteqv4.dat contient plus de paramètres et est plus précise pour la modélisation de N-NH_3, NO_2^-, NO_3^- et CNO^- que wateq4f.dat. Pour le reste des paramètres à l'étude, il était plus difficile de modéliser avec précision les phénomènes de sorption et coprécipitation car les particules colloïdales de Fe ont un impact majeur sur la mobilité des autres métaux.

7.5 Analyses minéralogiques aidant la précision des modèles

Lors de la modélisation avec le programme PHREEQC, celui-ci peut donner un grande nombre d'espèces minérales pouvant être présentes à l'équilibre selon l'indice de saturation. Afin de déterminer avec plus de précision la présence de certaines phases minérales, les sédiments formés lors des différents mélanges entreposés afin d'atteindre l'équilibre ont été filtrés puis séchés pour ensuite être analysés de près au MEB. En forçant la présence des phases connues dans PHREEQC avec l'option EQUILIBRIUM_PHASES, il est possible de modéliser avec plus de précision et c'est ce qui a été observé dans cette étude. En plus de permettre une prédiction plus précise, il est aussi possible de calculer les flux de chacune des phases minérales entrées dans le modèle, permettant ainsi d'avoir les quantités qui se dissolvent ou qui se solubilisent. Sans les analyses minéralogiques, il n'est pas possible de déterminer les phases minérales présentes avec certitude. Certaines phases amorphes sont plus difficilement identifiables au microscope mais en combinant les connaissances acquises de la littérature ainsi que les formes potentiellement présentes déterminées avec PHREEQC, il est possible d'orienter le minéralogiste afin de trouver les bonnes phases présentes. Cela a été un défi car les échantillons disponibles étaient en très petite quantité et une technique spéciale était nécessaire afin de mettre ceux-ci sur une section polie pouvant être insérée dans le TIMA, le microscope pouvant visualiser avec une meilleure précision.

7.6 Modélisations directes vs inverses

Différentes options de modélisation sont disponibles dans PHREEQC afin de pouvoir résoudre différents types de problèmes et ainsi raffiner et/ou valider les modélisations réalisées. En effet, il est possible d'utiliser la modélisation inverse afin d'identifier les phases minérales qui précipitent ou se dissolvent lors d'un mélange. Dans cette étude, cette approche a été utilisée dans le but de valider quels sont les flux des différentes phases minérales présentes dans les mélanges d'effluents préparés en laboratoire. En effectuant ce processus sur des effluents connus tout en ayant les analyses minéralogiques, il a été possible de valider la méthode. Les modélisations directes ont

ensuite été effectuées et cela a permis de démontrer que les mélanges n'avaient pas atteint l'équilibre car il y avait des différences au niveau des concentrations des différents contaminants, surtout lorsque le pH est acide et en présence de concentration élevée en Fe. Cette méthode est très utile afin de diminuer le nombre d'inconnus lors des différentes modélisations et permet d'augmenter le niveau de confiance des résultats obtenus.

7.7 Modélisation pour la prédiction

La modélisation avec PHREEQC permet de prédire la qualité de l'eau après mélange de différents effluents sur le long terme (AECOM, 2019). Au début de ce projet, la compagnie minière voulait savoir si l'effluent allait être impacté par le mélange de l'eau de la fosse DP servant comme parc à résidus lorsque celle-ci allait être pompée vers le TSF3E pour ensuite être mélangée avec le reste des effluents avant le traitement à l'usine HDS. Une simulation a été réalisée sur 5 années avec les données disponibles à ce moment en utilisant la base de données thermodynamique minteqv4.dat. Une des inquiétudes était la présence de CNO^- et $N\text{-}NH_3$ dans la fosse DP qui aurait pu affecter la toxicité rendu à l'effluent car ces derniers ne sont pas traités à l'usine HDS. Les différents ratios utilisés pour la prédiction sont présentés dans les tableaux 7.1 et 7.2.

Tableau 7.1 Ratios of the mix 1 DP into TSF3E

Pond	Volume ($\times 10^3$ m³)	Ratio
DP	582,576	0,621
TSF3E	355,644	0,379

Tableau 7.2 Ratios of the mix 2 into BB

Pond	Volume ($\times 10^3$ m³)								Total	Total with DP	Ratio
	May	Jun.	Jul.	Aug.	Sept.	Oct.	Nov.	Dec.			
TSF1	137,800	0	0	0	0	0	0	0	137,800	137,800	0,037
TSF2	42,282	172,800	92,160	0	0	84,000	162,000	66,000	619,242	619,242	0,168
TSF3E	11,040	4,140	2,520	2,160	3,000	63,060	192,720	37,920	316,560	899,136	0,244
NP	408,233	185,198	41,820	41,001	7,763	81,615	31,443	42,666	839,739	839,739	0,227
WR	139,026	298,868	235,946	57,181	25,095	191,964	124,290	123,923	1196,293	1196,293	0,324

Le tableau 7.3 présente les concentrations modélisées à l'équilibre dans TSF3E, après mélange avec DP. Au début, les concentrations augmentent pour ensuite se stabiliser vers la 5^e année. Les CNO^- augmentent pour atteindre une concentration de 3,04 mg/L dans TSF3E, alors que le $N\text{-}NH_3$

augmente rapidement dès la première année jusqu'à près de 30 mg/L pour atteindre une concentration de près de 48 mg/L après cinq ans. La salinité augmente aussi considérablement selon le paramètre. La concentration des métaux dans DP n'est pas élevé, leur concentration augmente que très légèrement.

Tableau 7.3 Predicted parameters for the mixture of DP into TSF3E for 5 years including the initial mean values

Parameter	Year 0	Year 1	Year 2	Year 3	Year 4	Year 5
Al	0,16	0,095	0,069	0,059	0,055	0,054
As	0,025	0,025	0,025	0,025	0,025	0,025
Ba	0,0085	0,048	0,062	0,068	0,070	0,071
Be	0,00020	0,00020	0,00020	0,00020	0,00020	0,00020
Br	0,45	2,93	3,87	4,22	4,36	4,41
H_2CO_3		62,9	71,5	74,7	76,0	76,48
HCO_3		83,5	116,8	129,4	134,1	135,9
Ca	183	434	530	566	580	585
Cd	0,0036	0,0057	0,0064	0,0067	0,0068	0,0069
Cl	6,4	58,1	77,7	85,1	87,9	89,0
Cr	0,0024	0,0047	0,0055	0,0058	0,0060	0,0060
Cu	0,0046	0,13	0,17	0,19	0,19	0,20
CNO^-	0,63	2,14	2,71	2,93	3,01	3,04
CN^-	0,003	0,066	0,090	0,10	0,10	0,10
F	0,38	0,35	0,33	0,33	0,33	0,33
Fe	0,023	1,39	1,91	2,11	2,18	2,21
K	8,5	39,5	51,1	55,6	57,3	57,9
Li	0,0083	0,032	0,040	0,044	0,045	0,045
Mg	20,7	119,1	156,4	170,6	175,9	178,0
Mn	0,016	7,33	10,11	11,16	11,55	11,71
$N\text{-}NH_3$	0,09	29,32	41,59	46,20	47,94	48,60
NO_2^-	0,44	54,24	63,58	67,12	68,46	68,96
NO_3^-	4,28	0,21	0,20	0,21	0,21	0,21
Na	31,1	182,5	239,8	261,6	269,9	272,9
Ni	0,0065	0,081	0,11	0,12	0,12	0,13
PO_4^{2-}	0,75	2,31	2,31	2,31	2,31	2,31
Pb	0,0028	0,0034	0,0036	0,0037	0,0038	0,0038
SO_4^{2-}	557	1352	1677	1799	1844	1862
Se	0,0018	0,0048	0,0059	0,0063	0,0065	0,0065
Si	0,13	1,11	1,52	1,68	1,74	1,76
Sr	0,27	1,38	1,80	1,96	2,02	2,04
U	0,00065	0,0012	0,0015	0,0016	0,0016	0,0016
Zn	0,038	0,41	0,55	0,61	0,63	0,64
pH	7,16	6,33	6,41	6,43	6,44	6,44

Le tableau 7.4 présente les concentrations à l'équilibre après modélisation du mélange complet dans BB en incluant DP sur cinq années. Les concentrations de CNO^- augmentent légèrement pour se stabiliser autour de 1 mg/L. La concentration de $N\text{-}NH_3$ se stabilise autour de 15 mg/L après

cinq ans. La concentration des métaux diminue légèrement pour la majorité puis se stabilise dû la dilution engendrée par la faible concentration de métaux dans DP. La salinité augmente légèrement sauf pour les SO_4^{2-} qui diminuent de près de la moitié. Le pH est aussi affecté légèrement à la hausse. Il est à noter que les concentrations à l'équilibre de NO_2^- et NO_3^- ne semblent pas réalistes pour ces prédictions. La toxicité associée à $N\text{-}NH_3$ pour une concentration d'environ 15 mg/L n'est historiquement pas problématique car l'effluent final a des épisodes saisonniers atteignant cette valeur, surtout en hiver dû à la méthode de gestion des eaux provenant de WWB vers WR. Cependant, considérant que les campagnes d'échantillonnage pour effectuer les modélisations ont été réalisées durant les saisons actives, l'apport supplémentaire de $N\text{-}NH_3$ en période hivernale pourrait potentiellement être problématique au niveau de la toxicité.

Tableau 7.4 Predicted parameters of BB after mixture of TSF1, TSF2, TSF3E, NP and WR for 5 years including the initial mean values

Parameter	Year 0	Year 1	Year 2	Year 3	Year 4	Year 5
Al	66,65	48,57	48,57	48,57	48,57	48,57
As	0,028	0,025	0,025	0,025	0,025	0,025
Ba	0,019	0,030	0,033	0,035	0,035	0,036
Be	0,0022	0,0013	0,0013	0,0013	0,0013	0,0013
Br	5,58	3,88	4,11	4,20	4,23	4,24
HCO_3^-		380,46	388,70	391,87	393,11	393,54
Ca	290,25	300,14	323,43	332,25	335,57	336,86
Cd	0,0051	0,0046	0,0048	0,0048	0,0049	0,0049
Cl	175,50	170,44	175,19	177,00	177,71	177,96
Cr	0,038	0,027	0,027	0,027	0,027	0,027
Cu	1,30	0,95	0,96	0,97	0,97	0,97
CNO^-	0,63	0,86	1,00	1,05	1,07	1,08
CN^-	0,028	0,018	0,024	0,026	0,027	0,027
F	0,49	0,43	0,43	0,43	0,42	0,42
Fe	302	223,10	223,21	223,27	223,32	223,32
K	4,73	11,96	14,82	15,91	16,32	16,47
Li	0,066	0,052	0,055	0,055	0,056	0,056
Mg	87,55	87,94	97,03	100,48	101,79	102,28
Mn	5,45	5,58	6,26	6,51	6,61	6,65
$N\text{-}NH_3$	2,03	9,93	13,07	14,26	14,71	14,88
NO_2^-	0,44	20,67	22,61	23,32	23,58	23,68
NO_3^-	9,41	18,46	18,86	19,03	19,10	19,12
Na	34,68	64,81	78,81	84,12	86,12	86,88
Ni	0,18	0,14	0,15	0,15	0,15	0,15
PO_4^{2-}	13,83	15,77	15,77	15,77	15,77	15,77
Pb	0,010	0,010	0,010	0,0098	0,0098	0,0098
SO_4^{2-}	1899	933	1010	1038	1050	1054
Se	0,027	0,018	0,018	0,018	0,018	0,018
Si	15,38	6,04	6,14	6,18	6,20	6,20
Sr	1,70	1,76	1,86	1,90	1,91	1,92
U	0,0053	0,0039	0,0040	0,0040	0,0040	0,0040

Zn	1,36	1,16	1,19	1,21	1,21	1,21
pH	2,63	2,72	2,72	2,73	2,73	2,73

7.8 Limites de PHREEQC

Les modélisations à l'aide de PHREEQC peuvent donner des résultats intéressants afin d'améliorer la gestion de l'eau sur un site minier. Il est cependant important de bien connaître les limites associées. En effet, le programme comporte certaines lacunes surtout en présence de bactéries, de concentration élevée en Fe et de faible pH tel qu'il a été possible de voir durant cette étude. De plus, lorsque les mélanges n'ont pas le temps d'atteindre l'équilibre, il devient difficile de prédire avec justesse les concentrations. Il est aussi important de bien connaître les limites des différentes bases de données thermodynamiques selon l'application à l'étude. Certains paramètres d'intérêt peuvent être présents dans une base de données mais pas dans l'autre, cela apporte certaines incertitudes quant à l'applicabilité à tout type d'effluent. Une combinaison de différentes bases de données peut être nécessaire afin d'avoir une vue d'ensemble complète lorsque tous les paramètres ne sont pas présents. Il a été possible de voir, par exemple, que la prédiction des composés azotés peut être erronée d'autant plus que ces composés peuvent être aussi régulé par l'activité bactérienne, telle la nitrification. Enfin, cet outil est tout de même en mesure de générer des données très utiles pour les opérateurs miniers, il faut s'assurer que la personne qui procède avec les modélisations connaisse bien les différentes limites.

7.9 Traitement avec le pilote d'ozonation en microbulles

Les essais réalisés avec le pilote d'ozonation par microbulles ont démontré l'importance de prétraiter les métaux avant de procéder à l'oxydation. Le fait que certains effluents n'étaient pas toxiques avant traitement et le devenaient par la suite est expliqué par la possible présence de nanoparticules d'oxydes métalliques. Vu que les échantillons ont été filtrés avec un filtre de 0,45 µm avant les bio essais et que la couleur rose demeurait, l'hypothèse de la présence de nanoparticules est plausible. Bien que l'oxydation permette de mieux traiter les métaux par la suite, la toxicité engendrée par cette manipulation est à considérer. L'oxydation avancée à l'aide de l'ozone en microbulles est surtout utile afin de traiter N-NH_3 et NO_2^-, ainsi que CNO^-, CN^- et SCN^- lorsque présents mais augmente la concentration de NO_3^-, qui est un des produits de l'oxydation finale des composés précédents, et est moins toxique. Dans des environnements sensibles, il est

toutefois important de ne pas transférer le problème vers une autre forme, même NO_3^-. Un traitement complet serait donc plus approprié en cas de concentration en NO_3^- trop élevée. Cela fait partie des limites de ce procédé. Une étape subséquente de dénitrification pourrait être ajoutée. Il est à noter que des essais en condition plus froide n'ont pas été testés dans cette présente étude car il a été démontré qu'il n'y avait un effet négligeable sur l'efficacité de traitement dans les travaux de maîtrise réalisés précédemment (Ryskie, 2017).

CHAPITRE 8 CONCLUSION ET RECOMMANDATIONS

Les sites miniers doivent gérer et souvent traiter de grands volumes d'eau contaminée dû à leurs opérations, soit par les changements géochimiques ou bien par l'ajout de produits chimiques dans les procédés d'extraction. Avec l'évolution des connaissances dans le domaine du traitement de l'eau et de l'écotoxicologie, des CEC sont de plus en plus considérés et leurs effets sur l'environnement démontrés. Des méthodes de traitement comme l'oxydation avancée à l'aide de l'ozone en microbulles peuvent aider à réduire les effets néfastes des CEC. Une bonne gestion de l'eau est aussi importante et des outils de modélisation numérique sont très utiles afin de prédire la qualité de l'eau.

L'objectif principal de cette étude est de prédire la spéciation des CEC à l'aide de PHREEQC ainsi que d'évaluer l'effet sur la toxicité aquatique sur le crustacé *D. magna* avant et après traitement d'effluents seuls et en mélanges à l'aide de l'ozonation en microbulles. Pour ce faire, une revue de littérature exhaustive a permis d'identifier les CEC et leurs effets sur la toxicité aquatique. Les différentes campagnes d'échantillonnage conjointement avec les données historiques ont permis de générer une géodatabase. L'utilisation de ces données à l'aide du programme PHREEQC et de la base de données thermodynamique wateq4f.dat a permis de modéliser les concentrations des différents CEC à l'équilibre. Les mélanges modélisés comparés aux mélanges préparés en labo ont permis de valider les modélisations par l'utilisation des commandes de modélisation directes et inverses. Les analyses minéralogiques ont été réalisées afin de valider les espèces minérales présentes dans les solides formés dans les mélanges des différents effluents. Les différents tests de traitabilité sur des mélanges d'effluents ont aussi été réalisés à l'aide du pilote d'ozonation en microbulles en traitant les métaux avant ou après l'ozonation afin de voir les effets sur la toxicité aquatique sur *D. magna* avant et après traitement.

Les résultats obtenus durant les différentes étapes de ce projet ont permis de tirer les conclusions suivantes :

- Les CEC sont présents dans les effluents miniers en différentes concentrations;
- Les effets écotoxicologiques des différents CEC diffèrent l'un de l'autre et dépendent des paramètres physico-chimiques de l'eau;

- Des méthodes de traitement utilisant l'ozone en microbulles et la filtration membranaire peuvent être utilisés pour le traitement des CEC en domaine minier, spécifiquement en climat froid et pour de très faibles concentrations;
- La combinaison d'analyses chimiques, isotopiques et minéralogiques avec des analyses statistiques et des approches de modélisation directe et inverse a permis de décrypter les processus clés contrôlant l'évolution géochimique des effluents miniers mixtes;
- La formation de minéraux secondaires tels que la schwertmannite, la jarosite et la goethite a été identifiée comme un processus clé contrôlant la géochimie des effluents miniers étudiés;
- La schwertmannite, la jarosite et la goethite peuvent incorporer Fe, SO_4^{2-}, K et Na à partir de la solution par incorporation directe dans les structures minérales et il est probable que d'autres métaux et métalloïdes (c'est-à-dire Li, Ti, U, Cr, Be, Al, Pb, Ni, Co, Se, Si, Cu, Mn, Zn) sont également immobilisés par ces phases par des processus de sorption ou de coprécipitation;
- La cinétique de formation de la schwertmannite, de la jarosite et de la goethite semble jouer un rôle important dans l'évolution géochimique des mélanges d'effluents, ces derniers restant souvent en déséquilibre par rapport à ces phases;
- L'activité biologique peut encore influencer la formation de minéraux secondaires;
- Les observations faites sur les solides formés au cours des expériences de laboratoire suggèrent fortement l'apparition de processus à médiation biologique, ce qui apporte certaines incertitudes supplémentaires aux modèles;
- Les approches de modélisation directe et inverse réalisées à l'aide de PHREEQC peuvent fournir des informations utiles sur la possible plage de concentrations de solides dissous dans les mélanges d'effluents miniers et sur les phases minérales susceptibles de contrôler l'évolution géochimique des mélanges;
- Les tests de traitabilité ont montré des résultats de traitement satisfaisants en utilisant l'ozone en microbulles et une précipitation chimique à l'aide de chaux et de floculant;

- L'efficacité de traitement du NH_3-N était > 90% pour les faibles concentrations (< 4 mg/L) et > 99% pour les concentrations plus élevées (54-58 mg/L);
- Alors que le traitement a montré une performance légèrement meilleure en utilisant l'ozone sans prétraitement des métaux, les essais biologiques ont montré que le prétraitement des métaux était nécessaire pour prévenir les problèmes de toxicité dus à la présence possible de nanoparticules d'oxydes métalliques générées par l'ozonation;
- Une couleur rose était encore présente dans l'eau des mélanges 4 et 5 sans prétraitement des métaux lors des bioessais, suggérant la présence possible de nanoparticules d'oxydes métalliques;
- La toxicité a été observée uniquement à une dilution de 50%, avec l'eau de contrôle pendant le bioessai, seulement pour les mélanges 4 et 5 sans prétraitement des métaux;
- La plus faible dureté de l'eau de contrôle pourrait avoir joué un rôle dans la toxicité, diminuant l'effet protecteur du Ca sur la toxicité des métaux lors de la dilution.

Afin de continuer les travaux présentés dans cette thèse, il est recommandé de :

- Caractériser les effluents en période hivernale afin d'avoir une meilleure vue d'ensemble de toutes les saisons;
- Filtrer les échantillons prélevés avec un filtre 0,45 µm et 0,1 µm, en plus de séparer les particules par centrifugation à haute vitesse afin de tenter d'éliminer complètement les particules colloïdales pouvant être présentes et ainsi diminuer les erreurs lors des modélisations;
- Observer la membrane poreuse de l'électrode de pH au MEB avant et après les mesures des échantillons afin de voir s'il y a colmatage de la membrane par des particules colloïdales;
- Réaliser des analyses microbiologiques en parallèle des mélanges afin de déterminer la présence de bactéries pouvant contrôler les processus géochimiques;
- Réaliser les mélanges à plus grande échelle afin d'obtenir une plus grande quantité de solides et ainsi améliorer la qualité des analyses minéralogiques;
- Laisser reposer les mélanges plus longtemps que deux semaines afin de tenter d'atteindre l'équilibre et ainsi valider les modèles avec plus de précision;

- Utiliser un autre logiciel de modélisation numérique qui incorpore les processus microbiologiques et géochimiques et comparer avec PHREEQC;
- Effectuer des modélisations complémentaires avec un modèle BLM qui identifie les phases labiles et biodisponibles des différents contaminants tout en réalisant des bioessais afin de prédire la toxicité aquatique;
- Mesurer la taille des bulles avec un équipement pouvant réaliser des analyses zeta et tenter de modifier les pressions d'opération afin de diminuer au minimum la taille des bulles;
- Combiner la filtration membranaire au pilote d'ozonation en microbulles, avant ou après, afin de voir l'efficacité de traitement;
- Pour une évaluation plus approfondie, une étape de polissage pourrait être effectuée pour éliminer la couleur et évaluer si le problème de toxicité est lié à la présence de nanoparticules d'oxyde métallique.

RÉFÉRENCES

AECOM. (2019). New Britannia Mill Water Quality Assessment. Memo for Hudbay Minerals Inc., 49 p.

Aguiar, A., Andrade, L., Grossi, L., Pires, W., Amaral, M. (2018). Acid mine drainage treatment by nanofiltration: A study of membrane fouling, chemical cleaning, and membrane ageing. *Separation and Purification Technology*, *192*, 185–195.

Altaee, A., AlZainati, N. (2020). Novel thermal desalination brine reject-sewage effluent salinity gradient for power generation and dilution of brine reject. *Energies*, *13*, 1756.

Alto, K., Broderius, S., Smith, L. (1978). *Toxicity of Xanthates to Freshwater Fish and Invertebrates*, Minnesota Environmental Quality Council: Minneapolis, MN, USA.

American Public Health Association (APHA). (2017). Standard Methods for the Examination of Water and Wastewater. Method 4500-NH_3 D. 23rd Ed. Washington, DC, USA.

Andrade, L., Aguiar, A., Pires, W., Miranda, G., Amaral, M. (2017). Integrated ultrafiltration-nanofiltration membrane processes applied to the treatment of gold mining effluent: Influence of feed pH and temperature. *Separation Science and Technology*, *52*, 756–766.

Andrés-Mañas, J.A., Ruiz-Aguirre, A., Acién, F.G., Zaragoza, G. (2018). Assessment of a pilot system for seawater desalination based on vacuum multi-effect membrane distillation with enhanced heat recovery. *Desalination*, *443*, 110–121.

Appelo, C.A.J., Postma, D., 2005. Geochemistry, Groundwater and Pollution (2nd). Balkema, Leiden, p. 678.

Babu, D.S., Nidheesh, P.V. (2021). A review on electrochemical treatment of arsenic from aqueous medium. *Chemical Engineering Communications*, *208*, 389–410.

Bach, L., Nørregaard, R.D., Hansen, V., Gustavson, K. (2016). *Review on Environmental Risk Assessment of Mining Chemicals Used for Mineral*, Scientific Report, DCE–Danish Centre for Environment and Energy: Roskilde, Denmark.

Baker, J.A., Gilron, G., Chalmers, B.A., Elphick, J.R. (2017). Evaluation of the effect of water type on the toxicity of nitrate to aquatic organisms. *Chemosphere*, *168*, 435–440.

Bale, C. W., Chartrand, P., Degterov, S., Eriksson, G., Hack, K., Mahfoud, R. B., Petersen, S. (2002). FactSage thermochemical software and databases. *Calphad, 26*(2), 189-228.

Balistrieri, L. S., Seal II, R. R., Piatak, N. M., Paul, B. (2007). Assessing the concentration, speciation, and toxicity of dissolved metals during mixing of acid-mine drainage and ambient river water downstream of the Elizabeth Copper Mine, Vermont, USA. *Applied Geochemistry, 22*(5), 930-952.

Ball, J. W. & D. K. Nordstrom (1991). "User's manual for wateq4f, with revised thermodynamic data base and test cases for calculating speciation of major, trace, and redox elements in natural waters." US Geological Survey.

Banks, D., Younger, P.L., Arnesen, R.T., Iversen, E.R., Banks, S.B. (1997). Mine-water chemistry: The good, the bad and the ugly. *Environmental Geology*, *32*, 157–174.

Barge, L. M., Cardoso, S. S., Cartwright, J. H., Doloboff, I. J., Flores, E., Macías-Sánchez, E., Sobrón, P. (2016). Self-assembling iron oxyhydroxide/oxide tubular structures: laboratory-grown and field examples from Rio Tinto. *Proceedings of the Royal Society A: Mathematical, Physical and Engineering Sciences, 472*(2195), 20160466.

Ben Ali, H.E., Neculita, C.M., Molson, J.W., Maqsoud, A., Zagury, G.J. (2019). Performance of passive systems for mine drainage treatment at low temperature and high salinity: A review. *Minerals Engineering*, *134*, 325–344.

Bethk C.M., Farrell, B., Sharifi, M. (2022). GWB Essentials Guide. The Geochemist's Workbench. March 25. 232 p.

Bigham, J., Nordstrom, D. K. (2000). Iron and aluminum hydroxysulfates from acid sulfate waters. *Reviews in Mineralogy and Geochemistry, 40*(1), 351-403.

Bogart, S.J., Woodman, S., Steinkey, D., Meays, C., Pyle, G.G. (2016). Rapid changes in water hardness and alkalinity: Calcite formation is lethal to *Daphnia magna*. *Science of the Total Environment*, *559*, 182–191.

Bokare, A.D., Choi, W. (2014). Review of iron-free Fenton-like systems for activating H2O2 in advanced oxidation processes. *Journal of Hazardous Materials*, *275*, 121–135.

Bondu, R., Cloutier, V., Rosa, E., Roy, M. (2020). An exploratory data analysis approach for assessing the sources and distribution of naturally occurring contaminants (F, Ba, Mn, As) in groundwater from southern Quebec (Canada). *Applied Geochemistry, 114*, 104500.

Bondu, R., Cloutier, V., Rosa, E., Benzaazoua, M. (2017). Mobility and speciation of geogenic arsenic in bedrock groundwater from the Canadian Shield in western Quebec, Canada. *Science of the Total Environment, 574*, 509-519.

Borrok, D. M., Nimick, D. A., Wanty, R. B., Ridley, W. I. (2008). Isotopic variations of dissolved copper and zinc in stream waters affected by historical mining. *Geochimica et Cosmochimica Acta, 72*(2), 329-344.

Botz, M. M. (2001). Overview of cyanide treatment methods. *Mining Environmental Management, Mining Journal Ltd., London, UK, 28*, 30.

Bowell, R.J. (2004). A review of sulfate removal options for mine waters. SRK Consulting, Cardiff, Wales, United Kingdom, 24 p.

Budaev, S.L., Batoeva, A.A., Tsybikova, B.A. (2014). Effect of Fenton-like reactions on the degradation of thiocyanate in water treatment. *Journal of Environmental Chemical Engineering*, *2*, 1907–1911.

Burrows, J.E., Cravotta, C.A. III, and Peters, S.C. (2017). Enhanced Al and Zn removal from coal-mine drainage during rapid oxidation and precipitation of Fe oxides at near-neutral pH. *Applied Geochemistry, 78*, 194-210.

Carrero, S., Fernandez-Martinez, A., Pérez-López, R., Cama, J., Dejoie, C., Nieto, J. M. (2022). Effects of aluminum incorporation on the schwertmannite structure and surface properties. *Environmental Science: Processes & Impacts,* 24, 1383-1391.

CCME (Canadian Water Quality Guidelines for the Protection of Aquatic Life). (2010). *Ammonia*, Canadian Council of Ministers of the Environment: Winnipeg, MB, Canada, pp. 1–8.

CCME. (2012). *Nitrate Ion*, Canadian Council of Ministers of the Environment: Winnipeg, MB, Canada, pp. 1–17.

CCME. (2020). Summary Table. Available online: http://st-ts.ccme.ca/en/index.html (accessed on 18 October 2020).

CEAEQ. (2016). Détermination de l'alcalinité de de l'acidité: méthode titrimétrique automatisée. MA. 315 – Alc-Aci 1.0, Rév. 3. Ministère du Développement durable, de l'environnement et de la lutte contre les changements climatiques du Québec, Qc, Canada, 12p.

CEAEQ. (2016). Détermination des cyanures: méthode colorimétrique automatisée avec l'acide isonicotinique et l'acide barbiturique – distillation manuelle. MA. 300 – CN 1.2, Rév. 4. Ministère du Développement durable, de l'Environnement et de la Lutte contre les changements climatiques du Québec, Qc, Canada, 26p.

CEAEQ. (2020). Détermination des anions: méthode par chromatographie ionique. MA. 300 – Ions 1.3, Rév. 6. Ministère de l'environnement et de la lutte contre les changements climatiques, Qc, Canda, 14p.

CEAEQ. (2020). Détermination des métaux: méthode par spectrométrie de masse à source ionisante au plasma d'argon. MA. 200 – Mét. 1.2, Rév. 7. Ministère de l'environnement et de la lutte contre les changements climatiques, Qc, Canada, 35p.

Centre d'Expertise en Analyse Environnementale du Québec (CEAEQ). (2021). Détermination de la toxicité: létalité (CL50 48h) chez la daphnie *Daphnia magna*. MA. 500 – D.mag. 1.1, Rév. 3. Ministère de l'environnement et de la lutte contre les changements climatiques du Québec, Qc, Canada, 18p.

Cesar, J., Mayer, B., Humez, P. (2021). A novel isotopic approach to distinguish primary microbial and thermogenic gases in shallow subsurface environments. *Applied Geochemistry, 131*, 105048.

Chad, S. J., Barbour, S. L., McDonnell, J. J., Gibson, J. J. (2022). Using stable isotopes to track hydrological processes at an oil sands mine, Alberta, Canada. *Journal of Hydrology: Regional Studies, 40*, 101032.

Chlot, S. (2013). Nitrogen and phosphorus interactions and transformations in cold-climate mine water recipients. Ph.D. Thesis, Lulea University of Technology, Lulea, Sweden.

Choi, J. Y., Lee, T., Cheng, Y., Cohen, Y. (2019). Observed crystallization induction time in seeded gypsum crystallization. *Industrial & Engineering Chemistry Research, 58*(51), 23359-23365.

Chung, T.S., Luo, L., Wan, C.F., Cui, Y., Amy, G. (2015). What is next for forward osmosis (FO) and pressure retarded osmosis (PRO)? *Separation and Purification Technology*, *156*, 856–860.

Cidu, R., Frau, F., Da Pelo, S. (2011). Drainage at abandoned mine sites: natural attenuation of contaminants in different seasons. *Mine Water and the Environment, 30*(2), 113-126.

Clark, I. D., Fritz, P. (1997). *Environmental isotopes in hydrogeology*: CRC press. 343 p.

climate-data.org. (2022). Historic Weather for Rouyn-Noranda, Québec, Canada. https://fr.climate-data.org/amerique-du-nord/canada/quebec/rouyn-noranda-21931/#climate-table (last access: January 20, 2022).

Cohen, B., Lazarovitch, N., Gilron, J. (2018). Upgrading groundwater for irrigation using monovalent selective electrodialysis. *Desalination*, *431*, 126–139.

Costis, S., Mueller, K., Coudert, L., Neculita, C.M., Reynier, N., Blais, J.F. (2021). Recovery potential of rare earth elements from mining and industrial residues: A review and case studies. *Journal of Geochemical Exploration*, *221*, 106699.

Coudert, L., Bondu, R., Rakotonimaro, T.V., Rosa, E., Guittonny, M., Neculita, C.M. (2020). Treatment of As-rich mine effluents and produced residues stability: Current knowledge and research priorities for gold mining. *Journal of Hazardous Materials*, 121920.

Coulton, R., Bullen, C., Hallett, C. (2003). The design and optimisation of active mine water treatment plants. *Land Contamination and Reclamation, 11*(2), 273-280.

Couture, P., Pyle, G. (2012). Field studies on metal accumulation and effects in fish. In *Homeostasis and Toxicology of Essential Metals*, Wood, C.M., Farrell, A.P., Brauner, C.J., Eds., Fish Physiology, Vol. 31, Part 1. Academic Press: Cambridge, MA, USA, pp. 417–473.

Craig, H., Gordon, L. I. (1965). Deuterium and oxygen 18 variations in the ocean and the marine atmosphere. Stable Isotopes in Oceanographic Studies and Paleotemperatures. Spoleto, July 26-30.

Cravotta, C. A. III (2021). "Interactive PHREEQ-N-AMDTreat water-quality modeling tools to evaluate performance and design of treatment systems for acid mine drainage." *Applied Geochemistry, 126*, 104845.

Cravotta, C.A. III, Goode, D.J., Bartles, M.D., Risser, D.W., Galeone, D.G. (2014). Surface-water and groundwater interactions in an extensively mined watershed, upper Schuylkill River, Pennsylvania, USA. *Hydrological Processes, 28*, 3574–3601.

D019. (2005). *Directive 019 Sur l'Industrie Minière*, Government of Quebec: Quebec, QC, Canada.

D019. (2012). *Directive 019 Sur l'Industrie Minière*, Government of Quebec: Quebec, QC, Canada.

Dauchy, J.W., Waller, T.W., Piwoni, M.D. (1980). Acute toxicity of cyanate to *Daphnia magna*. *Bulletin of Environmental Contamination and Toxicology*, *25*, 194–196.

Deleebeeck, N.M., De Schamphelaere, K.A., Heijerick, D.G., Bossuyt, B.T., Janssen, C.R. (2008). The acute toxicity of nickel to *Daphnia magna*: Predictive capacity of bioavailability models in artificial and natural waters. *Ecotoxicology and Environmental Safety*, *70*, 67–78.

di Biase, A., Wei, V., Kowalski, M.S., Bratty, M., Hildebrand, M., Jabari, P., Oleszkiewicz, J.A. (2020). Ammonia, thiocyanate, and cyanate removal in an aerobic up-flow submerged attached growth reactor treating gold mine wastewater. *Chemosphere*, *243*, 125395.

Douglas, M., Clark, I., Raven, K., Bottomley, D. (2000). Groundwater mixing dynamics at a Canadian Shield mine. *Journal of Hydrology, 235*(1-2), 88-103.

Drioli, E., Ali, A., Macedonio, F. (2015). Membrane distillation: Recent developments and perspectives. *Desalination*, *356*, 56–84.

Dubuc, J., Coudert, L., Lefebvre, O., Neculita, C.M. (2022). Electro-Fenton treatment of contaminated mine water to decrease thiosalts toxicity to *Daphnia magna*. *Science of the Total Environment*, 835, 155323.

Eary, L. E., Runnells, D. D., Esposito, K. (2003). Geochemical controls on ground water composition at the Cripple Creek mining district, Cripple Creek, Colorado. *Applied Geochemistry, 18*(1), 1-24.

Edraki, M., Golding, S., Baublys, K., Lawrence, M. (2005). Hydrochemistry, mineralogy and sulfur isotope geochemistry of acid mine drainage at the Mt. Morgan mine environment, Queensland, Australia. *Applied Geochemistry, 20*(4), 789-805.

Elliot, T., Younger, P.L. (2007). Hydrochemical and isotopic tracing of mixing dynamics and water quality evolution under pumping conditions in the mine shaft of the abandoned Frances Colliery, Scotland. *Applied Geochemistry, 22*(12), 2834-2860.

Elshorbagy, W., Chowdhury, R. (2013). *Water Treatment*, InTech: London, UK, 392.

Esparza, J.M., Cueva, N.C., Pauker, C.S., Jentzsch, P.V., Bisesti, F.M. (2019). Combined treatment using ozone for cyanide removal from wastewater: A comparison. *Revista Internacional de Contaminacion Ambiental*, *35*, 459–467.

Etteieb, S., Magdouli, S., Zolfaghari, M., Brar, S. (2020). Monitoring and analysis of selenium as an emerging contaminant in mining industry: A critical review. *Science of the Total Environment*, 134339.

Eytcheson, S.A., LeBlanc, G.A. (2018). Hemoglobin levels modulate nitrite toxicity to *Daphnia magna*. *Scientific Reports*, *8*, 1–8.

Fairbairn, D.J., Arnold, W.A., Barber, B.L., Kaufenberg, E.F., Koskinen, W.C., Novak, P.J., Rice, P.J., Swackhamer, D.L. (2016). Contaminants of emerging concern: Mass balance and comparison of wastewater effluent and upstream sources in a mixed-use watershed. *Environmental Science & Technology*, *50*, 36–45.

Fisheries and Environment Canada. (1977). *Metal Mining Liquid Effluent Regulations and Guidelines*, Report EPS 1-WP-77-1, Fisheries and Environment Canada: Ottawa, ON, Canada.

Flem, B., Reimann, C., Fabian, K., Birke, M., Filzmoser, P., Banks, D. (2018). Graphical statistics to explore the natural and anthropogenic processes influencing the inorganic quality of drinking water, ground water and surface water. *Applied Geochemistry*, *88*, 133–148.

Fordyce, F. (2007). Selenium geochemistry and health. *Ambio*, *36*, 94–97.

Foudhaili, T., Jaidi, R., Neculita, C.M., Rosa, E., Triffault-Bouchet, G., Veilleux, E., Coudert, L., Lefebvre, O. (2020). Effect of the electrocoagulation process on the toxicity of gold mine effluents: A comparative assessment of *Daphnia magna* and *Daphnia pulex*. *Science of the Total Environment*, *708*, 134739.

Frau, F., Ardau, C. (2003). Geochemical controls on arsenic distribution in the Baccu Locci stream catchment (Sardinia, Italy) affected by past mining. *Applied Geochemistry, 18*(9), 1373-1386.

Fujioka, T., Hoang, A.T., Okuda, T., Takeuchi, H., Tanaka, H., Nghiem, L.D. (2018). Water reclamation using a ceramic nanofiltration membrane and surface flushing with ozonated water. *International Journal of Environmental Research and Public Health*, *15*, 799.

Gaillardet, J., Viers, J., Duprée, B. (2003). Trace elements in river waters. In: *Treatise on Geochemistry*, Drever, J.I., Ed., Pergamon: Oxford, UK, pp. 225–272.

Gervais, M., Dubuc, J., Paquin, M., Gonzalez-Merchan, C., Genty, T., Neculita, C.M. (2020). Comparative efficiency of three advanced oxidation processes for thiosalts treatment in mine impacted water. *Minerals Engineering*, *152*, 106349.

Ghanem, H., Kravchenko, V., Makedon, V., Shulha, O., Oleksandr, S. (2019). Preliminary water purification from surfactants and organic compounds through ozone oxidation, intensified by electrical impulses. In Proceedings of the 2019 IEEE 6th International Conference on Energy Smart Systems (ESS), Kyiv, Ukraine, 17–19 April.

Giloteaux, L., Duran, R., Casiot, C., Bruneel, O., Elbaz-Poulichet, F., Goni-Urriza, M. (2013). Three-year survey of sulfate-reducing bacteria community structure in Carnoulès acid mine drainage (France), highly contaminated by arsenic. *FEMS Microbial Ecology*, *83*, 724–737.

Golder Associates Inc. (2009) *Literature Review of Treatment Technologies to Remove Selenium from Mining Influenced Water*, Teck Coal Limited: Calgary, AB, Canada.

GoldSim Technology Group. (2021). GoldSim User's Guide (Version 14.0), https://www.goldsim.com/Web/Customers/Education/Documentation/, October 2021.

Gonzalez, J. A., Ghobaeiyeh, F. V., Mckay, D. J. (2019). Process for treatment of mine impacted water. In: Google Patents.

Gonzalez-Merchan, C., Genty, T., Bussière, B., Potvin, R., Paquin, M., Benhammadi, M., Neculita, C.M. (2016). Influence of contaminant to hydrogen peroxide to catalyzer molar ratio in the advanced oxidation of thiocyanates and ammonia using Fenton-based processes. *Journal of Environmental Chemical Engineering*, *4*, 4129–4136.

Gonzalez-Merchan, C., Genty, T., Bussière, B., Potvin, R., Paquin, M., Benhammadi, M., Neculita, C.M. (2016). Ferrates performance in thiocyanates and ammonia degradation in gold mine effluents. *Minerals Engineering*, *95*, 124–130.

Gonzalez-Merchan, C., Genty, T., Paquin, M., Gervais, M., Bussière, B., Potvin, R., Neculita, C.M. (2018). Influence of ferric iron source on ferrate's performance and residual contamination during the treatment of gold mine effluents. *Minerals Engineering*, *127*, 61–66.

Gould, D.W., King, M., Mohapatra, B.R., Cameron, R.A., Kapoor, A., Koren, D.W. (2012). A critical review on destruction of thiocyanate in mining effluents. *Minerals Engineering*, *34*, 38–47.

Hamed, Y., Ahmadi, R., Demdoum, A., Bouri, S., Gargouri, I., Dhia, H.B., Choura, A. (2014). Use of geochemical, isotopic, and age tracer data to develop models of groundwater flow: a case study of Gafsa mining basin-Southern Tunisia. *Journal of African Earth Sciences, 100*, 418-436.

Hamel, B.L., Stewart, B.W., Kim, A.G. (2010). Tracing the interaction of acid mine drainage with coal utilization byproducts in a grouted mine: Strontium isotope study of the inactive Omega Coal Mine, West Virginia (USA). *Applied Geochemistry, 25*(2), 212-223.

Hamilton, S. J. (2004). Review of selenium toxicity in the aquatic food chain. *Science of the Total Environment, 326*(1-3), 1-31.

Health Canada. (2013). Guidelines for Canadian drinking water quality: Guideline technical document-Nitrate and nitrite. In *Water and Air Quality Bureau*, Healthy Environments and Consumer Safety: Ottawa, ON, Canada, 128.

Hem, J.D. (1985). *Study and interpretation of the chemical characteristics of natural water* (Vol. 2254): Department of the Interior, US Geological Survey.

Hendry, M.J., Barbour, S.L., Schmeling, E.E., Wassenaar, L.I., Shaw, S., Schabert, M.S. (2023). Quantifying denitrification in a field-scale bioremediation experiment. *Science of the Total Environment, 854*, 158762.

Hendry, M.J., Wassenaar, L.I., Barbour, S.L., Schabert, M.S., Birkham, T.K., Fedec, T., Schmeling, E.E. (2018). Assessing the fate of explosives derived nitrate in mine waste rock dumps using the stable isotopes of oxygen and nitrogen. *Science of the Total Environment, 640*, 127-137.

Hu, J., Chen, X., Chen, Y., Li, C., Ren, M., Jiang, C., Zheng, L. (2021). Nitrate sources and transformations in surface water of a mining area due to intensive mining activities: Emphasis on effects on distinct subsidence waters. *Journal of Environmental Management, 298*, 113451.

Huang, P., Wang, X. (2017). Applying environmental isotope theory to groundwater recharge in the Jiaozuo mining area, China. *Geofluids*, *2017*, 9568349.

Hube, S., Eskafi, M., Hrafnkelsdóttir, K.F., Bjarnadóttir, B., Bjarnadóttir, M.Á., Axelsdóttir, S., Wu, B. (2020). Direct membrane filtration for wastewater treatment and resource recovery: A review. *Science of the Total Environment*, *710*, 136375.

Jermakka, J., Wendling, L., Sohlberg, E., Heinonen, H., Vikman, M. (2015). Potential technologies for the removal and recovery of nitrogen compounds from mine and quarry waters in subarctic conditions. *Critical Reviews in Environmental Science and Technology*, *45*, 703–748.

Ji, Y., Li, L., Wang, Y. (2020). Selenium removal by activated alumina in batch and continuous-flow reactors. *Water Environment Research*, *92*, 51–59.

Ji, Z. (2018). Treatment of heavy-metal wastewater by vacuum membrane distillation: Effect of wastewater properties. *IOP Conference Series: Earth and Environmental Science*, *108*, 042019.

Johnson, C.A. (2015). The fate of cyanide in leach wastes at gold mines: An environmental perspective. *Applied Geochemistry*, *57*, 194–205.

Johnson, D.B. (2003). Chemical and microbiological characteristics of mineral spoils and drainage waters at abandoned coal and metal mines. *Water, Air and Soil Pollution*, *3*, 47–66.

Jouini, M., Neculita, C.M., Genty, T., Benzaazoua, M. (2020). Freezing/thawing effects on geochemical behaviour of residues from acid mine drainage passive treatment systems. *Journal of Water Process Engineering*, *33*, 101807.

Jung, H., Koh, D.-C., Kim, Y. S., Jeen, S.-W., Lee, J. (2020). Stable isotopes of water and nitrate for the identification of groundwater flowpaths: A review. *Water, 12*(1), 138.

Kang, S.W., Seo, J., Han, J., Lee, J.S., Jung, J. (2011). A comparative study of toxicity identification using *Daphnia magna* and *Tigriopus japonicus*: Implications of establishing effluent discharge limits in Korea. *Marine Pollution Bulletin*, *63*, 370-375.

Karanasiou, A., Kostoglou, M., Karabelas, A. (2018). An experimental and theoretical study on separations by vacuum membrane distillation employing hollow-fiber modules. *Water*, *10*, 947.

Katz, M. (1977). The Canadian sulphur problem. *Sulphur and Its Inorganic Derivatives in the Canadian Environment*, National Research Council of Canada, NRC Associate Committee on Scientific Criteria for Environmental Quality: Ottawa, ON, Canada, pp. 21–67.

Khuntia, S., Majumder, S.K., Ghosh, P. (2013). Removal of ammonia from water by ozone microbubbles. *Industrial & Engineering Chemistry Research*, *52*, 318–326.

Khuntia, S., Majumder, S.K., Ghosh, P. (2014). Oxidation of As(III) to As(V) using ozone microbubbles. *Chemosphere*, *97*, 120–124.

Khuntia, S., Majumder, S.M., Ghosh, P. (2012). Microbubbles-aided water and wastewater purification: A review. *Reviews in Chemical Engineering*, *28*, 191–221.

Kim, H.-J., Kim, Y. (2021). Schwertmannite transformation to goethite and the related mobility of trace metals in acid mine drainage. *Chemosphere, 269*, 128720.

Kimball, B.E., Mathur, R., Dohnalkova, A., Wall, A., Runkel, R., Brantley, S.L. (2009). Copper isotope fractionation in acid mine drainage. *Geochimica et Cosmochimica Acta, 73*(5), 1247-1263.

Klaus, J., McDonnell, J. (2013). Hydrograph separation using stable isotopes: Review and evaluation. *Journal of Hydrology, 505*, 47-64.

Kolliopoulos, G., Shum, E., Papangelakis, V.G. (2018). Forward osmosis and freeze crystallization as low energy water recovery processes for a water-sustainable industry. *Environmental Processes*, *5*, 59–75.

Konhauser, K.O. (1997). Bacterial iron biomineralisation in nature. *FEMS microbiology reviews, 20*(3-4), 315-326.

Kozlova, T., Wood, C.M., McGeer, J.C. (2009). The effect of water chemistry on the acute toxicity of nickel to the cladoceran *Daphnia pulex* and the development of a biotic ligand model. *Aquatic Toxicology*, *91*, 221–228.

Kratochvil, D. (2012). Sustainable water treatment technologies for the treatment of acid mine drainage. In Proceedings of the International Conference on Acid Rock Drainage (ICARD), Ottawa, ON, Canada, 20–26 May.

Krausmann, F., Gingrich, S., Eisenmenger, N., Erb, K.H., Haberl, H., Fischer-Kowalski, M. (2009). Growth in global materials use, GDP and population during the 20th century. *Ecological Economics*, *68*, 2696–2705.

Kurukulasuriya, D., Howcroft, W., Moon, E., Meredith, K., Timms, W. (2022). Selecting environmental water tracers to understand groundwater around mines: Opportunities and limitations. *Mine Water and the Environment*, 1-13.

Kynčlová, P., Hron, K., Filzmoser, P. (2017). Correlation between compositional parts based on symmetric balances. *Mathematical Geosciences, 49*(6), 777-796.

Laurence, D. (2011). Establishing a sustainable mining operation: An overview. *Journal of Cleaner Production*, *19*, 278–284.

Le Bourre, B. (2020). Protocole d'essais de traitement de l'azote ammoniacal par ozonation. RIME (Research Institute on Mines and Environment), UQAT (Université du Québec en Abitibi-Témiscamingue), Rouyn-Noranda, Qc, Canada, 28 p.

Lecomte, K.L., Pasquini, A.I., Depetris, P.J. (2005). Mineral weathering in a semiarid mountain river: its assessment through PHREEQC inverse modeling. *Aquatic Geochemistry, 11*(2), 173-194.

Lee, J., von Gunten, U., Kim, J.H. (2020). Persulfate-based advanced oxidation: Critical assessment of opportunities and roadblocks. *Environmental Science & Technology*, *54*, 3064–3081.

Lee, S.H., Kim, I., Kim, K.W., Lee, B.T. (2015). Ecological assessment of coal mine and metal mine drainage in South Korea using *Daphnia magna* bioassay. *Springer Plus*, *4*, 518.

Lefebvre, O., Moletta, R. (2006). Treatment of organic pollution in industrial saline wastewater: A literature review. *Water Research*, *40*, 3671–3682.

Lemly, A. D. (2002). Symptoms and implications of selenium toxicity in fish: the Belews Lake case example. *Aquatic Toxicology, 57*(1-2), 39-49.

Lewicka-Szczebak, D., Jędrysek, M.-O. (2013). Tracing and quantifying lake water and groundwater fluxes in the area under mining dewatering pressure using coupled O and H stable isotope approach. *Isotopes in Environmental and Health Studies, 49*(1), 9-28.

Lewis-Russ, A., Jia, K., Mills, R. (2019). New Britannia Mill Water Quality Assessment. AECOM Canada, Burnaby, BC, March 1.

Liu, C., Chen, Y., He, C., Yin, R., Liu, J., Qiu, T. (2019). Ultrasound-enhanced catalytic ozonation oxidation of ammonia in aqueous solution. *International Journal of Environmental Research and Public Health*, *16*, 2139.

Loganathan, K., Chelme-Ayala, P., Gamal El-Din, M. (2016). Pilot-scale study on the treatment of basal aquifer water using ultrafiltration, reverse osmosis and evaporation/crystallization to achieve zero-liquid discharge. *Journal of Environmental Management*, *165*, 213–223.

Lu, P., Zhang, G., Apps, J., Zhu, C. (2022). Comparison of thermodynamic data files for PHREEQC. *Earth-Science Reviews, 225*, 103888.

Maest, A., Prucha, R., Wobus, C. (2020). Hydrologic and water quality modeling of the Pebble Mine Project pit lake and downstream environment after mine closure. *Minerals, 10*(8), 727.

Majzlan, J., Plášil, J., Škoda, R., Gescher, J., Kögler, F., Rusznyak, A., Küsel, K., Neu, T.R., Mangold, S., Rothe, J. (2014). Arsenic-rich acid mine water with extreme arsenic

concentration: Mineralogy, geochemistry, microbiology and environmental implications. *Environmental Science & Technology*, *48*, 13685–13693.

Mandal, B.K., Suzuki, T. (2002). Arsenic round the world: A review. *Talanta*, *58*, 201–235.

Marcotte, P., Aubé, E., Dubé, C., Neculita, C.M. (2021). Performance of microbubbles ozonation for the removal of nitrogen-based contaminants in mine impacted water. Proceedings of the Symposium on Mines and the Environment, Rouyn-Noranda, Qc, Canada, June 14-16.

Marcotte, P., Neculita, C. M., Cloutier, V., Bordeleau, G., Rosa, E. (2022). Tracing the sources and fate of nitrogen at a Canadian underground gold mine. *Applied Geochemistry, 142*, 105238.

Marsidi, N., Hasan, H.A., Abdullah, S.R.S. (2018). A review of biological aerated filters for iron and manganese ions removal in water treatment. *Journal of Water Process Engineering*, *23*, 1–12.

MEND (Mine Environment Neutral Drainage). (2014). Study to identify BATEA for the management and control of effluent quality from mines. MEND Report 3.50.1, Hatch, Canada. 527 p.

Mendoza, O. T., Ruiz, J., Villaseñor, E. D., Guzmán, A. R., Cortés, A., Souto, S. A. S., Bustos, R. R. (2016). Water-rock-tailings interactions and sources of sulfur and metals in the subtropical mining region of Taxco, Guerrero (southern Mexico): A multi-isotopic approach. *Applied Geochemistry, 66*, 73-81.

Meschke, K., Hofmann, R., Haseneder, R., Repke, J.-U. (2020). Membrane treatment of leached mining waste–A potential process chain for the separation of the strategic elements germanium and rhenium. *Chemical Engineering Journal, 380*, 122476.

Meshref, M.N.A., Klamerth, N., Islam, M.S., McPhedran, K.N., Gamal El-Din, M. (2017). Understanding the similarities and differences between ozone and peroxone in the degradation of naftenic acids: Comparative performance for potential treatment. *Chemosphere*, *180*, 149–159.

Metal and Diamond Mining Effluent Regulation (MMER). (2018). SOR/2002-222 [http://lawslois.justice.gc.ca].

Migaszewski, Z. M., Gałuszka, A., Dołęgowska, S. (2018). Stable isotope geochemistry of acid mine drainage from the Wiśniówka area (south-central Poland). *Applied Geochemistry, 95*, 45-56.

Miklos, D.B., Remy, C., Jekel, M., Linden, K.G., Drewes, J.E., Hubner, U. (2018). Evaluation of advanced oxidation processes for water and wastewater treatment: A critical review. *Water Research*, *139*, 118–131.

Miller, J.R., Lechler, P.J., Mackin, G., Germanoski, D., Villarroel, L.F. (2007). Evaluation of particle dispersal from mining and milling operations using lead isotopic fingerprinting techniques, Rio Pilcomayo Basin, Bolivia. *Science of the Total Environment, 384*(1-3), 355-373.

Minister of Justice. (2021). MDMER (Metal and Diamond Mining Effluent Regulations), SOR/ 2002–222. Government of Canada, Ottawa, ON, Canada. https://laws-lois.justice.gc.ca/ PDF/SOR-2002-222.pdf.

Minister of Justice. (2019). *MMER (Metal and Diamond Mining Effluent Regulations),* SOR/2002–222, Government of Canada: Ottawa, ON, Canada.

Ministère de l'environnement et de la lutte contre les changements climatiques (MELCC). (2012). Directive 019 sur l'industrie minière. Gouvernement du Québec. http://www.mddefp. gouv.qc.ca/milieu_ind/directive019/directive019.pdf.

Miranda-Trevino, J.C., Pappoe, M., Hawboldt, K., Bottaro, C. (2013). The importance of thiosalts speciation: Review of analytical methods, kinetics, and treatment. *Critical Reviews in Environmental Science and Technology*, *43*, 2013–2070.

Molina, G.C., Cayo, C.H., Rodrigues, M.A.S., Bernardes, A.M. (2013). Sodium isopropyl xanthate degradation by advanced oxidation processes. *Minerals Engineering*, *45*, 88–93.

Mosley, L. M., Daly, R., Palmer, D., Yeates, P., Dallimore, C., Biswas, T., Simpson, S. L. (2015). Predictive modelling of pH and dissolved metal concentrations and speciation following mixing of acid drainage with river water. *Applied Geochemistry, 59*, 1-10.

Mousset, E., Loh, W. H., Lim, W.S., Jarry, L., Wang, Z., Lefebvre, O. (2021). Cost comparison of advanced oxidation processes for wastewater treatment using accumulated oxygen-equivalent criteria. *Water Research*, 200, 117234.

Mudder, T.I., Botz, M.M., Smith, A. (2001). *Chemistry and Treatment of Cyanidation Wastes*, 2nd ed., Mining Journal Books Limited: London, UK.

Muzinda, I., Schreithofer, N. (2018). Water quality effects on flotation: Impacts and control of residual xanthates. *Minerals Engineering*, *125*, 34–41.

Naidu, G., Ryu, S., Thiruvenkatachari, R., Choi, Y., Jeong, S., Vigneswaran, S. (2019). A critical review on remediation, reuse, and resource recovery from acid mine drainage. *Environmental Pollution*, 247, 1110–1124.

Neculita, C.M., Coudert, L., Rosa, E., Mulligan, C.N. (2020). Future prospects for treating contaminants of emerging concern in water and soils/sediments. In *Advanced Nano-Bio Technologies for Water and Soil Treatment* (pp. 589-605): Springer.

Neculita, C.M., Coudert, L., Genty, T., Drapeau, M., Ryskie, S., Fortier-Delay, S. (2018). Emerging contaminants in mine effluents: operational challenges of their treatment and research needs. 6th Mines & Environment Symposium, Rouyn-Noranda, QC, Canada, June 17-20.

Neculita, C.M., Coudert, L., Rosa, E. (2019). Challenges and opportunities in mine water treatment in cold climate. GEE2019: 17th International Environmental Specialty Conference, Concordia University, Montreal, QC, Canada, May 30-31.

Neculita, C.M., Rosa, E. (2019). A review of the implications and challenges of manganese removal from mine drainage. *Chemosphere*, *214*, 491–510.

Négrel, P., Lemiere, B., Machard de Grammont, H., Billaud, P., Sengupta, B. (2007). Hydrogeochemical processes, mixing and isotope tracing in hard rock aquifers and surface waters from the Subarnarekha River Basin,(east Singhbhum District, Jharkhand State, India). *Hydrogeology Journal, 15*(8), 1535-1552.

Nilsson, L., Widerlund, A. (2017). Tracing nitrogen cycling in mining waters using stable nitrogen isotope analysis. *Applied Geochemistry, 84*, 41-51.

Nordstrom, D. K. (2020). Geochemical modeling of iron and aluminum precipitation during mixing and neutralization of acid mine drainage. *Minerals, 10*(6), 547.

Nordstrom, D.K., Blowes, D.W., Ptacek, C.J. (2015). Hydrogeochemistry and microbiology of mine drainage: An update. *Applied Geochemistry*, *57*, 3–16.

Novak, L., Holtze, K., Wagner, R., Feasby, G., Liu, L. (2002). *Guidance Document for Conducting Toxicity Reduction Evaluation (TRE) Investigations of Canadian Metal Mining Effluents*, Prepared ESG International Inc. and SGC Lakefield for TIME Network, ON, Canada, 85.

OECD. (2012). *New and Emerging Water Pollutants arising from Agriculture*, OECD: Paris, France, 49.

Okamoto, A., Yamamuro, M., Tatarazako, N. (2015). Acute toxicity of 50 metals to *Daphnia magna*. *Journal of Applied Toxicology*, *35*, 824–830.

OLI Systems Inc. (2021). OLI versus PHREEQC. Tiré du site web https://www.olisystems.com/resources/technical-resources/oli-versus-phreeqc/.

Olías, M., Cánovas, C., Basallote, M.D., Lozano, A. (2018). Geochemical behaviour of rare earth elements (REE) along a river reach receiving inputs of acid mine drainage. *Chemical Geology*, *493*, 468–477.

Olvera-Vargas, H., Dubuc, J., Wang, Z., Coudert, L., Neculita, C.M., Lefebvre, O. (2021). Electro-Fenton beyond the degradation of organics: Treatment of thiosalts in contaminated mine water. *Environmental Science & Technology*, *55*, 2564–2574.

Papp, D. C., Baciu, C., Turunen, K., Kittilä, A. (2020). Applicability of selected stable isotopes to study the hydrodynamics and contaminant transport within mining areas in Romania and Finland. *Geological Society, London, Special Publications, 507*(1), 169-192.

Paquin, P.R., Gorsuch, J.W., Apte, S., Batley, G.E., Bowles, K.C., Campbell, P.G., Galvez, F. (2002). The biotic ligand model: A historical overview. *Comparative Biochemistry and Physiology Part C: Toxicology & Pharmacology*, *133*, 3–35.

Parkhurst, D.L., Appelo, C. (1999). User's guide to PHREEQC (Version 2): A computer program for speciation, batch-reaction, one-dimensional transport, and inverse geochemical calculations. *Water-resources investigations report, 99*(4259), 312.

Parkhurst, D.L., Appelo, C. (2013). *Description of input and examples for PHREEQC version 3: a computer program for speciation, batch-reaction, one-dimensional transport, and inverse geochemical calculations* (2328-7055). Retrieved from https://pubs.usgs.gov/tm/06/a43/

Persoone, G., Baudo, R., Cotman, M., Blaise, C., Thompson, K.C., Moreira-Santos, M., Han, T. (2009). Review on the acute *Daphnia magna* toxicity test—Evaluation of the sensitivity and the precision of assays performed with organisms from laboratory cultures or hatched from dormant eggs. *Knowledge and Management of Aquatic Ecosystems*, *393*, 1–29.

Pinto, P.X., Al-Abed, S.R., Balz, D.A., Butler, B.A., Landy, R.B., Smith, S.J. (2016). Bench-scale and pilot-scale treatment technologies for the removal of total dissolved solids from coal mine water: A review. *Mine Water and the Environment*, *35*, 94–112.

Plant, J.A., Kinniburgh, D.G., Smedley, P.L., Fordyce, F.M., Klinck, B.A. (2003). Arsenic and selenium. In: *Treatise on Geochemistry*, Holland, H.D., Turekian, K.K., Eds., Pergamon: Oxford, UK, pp. 17–66.

Plummer, L.N., Prestemon, E.C., Parkhurst, D.L. (1994). An interactive code (NETPATH) for modeling net geochemical reactions along a flow path, version 2.0. *Water-resources investigations report, 94*, 4169.

Range, B.M.K., Hawboldt, K.A. (2018). Adsorption of thiosulphate, trithionate, tetrathionate using biomass ash/char. *Journal of Environmental Chemical Engineering*, *6*, 5401–5408.

Range, B.M.K., Hawboldt, K.A. (2019). Removal of thiosalt/sulfate from mining effluents by adsorption and ion exchange. *Mineral Processing and Extractive Metallurgy Review*, *40*, 79–86.

Renzi, M., Blašković, A. (2019). Ecotoxicity of nano-metal oxides: A case study on *Daphnia magna*. *Ecotoxicology, 28*(8), 878-889.

Rey, N., Rosa, E., Cloutier, V., Lefebvre, R. (2018). Using water stable isotopes for tracing surface and groundwater flow systems in the Barlow-Ojibway Clay Belt, Quebec, Canada. *Canadian Water Resources Journal/Revue canadienne des ressources hydriques, 43*(2), 173-194.

Ricci, B.C., Ferreira, C.D., Aguiar, A.O., Amaral, M.C. (2015). Integration of nanofiltration and reverse osmosis for metal separation and sulfuric acid recovery from gold mining effluent. *Separation and Purification Technology*, *154*, 11–21.

Roach, B., Walker, T.N. (2017). Aquatic monitoring programs conducted during environmental impact assessments in Canada: Preliminary assessment before and after weakened environmental regulation. *Environmental Monitoring and Assessment*, *189*, 109.

Rostad, C.E., Schmitt, C.J., Schumacher, J.G., Leiker, T.J. (2011). An exploratory investigation of polar organic compounds in waters from a lead–zinc mine and mill complex. *Water Air Soil Pollution*, *217*, 431–443.

Royer-Lavallée, A., Neculita, C.M., Coudert, L. (2020). Removal and potential recovery of rare earth elements from mine water. *Journal of Industrial and Engineering Chemistry*, *89*, 47–57.

Ryskie, S. (2017). Traitement de l'azote ammoniacal dans les effluents miniers contaminés au moyen de procédés d'oxydation avancée. Mémoire de maîtrise, IRME, UQAT, QC, Canada, 129 p.

Ryskie, S., Gonzalez-Merchan, C., Neculita, C.M., Genty, T. (2020). Efficiency of ozone microbubbles for ammonia removal from mine effluents. *Minerals Engineering, 145*, 106071.

Ryskie, S., Neculita, C.M., Rosa, E., Coudert, L., Couture, P. (2021). Active treatment of contaminants of emerging concern in cold mine water using advanced oxidation and membrane-related processes: a review. *Minerals, 11*(3), 259.

Salifu, M., Hällström, L., Aiglsperger, T., Mörth, C.-M., Alakangas, L. (2020). A simple model for evaluating isotopic (18O, 2H and 87Sr/86Sr) mixing calculations of mine–Impacted surface waters. *Journal of Contaminant Hydrology, 232*, 103640.

Samaei, S.M., Gato-Trinidad, S., Altaee, A. (2020). Performance evaluation of reverse osmosis process in the post-treatment of mining wastewaters: Case study of Costerfield mining operations, Victoria, Australia. *Journal of Water Process Engineering*, *34*, 101116.

Sauvé, S., Desrosiers, M. (2014). A review of what is an emerging contaminant. *Chemistry Central Journal*, *8*, 15.

Schoepfer, V.A., Burton, E.D. (2021). Schwertmannite: A review of its occurrence, formation, structure, stability and interactions with oxyanions. *Earth-Science Reviews, 221*, 103811.

Schudel, G., Plante, B., Bussière, B., McBeth, J., Dufour, G. (2019). The effect of arctic conditions on the geochemical behaviour of sulphidic tailings. In: Proceedings of the Tailings and Mine Waste, Vancouver, BC, Canada, 17–20 November.

Schwartz, M., Vigneault, B., McGeer, J. (2006). *Evaluating the Potential for Thiosalts to Contribute to Toxicity in Mine Effluents*, Report presented for Thiosalts Consortium, Project: 602591, Report CANMET-MMSL 06-053 (CR), CANMET Mining and Mineral Sciences Laboratories (CANMET-MMSL): Ottawa, ON, Canada, 101.

Sengul, A. B., Asmatulu, E. (2020). Toxicity of metal and metal oxide nanoparticles: a review. *Environmental Chemistry Letters, 18*(5), 1659-1683.

Shaffer, D.L., Werber, J.R., Jaramillo, H., Lin, S., Elimelech, M. (2015). Forward osmosis: Where are we now? *Desalination*, *356*, 271–284.

Shand, P., Edmunds, W.M. (2008). The baseline inorganic chemistry of European groundwaters. In: *Natural Groundwater Quality*, Edmunds, M.W., Shand, P., Eds., Blackwell Publishing: Hoboken, NJ, USA, pp. 22–58.

Sharif, M., Davis, R., Steele, K., Kim, B., Kresse, T., Fazio, J. (2008). Inverse geochemical modeling of groundwater evolution with emphasis on arsenic in the Mississippi River Valley alluvial aquifer, Arkansas (USA). *Journal of Hydrology, 350*(1-2), 41-55.

Shaw, J.R., Dempsey, T.D., Chen, C.Y., Hamilton, J.W., Folt, C.L. (2006). Comparative toxicity of cadmium, zinc, and mixtures of cadmium and zinc to daphnids. *Environmental Toxicology and Chemistry*, *25*, 182–189.

Sierra, C., Saiz, J.R.Á., Gallego, J.L.R. (2013). Nanofiltration of acid mine drainage in an abandoned mercury mining area. *Water Air Soil Pollution*, *224*, 1734.

Simate, G.S., Ndlovu, S. (2014). Acid mine drainage: Challenges and opportunities. *Journal of Environmental Chemical Engineering.*, *2*, 1785–1803.

Simmons, J.A. (2012). Toxicity of major cations and anions (Na^+, K^+, Ca^{2+}, Cl^-, and SO_4^{2-}) to a macrophyte and an alga. *Environmental Toxicology and Chemistry*, *31*, 1370–1374.

Singh, R., Venkatesh, A., Syed, T. H., Surinaidu, L., Pasupuleti, S., Rai, S., Kumar, M. (2018). Stable isotope systematics and geochemical signatures constraining groundwater hydraulics in the mining environment of the Korba Coalfield, Central India. *Environmental earth sciences, 77*(15), 1-17.

Sivakumar, M., Ramezanianpour, M., O'Halloran, G. (2013). Mine water treatment using a vacuum membrane distillation system. *APCBEE Procedia*, *5*, 157–162.

Sivula, L., Vehniainen, E.R., Karjalainen, A.K., Kukkonen, J.V.K. (2018). Toxicity of biomining effluents to *Daphnia magna*: Acute toxicity and transcriptomic biomarkers. *Chemosphere, 210*, 304–311.

Skilhagen, S.E., Dugstad, J.E., Aaberg, R.J. (2008). Osmotic power—Power production based on the osmotic pressure difference between waters with varying salt gradients. *Desalination*, *220*, 476–482.

Skrzypek, G., Mydłowski, A., Dogramaci, S., Hedley, P., Gibson, J.J., Grierson, P.F. (2015). Estimation of evaporative loss based on the stable isotope composition of water using Hydrocalculator. *Journal of Hydrology, 523*, 781-789.

Smedley, P.L., Kinniburgh, D.G. (2002). A review of the source, behaviour and distribution of arsenic in natural waters. *Applied Geochemistry*, *17*, 517–568.

Spangenberg, J.E., Dold, B., Vogt, M.-L., Pfeifer, H.-R. (2007). Stable hydrogen and oxygen isotope composition of waters from mine tailings in different climatic environments. *Environmental Science & Technology, 41*(6), 1870-1876.

Speed, D. (2016). Environmental aspects of planarization processes. In *Advances in Chemical Mechanical Planarization (CMP)*, Elsevier: Amsterdam, The Netherlands, pp. 229–269.

Spellman, C.J. Jr., Smyntek, P.M., Cravotta, C.A. III, Tasker, T.L., & Strosnider, W.H.J. (2022). Pollutant co-attenuation via in-stream interactions between mine drainage and municipal wastewater. *Water Research, 214*, 118173.

Staicu, L.C., Morin-Crini, N., Crini, G. (2017). Desulfurization: Critical step towards enhanced selenium removal from industrial effluents. *Chemosphere*, *172*, 111–119.

Sun, Z., Forsling, W. (1997). The degradation kinetics of ethyl-xanthate as a function of pH in aqueous solution. *Minerals Engineering*, *10*, 389–400.

Takahashi, M., Chiba, K., Li, P. (2007). Formation of hydroxyl radicals by collapsing ozone microbubbles under strongly acidic conditions. *The Journal of Physical Chemistry B, 111*(39), 11443-11446.

Takano, B., Ohsawa, S., Glover, R.B. (1994). Surveillance of Ruapehu Crater Lake, New Zealand by aqueous polythionates. *Journal of Volcanology and Geothermal Research*, *60*, 29–57.

Turunen, K., Räsänen, T., Hämäläinen, E., Hämäläinen, M., Pajula, P., Nieminen, S.P. (2020). Analysing contaminant mixing and dilution in river waters influenced by mine water discharges. *Water, Air, & Soil Pollution, 231*(6), 1-15.

USEPA (US Environmental Protection Agency). (1980). *Ambient Water Quality Criteria for Zinc,* Office of Research and Development: Washington, DC, USA.

USEPA. (2013). *Aquatic Life Ambient Water Quality Criteria for Ammonia–Freshwater*, Office of Water: Washington, DC, USA.

Van Dam, R.A., Harford, A.J., Lunn, S.A., Gagnon, M.M. (2014). Identifying the cause of toxicity of a saline mine water. *PLoS ONE*, *9*, e106857.

Van Der Lee, J., De Windt, L., Lagneau, V., Goblet, P. (2003). Module-oriented modeling of reactive transport with HYTEC. *Computers & Geosciences, 29*(3), 265-275.

Van Geluwe, S., Braeken, L., Van der Bruggen, B. (2011). Ozone oxidation for the alleviation of membrane fouling by natural organic matter: A review. *Water Research*, *45*, 3551–3570.

Vengosh, A., Wang, Z., Williams, G., Hill, R., Coyte, R. M., Dwyer, G. S. (2022). The strontium isotope fingerprint of phosphate rocks mining. *Science of the Total Environment, 850*, 157971.

Vicente C., Valverde Flores J. (2017). Removal of lead and zinc from mining effluents by applying air micro-nanobubbles. *Journal of Nanotechnology*, *1*, 73–78.

Vinot, H., Larpent, J. (1984). Water pollution by uranium ore treatment works. *Hydrobiologia*, *112*, 125–129.

Vital, B., Bartacek, J., Ortega-Bravo, J., Jeison, D. (2018). Treatment of acid mine drainage by forward osmosis: Heavy metal rejection and reverse flux of draw solution constituents. *Chemical Engineering Journal*, *332*, 85–91.

Wagner, R., Liu, L., Grondin, L. (2002). *Toxicity Treatment Evaluation of Mine Final Effluent—Using Chemical and Physical Treatment Methods*, Technical paper, SGS Minerals Services: Canada.

Wang, J.L., Xu, L.J. (2012). Advanced oxidation processes for wastewater treatment: Formation of hydroxyl radical and application. *Critical Reviews in Environmental Science and Technology, 42*(3), 251-325.

Wang, X.Q., Liu, C.P., Yuan, Y., Li, F.B. (2014). Arsenite oxidation and removal driven by a bio-electro-Fenton process under neutral pH conditions. *Journal of Hazardous Materials*, *275*, 200–209.

Warnes, M.G.R., Bolker, B., Bonebakker, L., Gentleman, R., Huber, W. (2016). Package 'gplots'. *Various R programming tools for plotting data*.

Wasserlauf, M., Dutrizac, J.E. (1982). *The Chemistry, Generation and Treatment of Thiosalts in Milling Effluents: A Non-Critical Summary of CANMET Investigations 1976–1982*, Report: 82-4E, CANMET: Ottawa, ON, Canada, 104.

Watson, I.C., Morin, O., Henthorne, L. (2003). *Desalting Handbook for Planners*, Desalination Research and Development Program Report, Bureau of Reclamation: Washington, DC, USA, 72.

Wen, B., Zhou, A., Zhou, J., Liu, C., Huang, Y., Li, L. (2018). Coupled S and Sr isotope evidences for elevated arsenic concentrations in groundwater from the world's largest antimony mine, Central China. *Journal of Hydrology, 557*, 211-221.

Wen, B., Zhou, J., Zhou, A., Liu, C., Xie, L. (2016). Sources, migration and transformation of antimony contamination in the water environment of Xikuangshan, China: Evidence from geochemical and stable isotope (S, Sr) signatures. *Science of the Total Environment, 569*, 114-122.

Wolkersdorfer, C., Nordstrom, D.K., Beckie, R.D., Cicerone, D.S., Elliot, T., Edraki, M., Valente, T., Alves França, S.C., Kumar, P., Oyarzún Lucero, R.A., Gil, A.L. (2020). Guidance for

the integrated use of hydrological, geochemical, and isotopic tools in mining operations. *Mine Water and the Environment*, *39*, 204–228.

Wu, Y., Tian, W., Zhang, Y., Fan, W., Liu, F., Zhao, J., Lyu, T. (2022). Nanobubble technology enhanced ozonation process for ammonia removal. *Water, 14*(12), 1865.

Xiong, X., Wang, B., Zhu, W., Tian, K., Zhang, H. (2019). A review on ultrasonic catalytic microbubbles ozonation processes: Properties, hydroxyl radicals generation pathway and potential in application. *Catalysts*, *9*, 10.

Xu, Y., Lay, J., Korte, F. (1988). Fate and effects of xanthates in laboratory freshwater systems. *Bulletin of Environmental Contamination and Toxicology*, *41*, 683–689.

Yates, B.J., Zboril, R., Sharma, V.K. (2014). Engineering aspects of ferrate in water and wastewater treatment: A review. *Journal of Environmental Science and Health*, *49*, 1603–1614.

Yi, X., Su, D., Bussière, B., Mayer, K.U. (2021). Thermal-hydrological-chemical modeling of a covered waste rock pile in a permafrost region. *Minerals, 11*(6), 565.

Yi, Y., Zhong, J., Bao, H., Mostofa, K.M., Xu, S., Xiao, H.-Y., Li, S.-L. (2021). The impacts of reservoirs on the sources and transport of riverine organic carbon in the karst area: a multi-tracer study. *Water research, 194*, 116933.

Yim, J.H., Kim, K.W., Kim, S.D. (2006). Effect of hardness on acute toxicity of metal mixtures using *Daphnia magna*: Prediction of acid mine drainage toxicity. *Journal of Hazardous Materials*, *138*, 16–21.

Young, B., Delatolla, R., Abujamel, T., Kennedy, K., Laflamme, E., Stintzi, A. (2017). Rapid start-up of nitrifying MBBRs at low temperatures: nitrification, biofilm response and microbiome analysis. *Bioprocess and Biosystems Engineering, 40*(5), 731-739.

Yu, Y., Jin, Z., Qiu, J. (2021). Global isotopic hydrograph separation research history and trends: a text mining and bibliometric analysis study. *Water, 13*(18), 2529.

Zheng, T., Wang, Q., Zhang, T., Shi, Z., Tian, Y., Shi, S., Wang, J. (2015). Microbubble enhanced ozonation process for advanced treatment of wastewater produced in acrylic fiber manufacturing industry. *Journal of Hazardous Materials, 287*, 412-420.

Zuttah, Y. (1999). Destruction de l'ammoniac dans les effluents miniers. MSc thesis, Department of mines and metallurgy, Laval University, Qc, Canada, 107p.

ANNEXE A PROTOCOLE DE TRAITABILITÉ AVEC MÉTHODE CONVENTIONNELLE ET OZONATION

1. **Préparation floculant à 0,2% m/m**
   - 2 g de floculant sec dans 1 L eau (1000 g eau)
   - Bien agiter à faible vitesse pendant 5 minutes et laisser maturer au moins 1 h avant utilisation (bon max 5-7 jours une fois préparé)
2. **Préparation lait de chaux à 10% m/m**
   - 100 g de chaux hydratée dans 1 L d'eau
   - Bien agiter et réagiter avant chaque utilisation pour remettre la chaux en suspension
3. **Essai enlèvement des métaux avant ou après traitement à l'ozone**
   - Faire un prétest de précipitation pour valider le dosage de floculant idéal
   - Prendre 3 béchers de 500 mL et les remplir avec l'effluent à tester
   - Agiter les 3 bécher en même temps soit avec des plaques agitatrices ou un jar test
   - Ajuster le pH à 10 avec du lait de chaux
   - Ajouter un dosage de floculant différent dans chaque bécher soit 2 mg/L, 4 mg/L et 6 mg/L
   - Continuer d'agiter 2 minutes et ensuite arrêter l'agitation
   - Laisser décanter les flocs et regarder lequel des dosages donne le meilleur résultat selon la turbidité du surnageant
   - Noter ce dosage et réaliser le test à grande échelle avec celui-ci
   - Prendre des photos
4. **Prétraitement avant l'ozonation (une chaudière)**

   Faire cette partie pour tous les effluents et mélanges
   - Faire la même manipulation que l'étape précédente avec la chaudière complète directement dans celle-ci
   - Filtrer ensuite l'échantillon tel que décrit dans la procédure du pilote d'ozonation
   - Prendre les échantillons avant traitement pour analyse des métaux dissous (filtré) et totaux (non filtré), ions majeurs, NO_2^-, NO_3^- et (SCN^-, CNO^- pour fosse Doyon et mélange fosse Doyon et parc 3 ouest) avant traitement avec ozonation

- Analyser pH, conductivité, température, orp, alcalinité, N-NH_3 avant de débuter le traitement avec ozonation
- Prendre des photos

5. Traitement avec pilote d'ozonation

- Faire un essai de traitement avec une chaudière prétraitée selon l'étape précédente et un autre essai avec une chaudière non prétraitée et ce, pour chaque effluent et mélange
- Suivre la procédure du pilote d'ozonation
- Prendre les échantillons et mesures tel que décrit dans la procédure d'ozonation
- Prendre les échantillons après traitement pour analyse des métaux dissous (filtré) et totaux (non filtré), ions majeurs, NO_2^-, NO_3^- et (SCN^-, CNO^- pour fosse Doyon et mélange fosse Doyon et parc 3 ouest)
- Prendre des photos

6. Post traitement après l'ozonation (une chaudière)

Faire cette partie pour la fosse Doyon et mélange fosse Doyon + parc 3 ouest ainsi que sur les échantillons traités par ozonation qui sont devenus colorés

- Refaire l'étape 3 avec l'eau traitée par ozonation
- Refaire l'étape 4 avec le reste de l'eau traitée par ozonation
- Prendre un échantillon pour analyse de toxicité et l'envoyer au CEAEQ

Échantillonnage

2 chaudières de 20 L par mélange, dans chaque chaudière mettre les volumes suivant :

Échantillon 2 : Parc 3 Ouest (3,88 L par chaudière) et Fosse Doyon (16,12 L par chaudière)

Échantillon 3 : Parc 1 (9,52 L par chaudière) et Parc 2 (10,48 L par chaudière)

- Échantillon 1 : Fosse Doyon seule (aucun mélange terrain)
  - Un kit filtré sur place pour H2Lab
  - Une bouteille 1 L pour essai de toxicité
  - Deux chaudières pour tests ultérieurs en labo
  - Une bouteille pour analyses isotopiques
- Échantillon 2 : Mélange Fosse Doyon et Parc 3 Ouest

- Un kit filtré sur place (après mélange) pour H2Lab
- Une bouteille 1 L (après mélange) pour essai de toxicité
- Deux chaudières (après mélange) pour tests ultérieurs en labo
- Une bouteille (après mélange) pour analyses isotopiques

- Échantillon 3 : Mélange parc 1 et parc 2
  - Un kit filtré sur place (après mélange) pour H2Lab
  - Une bouteille 1 L (après mélange) pour essai de toxicité
  - Deux chaudières (après mélange) pour tests ultérieurs en labo
  - Une bouteille (après mélange) pour analyses isotopiques
- Échantillon 4 : Réservoir Ouest (aucun mélange terrain)
  - Un kit filtré sur place pour H2Lab
  - Une bouteille 1 L pour essai de toxicité
  - Deux chaudières pour tests ultérieurs en labo
  - Une bouteille pour analyses isotopiques
- Échantillon 5 : Bassin B (aucun mélange terrain)
  - Un kit filtré sur place pour H2Lab
  - Une bouteille 1 L pour essai de toxicité
  - Deux chaudières pour tests ultérieurs en labo
  - Une bouteille pour analyses isotopiques

ANNEXE B PROTOCOLE DE PRÉPARATION ET D'ANALYSE DE MÉLANGES D'EFFLUENTS MINIERS

Département, Institut de recherche Mines et Environnement (IRME)

Université du Québec à Abitibi- Témiscamingue (UQAT)

Mots clés : mélanges, eaux minières, écotoxicologie

Objectif de travail

L'objectif de ce travail est de préparer différents mélanges d'effluents miniers afin de reproduire ce qui se produit sur le site minier de la mine Westwood. Les différents mélanges et analyses permettront de valider les modélisations réalisées préalablement à l'aide du modèle PHREEQC. Les différentes concentrations à l'équilibre mesurées seront comparées avec les concentrations modélisées en plus d'une comparaison des résultats écotoxicologiques.

Démarches du travail

Le but de cette procédure de travail est de préparer des mélanges afin de valider les modélisations réalisées à l'aide du modèle PHREEQC. Les paramètres physico-chimiques seront mesurés avant et après mélanges, dans l'immédiat et deux semaines plus tard afin de considérer l'équilibre thermodynamique.

Laboratoire

Matériaux, matériels, réactifs

- Sonde multiparamétrique (pH, conductivité, température, POR, O_2 dissous)
- Chaudières de 20 L
- Cylindre gradué 2 L
- Contenant 5 L
- Bouteilles d'échantillonnage
    - 125 mL
    - 250 mL
    - 500 mL
    - 1 L
- Préservatifs
    - H_2SO_4
    - NaOH
    - HNO_3
- Eau distillée
- Seringues avec filtres 0,45 micron
- Bécher

- Tige en verre

Manipulations préalables

Il est nécessaire de procéder aux analyses avant de préparer les mélanges. Une partie des différents échantillons recueillies sera préparée dans les contenants avec et sans préservatif selon les différentes analyses à réaliser. Les paramètres *in situ* des différents points d'échantillonnage doivent aussi être prélevés à l'aide de la sonde multiparamétrique. Les analyses des isotopes de la molécule d'eau seront en même temps réalisées afin de permettre de valider les ratios des différents mélanges.

Préparation des mélanges

La préparation des mélanges sera réalisée sur le terrain directement afin de pouvoir prendre les valeurs *in situ* le plus rapidement possible. Tous les paramètres physico-chimiques des différents mélanges seront aussi analysés, les échantillons doivent être préparés dans les différentes bouteilles avec et sans préservatifs selon les paramètres puis envoyés pour analyses. L'analyse des isotopes de l'eau seront aussi réalisées. Le tableau 8.8 présente les différents volumes à insérer dans le contenant de 5 L afin d'obtenir 4 L de mélange. Il est nécessaire de préparer deux fois ce volume afin de pouvoir procéder aux analyses deux semaines plus tard.

Les quantités des différents mélanges restant seront ensuite préservés durant deux semaines afin d'atteindre les équilibres thermodynamiques puis les mêmes analyses seront réalisées afin de pouvoir comparer cet effet.

À noter que pour préparer le mélange complet Bassin B + Fosse, un volume sera prélevé du mélange Fosse Doyon + Parc 3O qui aura préalablement été préparé. Il faut donc prévoir de préparer trois fois le volume de Fosse Doyon + Parc 3O afin de compenser le volume prélevé.

Tableau 8.1 : Volumes nécessaires des différents points d'échantillonnage pour la préparation des mélanges

	Volumes pour préparer les mélanges (mL)				
Point échantillonnage	**Mélange 1**	**Mélange 2**	**Mélange 3**	**Fosse Doyon + Parc 3O**	**Mélange complet Bassin B + Fosse**
Parc 1	1904				92
Parc 2	2096		555		412
Parc 3 Est			60		212
Parc 3 Ouest				776	
Bassin Westwood		1484			
Bassin sud		2516			
Halde nord			2285		560
Réservoir ouest			1100		800
Fosse Doyon				3224	
Mélange Doyon + Parc 3O					1924

Points d'échantillonnage

Figure 8.1 : Carte du site avec les différents points d'échantillonnage

Tableau 8.2 : Volumes nécessaires pour la préparation de chaque échantillon incluant le préservatif selon les paramètres à analyser

Paramètre	Manipulation	Volume	Préservatif
pH, ORP, conductivité, température	Mesure in-situ avec sonde multiparamètres	N/A	N/A
Métaux dissous, soufre dissous	Filtration 0,45 microns	125 mL	HNO3
Métaux totaux, soufre total	N/A	125 mL	HNO3

Paramètre	Manipulation	Volume	Préservatif
Alcalinité, acidité, carbonate, bicarbonate, chlorures, nitrates, nitrites, sulfates, thiosulfates	N/A	1 L	Aucun
Azote ammoniacal, phosphore total	N/A	125 mL	H2SO4
Thiocyanates	N/A	125 mL	HNO3
Dureté	N/A	125 mL	HNO3
Cyanates, cyanure	N/A	125 mL	NaOH
Isotope de la molécule d'eau			

Protocole détaillé

1- Commander les bouteilles nécessaires chez H2Lab en indiquant les paramètres nécessaires à analyser et les différents points d'échantillonnage et numéros de mélanges
2- Préparer tout le matériel nécessaire avant de se rendre sur le site de la mine Westwood
3- Se rendre sur aux différents points d'échantillonnage, selon figure 8.18
4- Mesure *in situ* avec la sonde multiparamètres
5- Prise d'échantillons de chaque effluent et séparer dans les différents contenants avec le bon préservatif, bien identifier et envoyer pour analyse, selon tableau 8.9
6- Prise d'échantillon de chaque effluent dans une chaudière de 20 L
7- Avant de quitter le site, préparer les mélanges dans une chaudière de 5 L deux fois selon les données du tableau 8.8
8- Prendre les mesure *in situ* des mélanges avec la sonde multiparamètres
9- Préparer les échantillons de chaque mélange et séparer dans les différents contenants avec le bon préservatif, bien identifier et envoyer pour analyse, selon tableau 8.9
10- Préserver les chaudières de 5 L contenant les différents mélanges qui n'ont pas été touchées afin de refaire les manipulations 5 et 6 deux semaines plus tard

11- Observer tous les jours la coloration et prendre des photos en s'assurant d'avoir le même éclairage à chaque fois

12- Deux semaines plus tard, mélanger légèrement avec une tige de verre l'eau contenue dans les chaudières durant 30 secondes

13- Prendre les mesure *in situ* des mélanges avec la sonde multiparamètres

14- À l'aide d'un bécher, préparer les échantillons de chaque mélange et séparer dans les différents contenants avec le bon préservatif, bien identifier et envoyer pour analyse, selon tableau 8.9